NSF/ENG-87009

PB87 215836/AS

Illinois Institute of Technology
Chicago, Illinois 60616

Department of Civil Engineering
Armour College of Engineering

Report to the
National Science Foundation
Under Grant No.CEE 8313935

MECHANICAL BEHAVIOR OF CEMENTED SANDS

Surendra K. Saxena
and
Raj K. Reddy

Report No. IIT-CE-8701
June 1987

50272-101

REPORT DOCUMENTATION PAGE	1. REPORT NO. NSF/ENG-87009	2.	PB87-215836

4. Title and Subtitle
Mechanical Behavior of Cemented Sands

5. Report Date
June 1987

6.

7. Author(s)
S.K. Saxena; R.K. Reddy

8. Performing Organization Rept. No.
IIT-CE-8701

9. Performing Organization Name and Address
Illinois Institute of Technology
Department of Civil Engineering
Chicago, IL 60616

10. Project/Task/Work Unit No.

11. Contract(C) or Grant(G) No.
(C)
(G) CEE8313935

12. Sponsoring Organization Name and Address
Directorate for Engineering (ENG)
National Science Foundation
1800 G Street, N.W.
Washington, DC 20550

13. Type of Report & Period Covered

14.

15. Supplementary Notes

16. Abstract (Limit: 200 words)

This report evaluates the beneficial effects of artificial cementation in modifying loose sandy soils to safeguard against earthquake induced damage. The study has increased the data base of properties of uncemented and artificially cemented sands at different strain levels. Results indicate that unconfined compressive strength, tensile strength, shear strength, and deformation modulus increase considerably with cementation. The dynamic behavior of cemented sands was found to be greatly influenced by cement content and density and it was demonstrated that a small amount of cementation significantly increases the liquefaction resistance of uncemented sands. The data base was used to develop or modify relationships for deformation modulus, maximum dynamic shear modulus, dynamic shear damping, dynamic longitudinal moduls, etc. for use by practicing engineers.

17. Document Analysis a. Descriptors

Soil mechanics
Soil dynamics
Sands
Soil properties
Earthquakes
Triaxial tests

b. Identifiers/Open-Ended Terms

Cemented sands
Cementation

c. COSATI Field/Group

18. Availability Statement	19. Security Class (This Report)	21. No. of Pages
NTIS		189
	20. Security Class (This Page)	22. Price

(See ANSI-Z39.18) *See Instructions on Reverse* OPTIONAL FORM 272 (4-77)
(Formerly NTIS-35)
Department of Commerce

MECHANICAL BEHAVIOR OF CEMENTED SANDS

Surendra K. Saxena
and
Raj K. Reddy

Report to the
National Science Foundation
Grant No. CEE 83-13935

Principal Investigator
Surendra K. Saxena

Report No. IIT-CE-8701
Civil Engineering Department
Illinois Institute of Technology
Chicago, Illinois
June 1987

CONTENTS

Page

FORWARD v

ABSTRACT vi

LIST OF TABLES vii

LIST OF FIGURES viii

LIST OF SYMBOLS xiii

CHAPTER

I. INTRODUCTION 1

II. STATIC BEHAVIOR OF ARTIFICIALLY CEMENTED SAND 4

Introduction 4
Previous Studies 5
Experimental Investigations 9
Materials Used
Sample Preparation
Tests Conducted
Analysis of Test Results 16
Tensile Strength vs Unconfined compressive Strength
Shear Strength
Strength Generation
Deformation Modulus
Constitutive Behavior
Summary 45

III. DYNAMIC BEHAVIOR OF UNCEMENTED SANDS AT LOW STRAINS 49

Introduction 49

The Resonant Column Test 49
Review of Empirical Relations 50
Relations for G_{max}
Relations for E_{max}
Relations for D_s
Relations for D_l
Comments on Reported Empirical Relations 61
Investigations at I.I.T. 63
Test Equipment
Soil Type
Sample Preparation
Test Procedure
Analysis of Test Data 64
Dynamic Shear Modulus
Dynamic Young's Modulus
Dynamic Shear Damping
Dynamic Longitudinal Damping
Evaluation of Relationships 78
Summary 88

IV. DYNAMIC BEHAVIOR OF CEMENTED SANDS AT LOW STRAINS 89

Introduction. 89
Experimental Investigation 89
Test Materials
Sample Preparation
Test Setup and Procedure
Variables
Analysis of Test Results 92
Effect of Strain Amplitude
Effect of Confining Pressure
Effect of Cement Content
Effect of Void Ratio
Effect of Curing Period
Empirical Relations 103
Dynamic Shear Modulus
Dynamic Young's Modulus

Dynamic Shear Damping
Dynamic Longitudinal Damping
Correlations with Static Triaxial tests 117
Static Triaxial Tests
Variation of E with ϵ
Correlations with Dynamic Moduli
Correlations for Damping Ratios
Summary 123

V. CORRELATION BETWEEN DYNAMIC MODULI AND RESISTANCE TO LIQUEFACTION OF CEMENTED SANDS 124

Introduction 124
Scope of Present Study 124
Shear Wave Velocity 125
Summary of Experimental Investigation 126
Cyclic Triaxial Testing
Resonant Column Testing
Analysis of Experimental results 137
Liquefaction Resistance 137
Effect of Density
Effect of Cement Content
Effect of Curing Period
Correlation between Dynamic Moduli and Cyclic Strength 141
Correlations for Uncemented Sand
Correlations for Cemented Sand
Discussion on Correlations
Summary 160

VI. CONCLUSIONS AND RECOMMENDATIONS 162

BIBLIOGRAPHY 165

FORWARD

This report evaluates the beneficial effects of artificial cementation in modifying loose sandy soils to safeguard againest the earthquake induced damage. This work is the culmination of the first phase of the activity to understand the mechanical behavior of cemented sands. The study has increased the data base of the properties of uncemented and artificially cemented sands at different strain levels. The developed data base has been utilised to quantify the beneficial effects of artificial cementation of sands by developing or modifying relationships for deformation modulus, maximum dynamic shear modulus, dynamic shear damping and other for use by practicing engineers.

This work was conducted by the Illinois Institute of Technology,Chicago under the sponsorship of National Science Foundation under a grant CEE 83-13935. An interim report entitled " Behavior of Cement Stabilized Sands Under Static and Dynamic Loads", was submitted to NSF in September 1985. The support of the National Science Foundation is deeply appreciated and acknowledged.

The principal investigator for the entire research effort is Dr.Suren Saxena, Professor and Chairman, Civil Engineering Department. Much of the experimental work was done by Dr.Anestis Avramidis, then Research Assistant now Geotechnical Engineer, Woodward Clyde Associates. The analysis of test results and derivation of relationships was conducted by Raj Krishna Reddy, Research Assistant, Civil Engineering Department, Illinois Institute of Technology.

This report is authored by Prof.S.K. Saxena and R.K. Reddy. The overall support of the Civil Engineering Department, Illinios Institute of Technology is also greatfully acknowledged.

ABSTRACT

This research effort was aimed to increase the data base of the deterministic properties for uncemented and artificially cemented sands at different strain levels and to utilize the obtained data base to quantify the beneficial effects of artificial cementation of sands.

In all 152 static triaxial (drained) tests, 52 resonant column tests, 84 cyclic triaxial tests, 15 unconfined compression tests and 15 brazilian tests were conducted. Some of the testing equipment had to be modified for testing the stiff cemented sand specimens. All the specimens were prepared using the method of undercompaction– the method approved by the NRC. The variables considered were relative density, cement content, curing period and effective confining pressure.

The results indicated that unconfined compressive strength, tensile strength, shear strength and deformation modulus increase considerably with cementation. It was found that the dynamic behavior of cemented sands is greatly influenced by cement content and density. At very low strain amplitudes the dynamic moduli and damping ratios were increased at low levels of cementation, however with higher cement content though the moduli considerably increased, but the damping ratios were observed to be decreasing. It was clearly demonstrated that a small amount of cementation significantly increases the liquefaction resistance of uncemented sands. A good correlation between liquefaction resistance and dynamic moduli (and thus wave velocities) was also found possible for cemented sands but such correlation was examined for a particular confining pressure only.

The data base was then used to develop or modify relationships for tensile strength, deformation modulus, dynamic maximum shear and Young's moduli, dynamic shear and longitudinal damping ratios etc. for use by practicing engineers to modify the loose sandy soils to withstand the earthquake induced damage especially liquefaction.

LIST OF TABLES

Table		Page
2.1	Index Properties of Monterey No. O sand	12
2.2	Results from Brazilian & Unconfined Compression Tests . .	18
2.3	Values of ϕ and c for Cemented and Uncemented Monterey Sand	27
2.4	Values of Elastic Modulus Parameters	43
3.1	Reported Relationships for G_{max} Estimation	52
3.2	Values of k (Hardin and Drenevich, 1972)	53
3.3	Values of Constants for Eqn.3.1 (Isenhower,1979)	54
3.4	Values of K_{2max} for Eqn.3.3 (Seed and Idriss, 1970) . . .	56
3.5	Values of D_{max} for Eqn.3.10 (Hardin and Drenevich, 1972) .	58
3.6	Poisson's Ratio Values (Skoglund et al. 1976)	74
4.1	Variables and their Range of Values for Resonant Column Tests	95
5.1	Variables and their Range of Values for Cyclic Triaxial Tests	129
5.2	Values of a and b for Eqn.5.9	147

LIST OF FIGURES

Figure		Page
2.1	Grain Size Distribution for Monterey No.O Sand	11
2.2	Schematic of test set-up for Brazilian Tests	15
2.3a	Stress-strain response of uncemented and cemented sands for D_r=43%	21
2.3b	Volumetric strain versus Axial strain curves of uncemented and cemented sands for D_r=43%	22
2.4	Coefficient of Brittleness versus $\overline{\sigma}_c$ at Various D_r and CC values	24
2.5	Cohesion and Angle of internal friction at peak strength versus cement content after 15 days of curing	25
2.6	Strength Ratio versus Effective Confining Pressure	26
2.7	Strength envelope and Strain contours for dense uncemented Monterey sand (D_r=80%)	29
2.8	Strength envelope and Strain contours for loose uncemented Monterey sand (D_r=43%)	30
2.9	Variation of c and ϕ with axial strain for dense uncemented Monterey sand (D_r=80%)	32
2.10	Variation of c and ϕ with axial strain for loose uncemented Monterey sand (D_r=43%)	33
2.11	Strength envelope and Strain contours for cemented Monterey sand with D_r=43% and CC=2%	34
2.12	Strength envelope and Strain contours for cemented Monterey sand with D_r=43% and CC=5%	35
2.13	Strength envelope and Strain contours for cemented Monterey sand with D_r=43% and CC=8%	36
2.14	Variation of c and ϕ with axial strain for cemented Monterey sand with D_r=43% and CC=2%	38
2.15	Variation of c and ϕ with axial strain for cemented Monterey sand with D_r=43% and CC=5%	39
2.16	Variation of c and ϕ with axial strain for cemented	

Monterey sand with D_r=43% and CC=8% 40

2.17 Stress-strain response of Strongly Cemented Sands 46

2.18 Stress-strain response of Weakly Cemented Sands 47

3.1 Definitions of Strain amplitude, moduli and damping . . . 51

3.2 n versus γ relationship 60

3.3 Dynamic Shear Modulus versus shear strain amplitude for Monterey No. O sand with D_r= 25, 43, 60 and 80% 65

3.4 Dynamic longitudinal (or Young's modulus) versus longitudinal strain amplitude for Monterey No.O sand with D_r=25, 43, 60 and 80% 66

3.5 Dynamic shear damping versus shear strain amplitude for Monterey No. O sand with D_r=25, 43, 60 and 80% . 67

3.6 Dynamic Longitudinal damping versus longitudinal strain amplitude for Monterey No. o sand with D_r=25, 43, 60 and 80% 68

3.7 Effective confining pressure versus maximum shear modulus 69

3.8 Comparison of proposed relation and available relations for G_{max} for Monterey No. O sand 71

3.9 Comparison of Proposed relation for Monterey No O sand with reported relations for other types of soils 72

3.10 Grain size distribution and index properties of sand used by Skoglund et. al (1976) 73

3.11 Effective confining pressure versus maximum Young's modulus 76

3.12 Effect of relative density on D_s 79

3.13 Effect of relative density on D_l 80

3.14 Evaluation of relationship for maximum shear modulus . . 82

3.15 Evaluation of relationships for maximum shear modulus as compared to experimental results 83

3.16 Evaluation of relationship for maximum Young's modulus . 84

3.17 Evaluation of relationship for shear damping 85

3.18 Comparison of Shear Damping values for $\overline{\sigma}_0$= 98 kpa and e= 0.7253 86

3.19 Evaluation of relationship for longitudinal damping 87

4.1 Performance of Modified Drenvich Long-Tor Resonant Column Apparatus 91

4.2 Influence of Testing Sequence 93

4.3 Effect of saturation 94

4.4 Typical results From Resonant Column testing For the case of D_r= 25%, CC=2% and CP=15 days 96

4.5 Effect of Confining pressure on increase in maximum dynamic shear modulus 98

4.6 Effect of Confining pressure on increase in maximum dynamic Young's modulus 99

4.7 Effect of Cement Content on Dynamic Moduli and Damping Ratios 100

4.8 Effect of Density on Dynamic Moduli and Damping Ratios . 104

4.9 Effect of Curing Period on Dynamic Moduli and Damping Ratios 105

4.10 Comparison of measured and computed values of increase in dynamic maximum Shear Modulus 107

4.11 Comparison of Proposed relation with the relation developed by Chiang and Chae (1972) for maximum dynamic shear modulus 109

4.12 Comparison of Proposed relation with the relation developed by Acar and Tahir (1986) for maximum Dynamic Shear Modulus 111

4.13 Comparison of measured and computed values of increase in dynamic maximum Young's Modulus 113

4.14 Comparison of Proposed relation with experimental results for Dynamic Shear Damping 116

4.15 Variation of Young's Modulus with strain as determined by the Resonant Column and by the Static Triaxial Test 119

4.16 Correlation between Maximum Shear Modulus and Deviator

Stress (at 1% axial strain) of Static Triaxial Tests . . 121

4.17 Correlation between Maximum Dynamic Young's Modulus and Deviator Stress (at 1% axial strain) of Static Triaxial Tests 122

5.1 Typical Results from Cyclic Triaxial Test 130

5.2a Axial Strain vs Cycle Ratio for Uncemented Sand 131

5.2b Pore pressure vs Cycle Ratio for Uncemented Sand 132

5.2c Stress Ratio vs Loading Cycle Number for Uncemented Sand 133

5.3a Axial Strain vs Cycle Ratio for Cemented Sand 134

5.3b Pore Pressure Ratio vs Cycle Ratio for Cemented sand . . 135

5.3c Stress Ratio vs Loading Cycle Number for Cemented Sand 136

5.4 Effect of Density on Liquefaction Resistance for Uncemented Sand 138

5.5 Effect of Density on Liquefaction Resistance for Cemented Sand with CC=1% 139

5.6 Effect of Density on Liquefaction Resistance for Cemented Sand with CC=2% 140

5.7 Effect of Cement Content on Liquefaction Resistance . . . 142

5.8 Effects of Cement Content and Density on Stress Ratio to cause Liquefaction after 10 cycles . . . 143

5.9 Effects of Cement Content and Density on Stress Ratio to cause Liquefaction after 100 cycles 144

5.10 Effect of Curing period on Liquefaction Resistance 145

5.11 Dynamic Shear Modulus vs Liquefaction Resistance for Uncemented Sand 150

5.12 Dynamic Young's Modulus vs Liquefaction Resistance for Uncemented Sand 151

5.13 Effect of Specific Number of Cycles to cause Liquefaction on Correlation between Shear Modulus and Liquefaction Resistance for Uncemented Sand 153

5.14 Effect of Specific Number of Cycles to cause Liquefaction on

Correlation between Young's Modulus and Liquefaction Resistance for Uncemented Sand 154

5.15 Comparison of Correlations between Dynamic Shear Modulus and Liquefaction Resistance for Uncemented Sand . . . 155

5.16 Dynamic Shear Modulus vs Liquefaction Resistance for Cemented Sand with CC=1% 156

5.17 Dynamic Shear Modulus vs Liquefaction Resistance for Cemented Sand with CC=2% 157

5.18 Dynamic Young's Modulus vs Liquefaction Resistance for Cemented Sand with CC=1% 158

5.19 Dynamic Young's modulus vs Liquefaction Resistance for Cemented Sand with CC=2% 159

LIST OF SYMBOLS

Abbreviation	Term
B	Skempton's B parameter
B_c	Brittleness coefficient
c	Cohesion
C_c	Coefficient of curvature
CC	Cement content
CR	Cycle ratio
CP	Curing period
C_u	Coefficient of uniformity
D_l	Hysteretic damping ratio in compression
D_s	Hysteretic damping ratio in shear
D_r	Relative density
E_i, E_i^*	Initial Young's modulus or Deformation modulus
E, E^*	Dynamic Young's modulus
E_m, E_m^*	Maximum dynamic Young's modulus
e	Void ratio
G, G^*	Dynamic shear modulus
G_m, G_m^*	Maximum dynamic shear modulus
P_a	Atmospheric pressure
q_u	Unconfined compressive strength

S_{peak}	Peak strength
S_{resid}	Residual strength
SR	Stress ratio
U	Pore water pressure ratio
v_s	Shear wave velocity
γ	Shear strain amplitude
Δu	Excess pore water pressure
Δu_{max}	Maximum excess pore water pressure
ΔE	Increase in dynamic Young's modulus
ΔG	Increase in dynamic shear modulus
ΔD_s	Increase in dynamic shear damping
ΔD_l	Increase in dynamic longitudinal damping
ϵ	Longitudinal strain amplitude
ϕ	Angle of internal friction
ν	Poisson's ratio
ρ	Mass density
$\overline{\sigma}_c$	Effective confining pressure
$\overline{\sigma}_0$	Effective mean principal pressure
σ_d	Deviator stress
σ_t	Tensile strength
*	refers the values for cemented sands

Chapter I

INTRODUCTION

The investigation of the behavior of *cemented sands* is an important topic in both dynamic and static geotechnical engineering. Most sands are cemented in nature and thus the amount of cementation has a significant influence on their engineering properties. Little is understood of this important characteristic.

Naturally cemented sands are generally brittle and easily crushable. These exhibit softening behavior, dilation at relatively low confining pressure and high compressibility. Undisturbed sampling of such sands is immensely complicated because any sampling technique can clearly damage cementation bonds and cause crushing of the soil grains. Therefore even the limited studies involving naturally cemented sands were inconclusive. However Sitar et.al.(1980) and Rad and Clough (1982) showed that artificially cemented sands may be used to simulate and study the behavior of naturally cemented sands.

The study of artificially cemented sands is also useful to evaluate the feasibility of improving subgrades under highways and airport runways, stabilizing slopes in cuts and embankments, increasing soil bearing capacity.....Under such situations, the knowledge of modified static properties due to cementation is very important. The recent recognition of the importance of increase in dynamic properties of poor sandy deposits by artificial cementation to mitigate earthquake effects, machine foundation design, foundation isolation...necessitated the study of behavior of cemented sands under dynamic conditions.

The research described in this report is the culmination of the first phase of the activity at the Illinois Institute of Technology towards understanding the mechanical behavior of artificially cemented sands. *The aim of this study was to increase the data base of the deterministic properties for uncemented and artificially cemented sands at different strain levels and to utilise the obtained data base to quantify the beneficial effects of artificial cementation of sands. This data base has then been used to develop or modify relationships*

for deformation modulus, maximum dynamic shear modulus, dynamic shear damping, dynamic longitudinal moduls, etc. for use by practicing engineers.

The variables considered were cement content, curing period, density and effective confining pressure. The tests conducted include static triaxial tests, resonant column tests, cyclic triaxial tests and also unconfined and brazilian tests.

The second chapter of the report is devoted to a study of *static* behavior of artificially cemented sands. The studies of cemented sands from 1964 to 1982 by various investigators have been summarized and the results of the experimental investigation at I.I.T. from 1983 to 1986 involving static triaxial, unconfined compression and brazilian tests along with the analysis of test results. Based on studies todate, correlations among unconfined compressive strength, tensile strength and shear strength are developed and presented. A discussion of existing methods for the selection of deformation modulus is presented and a new alternate relation proposed.

The third chapter of the report examines the available empirical relations for maximum dynamic shear modulus and dynamic shear damping for sands at low strain amplitudes. Based on the results of resonant column tests on Monterey No. O sand conducted at I.I.T. new relations for the dynamic shear modulus and damping are proposed. Also proposed are the relations for dynamic longitudinal modulus and damping based on the results of tests.

The fourth chapter advances the understanding about the *beneficial effects of cementation* on dynamic behavior of sands at low strain amplitudes. The influence of important parameters such as cement content, effective confining pressure, density etc. is discussed in detail on the basis of results from resonant column tests. A newly proposed relationship for maximum dynamic shear modulus is compared with reported relationships. Empirical relations for maximum longitudinal modulus, dynamic shear and longitudinal damping are proposed afresh. The developed relationships are nondimensional.

In the fifth chapter the *correlation between resonant column test results and the cyclic triaxial test results* is investigated. Since the samples for both

types of tests were prepared identically by the method of undercompaction, any correlations developed would be free from sample preparation effects. The development of correlations became possible because of the maintainance of a one-to-one correspondance of the parameters such as cement content, curing period, density etc. for both types of tests during experimental investigation. If dynamic moduli (or wave velocities) are known from laboratory or field tests, the correlations could be helpful in determining the cyclic shear strength of soils. Then any existing methods like shear wave velocity test can be employed to identify the susceptibility of liquefaction. Such correlations will be helpful in evaluating the feasibility of strengthening poor sandy deposits by artificial cementation.

The final (sixth) chapter reports the conclusions and recommendations for future research in this area.

Chapter II

STATIC BEHAVIOR OF ARTIFICIALLY CEMENTED SAND

2.1 INTRODUCTION

Whenever soils with unsatisfactory properties are encountered on engineering projects, some form of soil stabilization is required. Many engineering projects, such as improvements of subgrades under highways and airport runways, stabilizing slopes in cuts and embankments, increasing soil bearing capacity under foundations etc. need stabilization.

There are many methods of soil stabilization. The description, merits and demerits of commonly used stabilization techniques are discussed in detail elsewhere (MIT, 1952; USNAEC, 1969, ASCE, 1982, etc.) and are not reported here. To stabilize the weak sandy deposits, the method of artificial cementation is becoming increasingly popular. The addition of a small amount of cementing material such as portland cement substantially improves engineering properties of sands.

The studies of cemented sands were performed at M.I.T. (Wissa and Ladd, 1964, 1965) involving only static triaxial tests. Bachus et al., (1981), Rad and Clough (1982) and Sitar et al. (1980) investigated the behavior of weakly cemented sands for static loading conditions and for soil slopes under earthquake conditions. Saxena and Lastrico (1978) and Dupas and Pecker (1979) studied the static properties of naturally cemented sands.

The present study is limited to artificially cemented sand with the following objectives;

(i) to briefly review the previous studies

(ii)to increase the data base for tensile strength and to correlate it with unconfined compressive strength.

(iii)to analyze the triaxial drained test results with cemented-stabilized Monterey No. 0 sand to obtain an understanding about

(a) Strength generation

(b) Initial tangent modulus

(c) Stress-strain characteristics

2.2 PREVIOUS STUDIES

Wissa and Ladd (1964, 65) were the first to study the properties of compacted stabilized soils (artificially cemented). They used two types of coarse soils; one coarse Ottawa uniform sand which entirely (100%) passed sieve #20 and 95% retained on sieve #30. The second was a medium Ottawa sand obtained by sieving well graded Ottawa sand and using the portion passed through sieve #40 and retained on sieve #60. The first type of soil has maximum and minimum dry densities of 1.78 g/cm^3 (112.3 lb/ft^2) and 1.541 gm/cm^3 (96.9 lb/ft^3) respectively, while the second type had maximum and minimum dry densities of 1.716 gm/cm^3 (107.9 lb/ft^3) and 1.44 gm/cm^3 (90.5 lb/ft^3) respectively. These dry densities of sand portion were obtained by air pluviation technique. The relative densities of the samples tested were: Coarse Ottawa sand; 43% and medium Ottawa sand; 62%, 64% and 75%. The samples tested were 8 cm in length and 3.57 cm in diameter. The stabilizer used was Portland cement Type 1. For coarse sand 5% by stabilizer dry weight of sand was used and for medium sand two proportions 5% by dry weight and 10% by dry weight were used. The exact weight of any sand for one sample was hand-blended with the appropriate amount of cement. The mixing water was then added and mixed thoroughly by hand. The samples were compacted in two part split mold in 10-15 layers using 10 soft tamping per layer applied with 0.5 in diameter tamper. The samples were first humid cured in desicant jars for three days and then were completely immersed in water for at least 24 hours before testing.

The samples were saturated under a back pressure of 10 kg/cm^2 (147 psi) for two hours and saturation was considered 100% when Skempton's B parameter was at least 0.90. Deaired water was used to saturate the samples. The samples were subject to consolidated undrained and consolidated drained triaxial tests. All tests were strain controlled with strain rate of 6% per hour. Final water content was determined at the end of the test. In the drained tests volume changes during shear were measured under the back pressure of

10 kg/cm^2 (147 psi) to the nearest 0.01%. The total number of tests conducted were 27 on sands and 107 on clays.

The influence of cementation was studied based on CID triaxial compression tests with Ottawa sand stabilized with different cement content and curing periods. Unlike uncemented sand, the cemented sand was found to cause Mohr's envelope with cohesion intercept and appreciably curved at lower confining pressures due to premature brittle fracture caused by inadequate confining pressure to close the submicroscopic shrinkage cracks due to hydration during curing. For example, a consolidation pressure of 10 kg/cm^2 was sufficient to avoid brittle fracture for the case of medium dense sand with CC=5%. This value, however was greater for higher cement contents.

Axial strain contours, indicate that at low strains the shearing resistance was due to the cementation between grains and no appreciable friction was mobilized. After about 0.6% axial strain the frictional resistance continued to increase and the cementation gradually broke down. On further straining ultimate conditions were reached at which time the continuous cementation between grains in the failure zone was completely destroyed and the effective stress-strength curve converged towards the origin on a $\overline{p}$ vs q plot. The maximum principal strength difference was found to occur when the sum of the shearing resistance due to friction and cementation reached a maximum. At this time, the slopes of the volumetric strain versus axial strain curve did not reach a maximum.

The second study appeared in the literature in 1978 by Saxena and Lastrico. In this investigation the naturally cemented sand of the Vincetown Formation in the New Jersey coast was studied. The Vincetown formation is composed of a variably cemented fine to medium greenish gray sand, with fine content ranging from 10% to 40% by weight. The D_{50} values of the sand range from 0.15 mm to 0.49 mm with natural water content varying from 20 to 40%. The material passing #200 sieve had liquid limits and plastic limits of 23-47% and 16-33% respectively. The material had specific gravity from 2.66 to 2.76 and the dry density ranged from 1.20 gm/cm^3 (75 pcf) to 1.60 gm/cm^3 (100

pcf). The sample had a length diameter ratio of greater than 2. The stabilizer was calcite cement and only samples with least cement content were tested. The samples were saturated under back pressure of 20.97 kg/cm^2 (44 ksf) and saturation was assumed 100% when B parameter had a value equal to or greater than 0.96. Isotropically consolidated triaxial tests were conducted on samples under various confining pressures. Pore pressures were measured in the tests. The rate of shear was 0.025 cm/min and the failure was assumed when the post shear behavior was observed or until 20% axial strain was reached. In total 92 triaxial tests were conducted.

The test results indicated no clear relation between initial porosity and friction angles and so also between density and strength because of variation in cementation. Besides, no correlation was observed between strain at failure or maximum deviator stress and confining stresses, thereby confirming the fact that the natural cemented sands possess inherent variation in strength. In general, the stress-strain curves were observed similar to that of a dilating or dense material, even though the tested samples were not dense enough (the cementation creates an "apparent high density"). It was also noted that cemented sands exhibit higher undrained shear strength at lower confining pressures and lower strain levels; however at higher strains, behavior was like uncemented sands. The axial strain contours on $\bar{p}$-q plots indicated breakage of cementation and increase in frictional resistance after certain strain levels.

Dupas and Pecker (1979) described static consolidated drained triaxial tests and dynamic triaxial tests to assess the static and dynamic behavior of cement treated sands. Samples were prepared by compaction with 5,7 and 9 percentages of cement to the dry weight of sand and at two different dry weights corresponding to 100 and 95 percentages of maximum standard proctor density and cured for 7 days. A consistent decrease in permeability was obtained with the increase of cement content and dry density. Based on static CID triaxial tests with small range of confining pressure (0.1 Mpa - 0.5 Mpa) and assuming straight line envelopes, it was concluded that friction angle does not change significantly whereas cohesion increases considerably with the increase in dry

density, curing period and cement content. They found that the stress-strain data can be approximated by hyperbola and the tangent Young modulus is expressed as below:

$$E_t = E_i \left(1 - \frac{R_f(1 - sin\phi)(\sigma_1 - \sigma_3)}{2ccos\phi + 2\sigma_3 sin\phi}\right)^2 \tag{2.1}$$

$$E_i = kP_a \left(\frac{\sigma_3 + ctan^{-1}\phi}{P_a}\right)^n \tag{2.2}$$

in which c, ϕ = drained strength parameters, σ_1, σ_3= principal stresses, E_i = initial Young modulus, P_a = atmospheric pressure and R_f, k and n are the parameters determined from test results. It was observed that k value decreases and n value increases as cement content increases, however R_f value was found constant.

A study on behavior of weakly cemented sands was also undertaken at Stanford University. In the earlier two reports (No. 44 and 52) by Sitar, Clough and Bachus (1980, 1981), the investigation studies natural and artificially cemented sands from Stanford Linear Accelerator site and along the Pacific coast. Samples from the above two sites (intact and reconstituted) were tested in unconfined compression and drained triaxial compression. About 50 tests were done on intact samples and nine on reconstituted ones. The intact samples were tested at natural water content, after soaking for two days, after soaking for four days and in oven-dry conditions. The reconstituted samples were tested at natural water content and under oven-dry conditions.

The tests on artificially cemented soils used 50% of Monterey sand #0 and 50% of Monterey sand #20. The sample dimensions were 7 cm in diameter and 13.8 cm in height. The stabilizer used was Portland cement (2% and 4% by dry weight of sand). The samples tested had relative densities of 60%, 74% and 90%. The samples were compacted in layers of constant thickness to assure uniform density and humid curing was used. Samples were cured for 3 to 28 days and a total of 28 unconfined compression tests were performed to determine the variations of strength with time. The results indicated that 80% of the 28 day strength had occurred during the first ten days of curing. Therefore, all samples later were cured for 14 days only. The tests performed on

artificially cemented sands consisted of four types of static tests: (a) unconfined compression tests (b) consolidated drained triaxial tests, (c) unconfined simple shear tests and (d) Brazilian tests. The dynamic tests were cyclic compression triaxial tests.

The latest report Rad and Clough, 1982 studies are directed to understand behavior of cemented sands subjected to static and dynamic loading under undrained conditions. The investigations involved more than 300 static drained and undrained strain controlled triaxial tests. Both naturally and artificially cemented sands, as well as uncemented sands were tested. For the artificially cemented samples 1, 2 and 4% cement was used and the relative density was ranging from 25 to 90%. The results of tests on uncemented sand samples formed a basis of comparison to the artificially cemented ones. The samples were prepared by a new method which involves application of an initial vacuum to the specimen, which in turn facilitates saturation under back pressure. The volume change was measured by a new device developed during the research which measures the volume change automatically.

The conventional field tests, such as SPT, CPT and Self boring pressuremeter tests were also conducted in the areas of naturally cemented soils. It was found that the SPT and CPT are of limited use whereas self boring pressuremeter is the best in-situ testing tool to determine the parameters of a weakly cemented sand.

2.3 EXPERIMENTAL INVESTIGATIONS

An experimental research program was initiated at the Illinois Institute of Technology (IIT) from 1983 through 1985 in order to understand the behavior of artificially cemented sand at different strain levels. The static tests conducted include permeability tests, and consolidated drained triaxial compression tests. The parameters considered were: relative density, cement content, curing period, and effective confining pressure. All the details of test results and conclusions have been reported in the interim report (Avramidis and Saxena, 1985) submitted to the National Science Foundation.

In this section a brief background of selected materials, the methods of

preparing samples, testing procedures and salient results of above investigation are presented. Results of further studies by newly conducted brazilian and unconfined compression tests are described. Finally, the large body of available data is thoroughly analyzed to fulfil the objectives mentioned earlier.

Materials Used: Monterey No. 0 sand and Portland cement type I (commercial grade) were used. The grain size distribution curve and index properties of Monterey No. 0 sand are given in Fig. 2.1 and Table 2.1 respectively.

Sample preparation: Specimens used in previous and current research were reconstituted by the method of undercompaction, proposed by Ladd (1978). To obtain the desired relative density with this method, a predetermined mass of sand must occupy certain volume inside the sample preparation mold.

The whole sample is made in layers. The lower layers are placed in a relatively loose condition (undercompacted) so as the compaction due to the subsequent layers above them will densify them to the desired relative density. Samples prepared with this method are more reproducible than those made with vibration or pluviation techniques (Ladd, 1978). Also, particle segregation is minimized during preparation and a wide range of uniform relative densities can be achieved.

All the uncemented specimens for static triaxial testing were prepared in the testing apparatus inside an aluminum split mold. However, all the cemented specimens for triaxial testing, brazilian tests and unconfined compression tests were prepared on a stand inside a plastic mold made out of PVC tubing. The details of this sample preparation set up are given in Avramidis and Saxena (1985).

All the specimens were prepared in six layers. In preparing the specimens, first the proper amount of dry cement per layer was weighed in a porcelain dish. The weight of cement was the desired percentage based on the dry weight of Monterey sand. Then the properly weighed amount of dry sand, per layer, was added and the two materials were mixed thoroughly by hand with-

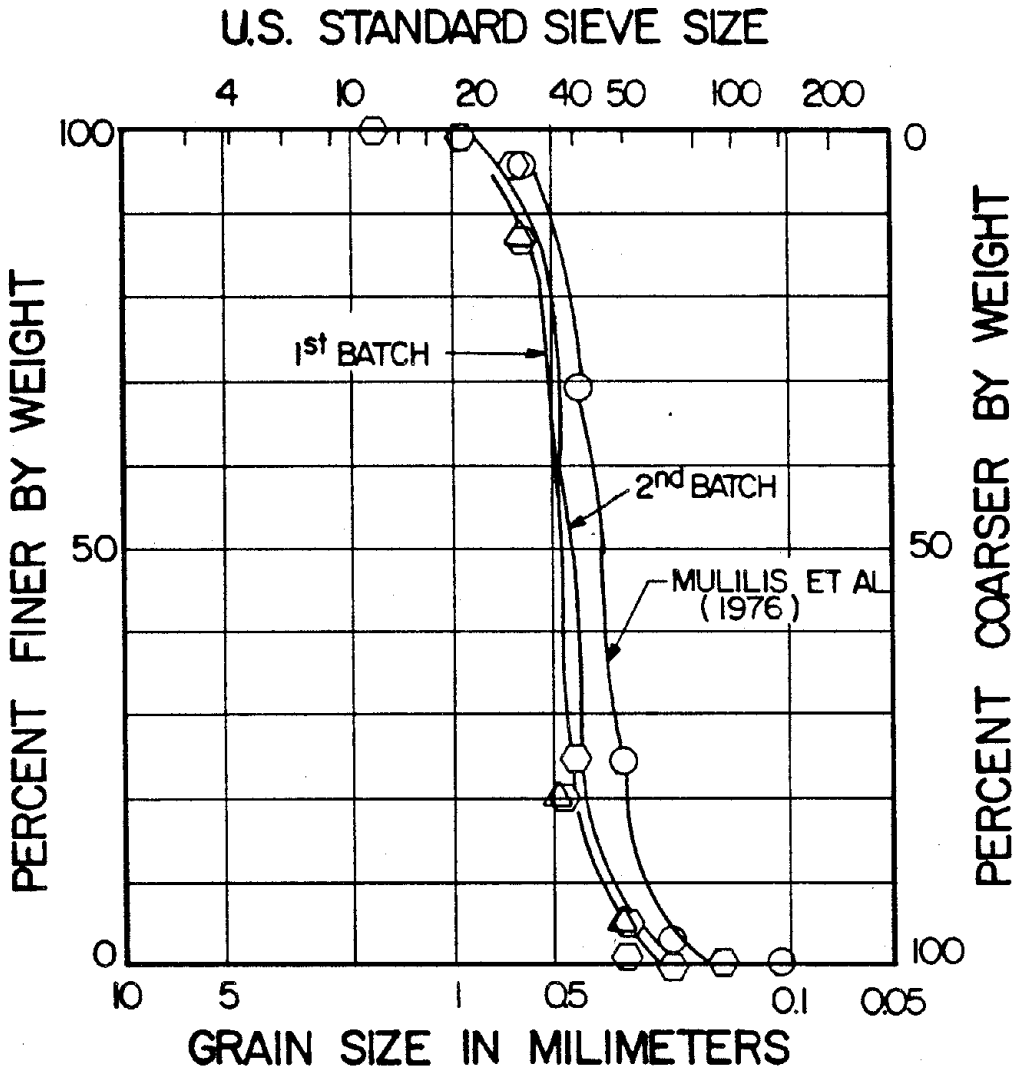

Fig.2.1 Grain Size Distribution for Monterey No.O Sand

Table 2.1 Index Properties of Monterey Sand

PROPERTIES	VALUES
U.S.C.S. Group Symbol	SP
Mean Specific Gravity	2.65
Particle Size Distribution Data	
Coefficient of Curvature, C_c	1.02
Coefficient of Uniformity, C_u	1.35
Mean Grain Size Diameter, D_{10}	0.44
Maximum Void Ratio*	0.85
Minimum Void Ratio*	0.56

* Based on Mulilis et. al. (1976)

out adding water until a mixture of uniform color appeared. The material was emptied into a larger porcelain dish where 8% water, based on the dry weight of the sand-cement mixture was added. The resulting sand-cement-water mixture was re-mixed thoroughly using a steel rod 0.635 cm in diameter. The wet homogeneous mixture was then placed inside the mold using a spoon, was leveled off, and subsequently compacted with a tamper. The degree of compaction used was 6%, and the procedure was repeated for the rest of the layers. The cemented samples were then cured below water for different days. The height to diameter ratio for the uncemented and cemented samples was between 2.0 and 3.0.

Tests conducted: The different static tests conducted previously and during current research are as follows:

(i) Static Drained Triaxial Tests

(ii) Brazilian Tests (or Splitting Tension Tests)

(iii) Unconfined Compression Tests

The materials and method of sample preparation are same for all above tests.

(i) Static Triaxial Tests: A total of 152 static strain controlled, isotropically consolidated drained triaxial compression tests were conducted on uncemented and cemented sands during the first phase of research at IIT (Avramidis and Saxena, 1985). The following test variables were considered:

Loading Strain Rate = 0.186% per minute

Effective Consolidation Pressure = 49 kpa, 245 kpa & 490 kpa

Relative Density = 43%, 60% and 80%

Cement Content = 0% (no cement), 2%, 5% and 8%

Curing period = 15 days, 30 days, 60 days and 180 days

After the specific curing period was completed, measurements of height and diameter of the specimen were obtained. The sample surrounded by two membranes, each having a thickness of 0.317 mm, was placed between the pedestals of the triaxial cell and the tip and bottom were sealed using two rubber O-rings. Uncemented specimens were prepared in a split mold which

was placed on the triaxial cell pedestal were also surrounded by two membranes. At this time, the space between the specimen and the cell chamber was filled with fresh deaired water.

To facilitate the saturation process, the specimens were flushed with carbon dioxide and then with fresh deaired water under a back pressure of 192 kpa. The effective confining pressure during saturation was 25 kpa. Some samples were also saturated under vaccum. No effect of carbon dioxide on the strength of samples was found. The saturation was considered adequate when Skempton's pore pressure parameter, B was equal or larger than 96%. With the triaxial testing set up used in this investigation, the coefficient of permeability was also determined. Subsequently the specimen was consolidated under specific effective confining pressure. The volume change during consolidation was obtained from water levels in the burette from which the preshear data such as void ratio etc. were obtained. Then the specimen was axially loaded to shear. During testing, the following parameters were monitored and recorded: 1) time, 2) axial deformation, 3) axial load, 4) volumetric change, 5) back pressure and 6) cell pressure.

The test results were plotted as stress versus strain, volumetric strain versus axial strain, and q versus $\bar{p}$ curves. Because of wide range of variables, enormous graphs were resulted and appended in Appendix B of the interim report (Avramidis and Saxena, 1985).

(ii) Brazilian Tests (or Splitting Tension Tests): A total of 15 specimens were tested with the test set-up schematically shown in Fig. 2.2. The following tests variables were considered.

Loading Strain Rate = 0.186% per minute

Relative Density= 25%, 43%, 60% and 80%

Cement Content= 1%, 2%, 5% and 8%

Curing period = 15 days

Length/Diameter Ratio = 2.0

The samples tested were prepared by method of undercompaction in the same way as for static triaxial tests. Circular steel plates with diameter

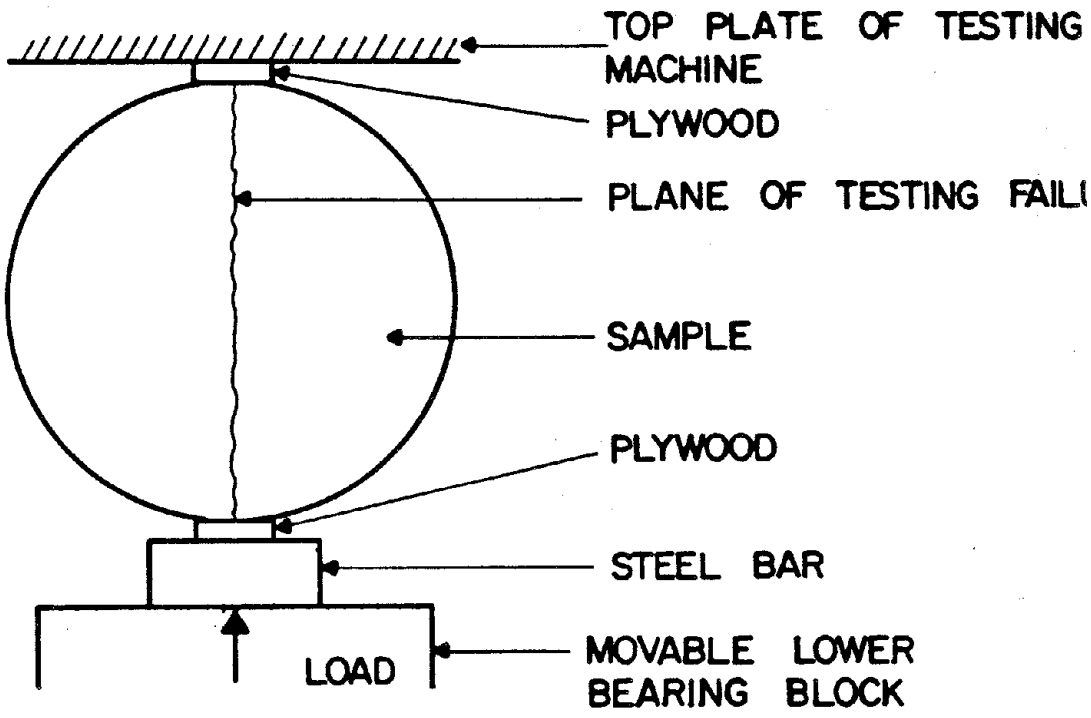

Fig.2.2 Schematic of test set-up for Brazilian Tests

slightly larger than the length of the samples were fixed to the top plate of testing machine and the lower bearing block of triaxial testing machine in such a manner that the load applied is distributed over the entire length of the specimen. Two bearing strips of 1 in. wide and 0.2 in. thick smooth plywood of a length equal to length of specimen were prepared. One of the plywood strips was placed in center of the lower bearing block. After precise measurement of length and diameter, the specimen, was placed on this lower plywood strip. The upper plywood strip was then placed lengthwise on top of the specimen. The movable lower bearing block was raised slowly until the sample and the plywood strips were gripped by the top plate. Load was then increased until the specimen failed. The loads at which first crack appeared and the sample failed, were recorded. No measurements for strains were made. The tensile strength of specimen was calculated using the following expression:

$$\sigma_t = \frac{2P}{\pi LD} \tag{2.3}$$

where σ_t = tensile strength in pounds per square inch, P = maximum applied load, in pounds, L = length in inches and D = diameter in inches.The results are summarized and discussed in the following sections.

(iii) Unconfined Compression Tests: In order to relate tensile strength of cemented sands with unconfined compressive strength of cemented sand with identical parameters, a total of 15 specimens were tested with the same testing parameters considered for tensile tests. The samples were prepared by the method of undercompaction described earlier and then tested without membranes in triaxial cell. The results are summarized and discussed in the next section.

2.4 ANALYSIS OF TEST RESULTS

Based on the previous studies, the behavior of cemented sand is found to be influenced by the following factors:

1. Strain level
2. Cement content, Type of cement
3. Density

4. Time
5. Effective Consolidation pressure
6. Grain Size distribution
7. Structure (soil fabric or grain arrangements)
8. Water content and Degree of Saturation
9. Method of Sample Preparation
10. Type of Test
11. Type of Sand, etc.

The aim of present study is to analyze the results of tests mentioned in the previous sections to comprehend the strength- deformation characteristics of cemented sand.

Tensile strength versus unconfined compressive strength: The results of brazilian tests and unconfined compression tests are summarized in Table 2.2. The unconfined compression test results reported by other investigators are also given in the Table 2.2.

Unlike sands, the cemented sands posses some tensile strength. Therefore to reveal the complete constitutive behavior of cemented sand, the results of tensile tests are essential in addition to compression tests. The tensile strength of cemented sand is not given much attention because of lack of practical and reliable testing technique. Clough and his colleagues (1980 and 1981) reported very few brazilian tests on cemented sand and stated that the tensile strength is about 10 to 14% of the unconfined compressive strength. They also stated that the cohesion intercept is about twice the tensile strength. In absence of sufficient experimental data, the present practice is to assume a parabolic stress-strain variation in tensile region. There is a great need of new research to establish some data base for tensile strength of cemented sands by adopting similar techniques that provided fairly good data for concrete, rocks, clay, etc. in tension.

In this study, several brazilian (or splitting tension) tests were conducted with the variables shown in Table 2.2 to provide a preliminary data base. A correlation between unconfined compression strength and tensile strength has

Table 2.2 Summary of Results from Brazilian and Unconfined Compression Tests

Cement Content %	Relative Density %	Tensile Strength kN/sqm	Unconfined Compressive Strength, kN/sqm		
			Rad & Clough 1982	Acar & Tahir 1986	Present Study
1	25	1.0	7.0	10.0	12.0
	35	---	---	15.0	---
	43	1.5	---	---	17.0
	50	---	20.0	19.0	---
	60	1.8	---	---	25.0
	80	2.2	30.0	28.0	33.0
2	25	5.3	25.0	22.0	24.0
	35	---	---	33.0	---
	43	8.8	---	---	43.0
	50	---	42.0	41.0	---
	80	11.0	55.0	54.0	58.0
4	25	---	---	48.0	---
	35	---	---	51.0	---
	50	---	---	59.0	---
	60	---	203.0	63.0	---
	75	---	275.0	69.0	---
	80	---	---	71.0	---
	90	---	350.0	77.0	---
5	25	24.4	---	---	181.0
	43	31.0	---	---	218.0
	60	39.0	---	---	247.0
	80	45.0	---	---	282.0
8	25	67.0	---	---	476.0
	43	72.0	---	---	495.0
	60	84.0	---	---	527.0
	80	90.0	---	---	564.0

been investigated in this study. Furthermore the tensile strength obtained from these tests will be used in Lade's model (i.e. to find the parameter 'a'). The various parameters obtained from this investigation are being used to verify existing constitutive models for cemented sands. More details will be provided by the authors elsewhere (Saxena and Reddy, 1987).

A statistical analysis on the available experimental data with cemented sand (Table 2.2) provided the following correlations between unconfined compressive strength q_u and shear strength parameter c'.

For low cementation

$$q_u = 2.1c' \tag{2.4}$$

For high cementation

$$q_u = 1.4c' \tag{2.5}$$

It may be noted that the Eqn. 2.4 was also suggested by Acar and Tahir (1986), however they use this equation to predict strength for all degrees of cementation. The experimental results obtained during this study clearly indicated that at high cementation levels Eqn. 2.4 overpredicts q_u and Eqn. 2.5 provides better results.

Similar investigation with brazilian test results and unconfined compression test results resulted the following correlation.

$$\sigma_t = -0.15q_u \tag{2.6}$$

This relation has been found valid at all cementation levels and leads to the discussion about the applicability of Griffith's theory of failure (1920) for cemented sand.

According to Griffith's theory, if $\sigma_1 > \sigma_3$ and $\sigma_1 + \sigma_3 < 0$, the failure envelope is expressed as below:

$$(\sigma_1 - \sigma_3)^2 = -8\sigma_t(\sigma_1 + \sigma_3) \tag{2.7}$$

For uniaxial compression condition ($\sigma_3 = 0, \sigma_1 = q_u$) we get

$$q_u = -8\sigma_t \tag{2.8}$$

However from Eqn. 2.6, one obtains

$$q_u = -6.7\sigma_t \tag{2.9}$$

Maclintock and Walsh (1962) and Brace (1963) suggested modifications to Griffith's theory and derived the following expression:

$$\frac{q_u}{\sigma_t} = \frac{4}{(1+\mu^2)^{1/2} - \mu} \tag{2.10}$$

in which μ = coefficient of friction for crack surface. Considering an average angle of internal friction value of 37 degrees for cemented sands (Table 2.3), and assuming $\mu = tan\phi$, the above expression reduces to Eq.2.8. The comparison of Eqns. 2.8 and 2.9 however, suggest a need for further investigations regarding the determination of coefficient of friction for crack surface (μ) and also the validity of parabolic strength envelope of Griffith's theory in the tensile stress region.

Shear Strength: Angle of internal friction and cohesion are the two important shear strength parameters of soils. But in general static loads on soils are carried by the five components of their shear resistance, namely cohesion, basic mineral friction, dilatancy, particle crushing and particle rearrangement. However, basic mineral friction, dilatancy, particle crushing and particle rearrangement, are usually considered to constitute the frictional resistance of soils.

The gross shearing resistance of soils is increased greatly when they are mixed with small amounts of cementing agents such as Portland cement, lime, etc., as it was shown by Wissa and Ladd (1965). Avramidis and Saxena (1985), based on the previously mentioned static triaxial tests results, explained and reconfirmed the conclusions of study by Wissa and Ladd (1965). Following are the brief conclusions reported in Avramidis and Saxena (1985) which formed the strong background for the present investigation:

1. The stress-strain response was greatly influenced by effective confining pressure ($\overline{\sigma}_c$) and cement content (CC) and to a smaller degree by curing period (CP) and relative density (D_r). Even a loose specimen stabilized with a small amount of cement could exhibit brittle behavior (Fig. 2.3).

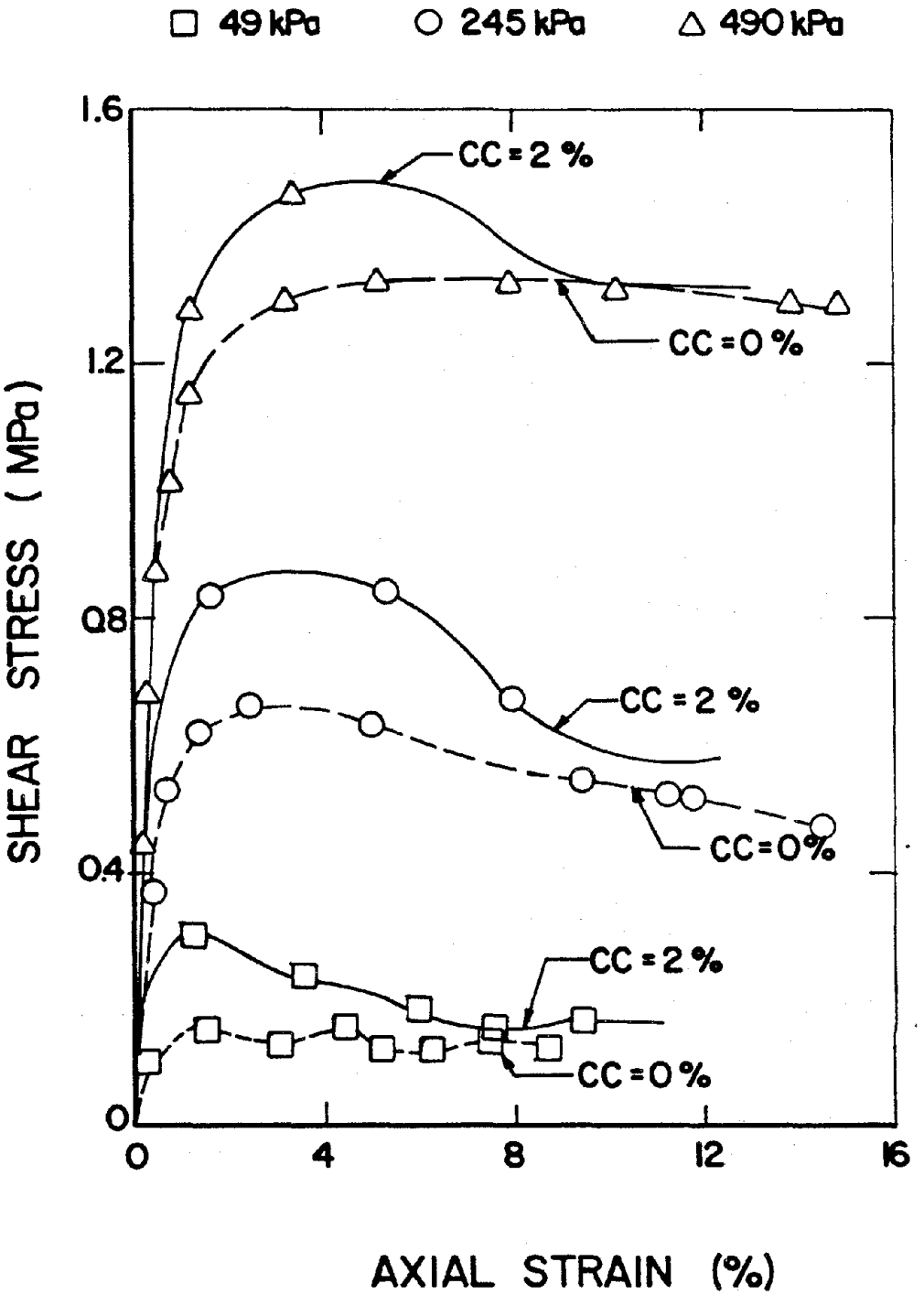

Fig.2.3(a) Stress-strain response of uncemented and cemented sands for D_r=43%

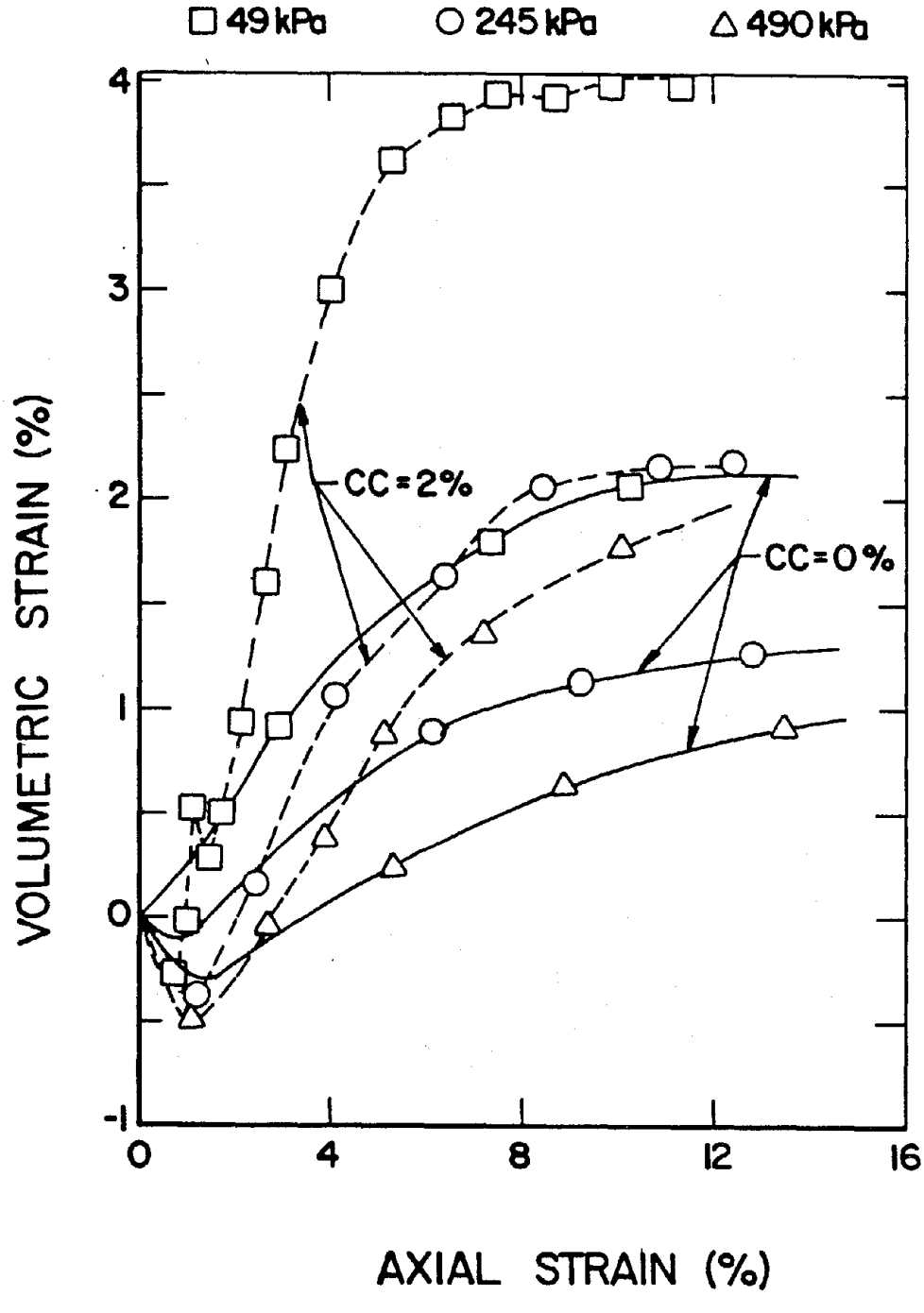

Fig.2.3(b) Volumetric strain versus Axial strain curves of uncemented and cemented sands for D_r=43%

2. In order to quantify the brittleness of cemented sands, the brittleness coefficient (B_c) was introduced. B_c was defined as the ratio of peak shear strength (S_{peak}) over its residual shear strength (S_{resid}). Brittle behavior was demonstrated more at low $\overline{\sigma}_c$ and large CC conditions (Fig. 2.4).

3. The residual strength of the uncemented sands was slightly lower than the corresponding one for the cemented sands at the same D_r and $\overline{\sigma}_c$ values.

4. An increase in the angle of internal friction and the cohesion intercept with increase in cement content was observed consistently (Fig. 2.5). Strength ratio, defined as the ratio of cemented peak strength to uncemented peak strength, decreases as $\overline{\sigma}_c$ increases and CC decreases (Fig. 2.6).

5. For the uncemented sand Mohr envelope at peak strength represents a condition where the maximum rate of volumetric expansion occurs. Whereas for the cemented sand it represents a condition where the summation of all strength components become maximum.

6. All the values of internal friction and cohesion for peak and residual stages for the range of variables considered are given in Table 2.3.

Though the above conclusions created the static quantitative behavioral basis, further study to investigate the strength generation (i.e. the variation of c and ϕ as strain increases), the initial Young's modulus and the stress-strain characteristics has been felt.

Strength Generation: The shearing resistance of uncemented sand has been very well understood because of significant research efforts by Hvorslev, Rowe, Ladanyi, Koerner and others. The mineral soils were noted to be nonplastic in the grain sizes tested and therefore the effective cohesion was considered as zero. Therefore the entire attention has to be focused on the effective angle of shearing resistance parameter ϕ . It has also been suggested by many investigators that the ϕ found from drained tests could be expressed by the following:

$$\phi = \phi_{mf} + \phi_{pc} + \phi_{pr} + \phi_d \tag{2.11}$$

where ϕ_{mf} = angle of basic mineral friction, ϕ_{pc} = angle of degradation or

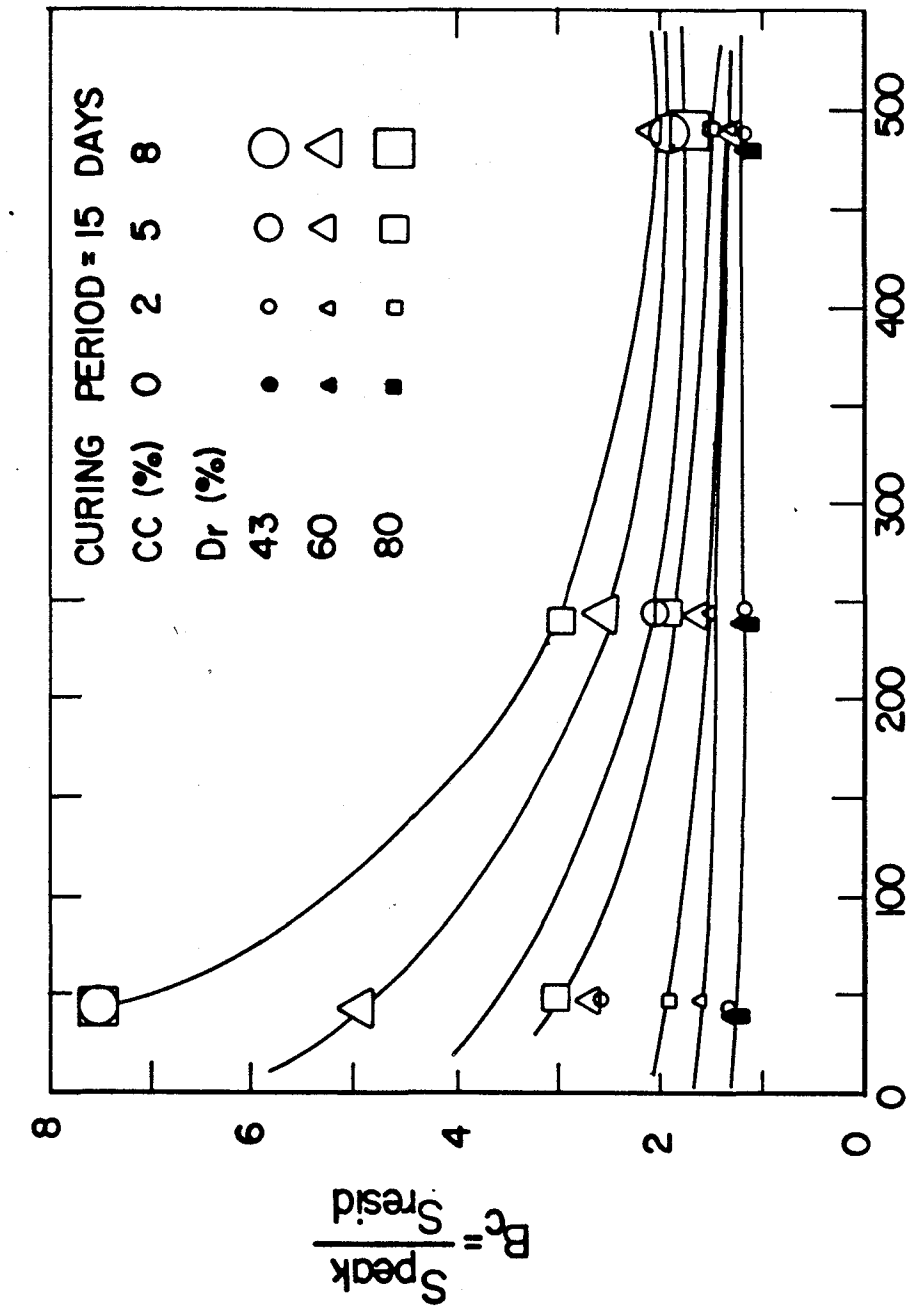

Fig.2.4 Coefficient of Brittleness versus $\bar{\sigma}_c$ at Various D_r and CC values

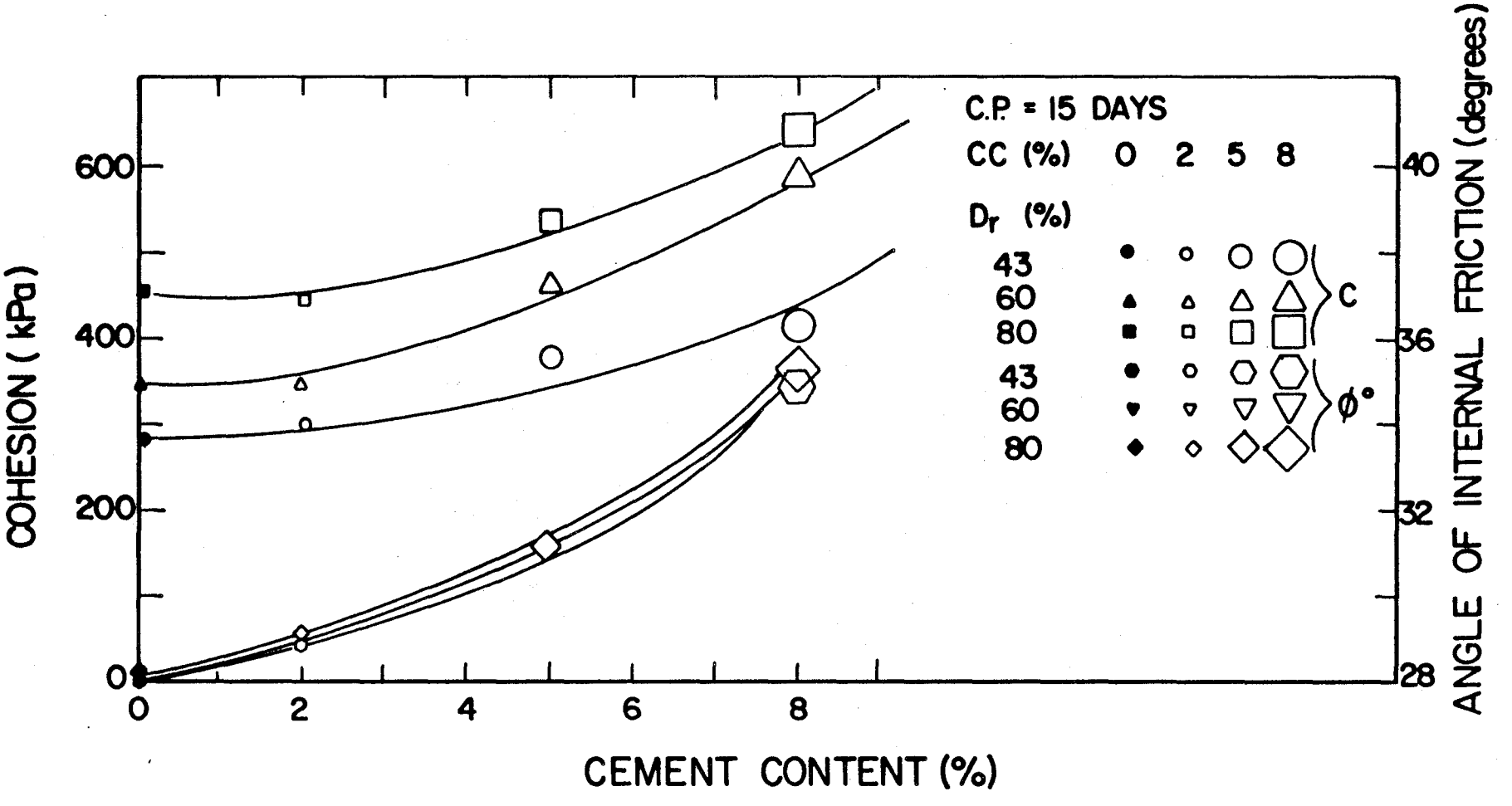

Fig.2.5 Cohesion and Angle of internal friction at peak strength versus cement content after 15 days of curing

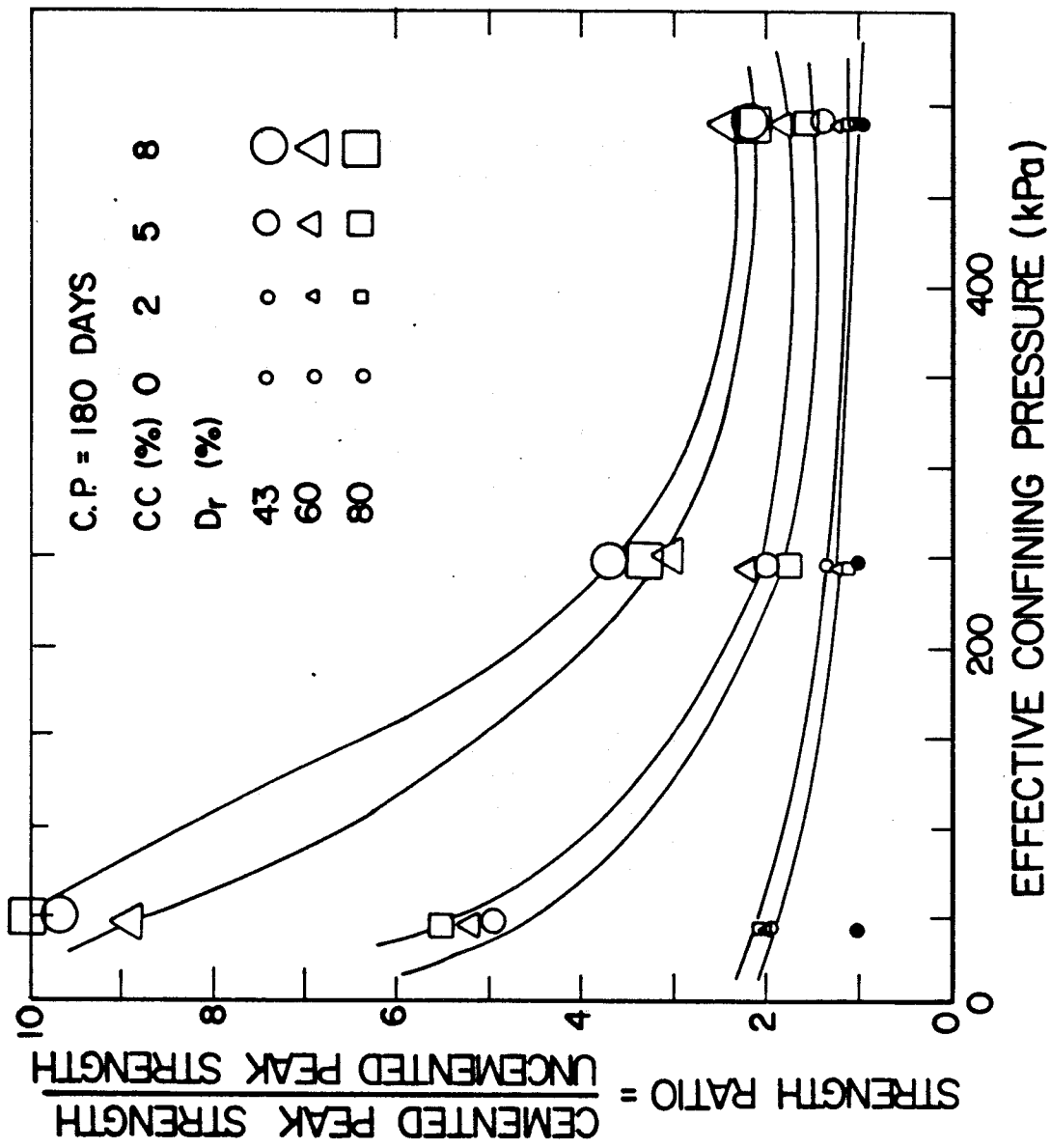

Fig.2.6 Strength Ratio versus Effective Confining Pressure

Table 2.3(a) Values of Internal Friction and Cohesion for Cemented Sands

CC %	Dr %		CP 15 days peak	CP 15 days resid.	CP 30 days peak	CP 30 days resid.	CP 60 days peak	CP 60 days resid.	CP 180 days peak	CP 180 days resid.
2	43	ϕ*	34.1	31.8	33.0	31.4	33.1	32.8	34.3	33.8
		c**	43.0	22.0	53.0	15.0	55.0	13.0	51.0	6.0
2	60	ϕ	34.9	33.7	33.2	32.0	35.2	34.3	35.6	34.4
		c	49.0	0.0	66.0	16.0	71.0	9.0	60.0	19.0
2	80	ϕ	36.9	32.9	36.3	32.0	35.3	34.4	37.4	34.9
		c	50.0	8.0	53.0	11.0	58.0	4.0	64.0	5.0
5	43	ϕ	35.6	35.3	35.4	34.9	35.9	32.9	36.1	35.2
		c	146.6	21.0	150.0	17.0	157.0	15.0	159.0	13.0
5	60	ϕ	37.3	36.9	36.9	36.9	37.8	35.2	36.9	36.3
		c	153.0	19.0	177.0	22.0	190.0	20.0	210.0	14.0
5	80	ϕ	38.7	34.6	39.2	36.9	38.5	37.8	38.0	38.0
		c	150.0	6.0	221.0	0.0	230.0	0.0	223.0	3.0
8	43	ϕ	36.3	36.3	36.9	35.8	37.8	37.1	37.8	37.8
		c	347.0	20.0	360.0	20.0	368.0	0.0	372.0	11.0
8	60	ϕ	39.8	39.6	40.3	39.9	39.8	39.8	39.4	36.6
		c	358.0	0.0	367.0	0.0	369.0	18.0	371.0	20.0
8	80	ϕ	40.9	40.9	42.0	40.5	42.4	38.0	43.4	39.8
		c	366.0	0.0	417.0	0.0	383.0	15.0	420.0	0.0

* Effective Angle of Internal Friction in Degrees
** Effective Cohesion in Kpa

Table 2.3(b) Values of ϕ and c for Uncemented Sand

Dr %	Peak $\bar{\phi}$	Peak $\bar{c}$	Residual $\bar{\phi}$	Residual $\bar{c}$
43	33.7	0.0	32.9	0.0
60	35.3	4.0	33.6	4.0
80	37.1	6.0	34.9	0.0

particle crushing, ϕ_{pr} = angle of reorientation or particle rearrangement, and ϕ_d = angle of dilatancy.

The above expression can be rewritten as

$$\phi = \phi_f + \phi_d \tag{2.12}$$

where ϕ_f is angle of interparticle friction or angle of internal friction and also can be termed as effective angle of shearing resistance. Therefore in order to find effective angle of shearing resistance ϕ_f , the ϕ_d has to be separated from measured angle of friction ϕ .

Uncemented Monterey No. 0 sand used in this investigation exhibited curved effective stress envelope in drained tests under dense conditions as shown in Fig 2.7. The slope of the envelope decreases with increasing consolidation pressure. Due to curvature, the Mohr envelope shows an increase in 'apparent' cohesion intercept with increasing consolidation pressure. However at high consolidation pressure, the curvature of the drained Mohr envelope and the apparent cohesion disappeared. Rowe stress-dilatancy equation as given below can be used to modify the stress difference (deviator stress) to account the influence of volume changes on the work done during shear.

$$(\sigma_1 - \sigma_3)_{modi} = \frac{\overline{\sigma}_1}{(1 + \frac{d\epsilon_v}{d\epsilon})} - \overline{\sigma}_3 \tag{2.13}$$

For sands the Mohr envelope using the modified stress difference results in a straight line.

In case of loose sand, the effective stress envelope in drained tests was straight line as shown in Fig. 2.8. Therefore the cohesion is always zero and no need of Rowe stress-dilatancy correction arises.

Axial strain contours have been drawn on the drained $\overline{p}$ versus q plot as shown in Fig. 2.7 and Fig. 2.8. It may be noticed that these results are similar to those reported by Wissa and Ladd (1965). The slopes initially increased with increasing axial strain in loose conditions mainly because the mineral to mineral friction between grains until failure. Whereas in case of dense sands when the volume of the samples reached a minimum, on further straining the

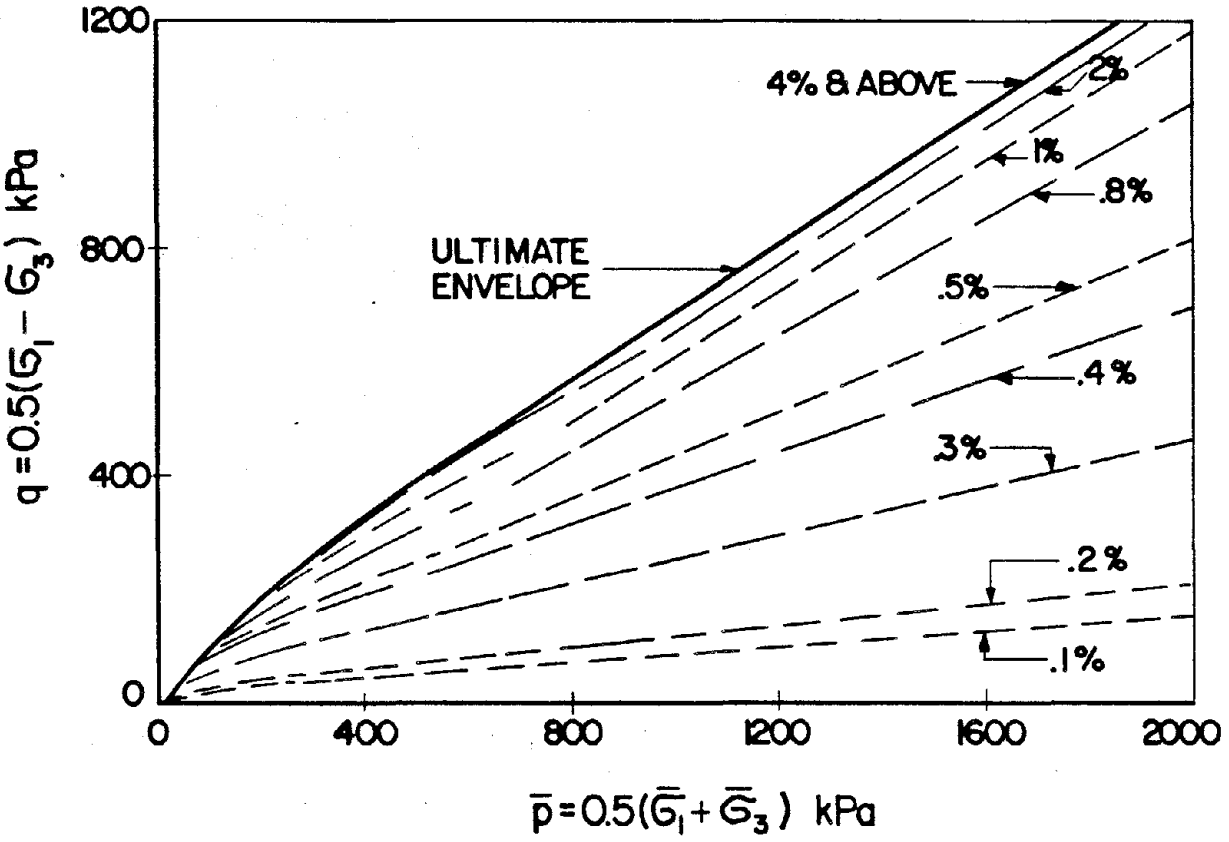

Fig.2.7 Strength envelope and Strain contours for dense uncemented Monterey sand (D_r=80%)

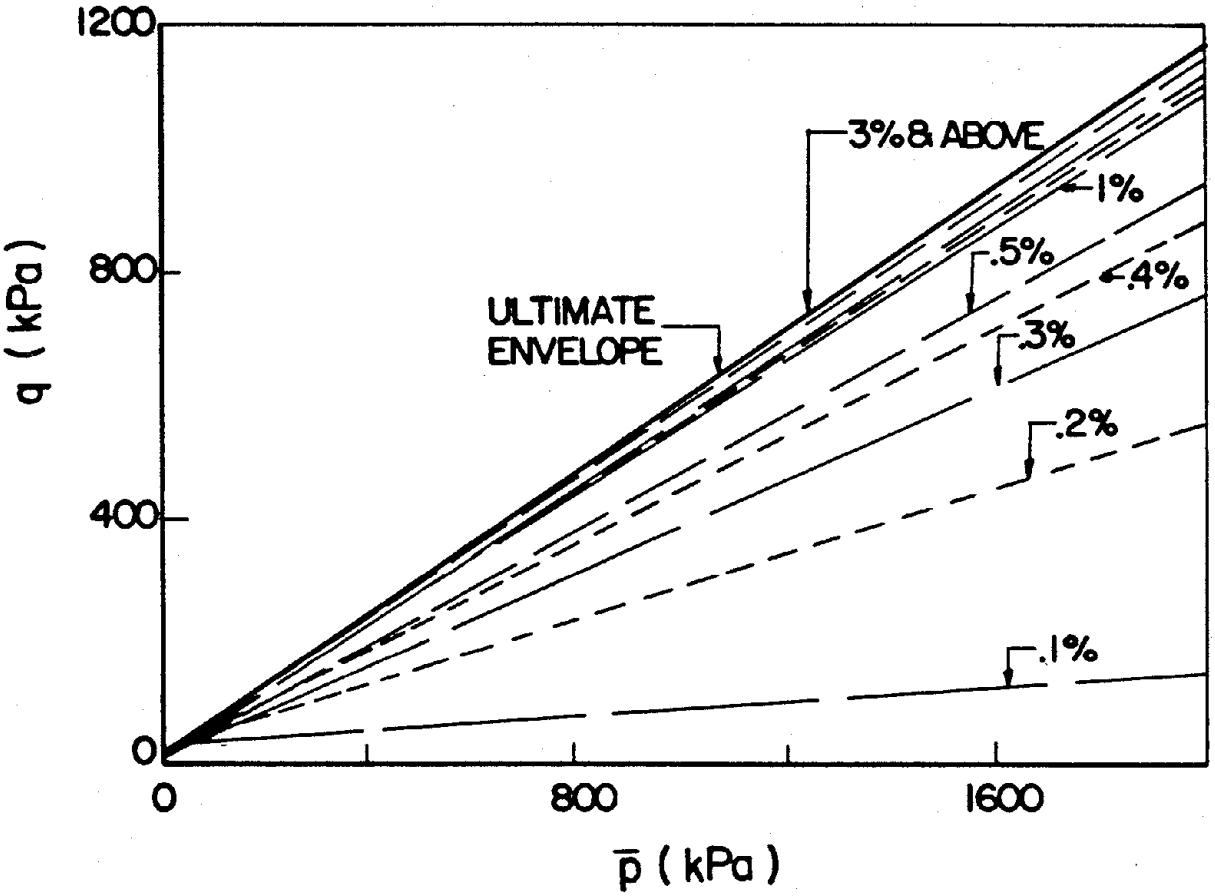

Fig.2.8 Strength envelope and Strain contours for loose uncemented Monterey sand (D_r=43%)

samples started to dialate at a gradually increasing rate, causing an increase in the slopes of the strain contours until maximum rate of dilatancy occurs. On further straining, the rate of dilatancy decreases and therefore, the slopes decreased until ultimate conditions were reached.

Figures 2.9 & 2.10 show the variation of gross cohesion (c) and gross angle of internal friction (ϕ) with axial strain. The reported values of the strength parameters (c and ϕ) are deduced indirectly from q -$\overline{p}$ envelopes, using the following well known formulas:

$$\phi = sin^{-1}(tan\alpha) \tag{2.14}$$

$$c = \frac{a}{cos\phi} \tag{2.15}$$

where α is the inclination of the q - $\overline{p}$ envelope and a is the q intercept of the q - $\overline{p}$ envelope. It can be concluded that at relatively small strain, the mobilization of friction occurs and remains same on further straining.

Only few investigators studied the effect of artificial cementation of sand (Wissa and Ladd, 1965; Dupas and Pecker, 1979, etc.) In all the studies, Mohr Coulomb strength criterion was used. The strength was represented by two components namely cohesion and friction. Avramidis and Saxena (1985) demonstrated that the shear strength of artificially cemented sands is influenced by cement content and curing period because the cement tends to bond the sand grains together. Besides all these, the present investigation revealed that the shear strength of cemented sand is strongly dependent on strain level. This strain dependent behavior was not adequately studied quantitatively by previous researchers.

The use of strain contours to separate the frictional and cohesive resistance is open to question when it is applied to fine-grained soils since large decrease in void ratio occur with increasing consolidation pressure, and/or applied load during shear of the sample, therefore, the fabric changes with these loads. As the void ratio decreases, the number of mineral to mineral contacts increase which will increase the frictional resistance during shear.

The strain contours of cemented sand with different ratios for a specific Dr = 43% are shown in Figs. 2.11 through 2.13. The rates at which the cohesive

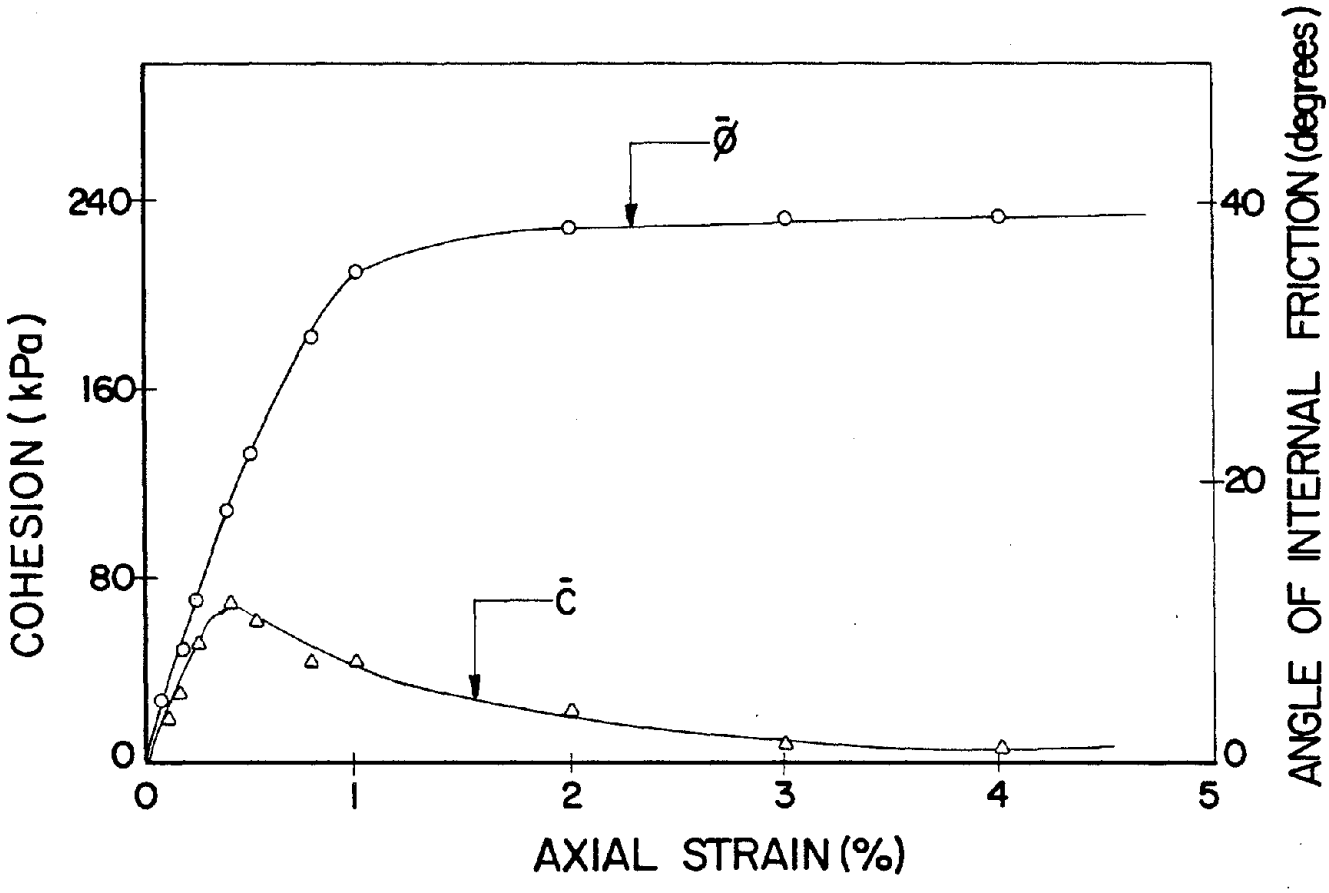

Fig.2.9 Variation of c and ϕ with axial strain for dense uncemented Monterey sand (D_r=80%)

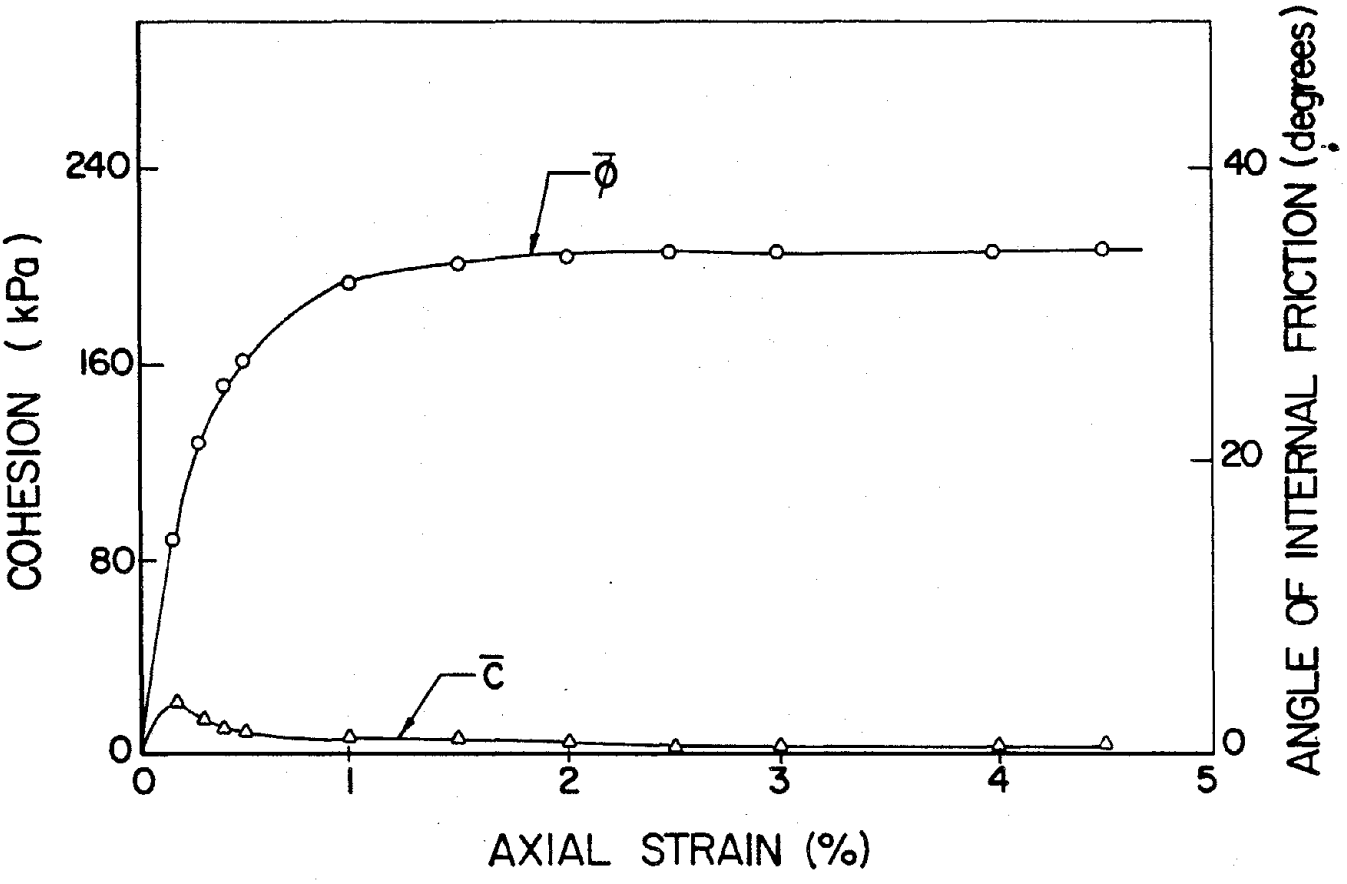

Fig.2.10 Variation of c and ϕ with axial strain for loose uncemented Monterey sand (D_r=43%)

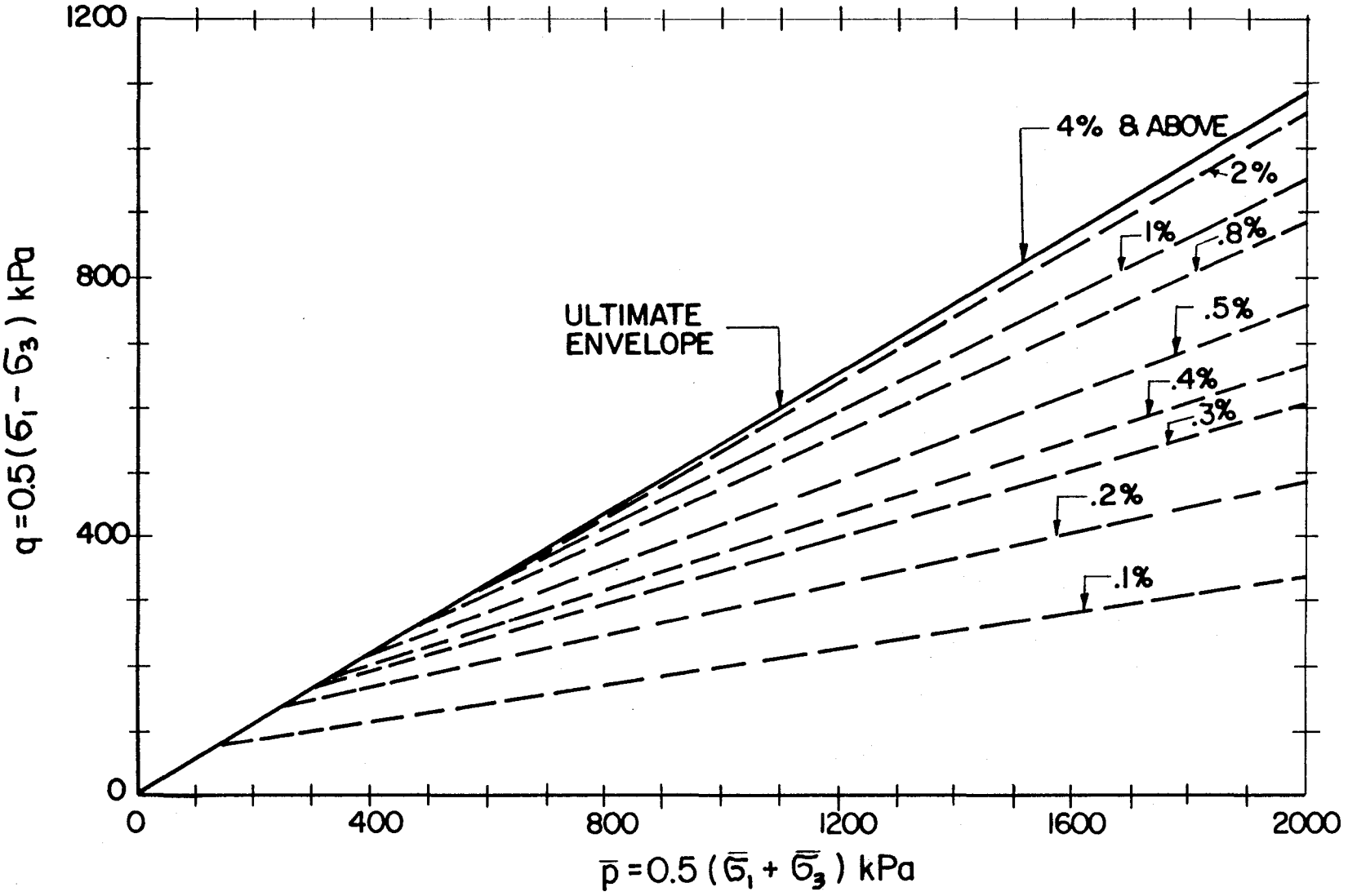

Fig.2.11 Strength envelope and Strain contours for cemented Monterey sand with D_r=43% and CC=2%

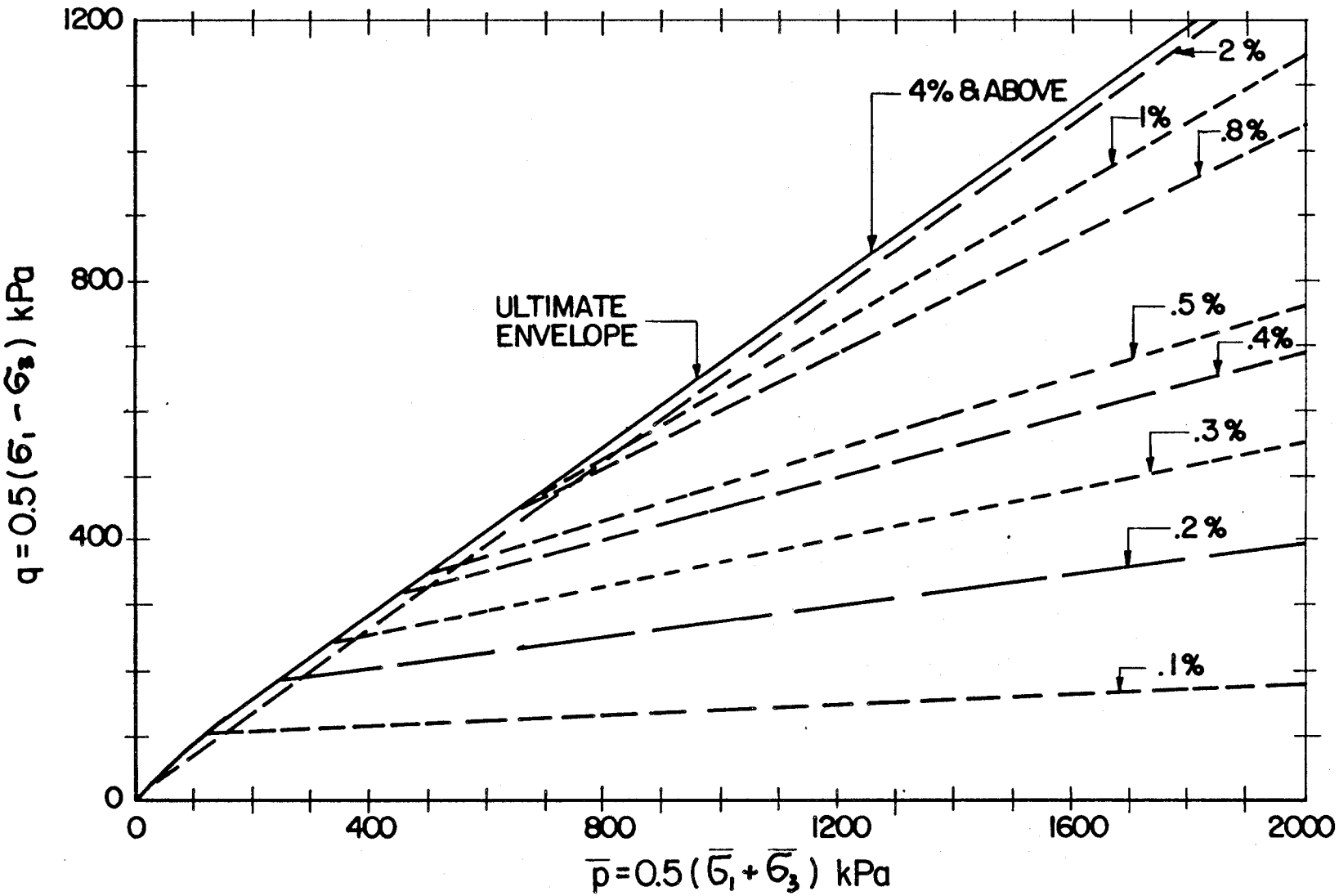

Fig.2.12 Strength envelope and Strain contours for cemented Monterey sand with D_r=43% and CC=5%

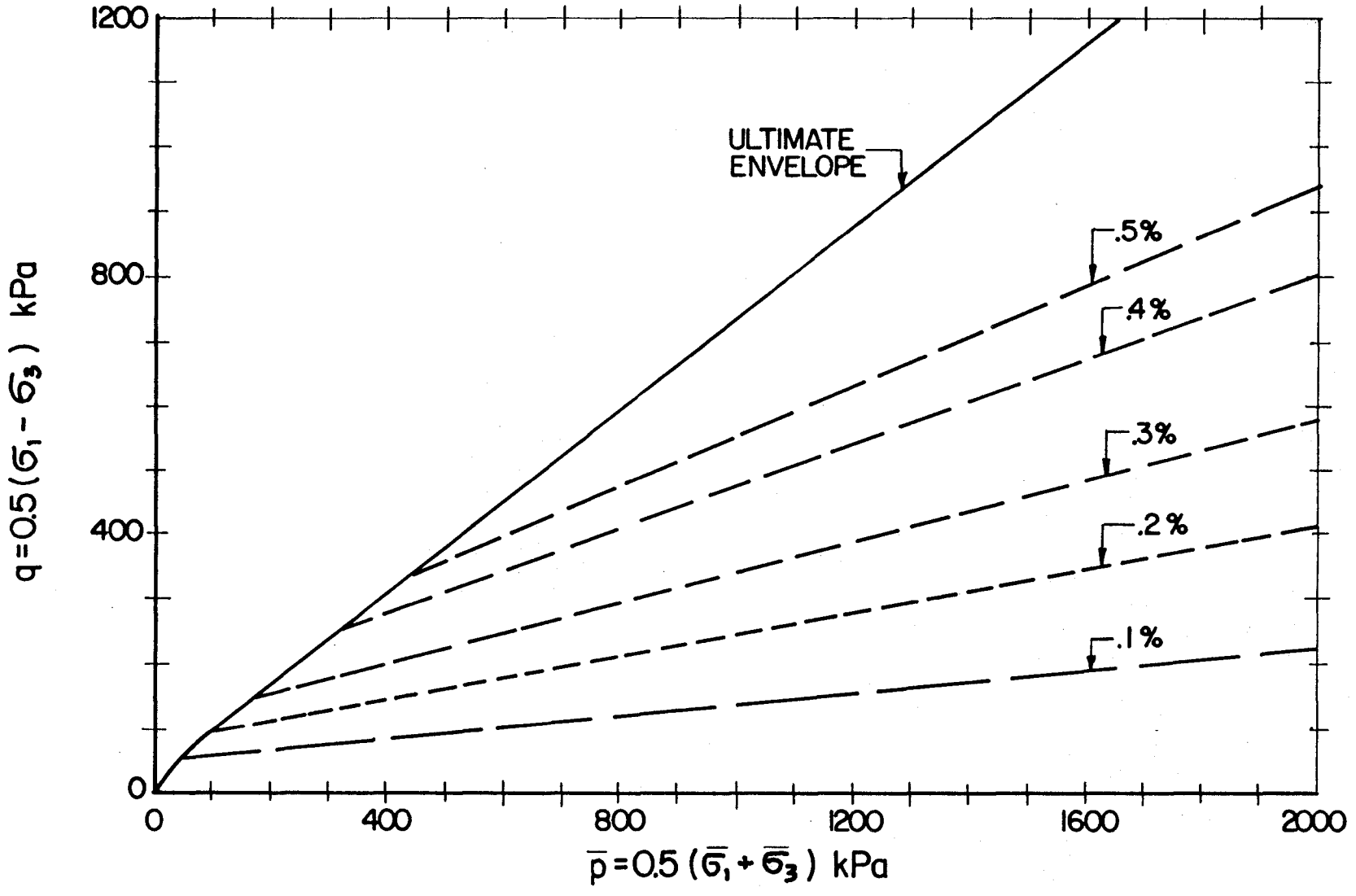

Fig.2.13 Strength envelope and Strain contours for cemented Monterey sand with D_r=43% and CC=8%

and frictional resistance change with increasing axial strain as obtained from intercept and slope of strain contours (Eqn. 2.14 and Eqn. 2.15), are shown in Fig. 2.14 through 2.16.

From these results, it may be concluded that at small axial strains, most of the shear strength is contributed from cohesion and with increasing axial strain, frictional resistance increases. After the cohesive resistance approaches its maximum value around 0.25 - 0.85% strain, the contribution of cohesion drops fast and the mobilization of frictional resistance increases relatively quickly. The frictional resistance becomes maximum as the stress path touches the Mohr-Coulomb envelope.

Deformation Modulus: The stress-strain response of cemented sands is predominantly elastic during the initial stages of loading. Sitar and Clough (1983) assumed stress-strain variation of cemented soil linear upto peak strength in a finite element analysis to study the behavior of cemented soil slopes. The post failure constitutive behavior was not considered in their study perhaps because the post failure deformations of the sliding mass are irrelevant as it collapses and disintegrates. However, they recognized that after the peak, the brittle nature of the failure and subsequent softening, make it extremely difficult to duplicate the exact behavior by simple models. Yielding, therefore, occurs just before the peak and well before the peak in cases of strongly and weakly cemented sands respectively. Therefore, it should be understood that the consideration of elastic response upto peak stress state is a crude approximation for weakly cemented sands and may be a reasonable approximation for strongly cemented sands. Finally, the success of elastic model for cemented sand for prefailure conditions greatly depends on the method of selecting elastic modulus. Even the advanced constitutive models require initial or elastic modulus as input. In this study, the results of triaxial (drained) tests are used to investigate the affecting factors and the selection methods of elastic modulus for cemented sands.

Elastic modulus or deformation modulus is considered equal to initial tangent modulus from stress-strain curves of drained triaxial tests. The parameters that effect the modulus are confining pressure, cement content, curing

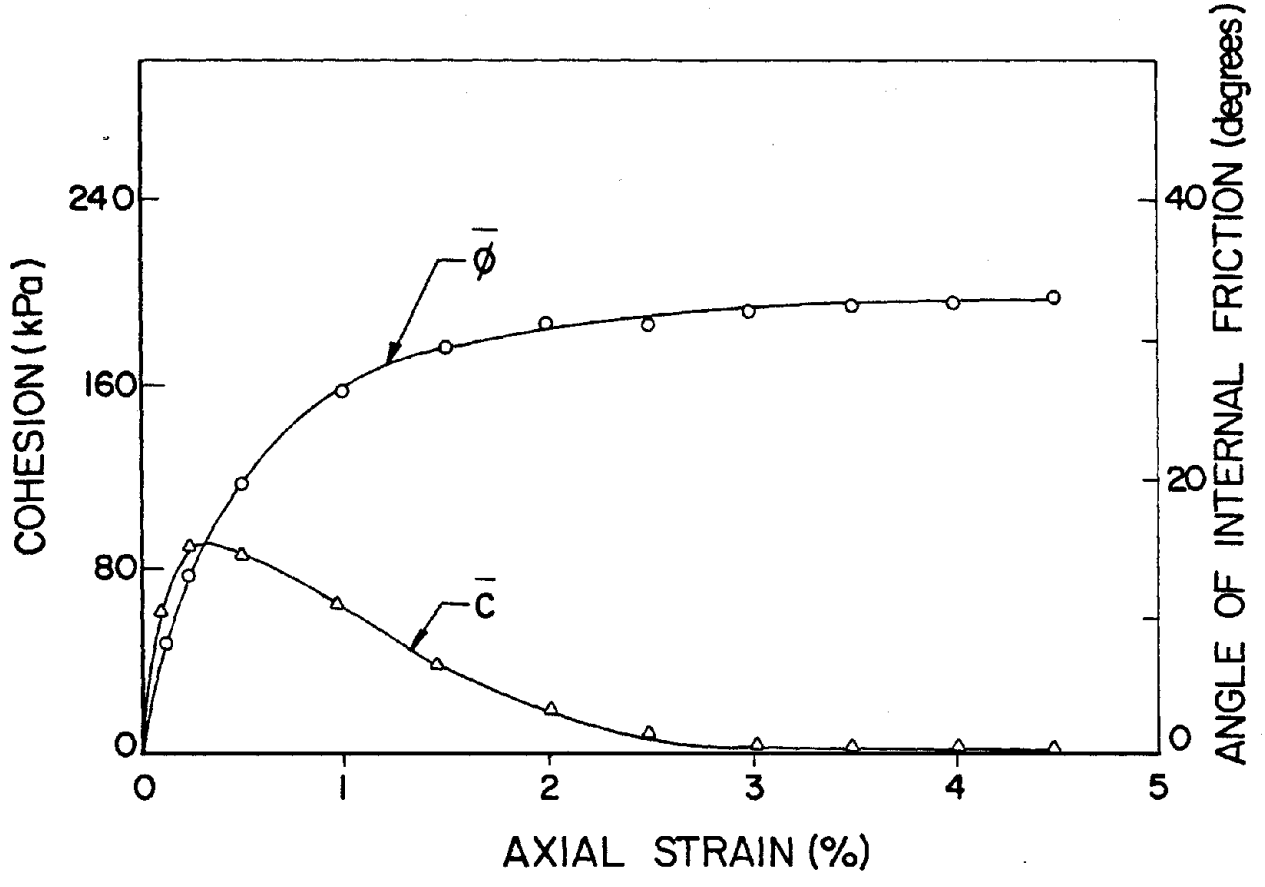

Fig.2.14 Variation of c and ϕ with axial strain for cemented Monterey sand with D_r=43% and CC=2%

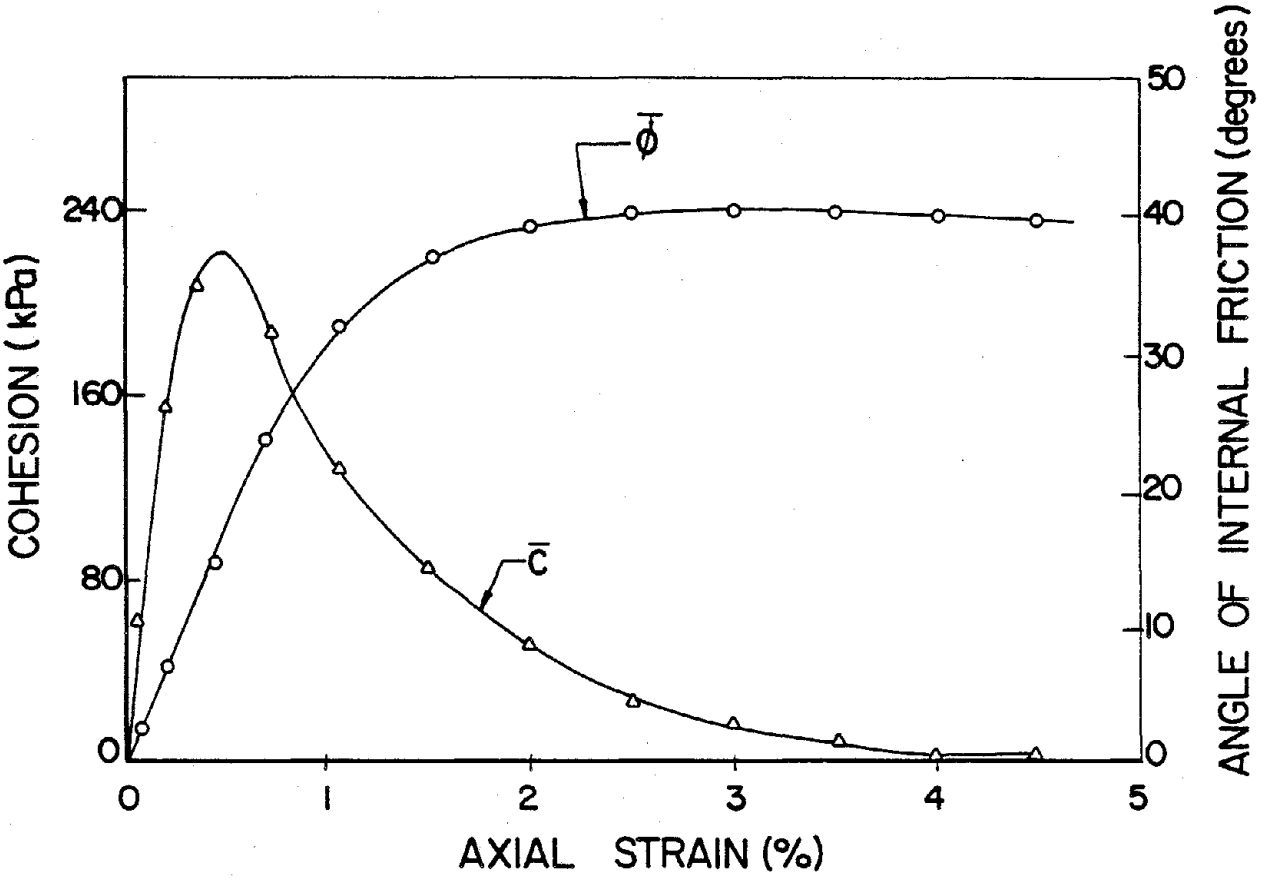

Fig.2.15 Variation of c and ϕ with axial strain for cemented Monterey sand with D_r=43% and CC=5%

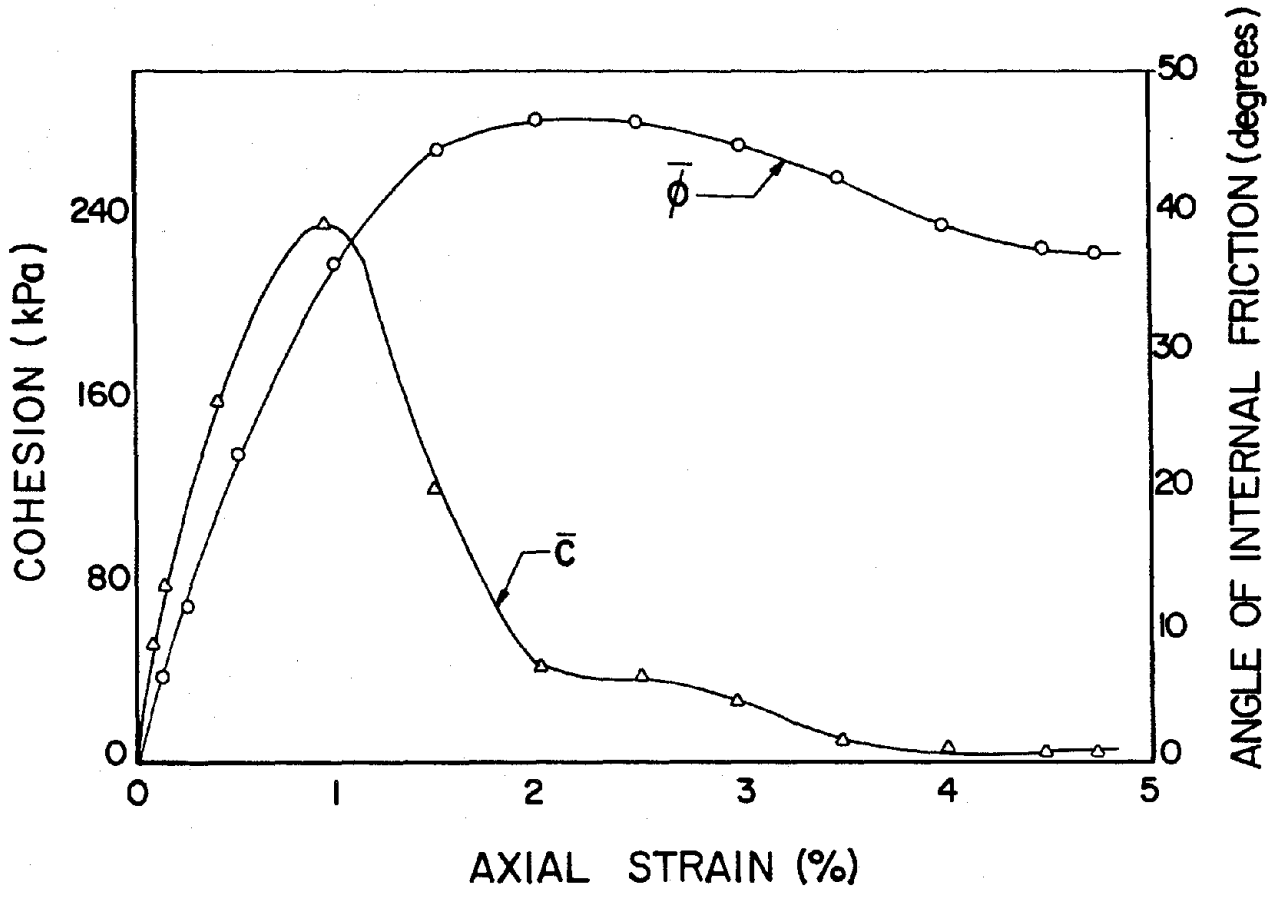

Fig.2.16 Variation of c and ϕ with axial strain for cemented Monterey sand with D_r=43% and CC=8%

period and density. All these variables tend to increase the initial tangent modulus values, however, the effects of cement content and confining pressure are significant.

All the previous investigators found that $(\overline{\sigma}_3/P_a)$ versus (E_i/P_a) represents "reasonably" a straight line on the log-log scale for cemented sands. Such an idea is adopted based on Janbu (1963) and Wong and Duncan (1974), who first found such relationship for uncemented sands and the equation of this straight line was given as below:

$$E_i = kP_a(\frac{\overline{\sigma}_3}{P_a})^n \tag{2.16}$$

where $\overline{\sigma}_3$ = effective confining pressure, E_i = initial tangent modulus and P_a = atmospheric pressure.$\overline{\sigma}_3$, E_i and P_a are expressed in same units. k and n are parameters which depend on soil condition and are determined from tests (k is the intercept at $(\overline{\sigma}_3/P_a) = 1$ and n is the slope of the line). In case of sands, k is directly related to stiffness and n exhibits the effect of confining pressure and relates the frictional component of strength.

Obviously for cemented sand, the initial tangent modulus not only depends on $\overline{\sigma}_3$ but also on density, cement content, curing time, etc. In order to account the effect of cement content drained shear strength parameters c' and ϕ were included in the above equation and the modified equation was given by Dupas and Pecker as below:

$$E_i = kP_a\left(\frac{\overline{\sigma}_3 + ctan^{-1}\phi}{P_a}\right)^n \tag{2.17}$$

Dupas and Pecker (1979) observed that the influence of density, cement content and curing time are indirectly accounted by the term $ctan^{-1}\phi$. It is concluded that k values decrease and the n values increase as the cement content increases. On the other hand, researchers at Stanford University (Sitar et al 1980, Bachus et al 1981, etc.) adopted equation 2.16 because, in their view, it is most conveniently used by geotechnical engineers. They found that k values increase and the n values decrease as the cement content increases. This variation of k and n in equation 2.16 is just contrary to the observation of Dupas

and Pecker (1979). The results of present study are therefore useful to evaluate these conflicting conclusions. Undoubtedly, all straight line relationships are liked by practicing engineers, however accuracy should not be sacrificed for simplicity when using such relations.

The values of initial tangent modulus are obtained for different effective confining pressures based on stress-strain data from triaxial (drained) tests with wide range of variables such as density, cement content, curing time, etc. A set of k and n values are obtained by plotting $(\overline{\sigma}_3/P_a)$ versus (E_i/P_a) on log-log scale. Also a set of k and n values are obtained by plotting $(\overline{\sigma}_3 + ctan^{-1}\phi)/P_a$ versus E_i/P_a . All the values of k and n are summarized in Table 2.4 for different values of the variables considered in the experimental investigations at I.I.T.

The present investigation revealed that the following expression for E_i (obtained by translation of axes) also gives the same results as obtained from Eqn. 2.17;

$$E_i = kP_a\left(\frac{\overline{\sigma}_3 + ccot\phi}{P_a}\right)^n \tag{2.18}$$

Inspite of inclusion of c and ϕ in the expression for E_i (Eqns. 2.17 and 2.18), the values of k and n still remained dependent on the cementation level.

An alternate expression for initial Youngs modulus for cemented sand (E_i^*) can be expressed in terms of initial Youngs modulus of uncemented sand (E_i) as below;

$$E_i^* = RE_i \tag{2.19}$$

where R can be called modulus ratio. The value of R, in general depends on cement content, density, curing period and effective confining pressure. A statistical analysis with the experimentally determined modulus values provided the following relationship for R;

$$logR = log(1 + C - eC) + (0.71 - 1.3e)(C)^{(2.2-2.4e)}log(\frac{\overline{\sigma}_3}{P_a}) \tag{2.20}$$

where C is the cement content (CC) expressed in percentage and e is the void ratio. The effect of curing period is to increase the modulus. However after initial few days of curing the increase in modulus is not very significant therefore

Table 2.4 Values of Elastic Modulus Paramaters

Cement Content %	Relative Density %	Elastic Modulus Parameters			
		Eqn 2.16 (text)		Eqn 2.17 or Eqn 2.18 (text)	
		k	n	k	n
0	43	675.0	0.88	675.0	0.88
	60	749.0	0.85	713.2	0.875
	80	877.0	0.81	820.2	0.845
2	43	1082.8	0.57	660.57	0.815
	60	1252.0	0.61	683.34	0.900
	80	1598.5	0.67	923.02	0.940
5	43	1613.2	0.42	555.31	0.90
	60	2003.0	0.47	525.76	1.06
	80	2781.6	0.52	584.68	1.20
8	43	2170.7	0.27	396.87	0.95
	60	2549.2	0.31	436.51	1.02
	80	3684.5	0.38	449.61	1.23

it has not been incorporated in the above expression for R. The modulus ratio (R) can also be related to unconfined compressive strength (q_u) as follows;

$$R = a(\frac{\overline{\sigma}_3}{P_a})^b \tag{2.21}$$

$$a = 2(\frac{q_u}{P_a})^{0.29} \tag{2.22}$$

$$b = (\frac{q_u}{P_a}) - 0.40...for \frac{q_u}{P_a} < 0.25 \tag{2.23a}$$

$$b = 0.7(\frac{q_u}{P_a}) - 0.57...for \frac{q_u}{P_a} < 0.50 \tag{2.23b}$$

$$b = 0.2(\frac{q_u}{P_a}) - 0.86...for \frac{q_u}{P_a} < 3.00 \tag{2.23c}$$

$$b = 0.22(\frac{q_u}{P_a}) - 1.70...for \frac{q_u}{P_a} < 6.00 \tag{2.23d}$$

In summary, the elastic modulus for artificially cemented sands can be found using any of above mentioned relationships. If unconfined compressive strength is known, the modulus can be easily computed from Eqn. 2.19 by knowing modulus ratio from Eqns. 2.21, 2.22 and 2.23.

Stress-Strain Characteristics or Constitutive Behavior: Unlike metals, the stress-strain response of soils is complicated. The artificially cemented sands tend to possess dilatant brittle nature. Based on the results of drained triaxial test results of Avramidis and Saxena (1985), the present study is devoted to describe the constitutive behavior of cemented sands.

The typical stress-strain variation of strongly cemented sands is depicted qualitatively in Fig 2.17. During the initial stages of loading (OA), a linear elastic response (almost upto the peak) can be observed because of cementation which prevents intergranular movement. The initiation of cement bond breaking starts just before peak (A), afterwhich the gradual nonlinear softening occurs due to progressive breaking of cement bonds (A to B). The gradual softening behavior is mainly because of high confining pressure which offers resistance to dilation. When complete breakdown of cementation occurs (B), a rapid nonlinear softening is exhibited (BC). After the residual state (C), the strength remains constant and is mainly due to frictional resistance of sand.

As can be seen from the same figure, at low confining pressures because of insufficient resistance for dilation, the gradual softening (AB) does not occur.

The behavior of weakly cemented sands is different from that of strongly cemented sands (Fig. 2.18). The elastic range (OA) is very small and the yielding of cement bonds start well before the peak. The complete breakdown of cementation occurs almost near the peak. Further straining causes gradual and sudden nonlinear softening under high and low confining pressures respectively. Finally residual strength is attained. It may be pointed out that the behavior of weakly cemented sands is almost similar to that of uncemented dense sand.

The results also indicate decrease in volume during the initial stages of loading afterwhich continuous increase in volume occurs. It has been concluded by previous investigators that the peak strength represents the maximum rate of volumetric expansion in cases of uncemented sands, whereas, in case of cemented sands it represents the culmination of the contribution of cementation and dilation followed later by the residual strength. The peak and residual strengths indicate the degree of brittleness of soil. Brittleness coefficient (B_c) may be used to quantify the brittleness. The brittleness of cemented sands is found more at low confining pressures and at high cement contents.

In order to quantify the above described stress-strain behavior, the four popular types of constitutive models namely 1) Hyperbolic model (Duncan and Chang model), 2) Elasto-plastic model (Lade's model), 3) cap models and 4) Endochronic model are under investigation by the authors for applicability and duplicating the behavior of cemented sands.

2.5 SUMMARY

The extensive experimental program undertaken in this study increased the data base for cemented sand under static conditions. The different types of tests such as triaxial tests, unconfined compression tests etc. were conducted on the specimens prepared identically with one-to-one correspondence between the involved variables. Therefore the relationships developed among q_u, c' and σ_t are free from sample preparation effects. The static triaxial test results helped to quantify the beneficial effects of artificial cementation of sand. The

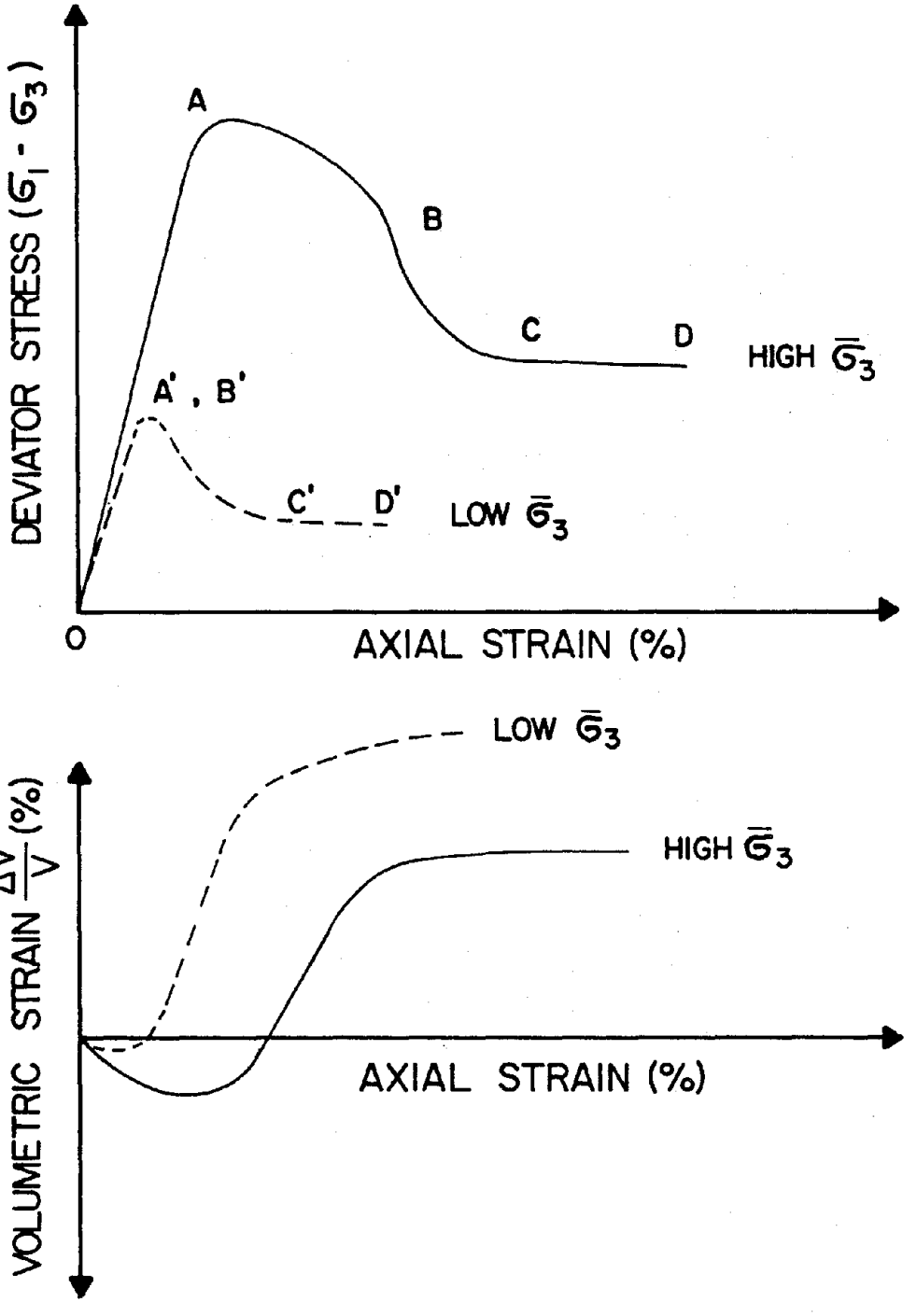

Fig.2.17 Stress-strain response of Strongly Cemented Sands

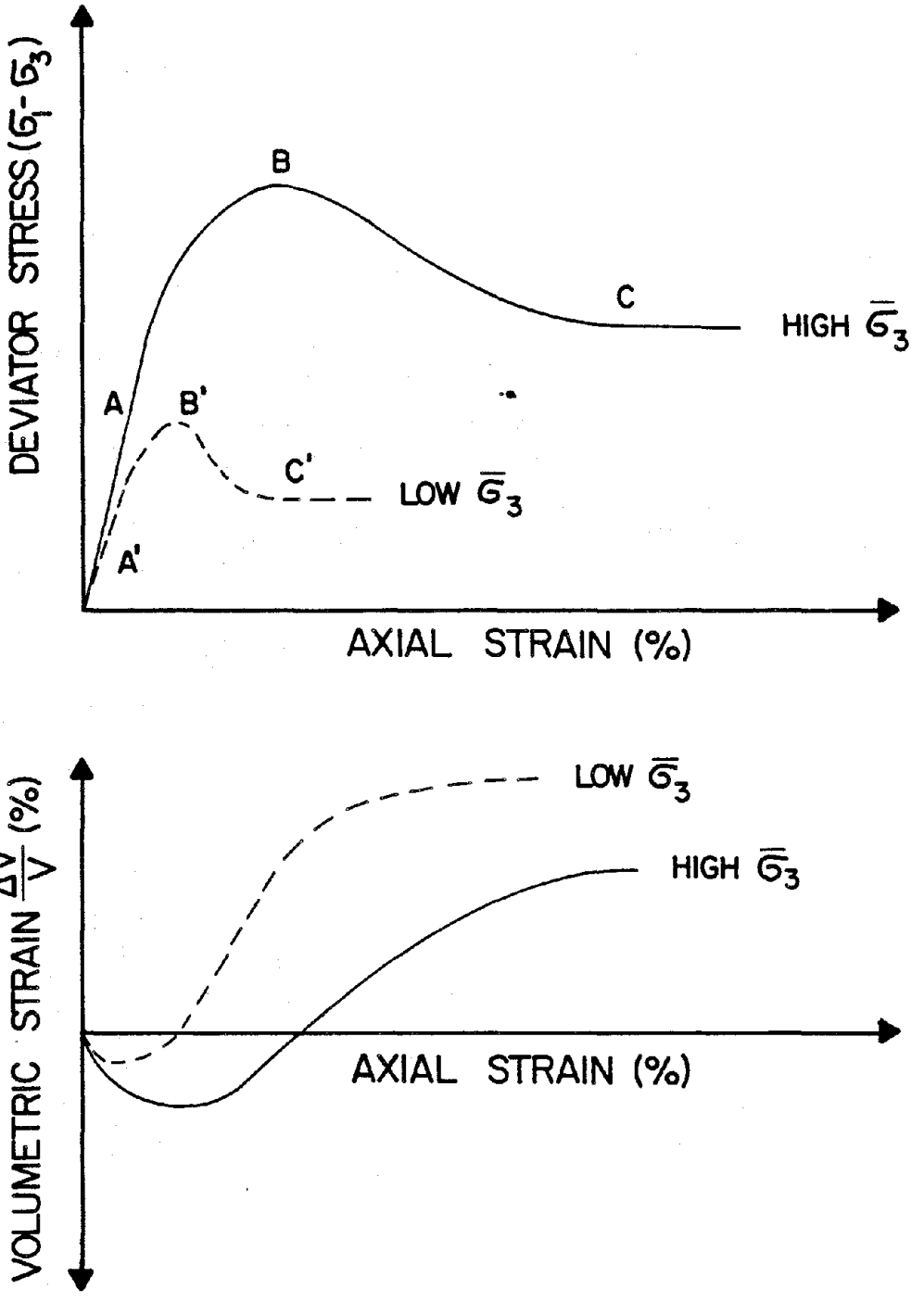

Fig.2.18 Stress-strain response of Weakly Cemented Sands

strain dependent behavior (or strength generation) is adequately studied and it is found that at small axial strains (0.25 - 0.85%) most of the shear strength is contributed from cohesion and with increasing axial strain, frictional resistance increases until the stress path touches the failure envelope. Also, the selection methods of deformation modulus are reviewed and an alternate new relationship is proposed. Finally a qualitative description of constitutive behavior is given in order to examine the validity of existing constitutive models for cemented sand in future research.

Chapter III

DYNAMIC BEHAVIOR OF UNCEMENTED SANDS AT LOW STRAINS

3.1 INTRODUCTION

The progress of advanced computational methods for dynamic soil-structure interaction analyses, has necessitated the accurate determination and estimation of dynamic soil properties. The design of engineering structures such as radar tower, power plants etc. require the dynamic properties of soils at low strain amplitude and high frequencies. The Resonant Column Test, in such circumstances is an indispensable tool and provides the values of dynamic moduli and damping ratio. The test though unique is not very commonly used. As such any empirical relationships which can provide the modulus and damping values close to those obtained from resonant column tests are of great help to practicing engineers. This chapter reviews such reported empirical relations for dynamic moduli and damping values for sands, discusses their limitations and proposes new relations based on recent experimental data of resonant column tests.

3.2 THE RESONANT COLUMN TEST

The most common types of laboratory tests used to investigate the dynamic behavior of soils are cyclic triaxial test, resonant column test, simple shear test and torsional shear test. Each of these tests has advantages and disadvantages when compared to others (Woods, 1978). The resonant column test is the most recommended test to evaluate dynamic moduli and damping values of soils at strains ranging from 10^{-4} to $10^{-2}\%$.

The basic principle of the resonant column device is to excite a confined cylindrical solid or hollow specimen of soil with either one end rigidly fixed at the base or free in a fundamental mode of vibration, typically in torsional or axial vibration. Once the fundamental mode of vibration is established, measurements are made of the resonance frequency and amplitude of vibration from which wave propagation velocities and strain amplitudes are calculated using the theory of elasticity. From the measured velocities of waves, longitudinal and shear moduli can be computed. By considering single degree of freedom system

with linear viscous damping (Kelvin-Voight Model) and free vibration damping values are calculated. The mathematical expressions and computer programs for data reduction are overviewed by many authors, the recent among them being Drenevich (1985) and Avramidis and Saxena (1985).

The definitions of moduli, damping and strain amplitude commonly adopted in analyzing resonant column test data and used in this chapter, are as shown in Fig. 3.1. Hardin (1970) describes the different methods of resonant column testing and the computation of results.

3.3 REVIEW OF EMPIRICAL RELATIONS

In this section the existing relationships for evaluating dynamic maximum shear modulus (G_{max}), dynamic maximum Young's modulus (E_{max}) and dynamic shear damping (D_s) are reviewed.

Relations for G_{max}: A summary of reported equations for estimating G_{max} is provided in Table 3.1 based on Chung, et. al. (1984). In the Hardin and Drenvich (1972) equation, the value of k depends on plasticity index of soil (provided in Table 3.2). However, this relationship is found to be applicable for e = 0.4 to 1.2 only. For higher values of void ratio, this relationship underestimates G_{max}, and as such a modified equation proposed by Hardin (1978), provides better results. Isenhower (1979) conducted resonant column tests with highly plastic silts and developed the following form of empirical relation for G_{max};

$$ln(G_{max}) = A+Bln(\overline{\sigma}_0)+Cln(\rho)+Dln(\overline{\sigma}_0)ln(\rho)+E[ln(\overline{\sigma}_0)]^2+F[ln(\rho)]^2 \quad (3.1)$$

The units of G, $\overline{\sigma}_0$ and ρ and the values of constants A,B,C,D,E and F are given in Table 3.3. Ohsaki and Iwasaki (1973) suggests the following correlation for estimating G_{max} at strains less than $10^{-4}\%$, from Standard Penetration Test;

$$G_{max} = 1200N^{0.8} \quad (3.2)$$

where N = Number of blows in a standard penetration test and units for G_{max} are tons per square meter. The above equation, nevertheless, does not distinguish type of soil nor the effect of the depth of embedment. Seed and Idriss

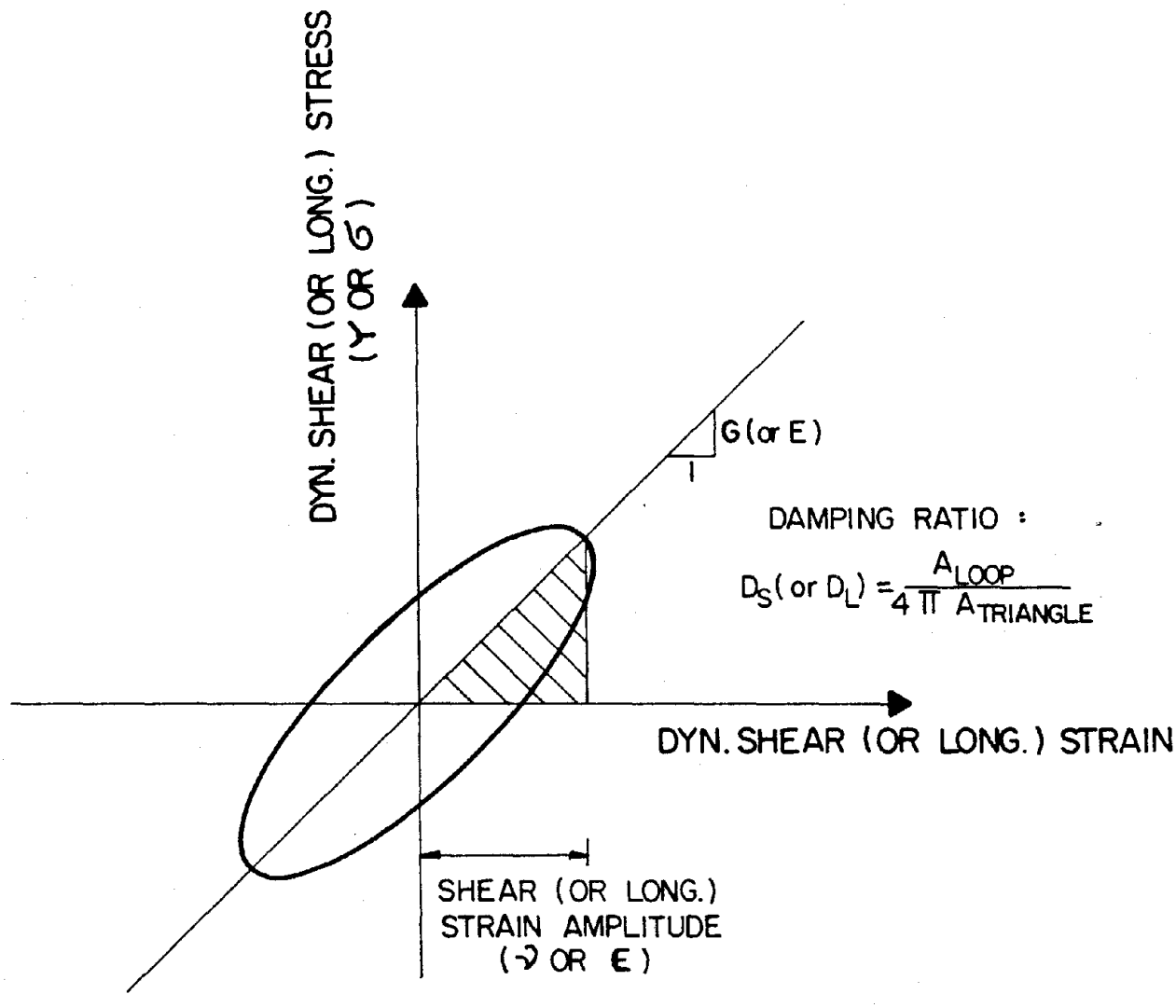

Fig.3.1 Definitions of Strain amplitude, moduli and damping

Table 3.1 Reported Relationships for G_{max} estimation

Soil Type	Empirical Relation	Strain γ	Valid Units G_{max}	Valid Units $\overline{\sigma}_0$	Ref.
Ottawa Sand	For $\overline{\sigma}_0 > 2000$ Psf $G_{max} = [(32.17 - 14.8e)^2/(1+e)]\overline{\sigma}_0{}^{0.5}$ For $\overline{\sigma}_0 < 2000$ Psf $G_{max} = [(22.52 - 10.6e)^2/(1+e)]\overline{\sigma}_0{}^{0.6}$	10^{-5}	Psi	Psf	Hardin (1965)
Kaolin Clay	$G_{max} = 1230[(2.973 - e)^2/(1+e)]\overline{\sigma}_0^{0.5}$	10^{-4}	Psi	Psi	Hardin & Black (1968)
Clays and Sands	$G_{max} = 1230[(2.97 - e)^2/(1+e)]\overline{\sigma}_0^{0.5}$	10^{-5}	Psi	Psi	Hardin and Drenevich (1972)
Clean Sands	$G_{max} = 900[(2.17 - e)^2/(1+e)]\overline{\sigma}_0^{0.4}$	10^{-6}	kg/cm^2	kg/cm^2	Iwasaki & Tatsuoka (1977)
Clays and Sands	$G_{max} = [625(OCR)^k/(0.3+0.7e^2)](P_a\overline{\sigma}_0)^{0.5}$	10^{-5}	any units	same as G_{max}	Hardin (1978)
Mont. No.O Sand	$G_{max} = 1230[(2.973 - e)^2/(1+e)]\overline{\sigma}_0^{0.5}$	10^{-5}	Psi	Psi	Drenevich (1978)
Sand	$G_{max} = 840[(2.17 - e)^2/(1+e)]\overline{\sigma}_0^{0.5}$	10^{-6}	kg/cm^2	kg/cm^2	Kokusho (1980)
Mont. No.O Sand	$G_{max} = [523/(0.3+0.7e^2)]P_a^{0.52}\overline{\sigma}_0^{0.48}$	10^{-5}	any units	same as G_{max}	Chung & Others (1984)

Table 3.2 Values of k (Hardin and Drenevich, 1972)

PLASTICITY INDEX PI	CONSTANT k
0	0
20	0.18
40	0.30
60	0.41
80	0.48
> 100	0.50

Table 3.3 Values of Constants for Eqn 3.1 (Isenhower, 1979)

CONSTANT	VALUES BASED ON		
	SOILD SPECIMEN	HOLLOW SPECIMEN	BOTH
A	-505.7	535.8	445.6
B	-62.3	17.9	65.2
C	1082.3	-1009.9	-963.2
D	61.1	-15.4	-69.0
E	-1.9	-0.1	2.0
F	-567.0	484.4	529.7

Note: G is in Psf, $\bar{\sigma}_o$ is in Psi, and ρ is in Slugs/cu ft.

(1970) proposed the equation for estimating G_{max} for sands as follows:

$$G_{max} = 1000 K_{2max} (\overline{\sigma}_0)^{0.5} \tag{3.3}$$

In this equation the units of G_{max} and $\overline{\sigma}_0$ are pounds per square feet and K_{2max} is an empirical factor which varies according to density. The values of K_{2max} obtained by geophysical tests are presented in Table 3.4. Anderson et. al. (1978) based on cross hole test field data and laboratory test data concluded that Equation (3.3) underestimates; and that proposed by Iwasaki (1973) overestiamtes the value of G_{max} for sandy soils.

Hardin and Drenvich (1972) proposed an approximate method of computing G at any strain level γ. Assuming hyperbolic stress-strain relations, the following expressions are obtained.:

$$(G/G_{max}) = \frac{1}{1 + (\gamma/\gamma_r)} \tag{3.4}$$

$$\gamma_r = \tau_{max}/G_{max} \tag{3.5}$$

and

$$\tau_{max} = \left[\left[\frac{(1+K_0)}{2} \overline{\sigma}_v sin\overline{\phi} + \overline{c} cos\overline{\phi} \right]^2 - \left[\frac{(1-K_0)}{2} \overline{\sigma}_v \right]^2 \right]^{0.5} \tag{3.6}$$

where K_0= coefficient of lateral strain at rest

γ_r= reference strain

and $\overline{\sigma}_v$= effective vertical stress.

Edil and Luh (1978) developed equations which can also be used to find G at given strain level γ. According to these investigators, for strains less than $0.25 \text{x} 10^{-4}$ radians, the values of G are found to be nearly constant and hence it can be taken as G_{max} (however in the publication G at $\gamma = 0.25 \text{x} 10^{-4}$ is termed as reference dynamic shear modulus G_0). The developed equations are:

$$\frac{G}{G_{max}} = 1.004 - 345.4\gamma \tag{3.7}$$

$$G_{max} = 10^4 [-5.899 + 0.305 (\overline{\sigma}_0)^{0.5} exp(D_r) + 4.02 (\overline{\sigma}_0)^{0.25}] \tag{3.8}$$

where G, G_{max} and $\overline{\sigma}_0$ are in KN/m^2; γ in radians and D_r (relative density) is a fraction of one. Expression in terms of void ratio was also provided.

Table 3.4 Values of K_{2max} for Eqn 3.3

(Seed and Idriss, 1970)

SOIL	LOCATION	DEPTH (ft)	K_{2max}
Loose moist sand	Minnesota	10	34
Dense dry sand	Washington	10	44
Dense saturated sand	S. California	50	58
Dense saturated sand	Georgia	200	60
Dense saturated silty sand	Georgia	60	65
Dense saturated sand	S. California	300	72
Extremely dense silty sand	S.California	125	86
Dense dry sand (slightly cemented)	Washington	65	166
Moist clayey sand	Georgia	30	119

Sherif and Ishibashi (1976) conducted torsional simple shear tests on four types of sands and proposed the correlation as

$$G_{eq} = 2.8\overline{\phi}\gamma^{-0.6}(\overline{\sigma}_c)^{0.85} \tag{3.9}$$

where G_{eq} is the equivalent dynamic shear modulus corresponding to the second cycle; $\overline{\phi}$ is the angle of internal friction, γ is the shear strain and $\overline{\sigma}_c$ is the effective confining pressure, the units of $\overline{\sigma}_c$ and G_{eq} are in Kpa. In the above correlation, the density (or void ratio) effects are reflected by an appropriate selection of ϕ.

Relations for Estimation of E_{max}: Currently the normal practice has been to calculate E_{max} from the estimated values of G_{max} using "appropriate poisson's ratio" (Hardin, 1978). This chapter also elaborates the effect of Poisson's ratio on the values of moduli from empirical relations.

Relations for Dynamic Shear Damping: Empirical relations for dynamic shear damping are not well established. Hardin and Drenevich (1972) proposed a relation for shear damping as given by:

$$D = D_{max}(1 - \frac{G}{G_{max}}) \tag{3.10}$$

The value of G_{max} can be obtained by choosing any relation in Table 3.1. However determination of D_{max} is slightly more cumbersome (D_{max} is the value of damping ratio when shear modulus theoretically equals to zero). Based on experimental data, empirical relations for D_{max} are proposed for various soils and are given in Table 3.5. It can be seen that for sands D_{max} depends on number of cycles of loading N; whereas, for silts and clays it depends also on frequency f and mean principal effective stress $\overline{\sigma}_0$. Therefore knowing G_{max}, D_{max} and G for any strain, the damping value D can be obtained.

Hardin (1968) proposed an empirical equation for damping ratio of clean dry sands for shear strains of 10^{-4} or less and confining pressures ($\overline{\sigma}_0$) varying from 0.24 to 1.63 kg/cm^2, based on comprehensive resonant column tests, as follows

$$D = 4.5\gamma^{0.2}(\overline{\sigma}_0)^{0.5} \tag{3.11}$$

Table 3.5 Values of D_{max} for Eqn 3.10 (Hardin and Drenevich, 1972)

SOIL TYPE	VALUE OF D_{max} %
Clean dry Sands	$33 - 1.5 \text{ Log } N$
Clean saturated sands	$28 - 1.5 \text{ Log } N$
Saturated Lick Creek silt	$26 - 4(\bar{\sigma}_o)^{0.5} + 0.7\, f - 1.5 \text{ Log } N$
Various saturated cohesive soils including Rhodes Creek Clay	$31 - (3 + 0.03\, f)(\bar{\sigma}_o)^{0.5} + 1.5\, f - 1.5 \text{ Log } N$

Note: f is in cycles per second and $\bar{\sigma}_o$ is in Kg/sq cm.

where $\overline{\sigma}_0$ is in pounds per square feet. and γ as fraction of one. Tatsuoka et. al. (1978) found that the exponent of $\overline{\sigma}_0$ in the above equation is dependent on strain level as shown in Fig. 3.2. It is reported that the void ratio has no effect on damping and proposed a relation (Eqn. 3.12) to evaluate damping ratio at any confining pressure, provided the value of damping ratio at a specific confining pressure is known

$$\frac{D_1}{D_2} = \left(\frac{\overline{\sigma}_{01}}{\overline{\sigma}_{02}}\right)^n \tag{3.12}$$

The values of n are obtained from Fig. 3.2. Sherif et. al. (1977) established an empirical equation for damping at N = 2 (based on cyclic torsional shear tests on dry Ottawa sand) as:

$$D = (50 - 0.6\overline{\sigma}_0)\gamma^{0.3} \tag{3.13}$$

In the above equation D and γ are in percentages and $\overline{\sigma}_0$ in pounds per square inch. In an attempt to evolve a general relationship, a soil gradation and sphericity factor F, and correlation factor for number of cycles are introduced and the subsequent expression for damping is:

$$D = \frac{(50 - 0.6\overline{\sigma}_0)}{38}(73.3F - 53.3)(1.01 - 0.046 log N_c)\gamma^{0.3} \tag{3.14}$$

Typically F varies from 1.0 to 2.0. In the above expression damping D and shear strain γ are in percentages and $\overline{\sigma}_0$ units are psi.

Edil and Luh (1978) observed significant effect of number of cycles on damping for Ottawa Sand and other such dry sands and found the correlations expressed in Eqn. 3.15. D_{max} is the damping ratio defined at number of cycles, N equal to 1000.

$$\frac{D}{D_{max}} = 1.131 - 0.453 log N \tag{3.15a}$$

$$D_{max} = 0.70 + 7800\gamma D_r^{0.5} - 0.36\gamma^{0.33}(\overline{\sigma}_0/98)^3 \tag{3.15b}$$

where D and D_{max} are in percentages, D_r in decimal form, $\overline{\sigma}_0$ in KN/m2, γ in radians and N is dimensionless.

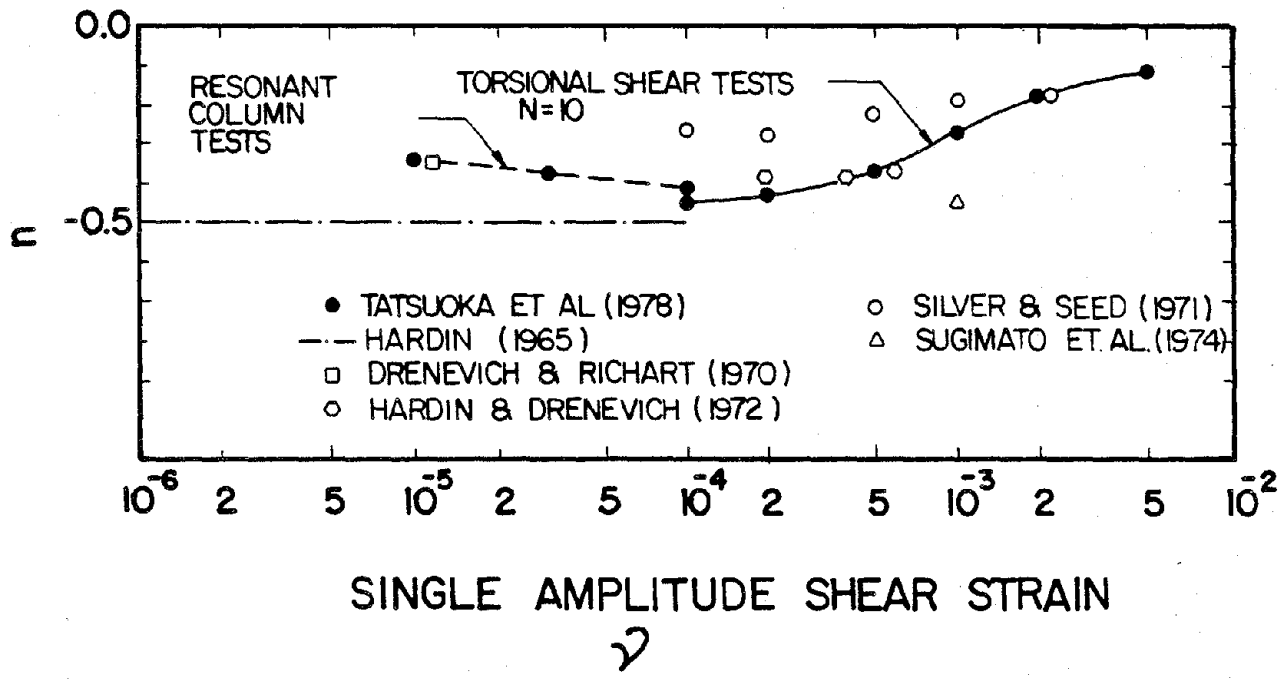

Fig.3.2 n versus γ relationship

Relations for Dynamic Longitudinal Damping: In dynamic response of soils, the predominant energy input comes from shear waves. Consequently, shear or torsional damping being the most important many investigators tried to develop relations for shear damping. There may be situations where the longitudinal damping needs to be considered (Marcuson and Curro, 1981). As of today no reliable empirical relation for dynamic longitudinal damping is reported in the literature. However, it is the present practice to assume longitudinal damping about 3% for strains less than 10^{-4} and 12% for strains above 10^{-4}.

3.4 COMMENTS ON REPORTED EMPIRICAL RELATIONS

The development of simple equations to make preliminary estimates of soil moduli and damping at low strain amplitudes as initiated by Hardin and Drenevich (1972) is indeed necessary for engineers. Though the relationships reported in the literature are based on exhaustive test data and well accepted there is always a room to verify and discuss these relations in view of new experimental data.

It has been recognized that the development of unique expressions for moduli and damping which can account for all the factors would be difficult, if not impossible. The factors affecting moduli and damping values can be listed as follows:

1. Type of soil
2. Mode of vibration
3. Strain Amplitude
4. Effective mean normal stress
5. Void ratio
6. Number of cycles
7. Prestrain
8. Moisture content
9. Stress History (OCR)
10. Frequency
11. Preloading

12. Capillary action
13. Strain rate
14. Sampling and sample preparation
15. Specimen geometry
16. Saturation
17. Grain size characteristics
18. Time
19. Temperature
20. Testing technique and apparatus
21. Data interpretation etc.

However depending on the situation, only few of the above factors may be important (Edil et. al. 1978, Avramidis and Saxena 1985 etc.). Therefore, for any reported relation its limitation should be well understood. For example, Hardin and Drenevich (1972) relations are mostly based on tests on clean Ottawa Sand, Lick Creek Silt and the data obtained from other investigators with other soils at low confining pressures. Later many Japanese investigators (Iwasaki et. al. 1977, Tatsuoka et. al. 1978 etc.) in their series of investigations relating to moduli and damping values for different soils found that the grain size distribution, percent fines etc. affect the dynamic characteristics of sandy soils. Isenhower (1979) also observed that the relation developed by Hardin (1978) for normally consolidated soils results in an average error in the values of shear modulus upto 12.7% (Table 3.1). On the other hand the relation developed by Isenhower (1979) , given as Eq. 3.1, is lengthy and involves too many constants and yet has an average error upto 8.8%. Chung et. al. (1984) found that the widely used equation of Hardin and Drenevich (1972) predicts moduli that are slightly lower than the average of the test results for Montrey No. 0 sand, though their tests results are limited to only one value of void ratio (e = 0.676).

It can be said that the relations for shear modulus are better established and relations for shear damping are yet at best in their infancy. No relations for dynamic longitudinal modulus and longitudinal damping are available.

In the following section, investigations conducted at Illinois Institute are reported along with proposed relations.

3.5 INVESTIGATIONS AT IIT

In this chapter the data of only resonant column tests on dry Monterey No. 0 sand specimens is reported.

Test Equipment: During this investigation all tests are conducted with the Modified Drenvich Longitudinal and Torsional Resonant Column device. The device can accommodate cylindrical soil specimens of nominal height of 135mm and a nominal diameter of 71.12 mm. The samples can be subjected to desired confining pressure. The samples are fixed at the base with excitation forces applied at the top. The apparatus is capable of applying both longitudinal and torsional excitations. Also, samples can be tested either in dry condition or completely saturated condition. For the complete details of the apparatus, please see Avramidis and Saxena (1985).

Soil Type: Monterey No. 0 sand is used in all the tests. This soil has been chosen because of its wide use by different geotechnical researchers and to extend the work of Chung et. al. (1984) for different void ratios. The grain size distribution and index properties are shown in Fig. 2.1 and Table 2.1 respectively.

Sample preparation: All the samples are prepared by method of undercompaction developed by Ladd (1978). The samples are prepared at relative densities of 25,43,60 and 80 percent.

Test procedure: The details of test procedure and data reduction method can be found in Avramidis and Saxena (1985). Dry samples of different relative densities mentioned above are tested at effective confining pressures of 49, 98, 196, 392 and 588 kpa in such a way that the system response could be studied at different low strain amplitudes. All the tests are carried out in a single stage.

The variations of dynamic shear modulus (G) and dynamic longitudinal modulus (E) with strain at different densities under different confining pressures are shown in Fig. 3.3 and Fig. 3.4 respectively. Whereas corresponding dy-

namic shear damping (D_s) and dynamic longitudinal damping (D_l) variations are shown in Fig. 3.5 and Fig. 3.6 respectively.

3.6 ANALYSIS OF TEST DATA

The research todate has shown that the moduli values decrease as strain increases. However, at very low strains of the orders below $10^{-3}\%$, the moduli are assumed to be constant and are termed as maximum moduli. The limit of strain for maximum moduli consideration is reported differently by different investigators (Table 3.1). In the present study, shear modulus is considered as maximum for strains less than $10^{-3}\%$, and Young's modulus as maximum for strains less than $10^{-4}\%$. Observations about the increase in damping ratio and decrease in moduli with strains are presented and discussed (Fig. 3.3-3.6).

Dynamic Shear Modulus: A modified relationship among G_{max}, e and $\overline{\sigma}_0$ is presented based on the test results. The test results shown in Fig. 3.3 are plotted as shown in Fig. 3.7. The following empirical equation closely approximating the test data of Fig. 3.3, is obtained by regression analysis.

$$G_{max} = \frac{428.2}{(0.3 + 0.7e^2)}(P_a)^{0.426}(\overline{\sigma}_0)^{0.574} \tag{3.16}$$

The coefficients in the above expression differ from those reported in earlier investigations (Table 3.1). It may be pointed out that the above relation is based on tests on dry Monterey No. 0 sand for strains less than $10^{-3}\%$, void ratios 0.618 to 0.7775 (D_r = 25 to 80%) and effective confining pressure from 49 to 588 kpa.

The void ratio function $1/(0.3+0.7e^2)$ is adopted as per Hardin (1978). With this function G_{max} can become zero, only when void ratio approaches infinity, which appears logical.

The relation as presented in Eq. 3.16 has two major advantages compared to those proposed previously. This equation is applicable for all systems of units because it is dimensionally correct. The second advantage is that this equation allows the shear modulus to approach zero only when void ratio approaches infinity (other recent relations-Hardin, 1978 and Chung et al., 1984-do also have the same).

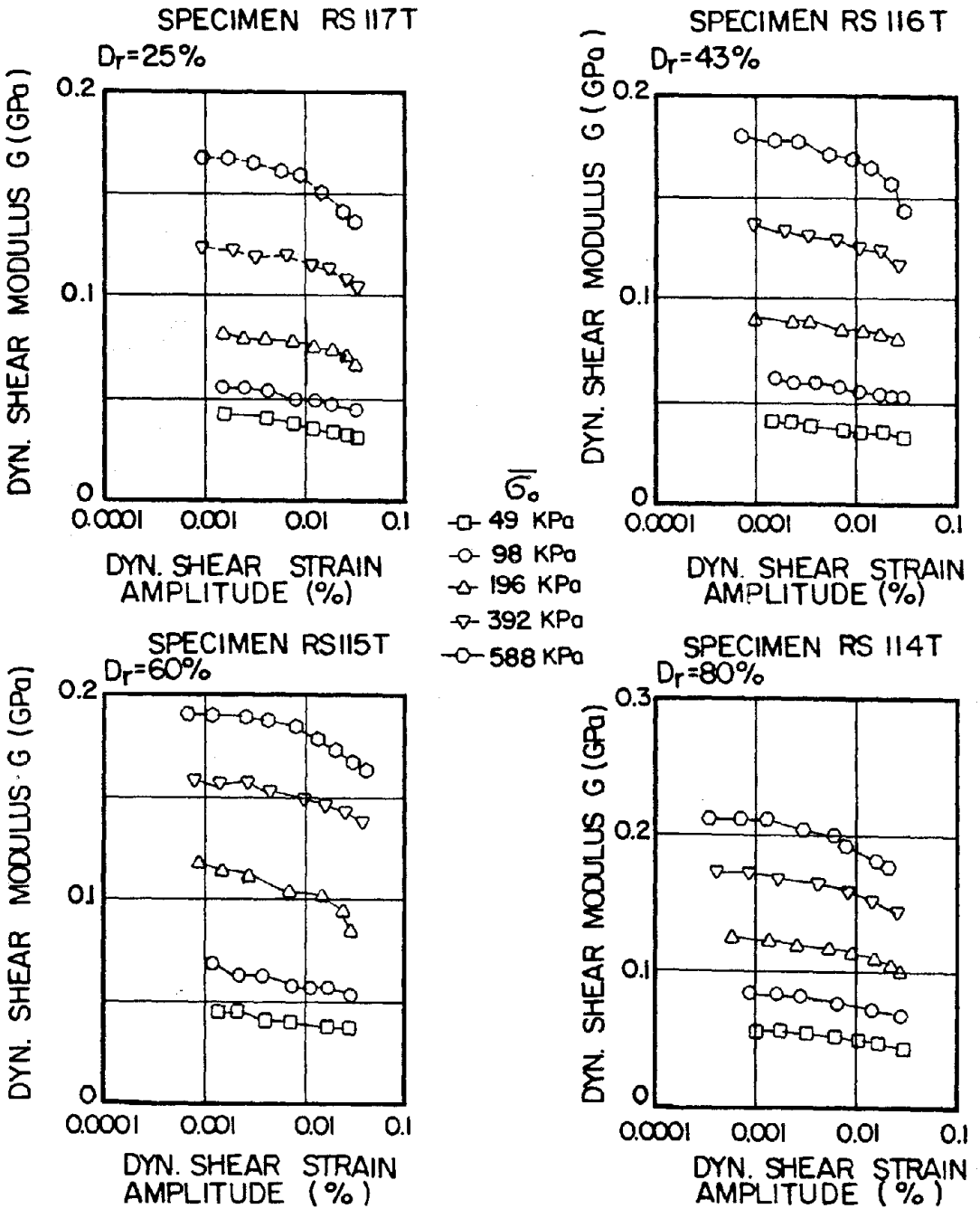

Fig.3.3 Dynamic Shear Modulus versus shear strain amplitude for Monterey No.O sand with D_r=25, 43, 60 and 80%

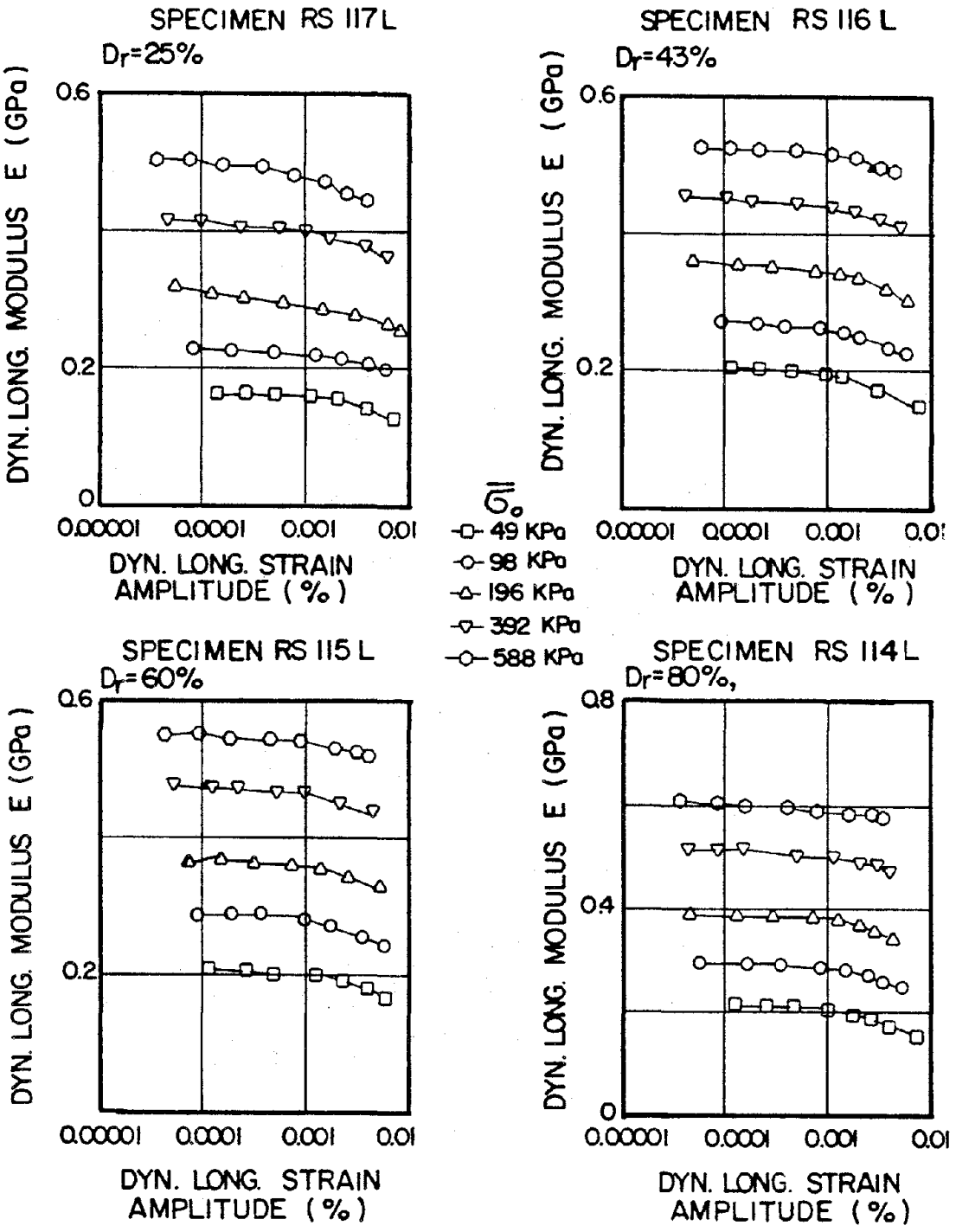

Fig.3.4 Dynamic Young's Modulus versus Longitudinal Strain amplitude for Monterey No.O sand with D_r=25, 43, 60 and 80%

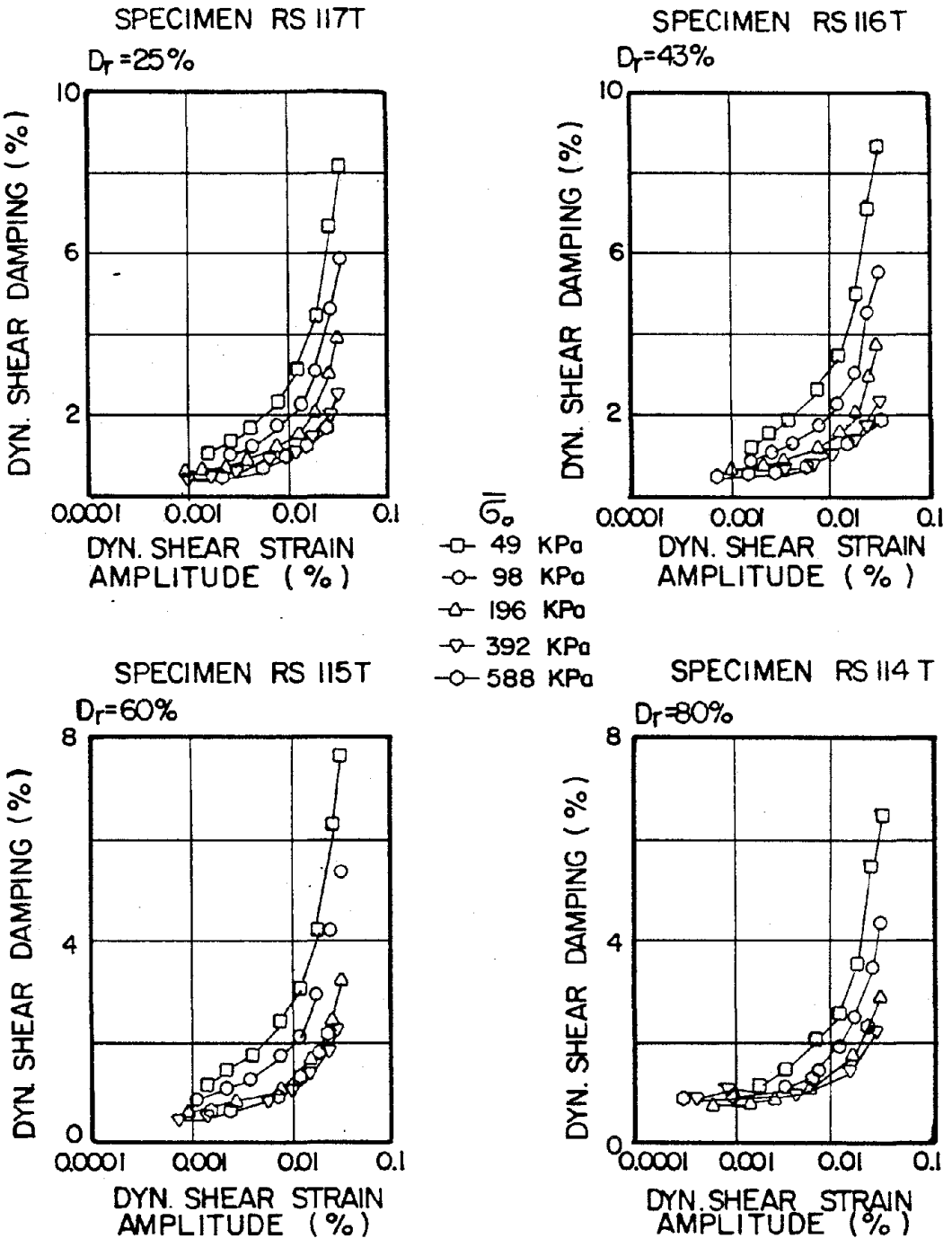

Fig.3.5 Dynamic Shear Damping versus Shear Strain Amplitude for Monterey No.O sand with D_r=25,43,60 and 80%

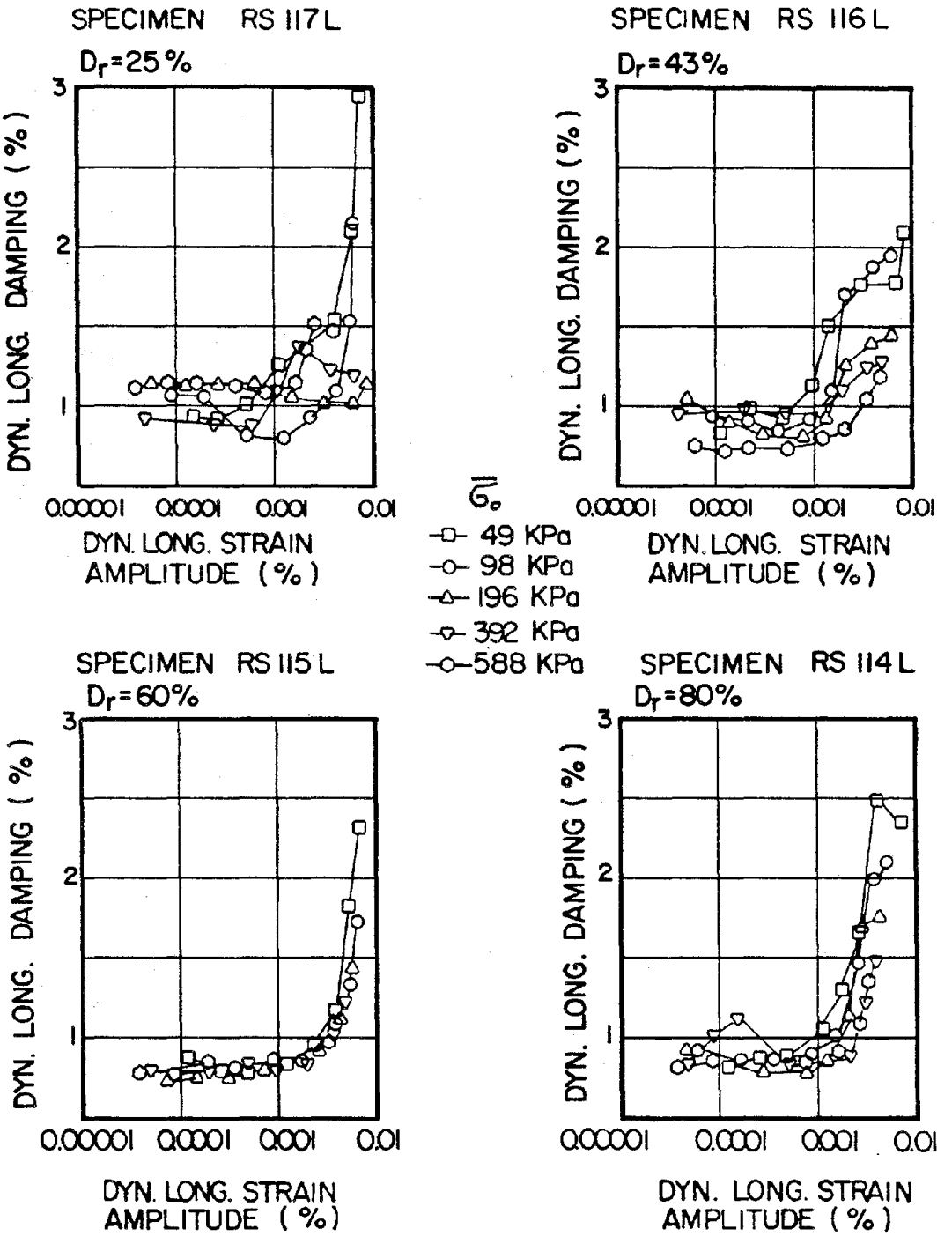

Fig.3.6 Dynamic Longitudinal Damping versus Longitudinal Strain Amplitude for Monterey No.O sand with D_r=25, 43, 60 and 80%

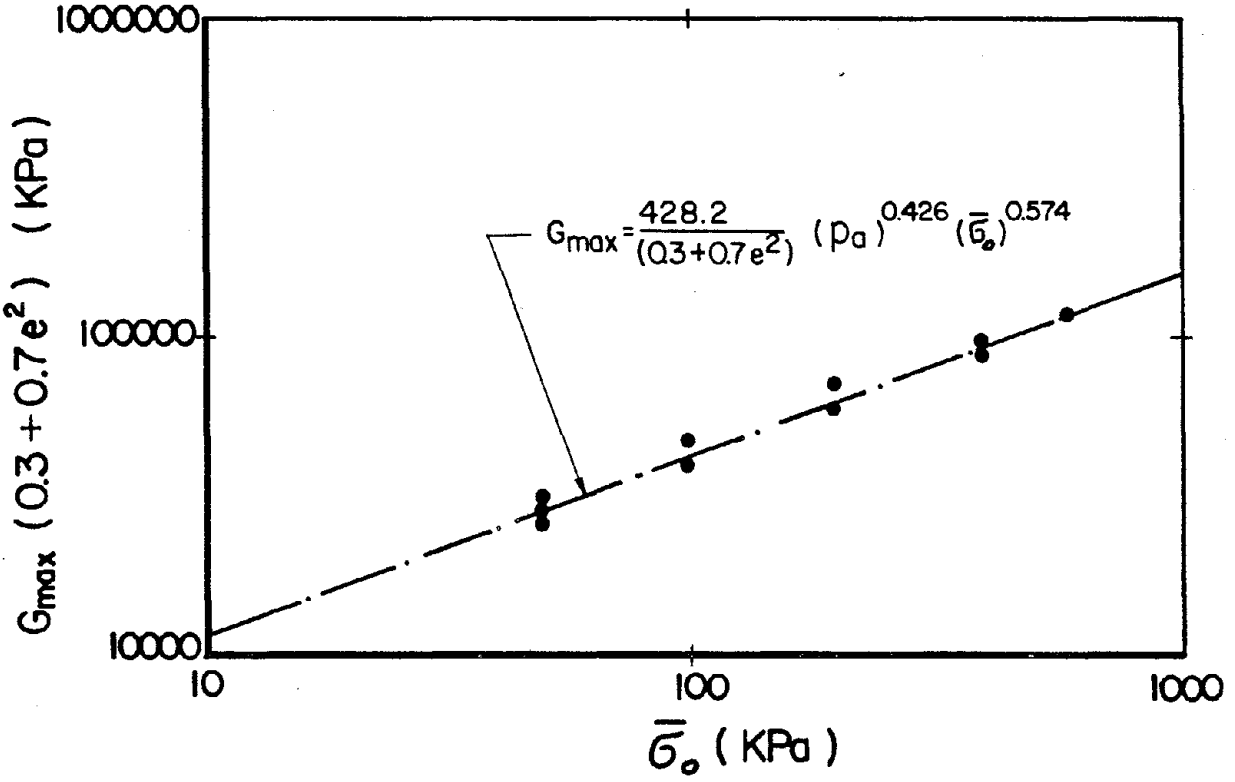

Fig.3.7 Effective Confining Pressure versus Maximum Shear Modulus

Chung et.al. (1984) reported the data from resonant column testing using Monterey No. 0 sand with similar sample preparation technique for e = 0.676 (D_r= 60%) and $\overline{\sigma}_0$ = 10 to 300 kpa. Defining maximum shear modulus at strain less than 10^{-3}% a relation was developed by Chung et al. (Table 3.1). However, their results are limited to one value of void ratio (e = 0.676). Drenevich (1978) conducted tests on Monterey No. 0 sand for the variables mentioned in Table 3.1 and obtained a relation also shown in Table 3.1. Since the soils used and testing technique are same, a comparison for G_{max} from these relations with Eqn. 3.16 for e = 0.676 (D_r = 60%) and effective confining pressure of 49,98,196,392 and 588 kpa is shown in Fig. 3.8. It can be observed that Eqn. 3.16 predicts G_{max} close to the results of Chung et. al. (1984). The Drenevich (1978) relation overpredicts the G_{max} values, and the difference is significant at high confinining pressures.

Figure 3.9 presents such relationships for different soils along with the names of investigators. It may be noted that relations developed for a kind of soil may provide incorrect results for another.

Dynamic Young's Modulus: The moduli values shown in Table 3.7 are compiled from the excellent work reported by Skoglund et. al. (1976) and are average values obtained by six investigators on uniform sand with grain size distribution and index properties shown in Fig. 3.10. with an average void ratio of 0.635. The poisson's ratio (ν) values are computed from theory of elasticity and listed in the Table 3.6. It can be observed that the values of dynamic longitudinal moduli are about 2 to 3 times the dynamic shear modulus at the same confining pressure. However, such a conclusion may not be true all the time because of the basic variations in longitudinal vibration from those of torsional ones. The poisson's ratio values obtained appear reasonable for sands. Importantly, the poisson's ratio, as can be seen from the values in the table, decreases with an increase in the confining pressure.

Skoglund et. al. (1976) and Marcuson et. al. (1981) also deal with dynamic longitudinal modulus but only for cohesive soils. The derivation of E_{max} from G_{max} requires an input of poisson's ratio. Herein, the effect of the

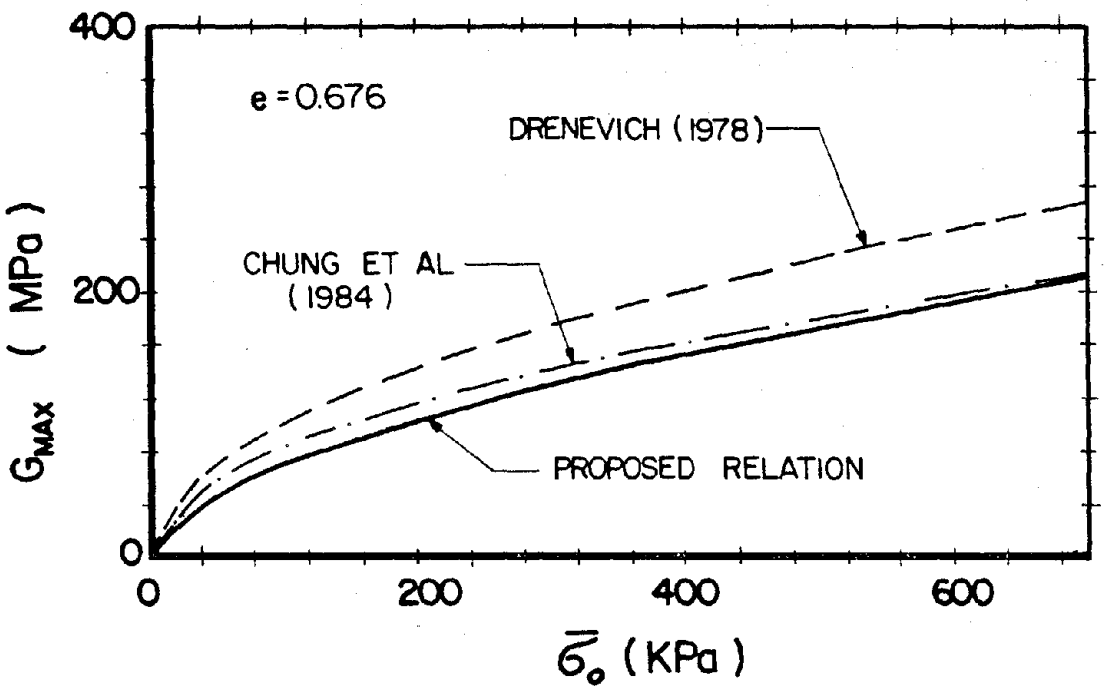

Fig.3.8 Comparison of Proposed Relation and Available Relations for G_{max} for Monterey No.O sand

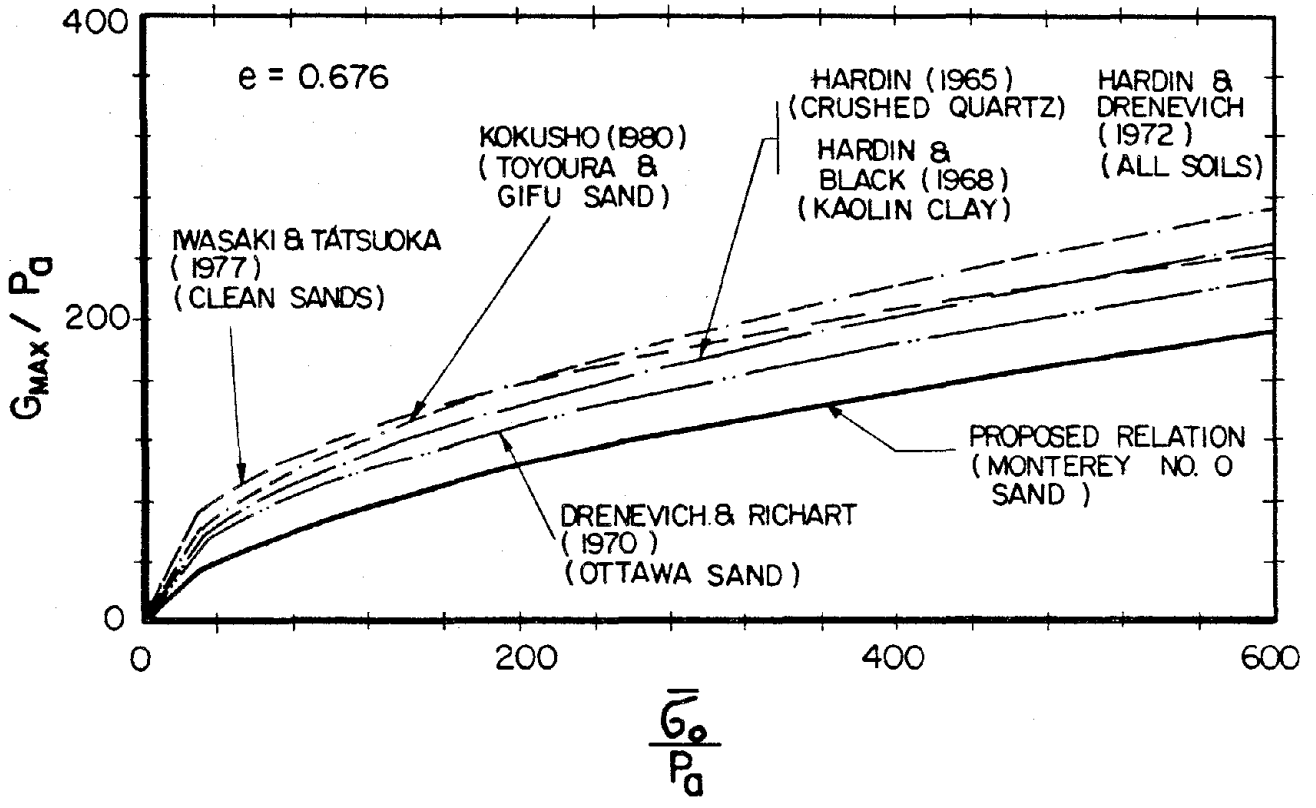

Fig.3.9 Comparison of Proposed Relation for Monterey No. O sand with Reported Relations for Other Types of Soils

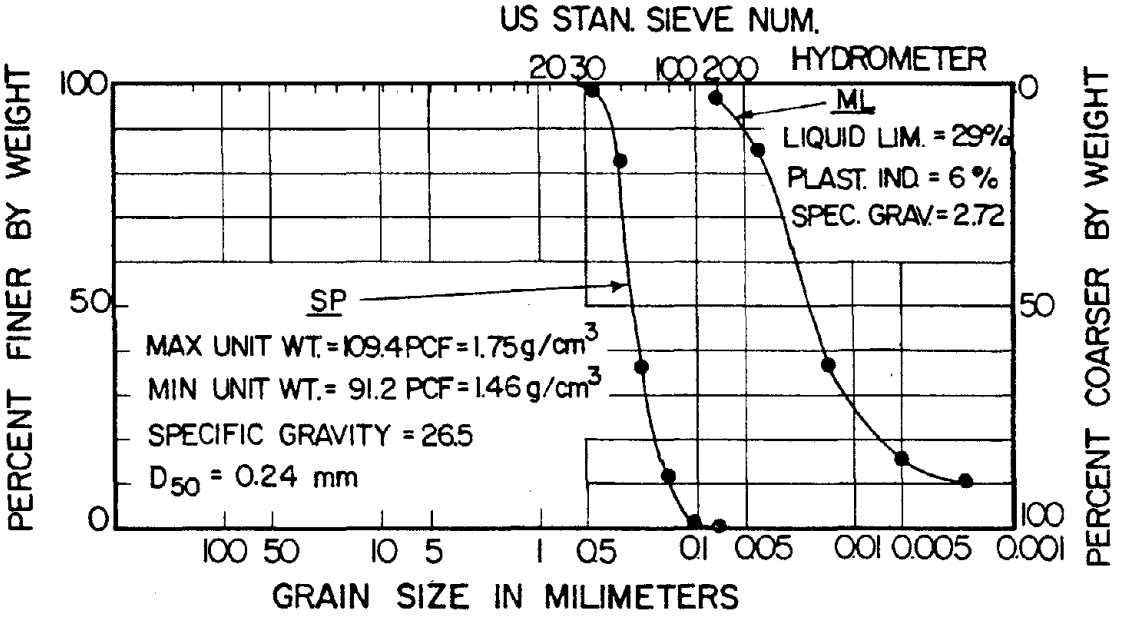

Fig.3.10 Grain Size Distribution and Index Properties of sand used by Skoglund et.al.(1976)

Table 3.6 Poisson's Ratio Values based on Skoglund et al., 1976

Effective Confining Pressure (N/ sq in)	Max. Dyn. Shear Modulus (Kips/sq in)	Max. Dyn. Young's Modulus (Kips/sq in)	Poisson's Ratio
6.9	12.7	34.3	0.35
13.8	18.3	48.0	0.31
27.6	25.4	64.1	0.26

value of poisson's ratio on E_{max} is discussed. The values of dynamic poisson's ratio are matter of disagreement among researchers. For example, Ohsaki and Iwasaki (1973) observed that i) dynamic poisson's ratio increases with decrease of shear modulus and approaches to 0.5 and ii) different soil types cause no definite difference in values of poisson's ratio. On the other hand, Hara (1970, 1973) based on static and dynamic triaxial tests on clays disagrees with above observations and concluded that dynamic poisson's ratios are not significantly influenced by the moduli, shear strain levels and frequencies or load application. The relation developed by Ohasaki and Iwasaki for sandy soils, is presented as follows:

$$\nu = 0.2 + 0.3\left[1 - \frac{1}{16(logG_{max} - 2)^2}\right]^2 \tag{3.17}$$

for $5000 < G_{max} < 100\ 000$

The units of $G_{max}$are in tons per square meter.

A relationship developed based on this investigation is presented. The test results for dynamic longitudinal (or Young's) modulus E versus dynamic strain are shown in Fig. 3.4. The moduli at strains less than $10^{-4}\%$ are assumed as constant and are called maximum moduli (E_{max}). Assuming the void ratio function same as used in Eqn. 3.16, the maximum dynamic longitudinal moduli are plotted in Fig. 3.11 and can be closely approximated by regression analysis as:

$$E_{max} = \frac{1703.57}{(0.3 + 0.7e^2)}(P_a)^{0.61}(\overline{\sigma}_0)^{0.39} \tag{3.18}$$

Since no such relation and no experimental data on Monterey No. 0 sand with samples prepared from the method of undercompaction are available, no attempt is made herein to verify the validity of Eqn. 3.18. From the relations for estimation of G_{max} and E_{max} (i.e. Equn. 3.16 and 3.18), the ratio of maximum dynamic longitudinal modulus E_{max} to maximum dynamic shear modulus G_{max} is obtained and is given in Eqn. 3.19.

$$E_{max} = 3.98G_{max}(P_a/\overline{\sigma}_0) \tag{3.19}$$

From the theory of elasticity, poisson's ratio can be expressed as:

$$\nu = 0.5(E_{max}/G_{max}) - 1 \tag{3.20}$$

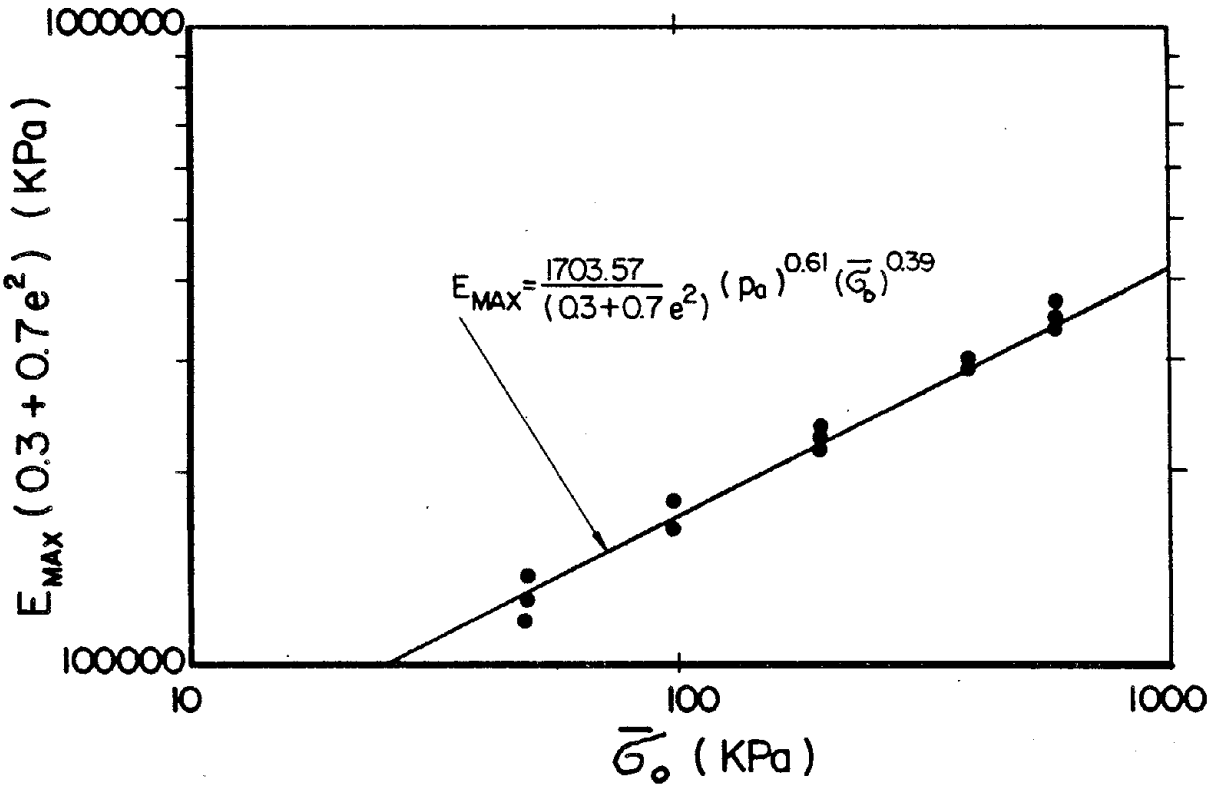

Fig.3.11 Effective Confining Pressure versus Maximum Young's Modulus

Substituting from Eqn. 3.19, the empirical equation for dynamic poisson's ratio becomes as given in Eqn. 3.21:

$$\nu = 2(P_a/\overline{\sigma}_0)^{0.184} - 1.0 \tag{3.21}$$

Eqn. 3.21 suggests that poisson's ratio is dependent on effective confining pressure and as confining pressure increases the poisson's ratio decreases. Similar observation was made by Skoglund et. al. (1976). Hardin and Richart (1963) found that the poisson's ratio for sands can be 0.1, whereas Ohsaki and Iwasaki (1973) observed from field data that the poisson's ratio for sandy soils can approach 0.5. Considering these values, the Eqn. 3.21 is valid for $5 < (\overline{\sigma}_0/P_a) < 25$.

The difficulty for finding poisson's ratio values from empirical relations such as Eqn. 3.21 has been recognized by many investigators long ago (Biot 1956, Wilson and Dietrich 1960, Hardin and Richart 1963, Wilson et. al. 1978, etc.) It may be noted that a small error in the ratio of longitudinal and shear moduli can produce very large error in poisson's ratio values. Hence, Poisson's ratios computed from empirical relations are not considered to be reliable.

According to Woods (1978) "a variety of "special" resonant column devices have recently been developed. Both shear modulus, G, and Young's moduli, E, can be measured in the same sample. This may be very important in the near future in resolving uncertainties regarding poisson's ratio,ν ."

Dynamic Shear Damping: The variation of dynamic shear damping with dynamic shear strain, effective confining pressure and density (or void ratio) is shown in Fig. 3.5. The effect of density on dynamic shear damping is insignificant as can be observed from Fig. 3.12. This fact supports the observations of Hardin (1965), Tatsuoka et. al. (1978), Sherif et.al (1977) etc. The data in Fig. 3.6 can be best expressed by the Eqn. 3.22

$$D_s = 9.22(\frac{\overline{\sigma}_0}{P_a})^{-0.38}\gamma^{0.33} \tag{3.22}$$

where $\overline{\sigma}_0$ is the effective confining pressure (or effective mean normal pressure), P_a is the atmospheric pressure and γ is the dynamic shear strain. The units of

$\overline{\sigma}_0$ and P_a must be the same and γ must be expressed in percentage, hence the resulting value of damping would be in percent. The Eqn. 3.22 has a distinct advantage over the reported relations. It applies for all systems of units because it is non-dimensional.

Dynamic Longitudinal Damping: Fig. 3.7 shows the values of dynamic longitudinal damping D_l from resonant column tests on dry Monterey No. 0 sand under longitudinal mode of vibration. Fig. 3.13 depicts the negligible effect of density on dynamic longitudinal damping values (D_l). Based on the statistical analysis on the data, the dynamic longitudinal damping can be expressed by Eqn. 3.23.

$$D_l = (\frac{\overline{\sigma}_0}{P_a})^{-0.13} \epsilon^{0.33} \tag{3.23}$$

Eqn. 3.23 is also non-dimensional. The strain (ϵ) and damping are expressed in percentage.

Comparing Eqns. 3.22 and 3.23, the dynamic longitudinal damping (D_l) can be related to dynamic shear damping (D_s) and is expressed by Eqn. 3.24.

$$D_l = 1.08 D_s (\frac{\overline{\sigma}_0}{P_a})^{0.25} \tag{3.24}$$

It should be noted that D_l is the dynamic longitudinal damping in longitudinal mode of vibration and D_s is the dynamic shear damping in torsional mode of vibration. Depending upon the predominate mode of vibration, one of these values should be considered. In a real situation, both dynamic longitudinal and shear dampings exist in any vibration condition. The values of dynamic shear damping in longitudinal mode of vibration and dynamic longitudinal damping in torsional mode of vibration are difficult to assess, hence the proposed relations may help in estimating such values.

3.7 EVALUATION OF RELATIONSHIPS

The accuracy, applicability and comparison of developed relations are discussed in this section.

Fig. 3.14 clearly depicts that the proposed relation for maximum dynamic shear modulus, G_{max} (Eqn. 3.16) best fits the experimentally measured data. The experimental data are based on well controlled resonant column tests

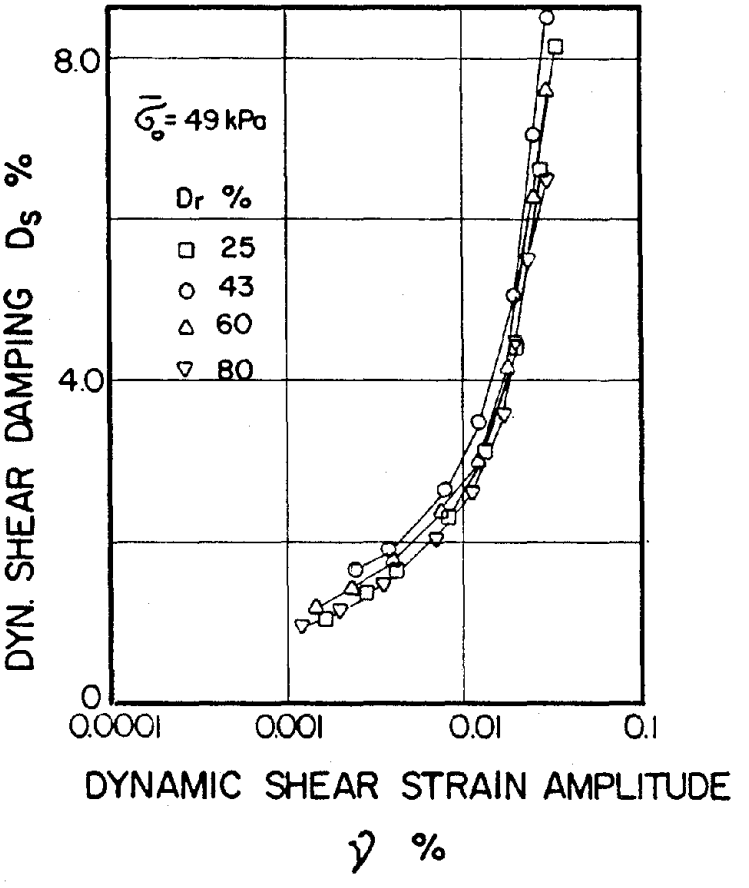

Fig.3.12 Effect of Relative Density on D_s

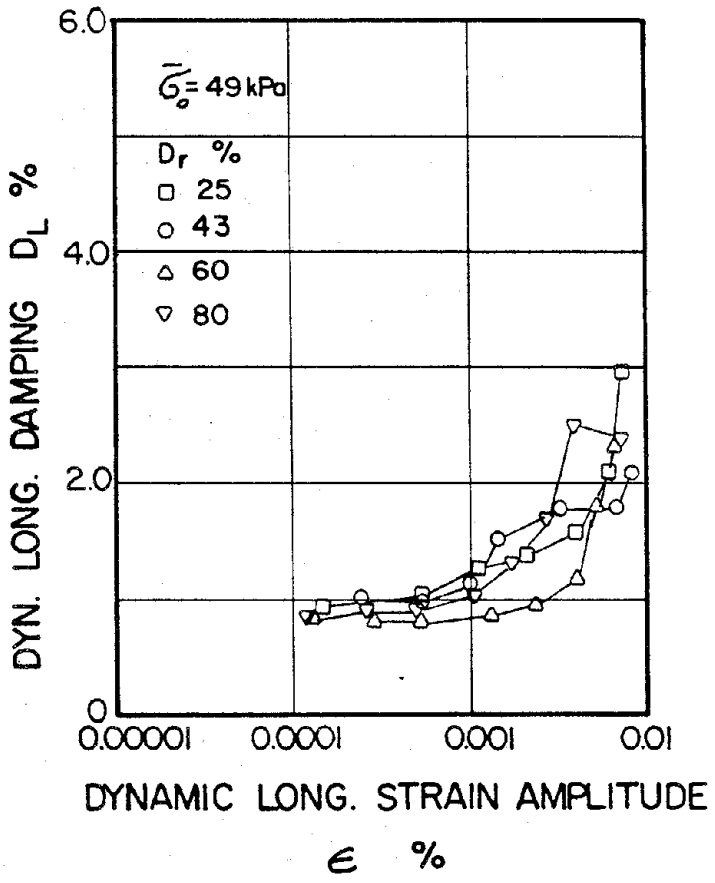

Fig.3.13 Effect of Relative Density on D_l

with samples prepared by the method of undercompaction. Therefore, the relation predicts reliable modulus for Monterey No. 0 sand and similar type of sands.

As a matter of interest, the G_{max} values from different reported relations are compared with the measured values (Fig.3.15). It can be inferred that the relation proposed by Seed and Idriss (1970) with density factor k_{2max} equals to 40, also produces similar results as the measured values. However, the k_{2max} value which depends on density conditions is hard to select correctly. The relation proposed by Chung et. al. (1984), Fig. 3.15-predicts the measured G_{max} at higher confining pressures. However at low confining pressures, the difference between the predicted and measured values is significant, perhaps because the relation is based on very limited test data. The relation proposed by Edil and Luh (1978) underestimates at lower confining pressures. The relations proposed by Hardin (1978) and Drenevich (1978) are found to overpredict G_{max} values in case of Monterey No. 0 sands. The difference may be attributed to the type of soil, testing technique, sample preparation etc. being different from those adopted in this study.

The proposed equation for dynamic longitudinal modulus, E_{max} (Eqn. 3.18) fits the experimentally determined values (Fig.3.16). The relation may be helpful in a situation where longitudinal mode of vibration is dominant. More field and laboratory test data is however needed to put this relation to a firm foundation.

The measured dynamic shear and longitudinal dampings are compared with computed values from proposed relations in Fig. 3.17 and 3.19 respectively. The large difference between computed and measured values is mainly caused by experimental error associated with the determination of damping. Fig. 3.18 shows the variation of dynamic shear damping with dynamic shear strains for a particular case of effective confining pressure equal to 98 kpa and relative density equals to 43% (e = 0.72353). At low strains, there is no appreciable difference among measured values, proposed and reported relations. However at large strains, the difference in value of damping is very significant.

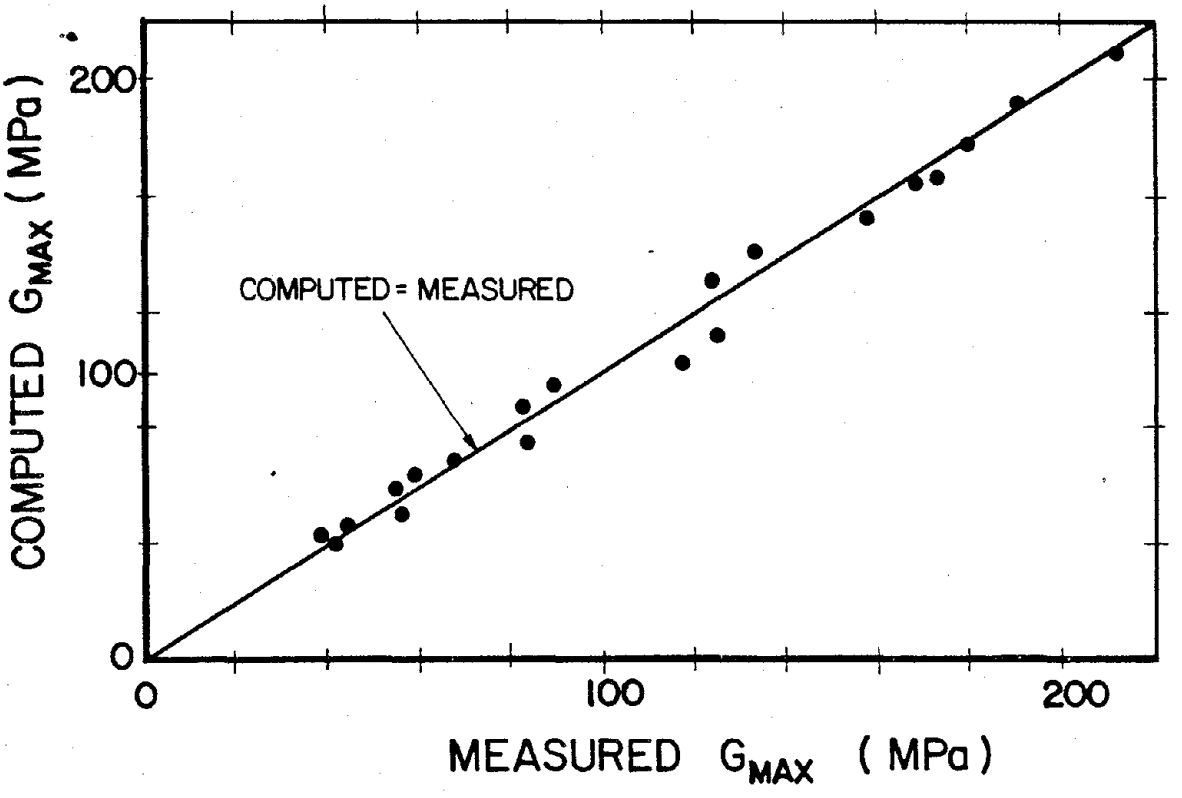

Fig.3.14 Evaluation of Relationships for Maximum Shear Modulus

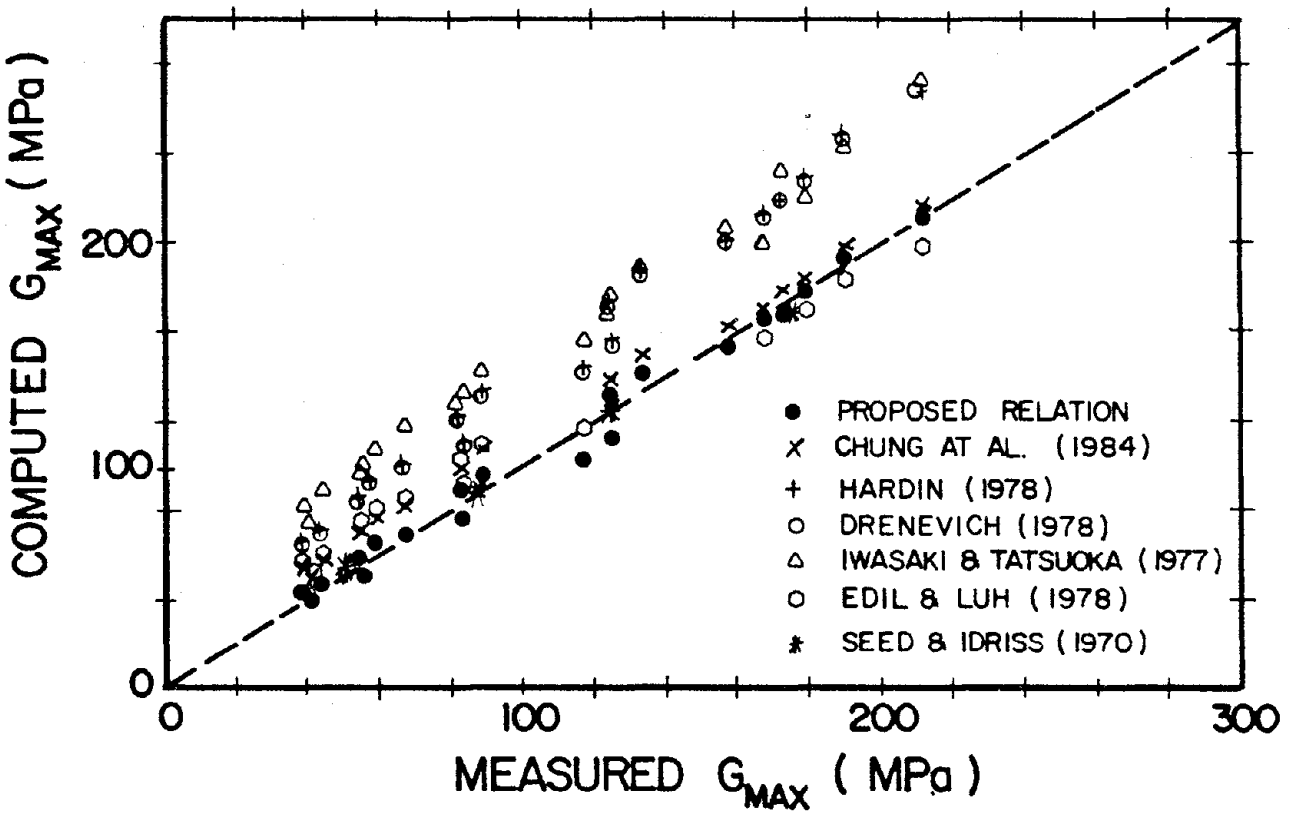

Fig.3.15 Evaluation of Relationships for Maximum Shear Modulus as compared to Experimental Results

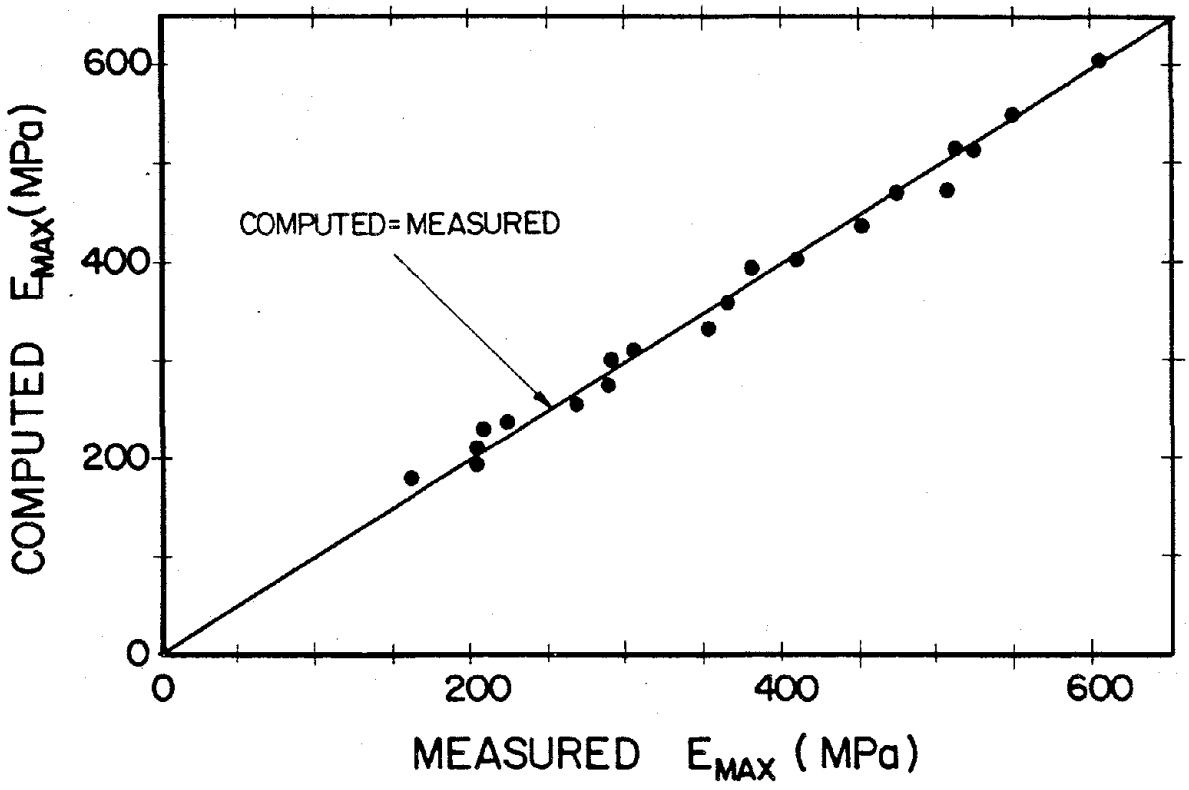

Fig.3.16 Evaluation of Relationship for Maximum Young's Modulus

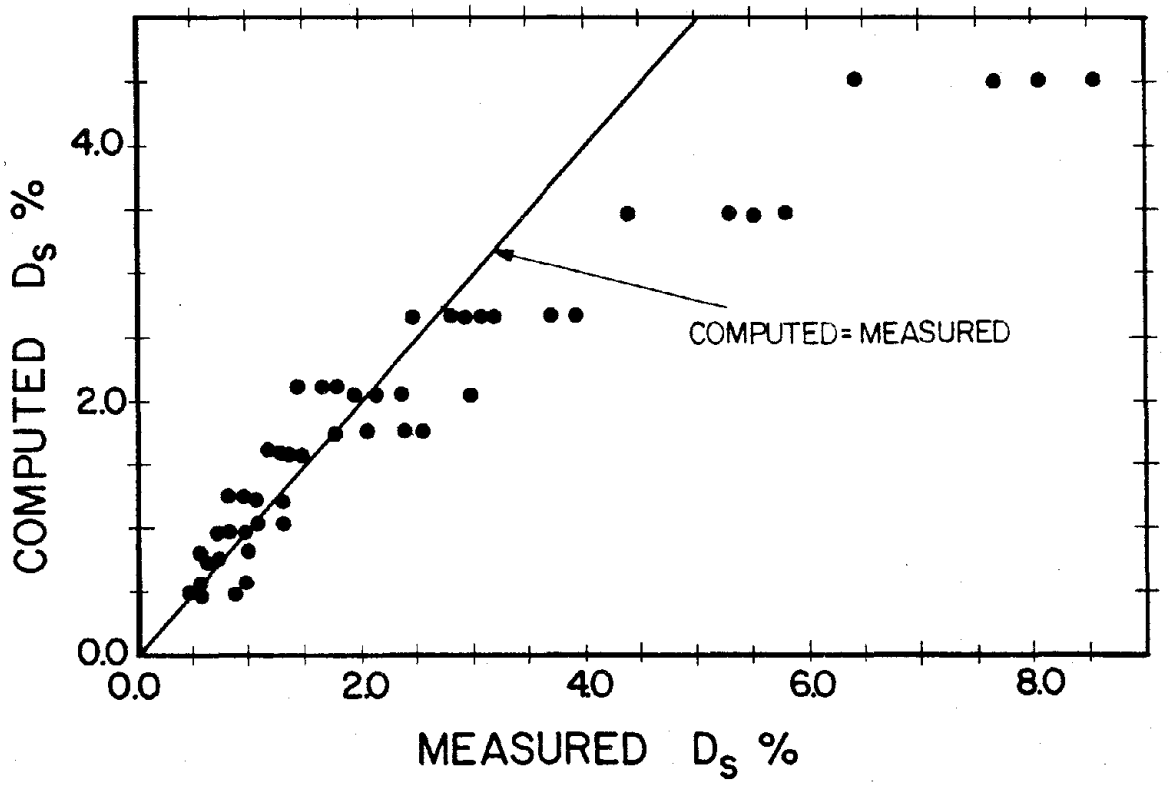

Fig.3.17 Evaluation of Relationship for Shear Damping

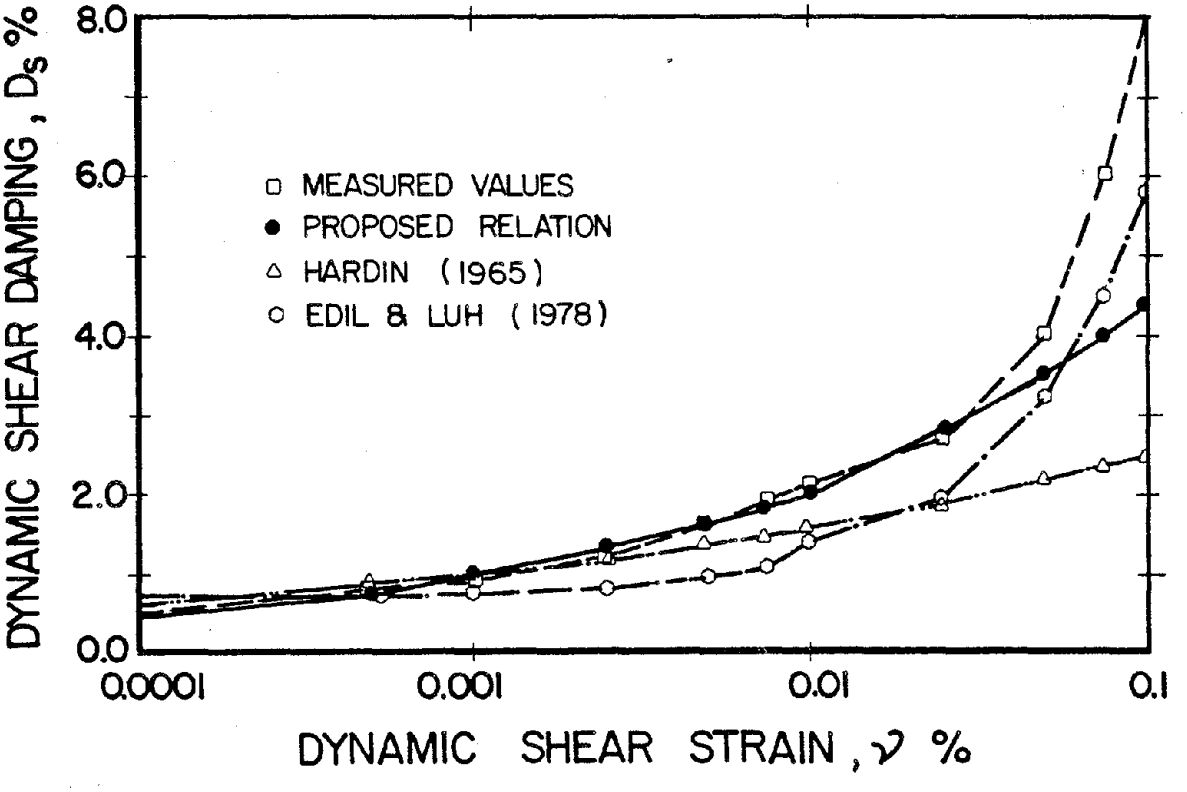

Fig.3.18 Comparison of Shear Damping values for $\bar{\sigma}_0$= 98 Kpa and e=0.7253

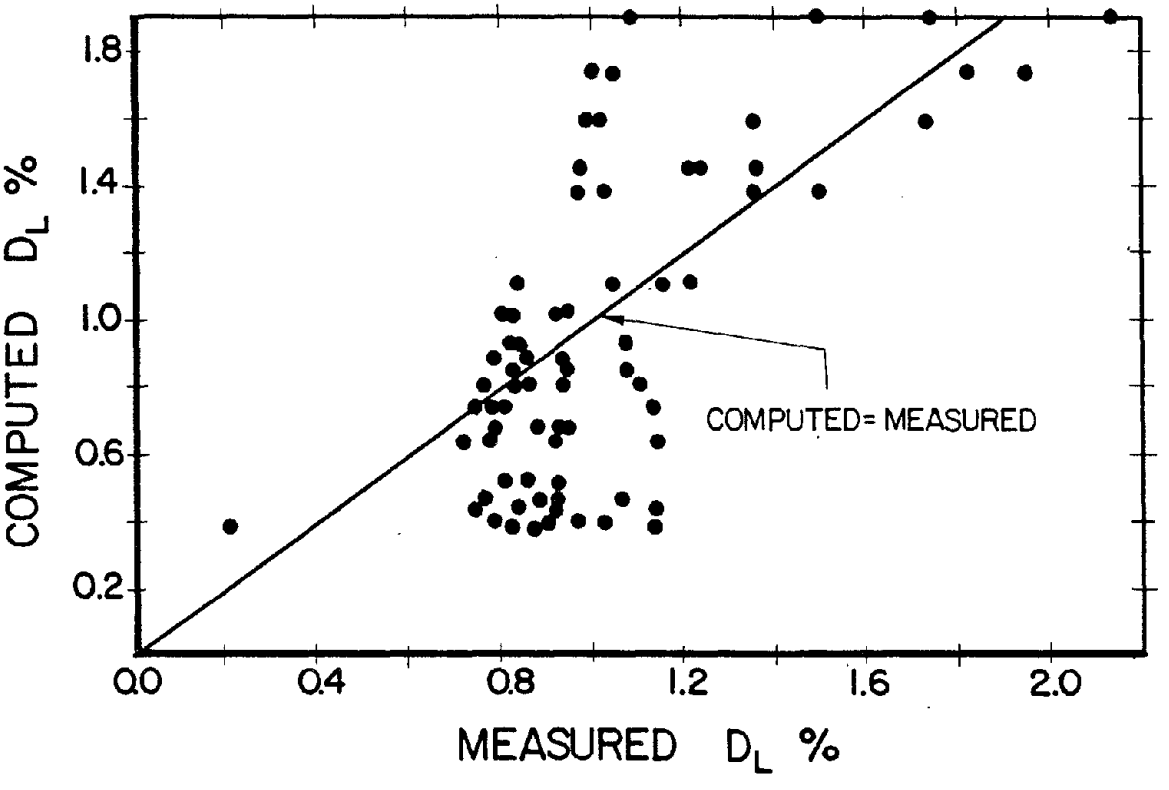

Fig.3.19 Evaluation of Relationship for Longitudinal Damping

3.8 SUMMARY

The following conclusions are drawn from this study:

1. The reported relations for dynamic shear modulus (G_{max}), dynamic Young's modulus (E_{max}), dynamic shear damping (D_s) and dynamic longitudinal damping (D_l) for sands at low strain levels are listed and discussed.

2. Based on experimental results with resonant column device on Monterey No. 0 sand, new and modified relations for G_{max}, E_{max}, D_s and D_l are proposed. These relations being non-dimensional can be used for any system of units.

3. An expression for computation of dynamic poisson's ratio is given and its validity discussed.

4. The developed relations for G_{max} and D_s are compared with experimental results and other reported relations. It is found that hitherto previously reported relations overpredict moduli and underpredict damping in case of Monterey No. 0 sand.

5. The relation of E_{max} and D_l are proposed afresh. More field and experimental results are required to establish these relations accurately.

Chapter IV

DYNAMIC BEHAVIOR OF CEMENTED SANDS AT LOW STRAINS

4.1 INTRODUCTION

The dynamic properties of uncemented sands, namely dynamic shear and Young's moduli and damping ratios under conditions of high frequency of loading, often ranging from approximately 20 Hz to 1000 Hz and small strain amplitudes of the order of approximately 10^{-6} to 10^{-4} rad or m/m, based on modified Drenevich resonant column tests are given in greater detail in chapter III. Stabilization of sand with cement to improve its properties has been in practice since long time. Considerable research is reported on static behavior of artificially and naturally cemented sands (Wissa and Ladd, 1965; Saxena and Lastrico, 1978; Dupas and Pecker, 1979; Clough et. al., 1983; Avramidis and Saxena, 1985 etc.). However information available regarding dynamic aspects of cemented sands especially at low strains is limited. Cyclic triaxial tests on cemented sands by Salomone et.al. (1978), Frydman et. al. (1980), Clough et.al. (1983), Avramidis and Saxena (1985) etc. helped in understanding liquefaction phenomenon. Chiang and Chae (1972) and Acar and El-Tahir(1986) reported resonant column test results with cement-treated sands, but tests conducted were only in torsional mode and at relatively low confining pressures.

This chapter describes the results of modified Drenevich resonant column tests on artificially cemented sands under both torsional and longitudinal modes of vibration. It discusses the effect of different variables such as cement content (CC), effective confining pressure ($\overline{\sigma}_0$), void ratio (e) etc. on dynamic shear modulus (G^*), dynamic Young's modulus (E^*), dynamic shear damping (D_s^*) and dynamic longitudinal damping (D_l^*). The newly developed empirical relations and their evaluation are revealed. A discussion on correlation of dynamic moduli and damping ratios with static triaxial test results is also given.

4.2 EXPERIMENTAL INVESTIGATION

Test Materials: The materials employed are Monterey No. 0 sand

and Portland Cement Type I. The index properties and grain size distribution of the sand used are shown in Table 2.1 and Fig. 2.1 respectively.

Sample Preparation: All the samples are reconstituted by method of undercompaction (Ladd, 1980) on a stand inside a plastic mold made out of PVC tubing. The samples are prepared in 8 layers with 6% degree of undercompaction. Depending on desired density and cement content, the proper amounts of dry sand and dry cement per layer are mixed thoroughly first and then 8% water (based on dry weight of cement and sand) is added. The wet homogeneous mixture is placed inside the mold and compacted with a tamper. The procedure is repeated for the rest of the layers. The sample in the mold is then cured after placing filter paper and perforated lucite plate at either ends. When extruded from the mold, the diameter and height of samples are 71.12mm and 177.8 mm respectively.

Test Setup and Procedure: The Drenevich type Long-Tor resonant column apparatus has been successfully used for testing sand and clay specimen. However, when cemented sand samples were tested with this device, inconsistent results are obtained. The inconsistency is attributed to the significant stiffeness of sample relative to the stiffeness of the device. Consequently the device was modified and the overall stiffeness of the apparatus considerably increased. The modified device was recalibrated and its performance verified by conducting tests on uncemented sands and comparing the results with those obtained with the original setup under similar conditions (Fig. 4.1).

The sample is saturated and subsequently consolidated at desired confining pressure. Knowing that the specimen is stiffer in compression than in shear, it is tested first in longitudinal vibratory mode by increasing confining pressure. When this is complete and when the sample is consolidated at the highest confining pressure, the testing is continued in the torsional mode by reducing the confining pressure. Fig. 4.2(a) shows that the dynamic shear modulus remains the same irrespective of fact that it is obtained by testing virgin specimens or by testing specimens which were first subjected to the longitudinal vibratory mode. On the other hand the testing sequence in Fig. 4.2(b)

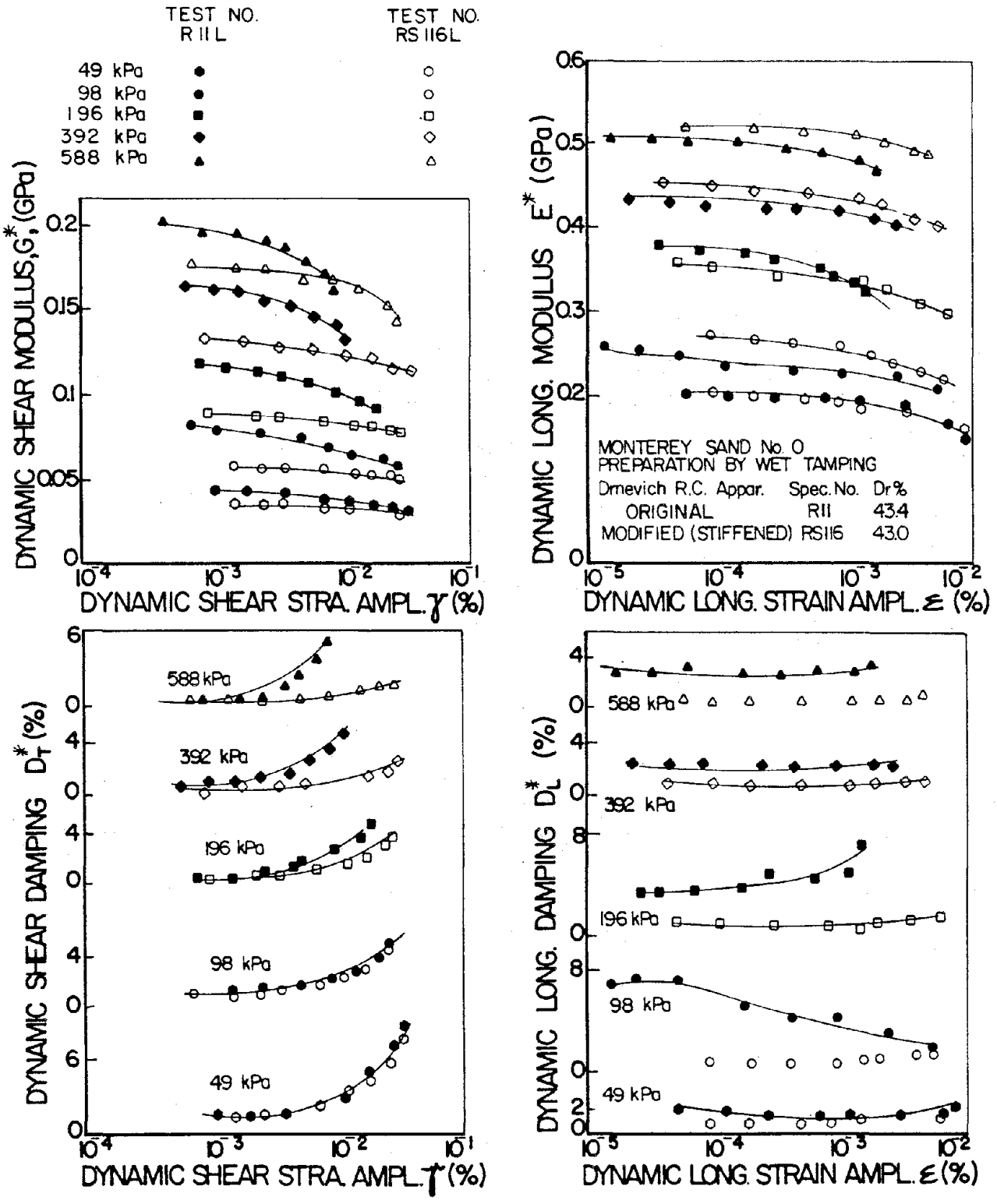

Fig.4.1 Performance of Modified Drenevich Long-Tor Resonant Column Apparatus

indicates that there is a difference in the value of dynamic Young's modulus obtained using a virgin or a pretested specimen. This difference varies with the confining pressure and is found to be less than 10% on the basis of tested samples. For each confining pressure, the stress amplitude is varied and the readings of LVDT and natural frequency are noted. From initial few tests, the effect of saturation has been found negligible (Fig.4.3). Therefore it was decided to test only dry samples. The test results are utilised to calculate dynamic strains (γ or ϵ) dynamic moduli (G^* or E^*) and dynamic damping ratios (D_s^* or D_l^*). Fig. 3.1 shows the definitions followed in this study. Typical results for a specific case of relative density (D_r) = 25%, CC = 2% and CP = 15 days are presented in Fig. 4.4.

Variables: The different variables and their range of values considered in this investigation are given in Table 4.1.

4.3 ANALYSIS OF TEST RESULTS

There are several factors influencing the dynamic properties of soils (chapter III). However, depending upon the situation only few of them may have major impact on the dynamic behavior. The main objective of this study is to investigate the beneficial effects of cementation on the dynamic behavior of sands at low strain amplitudes. Therefore, this section concentrates on the effects of important parameters namely strain amplitude, effective confining pressure, void ratio, cement content and curing period on dynamic moduli and damping ratios of cemented sands.

Effect of Strain Amplitude: The typical results presented in Fig. 4.4 clearly show that G^* and E^* decrease and damping ratios (D_s^* and D_l^*) increase with increase in strain amplitude. This trend is observed in all the tests. The decrease in moduli is mainly due to the nonlinearity of soils and the increase in damping ratios is caused by energy absorption due to particle rearrangement. Importantly, it is observed that for strains less than 10^{-4}%, the G^* and E^* values remain constant, hence are called maximum dynamic shear modulus (G_m^*) and maximum dynamic Young's modulus (E_m^*) respectively. Any dynamic stress-strain relation should capture the nonlinear variation of

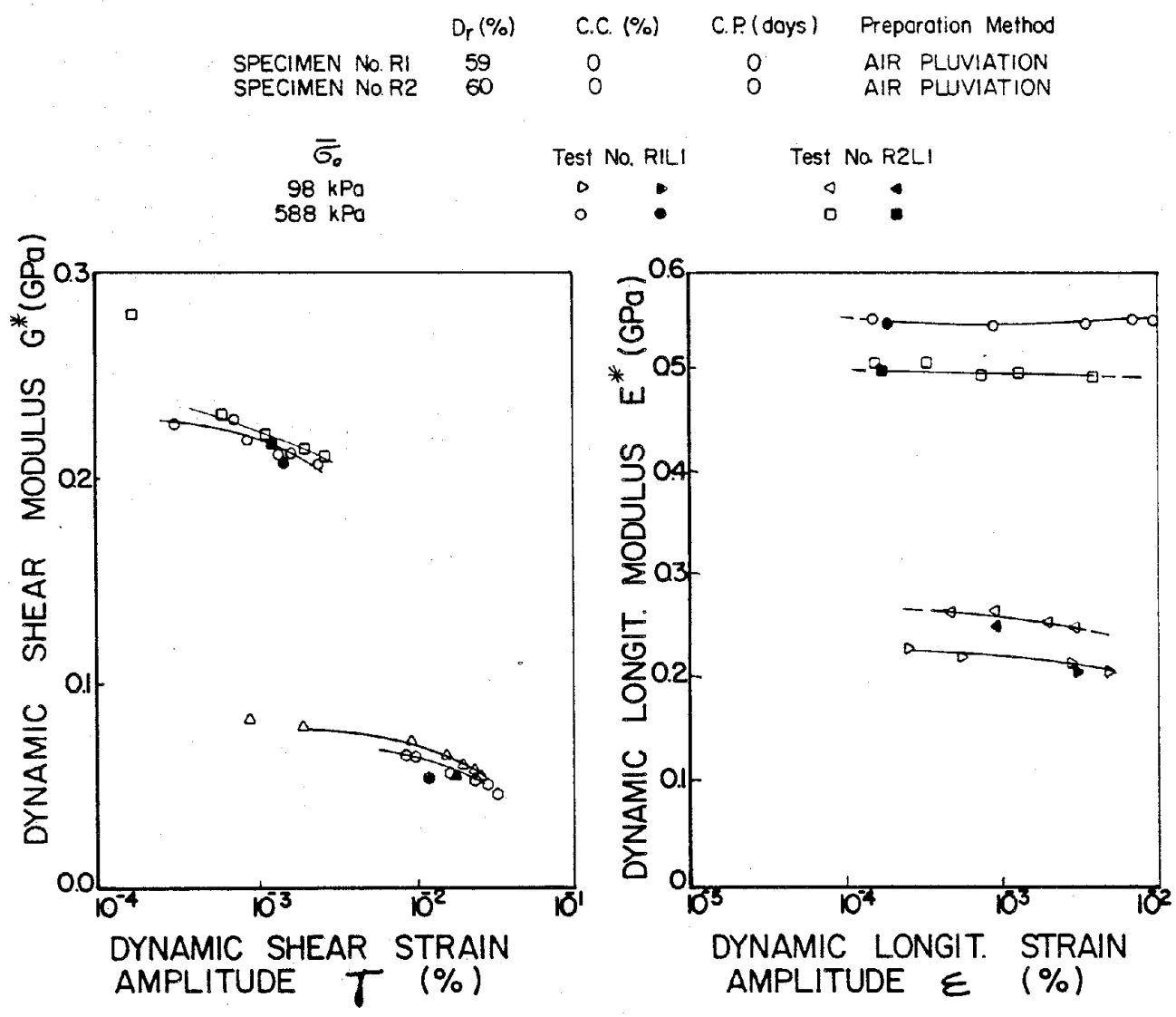

Fig.4.2 Influence of Testing Sequence

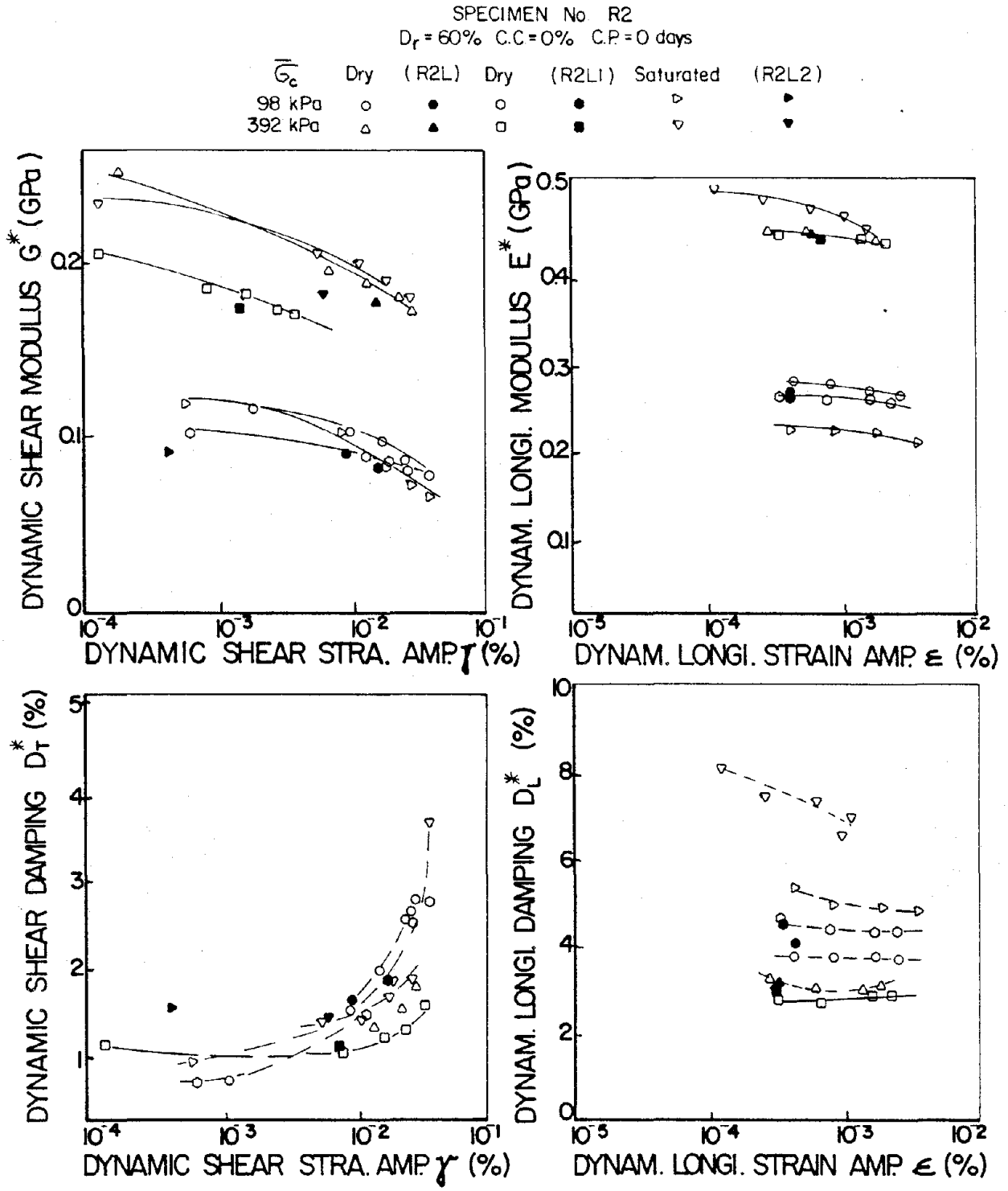

Fig.4.3 Effect of Saturation

Table 4.1 Variables and their Range of Values for Resonant Column Testing

VARIABLE	SYMBOL	UNITS	RANGE OF VALUES
Void Ratio	e	-	0.7775, 0.7253, 0.6760, 0.6180
Cement Content	CC	%	0, 1, 2, 5, 8
Effective Confining Pressure	$\bar{\sigma}_0$	Kpa	49, 98, 196, 392, 588
Curing Period	CP	Days	15, 30, 60

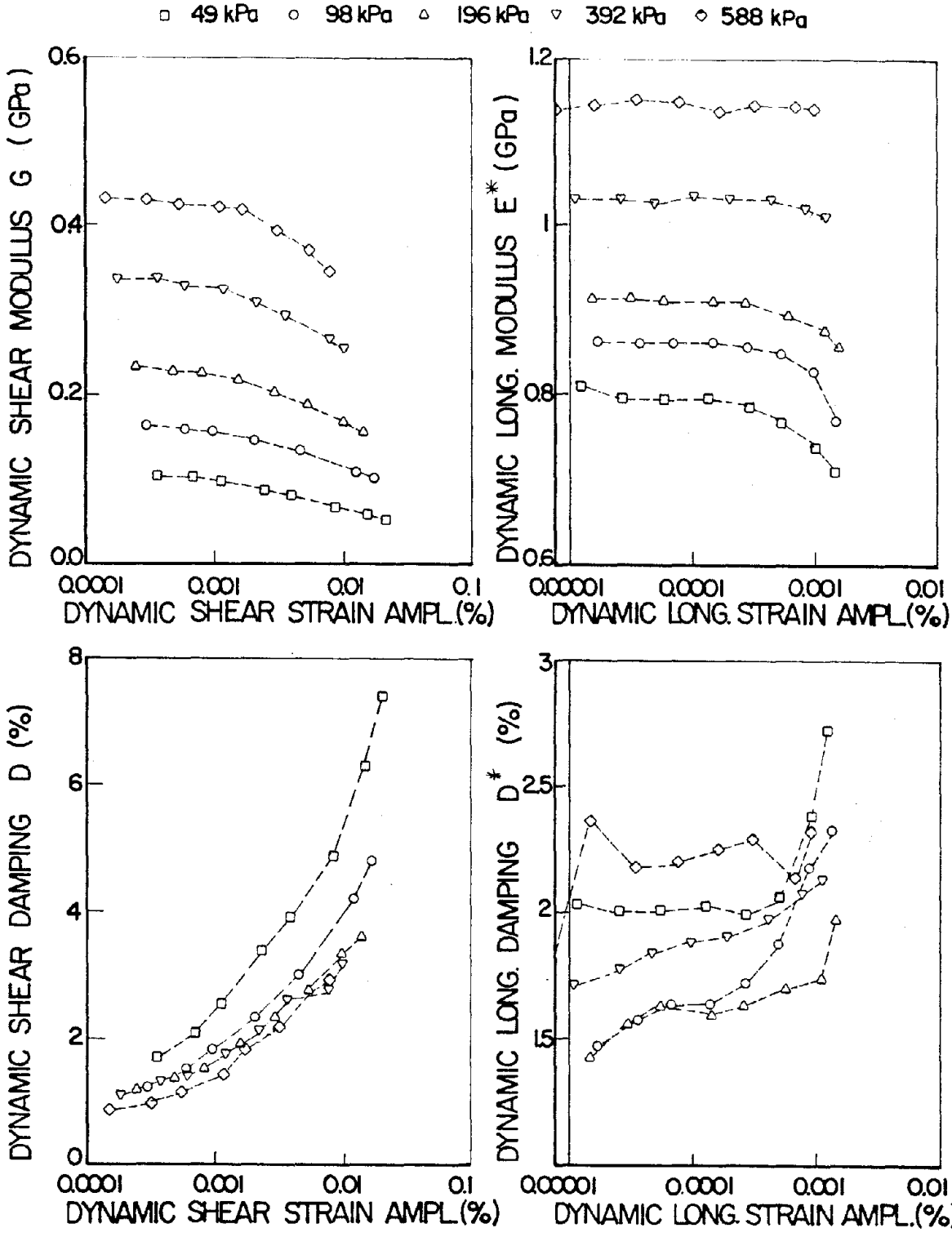

Fig.4.4 Typical Results from Resonant Column Testing for the case of D_r= 25%,CC=2% and CP=15 days

G^* and E^* for strains greater than $10^{-4}\%$. The increase of D_s^* and D_l^* with strain is also nonlinear. Generally D_l^* are found smaller than D_s^* for similar conditions. The shape of D_l^* versus ϵ curves is more often erratic than D_s^* versus γ curves.

Effect of Confining Pressure: Fig. 4.4 depicts the effect of confining pressure. Other tests with different parameters also showed similar trends. As the effective confining pressure ($\overline{\sigma}_0$) increases, the G^* and E^* are increased, whereas D_s^* and D_l^* are decreased. The increase in G^* and E^* due to cementation (i.e. ΔG_m and ΔE_m) versus $\overline{\sigma}_0$ for different cement contents on log-log scale are found to be straight lines as shown in Figs. 4.5 and 4.6 respectively. It can be concluded from Fig. 4.5 that in the lower cementation range where the sample is softer, the effect of $\overline{\sigma}_0$ on ΔG_m is more pronounced than in the higher cement content values where the sample is stiffer. This is mainly because of larger changes in void ratio due to the initial lower confining pressure causing the soil to become stiffer faster. Fig. 4.6 leads to an interesting conclusion. It shows that effective confining pressure ($\overline{\sigma}_0$) does not contribute to the increased dynamic maximum Young's modulus (ΔE_m) of cemented sands. The D_s^* and D_l^* decrease as confining pressure increases because at higher confining pressures there are more intergrain contacts thus there are more wave pathways, and therefore, less energy is expected to be dissipated during wave propagation.

Effect of Cement Content: This is the most important parameter for cemented sands. The values of G* and E* increase as the cement content increases with all other parameters kept constant, as shown in Fig. 4.7. It may be noted that there is large increase of these values with the increase of cement content from 2% to 5% (Fig. 4.5 and Fig.4.6). A definite increase of D_s^* and D_l^* is observed (Fig 4.7) with lower ranges of cementation and a subsequent decrease in these values at higher ranges of cementation. It is also seen that the effect of cement content is larger on D_l^* than D_s^*.

Usually as a material becomes stiffer, that is, as its elastic modulus increases (in this case due to increase of cement content), its damping ratio expected to be reduced. Accordingly, the above described behavior of the increase

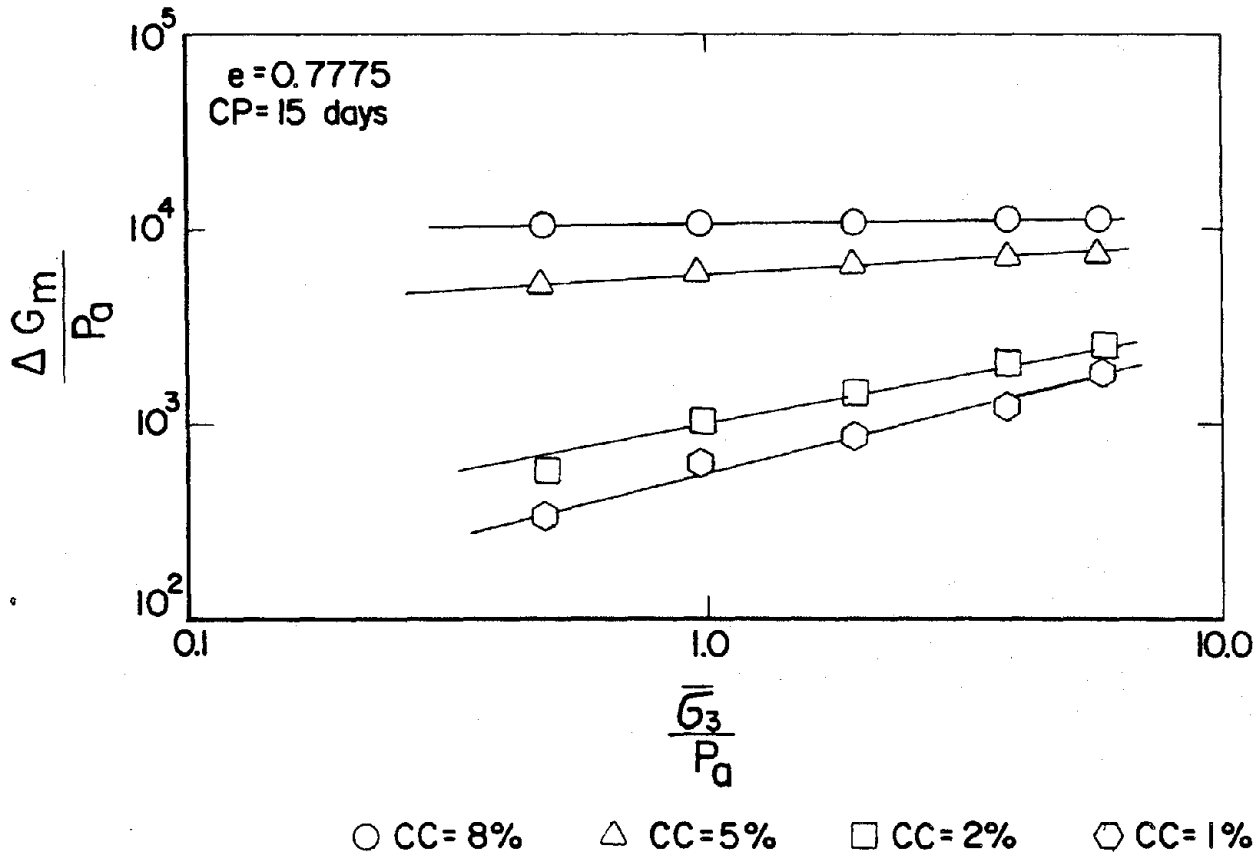

Fig.4.5 Effect of Confining Pressure on Increase in Maximum Dynamic Shear Modulus

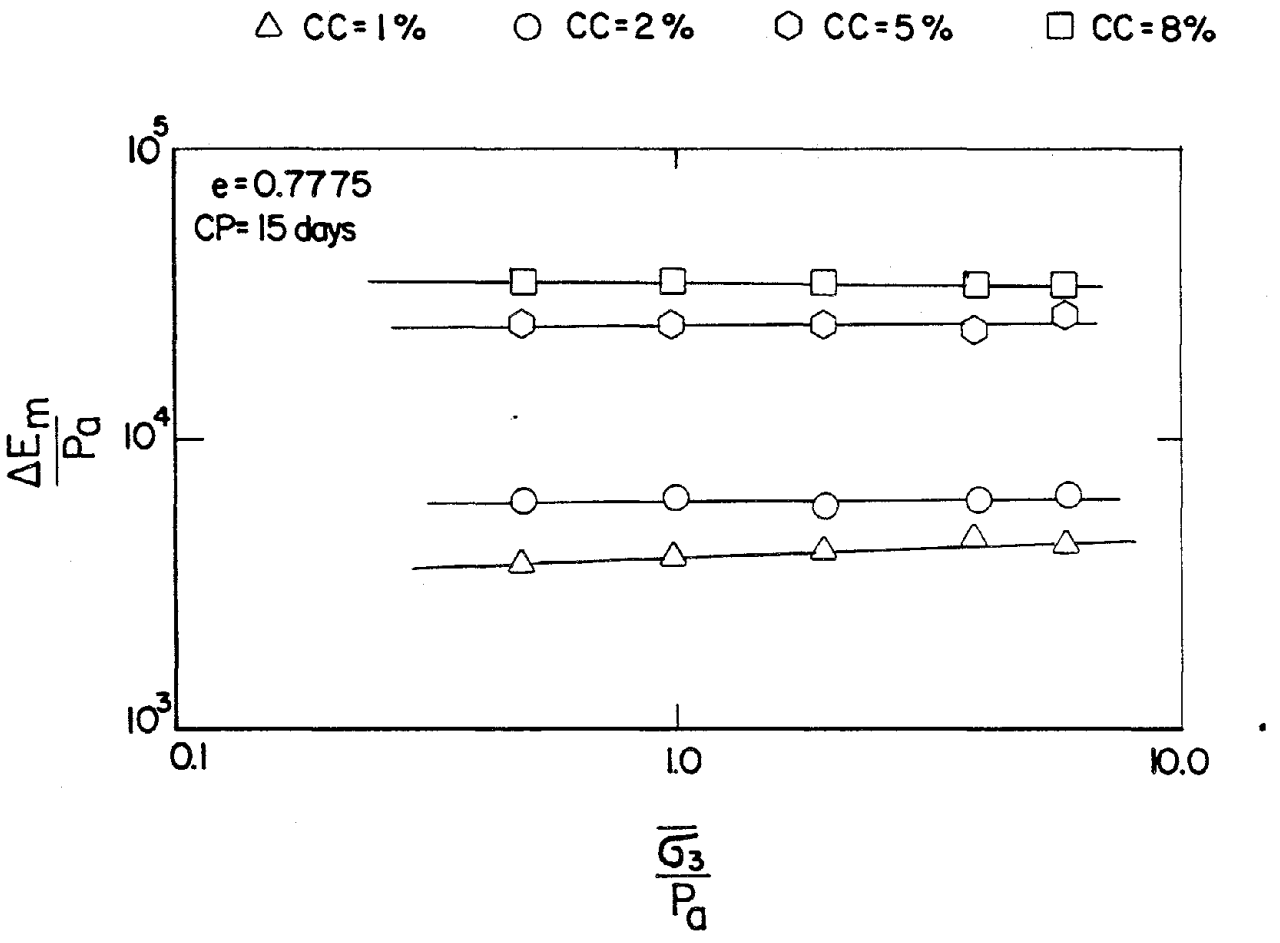

Fig.4.6 Effect of Confining Pressure on Increase in Maximum Dynamic Young's Modulus

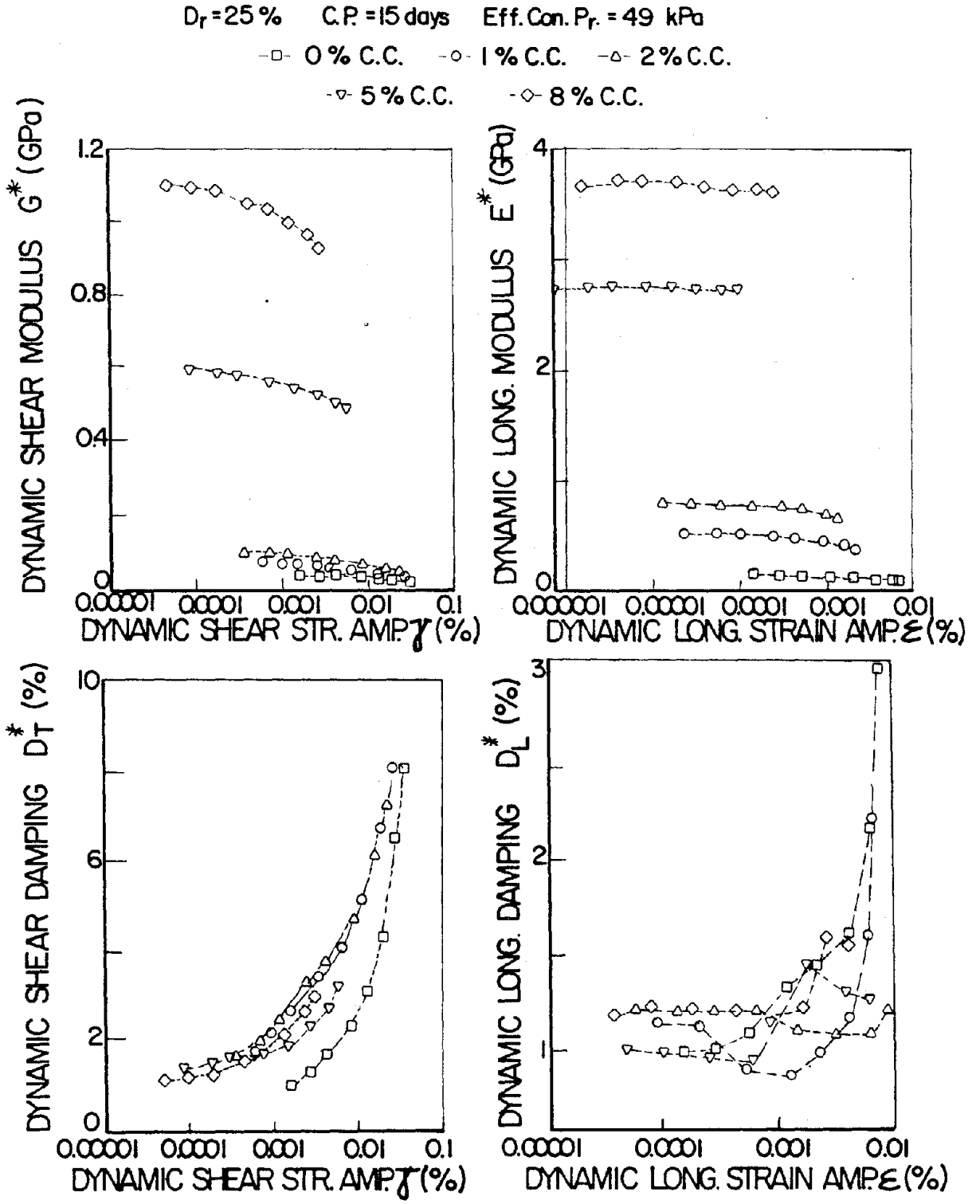

Fig.4.7 Effect of Cement Content on Dynamic Moduli and Damping Ratios

of D_s^* and D_l^* with increasing cement content from 0% to 5% is unexpected by a first glance, and may be explained adequately using the following postulate. Since the damping ratio in soils is related to the amount of energy dissipated during wave propagation through its mass (energy spent to rearrange the grains through interslippage or through crushing of the asperities of individual grains at their contacts), the energy spent for the wave to propagate through a weakly cemented sand sample should be larger than the energy spent by the wave propagation through a similar clean, uncemented specimen (prepared under similar condition same relative density, effective confining pressure, etc.). To clarify this point, the following hypothetical cases will be considered.

Case 1: Assume that there are two dry similar specimens, one constituted of clean sand and the other of a similar sand and dry Portland cement in the same quantity. The latter of the two specimens will be associated with greater damping ratio because the Portland cement particles will "stick" around the originally clean sand grains and therefore, the contacts between the individual grains will become less clean and thus more energy will be spent for the wave to propagate through.

Case 2: Assume that there are two similar specimens, one constituted of clean sand and the other of Portland cement paste in which many sand grains similar to those of the clean sand constituting the first sample are spread. In this case the Portland cement paste specimen, when allowed to solidify, will have the lowest damping ratio because less amount of energy is dissipated during the propagation of the wave through the solid and continuous cement matrix than through the contacts between the clean sand grains of the clean sand specimen.

Case 3: Assume that there are two similar specimens. The first constituted of clean sand and the second of a similar type of sand mixed with a small amount of Portland cement and adequate water. In the second specimen the clean grains of the sand will become dirty due to the sticking of the cement particles on the sand grains and at the same time, depending on the amount of the cement in the mixture, a number of bonds varying in strength will be created between the sand grains. At small cementation levels the effect of the

presence of Portland cement is to coat the areas of the contacts between the individual sand grains and thus increase the damping ratio. At high cementation levels on the other hand, the similar effect is to create more and stronger bonds and thus reduce the damping ratio.

Summarizing, as the cement content increases, from nearly zero percent to a level at which the "coating of the sand grains" effect is governing the dissipative mechanism for the wave propagation through the soil, the damping ratios should increase to its maximum value, and then should start decreasing with a further increase in cement content. This will happen because of the increase in the number of the created strong cementing bonds and, governs the dissipative mechanism by reducing the damping ratio. According to the above described postulate from the experimental results of this study the cement content at which the peak damping ratios are reached should lie between the values of 5% and 8% as it may be concluded from Figure 4.7. This value of the cement content may vary depending for example on the effective confining pressure. The fact that the damping ratio during wave propagation increases as the degree of coating (cleanliness) decreases was also observed by Duffy and Mindlin (1957) who performed experiments to determine compressional wave velocities and associated rates of energy dissipation in bars consisted of face-centered cubic arrays of spheres. In their findings amongst other conclusions they reported that "improper cleaning of the balls (using only acetone for instance) easily doubled the values obtained for W_T." In their experiment the energy loss per cycle of vibration was defined as W_T.

At this point it may be also mentioned that a similar increase in the damping ratio by increasing the amount of additives (Type I Portland cement, lime, lime-fly ash) was observed by Chiang and Chae (1972) and by Chae and Chaing (1978), however an explanation of the observed behavior was not provided. In their work they measured torsional damping ratios, D_s^*, which continuously were increased in the full range of cement content considered from 0% to 6%.

Effect of Void Ratio: The effects of relative density, grain size and

grain size distribution are indirectly reflected by void ratio (e). Fig. 4.8 shows that G^* and E^* increase as the void ratio decreases. The increase of G^* and E^* with decrease of void ratio strongly depends on the increase in effective confining pressure; especially at lower cementation range because of the effect of consolidation under these conditions is more pronounced. In general, the rate of increase of G^* and E^* with e is reduced with the decrease of e. It may be observed from Fig. 4.8 that D_s^* and D_l^* are not affected strongly by e.

Effect of Curing Period: As curing period (CP) increases G^* and E^* increase (Fig. 4.9). This is attributed to the fact that with time the cement is hydrated and the bonds become stronger. The increase of moduli with CP is greater at lower ranges of CP and relatively smaller at higher ranges of CP. Also, the rate of increase of moduli with CP is not affected by the increase in the $\overline{\sigma}_0$. It is observed from Fig. 4.9 that CP does not strongly affect damping ratios (i.e. D_s^* and D_l^*).

4.4 EMPIRICAL RELATIONS

Stabilization of sands with cement is a very valuable concept in the design of foundations and pavements to withstand dynamic loads. If dynamic properties of such cemented sands namely G^*, E^*, D_s^* and D_l^* are required at low strains, the resonant column testing is the most accepted solution. The test though unique is not very commonly used. Therefore any empirical relations developed based on reliable resonant column test results are very helpful for preliminary estimation of dynamic properties of soils at low strain levels.

Strain amplitude, effective confining pressure and void ratio are the three important parameters affecting the moduli and damping ratios of uncemented sands (chapter III). But in case of cemented sands the problem is complicated by the additional two major parameters i.e. cement content and curing period. Based on extensive resonant column test results described in the previous sections, interrelationship among these parameters for maximum moduli (G_m^* and E_m^*) and damping ratios (D_s^* and D_l^*) are developed and are presented in this section. Two equations for each moduli are proposed because of large difference in the behavior of cemented sands at low and high cemen-

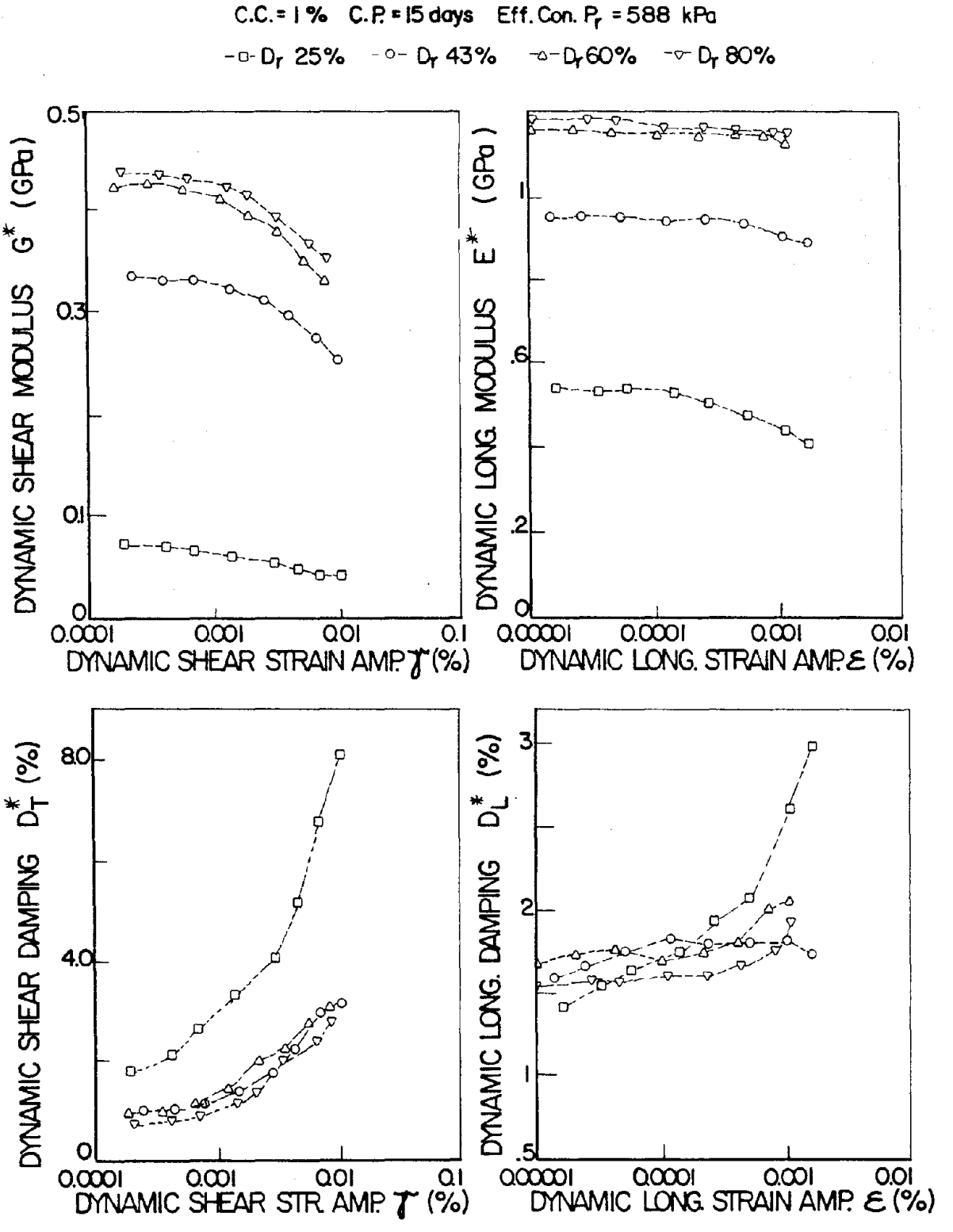

Fig.4.8 Effect of Density on Dynamic Moduli and Damping Ratios

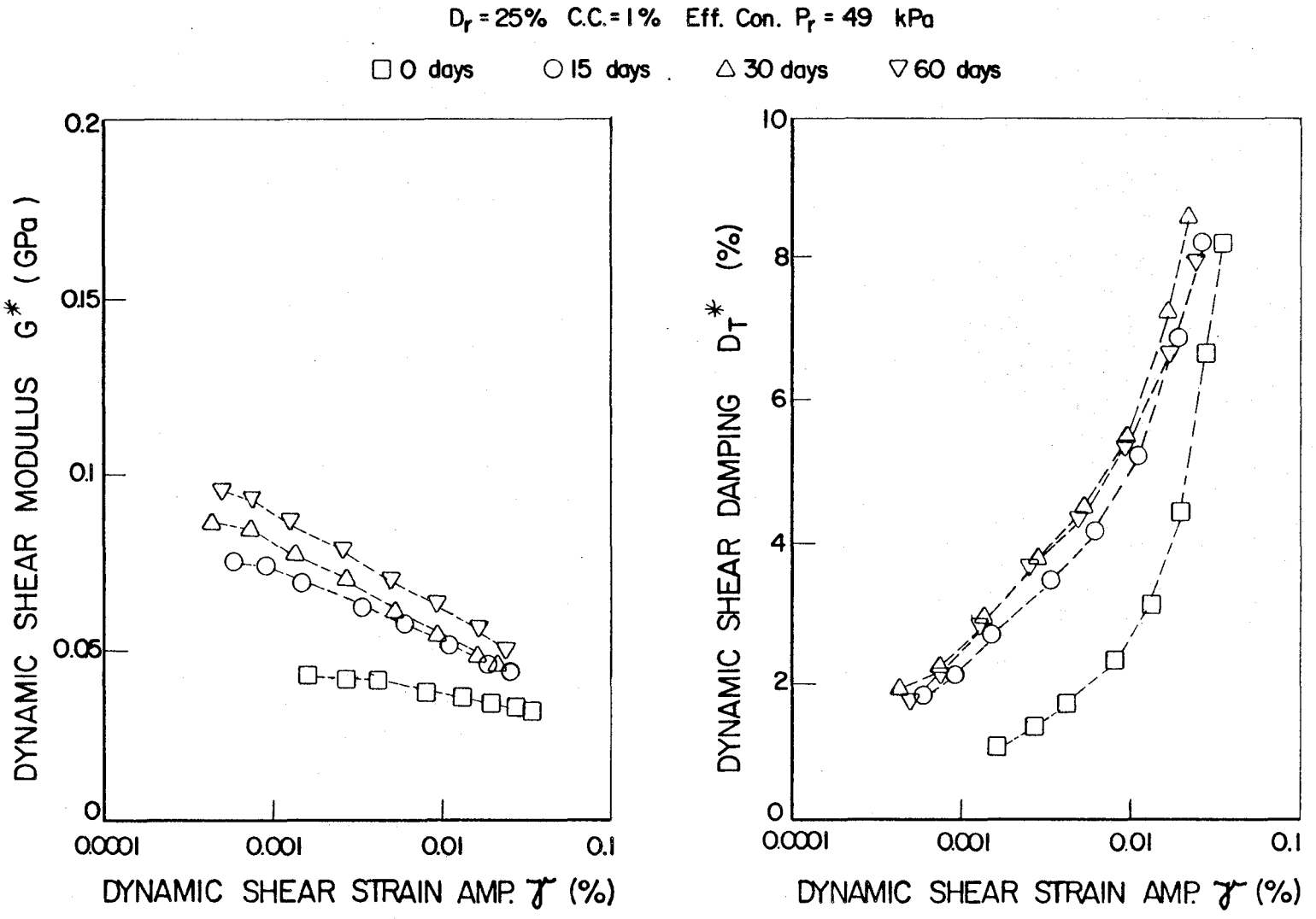

Fig.4.9 Effect of Curing Period on Dynamic Moduli and Damping Ratios

tation conditions as explained in the previous section. Also since the effect of curing is not very significant after initial few days, all the relations are developed for curing period of 15 days.

Dynamic Shear Modulus: The dynamic shear modulus (for$\gamma < 10^{-4}\%$) of cemented sand (G_m^*) may be expressed as the summation of dynamic shear modulus (for $\gamma < 10^{-4}\%$) of uncemented sand (G_m) and increase in modulus due to cementation (ΔG_m). The increase in dynamic shear modulus (ΔG_m) depends on cement content (CC), effective confining pressure ($\overline{\sigma}_0$), void ratio (e) and curing period (CP). Hence, we have

$$G_m^* = G_m + \Delta G_m \tag{4.1}$$

In nondimensional form

$$\frac{\Delta G_m}{P_a} = \frac{G_m^* - G_m}{P_a} \tag{4.2}$$

Based on regression analysis, relation for increase in maximum dynamic shear modulus (ΔG_m) due to cementation is obtained and given below;

$$\frac{\Delta G_m}{P_a} = \frac{172}{(e - 0.5168)}(CC)^{0.88}\left(\frac{\overline{\sigma}_0}{P_a}\right)^{(0.515e - 0.13CC + 0.285)} \tag{4.3}$$

$$\frac{\Delta G_m}{P_a} = \frac{773}{e}(CC)^{1.2}\left(\frac{\overline{\sigma}_0}{P_a}\right)^{(0.698e - 0.04CC - 0.2)} \tag{4.4}$$

Equation 4.3 is based on test results with CC $< 2\%$ whereas equation 4.4 is applicable at higher cementation but CC $< 8\%$. CC and e are expressed in percentage and decimal form respectively. The units of $\overline{\sigma}_0$ are same as atmospheric pressure P_a. Once ΔG_m is known, G_m^* can be found from eqn. 4.2. The following equation proposed in chapter III is also easy to evaluate G_m

$$G_m = \frac{428.2}{(0.3 + 0.7e^2)}(P_a)^{0.426}(\overline{\sigma}_0)^{0.574} \tag{4.5}$$

The ΔG_m values calculated based on Eqn. 4.3 and 4.4 are comparable with measured values as shown in Fig. 4.10.

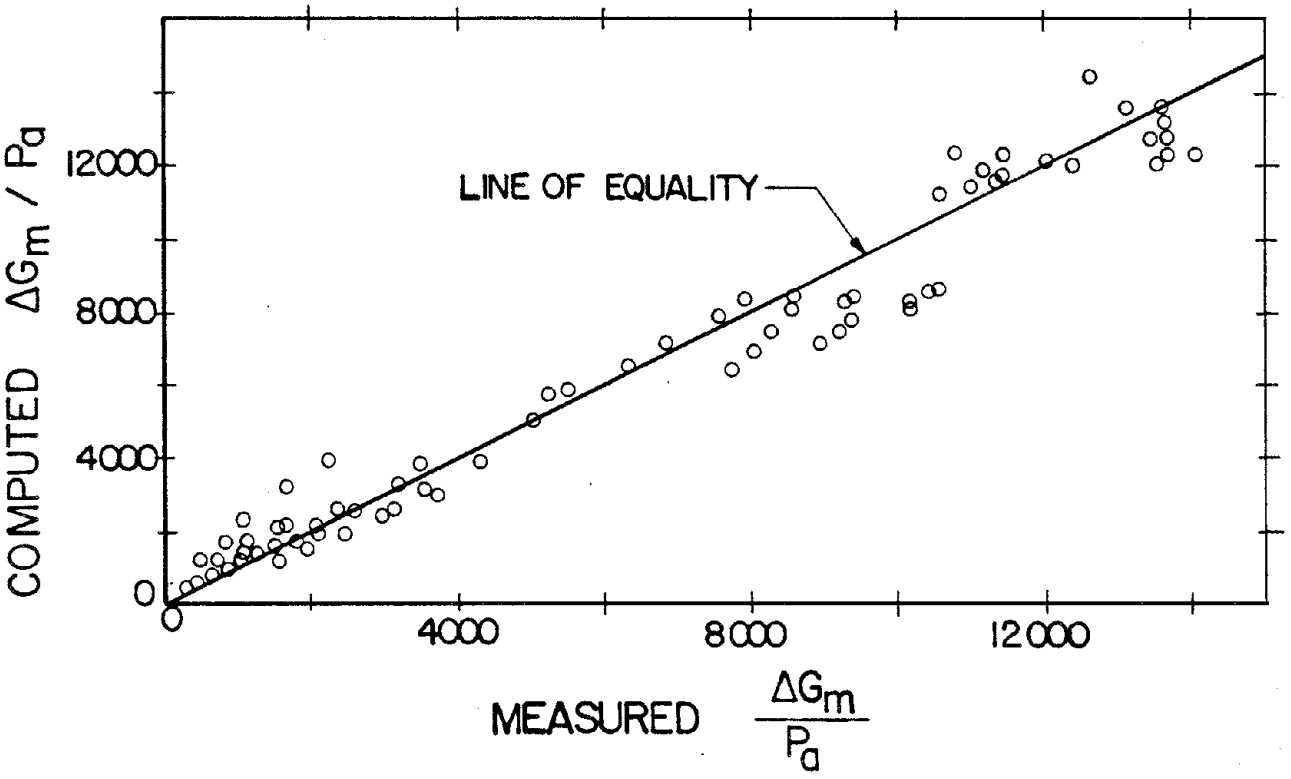

Fig.4.10 Comparison of Measured and Computed values of increase in Dynamic Maximum Shear Modulus

It is interesting to note that Chae and Chiang (1972) observed no effect of void ratio on the increase of dynamic shear modulus (ΔG_m) of cemented sands and proposed the following equation:

$$G_m^* = (G_m - 0.343CC(\overline{\sigma}_0)^{0.5})(\overline{\sigma}_0)^{0.06CC} \tag{4.6}$$

G_m^* and G_m are dynamic shear moduli, in psi, of cement-treated and untreated sands, respectively, and CC is the cement content in percent. For calculating G_m, they recommended Hardin and Drenevich (1972) relations. For example for round-grained sand, the eqn. for G_m is given as below:

$$G_m = 2630\frac{(2.17 - e)^2}{(1 + e)}(\overline{\sigma}_0)^{0.5} \tag{4.7}$$

G_m and $\overline{\sigma}_0$ are expressed in psi.

As a matter of interest, a comparison between the relation proposed by Chae and Chiang (1972) and the newly developed relations (eqns. 4.3 and 4.4) is made for two specific cases, one with CC = 2% and e = 0.7253 and the other with same void ratio but CC = 6% as shown in Fig. 4.11. The difference can be attributed to the following factors:

(a) Mainly the relation proposed by Chiang and Chae(1972) is based on experimental results with limited range of parameters.

(b) In their relationship, the increase of G_m is independent of density.

(c) The type of sand used by them is uniform which may have significant difference in behavior than Monterey No. 0 sand because of difference in grain size and grain size distribution.

The proposed relation for G_m^* (eqns. 4.1-4.4) has the following advantages:

(a) It is non-dimensional, hence adoptable to any system of units.

(b) The effect of density (or void ratio) on increase of modulus is accomodated.

(c) The relation is based on extensive tests with wide range of parameters.

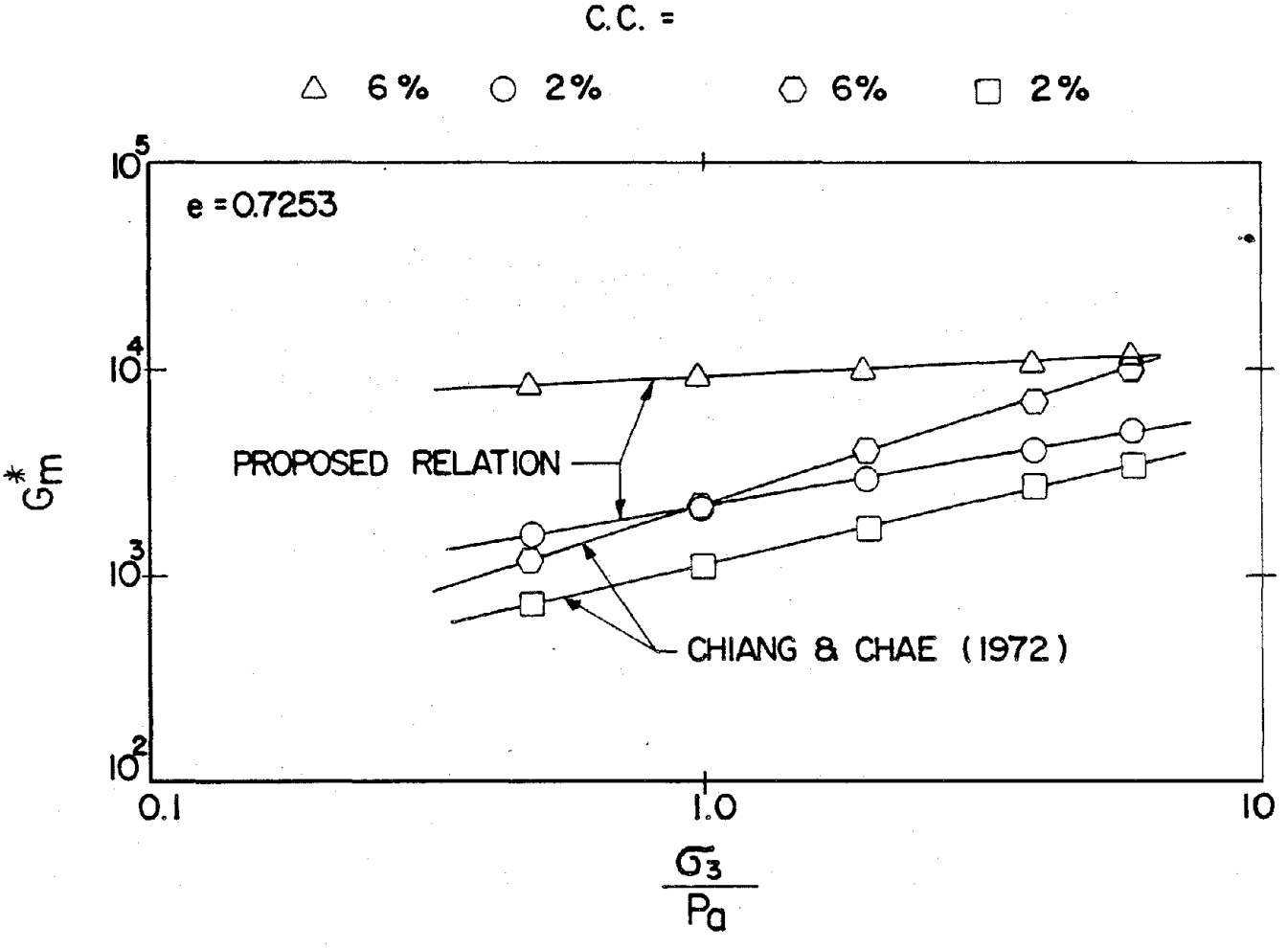

Fig.4.11 Comparison of Proposed Relation with the Relation developed by Chiang and Chae(1972) for Maximum Dynamic Shear Modulus

In a recent study on artificially cemented sand Acar and El-Tahir(1986) proposed the following relationship for maximum shear modulus:

$$G_m^* = R\frac{631}{(0.3+0.7e^2)}(P_a)^{0.57}(\overline{\sigma}_0)^{0.43} \tag{4.8}$$

where R is called stiffness ratio and is given by following equation in terms of cement content and void ratio:

$$R = 1 + (CC)^{0.49} - 2(CC)^{0.1}e^{4.6} \tag{4.9}$$

Acar and El-Tahir (1986) assume that there is no effect of confining pressure on the increase in maximum shear modulus for cemented sand. As explained earlier, indeed there will be significant effect of $\overline{\sigma}_0$ on maximum shear modulus at lower cementation. A comparison between the proposed relation and the relation developed by Acar and Tahir (1986) at low and high cementation levels is shown in Fig.4.12.

Dynamic Young's Modulus: As compared to dynamic shear modulus (G^*), the literature on dynamic Young's modulus (E^*) for uncemented sands is little and especially extremely scarce for cemented sands. It is the general practice to compute E^* from G^* using "appropriate" dynamic poisson's ratio (ν). In this section an empirical relation for maximum dynamic Young's modulus (E_m^*) of cemented sands is proposed for the first time. Also an attempt is made to determine the dynamic poisson's ratio with the test results in longitudinal and torsional modes on the same cemented sand sample in modified resonant column device.

The maximum dynamic Young's modulus (E_m^*) is expressed as below;

$$E_m^* = E_m + \Delta E_m \tag{4.10}$$

in which E_m = maximum dynamic Young's modulus ($\epsilon < 10^{-4}\%$) of uncemented sand and ΔE_m = increase in modulus because of cementation effects. In nondimensional form, the above expression can be written as:

$$\frac{\Delta E_m}{P_a} = \frac{E_m^* - E_m}{P_a} \tag{4.11}$$

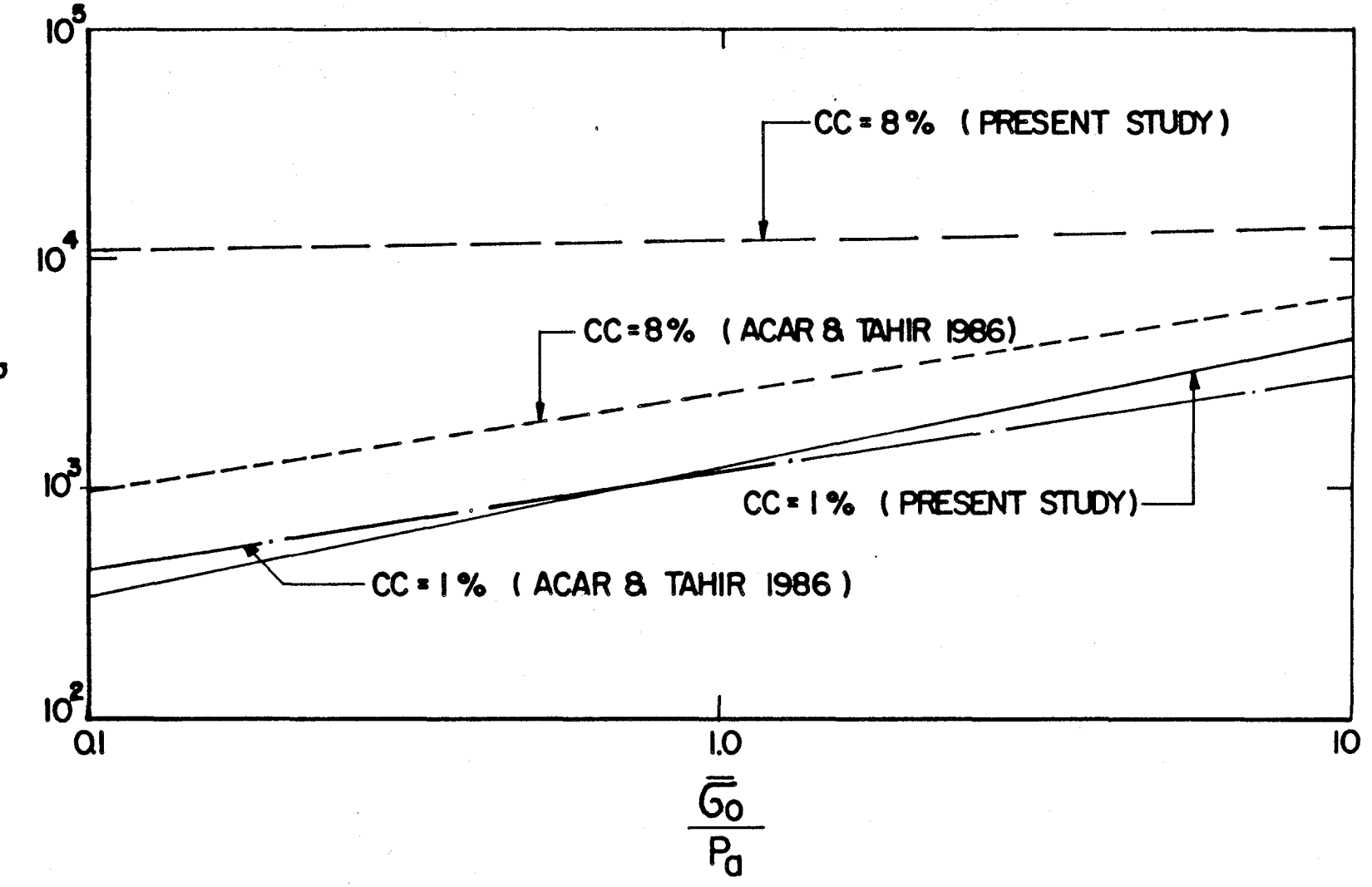

Fig.4.12 Comparison of Proposed Relation with the Relation developed by Acar and Tahir(1986) for Maximum Dynamic Shear Modulus

The maximum dynamic Young's modulus (E_m) of uncemented sands can be determined using the relation proposed in chapter III as given below:

$$E_m = \frac{1703.57}{(0.3 + 0.7e^2)}(P_a)^{0.61}(\overline{\sigma}_0)^{0.39} \tag{4.12}$$

in which $\overline{\sigma}_0$ and P_a are in same units.

Based on regression analysis, the following two relations are obtained to find the increase in dynamic Young's modulus (ΔE_m) due to cementation effects;

For low cementation range (CC < 2%)

$$\frac{\Delta E_m}{P_a} = \frac{2193.4}{(e - 0.2262)}(CC)^{(2.03-1.739e)} \tag{4.13}$$

For high cementation ranges (CC <8% and CC > 2%)

$$\frac{\Delta E_m}{P_a} = \frac{2930.5}{(e - 0.4921)}(CC)^{(2.692e-1.44)} \tag{4.14}$$

Therefore, knowing E_m and ΔE_m (eqns. 4.12, 4.13 and 4.14), the value of E_m^* (eqn. 4.10 or 4.11) for cemented sands can be determined.

Figure 4.13 shows a good agreement between experimentally measured values and the values calculated based on proposed relations for ΔE_m. As explained in the earlier sections, the effect of $\overline{\sigma}_0$ on ΔE_m at all densities is negligible (Fig. 4.6). Therefore the relations for ΔE_m (eqn. 4.13 and 4.14) do not include $\overline{\sigma}_0$.

At this point, it may be interesting to investigate into the dynamic poisson's ratio (ν) of cemented sands. The dynamic poisson's ratio (ν) as per theory of elasticity can be expressed as:

$$\nu = 0.5(E_m^*/G_m^*) - 1.0 \tag{4.15}$$

Without surprise, it is noticed that the dynamic poisson's ratios computed, based on the above equation substituted from the developed empirical relations for E_m^* and G_m^* are meaningless. It is explained in chapter III and also by other investigators that the small difference in moduli ratio (E_m^*/G_m^*) causes very significant error in computed ν . Therefore, ν values for cemented

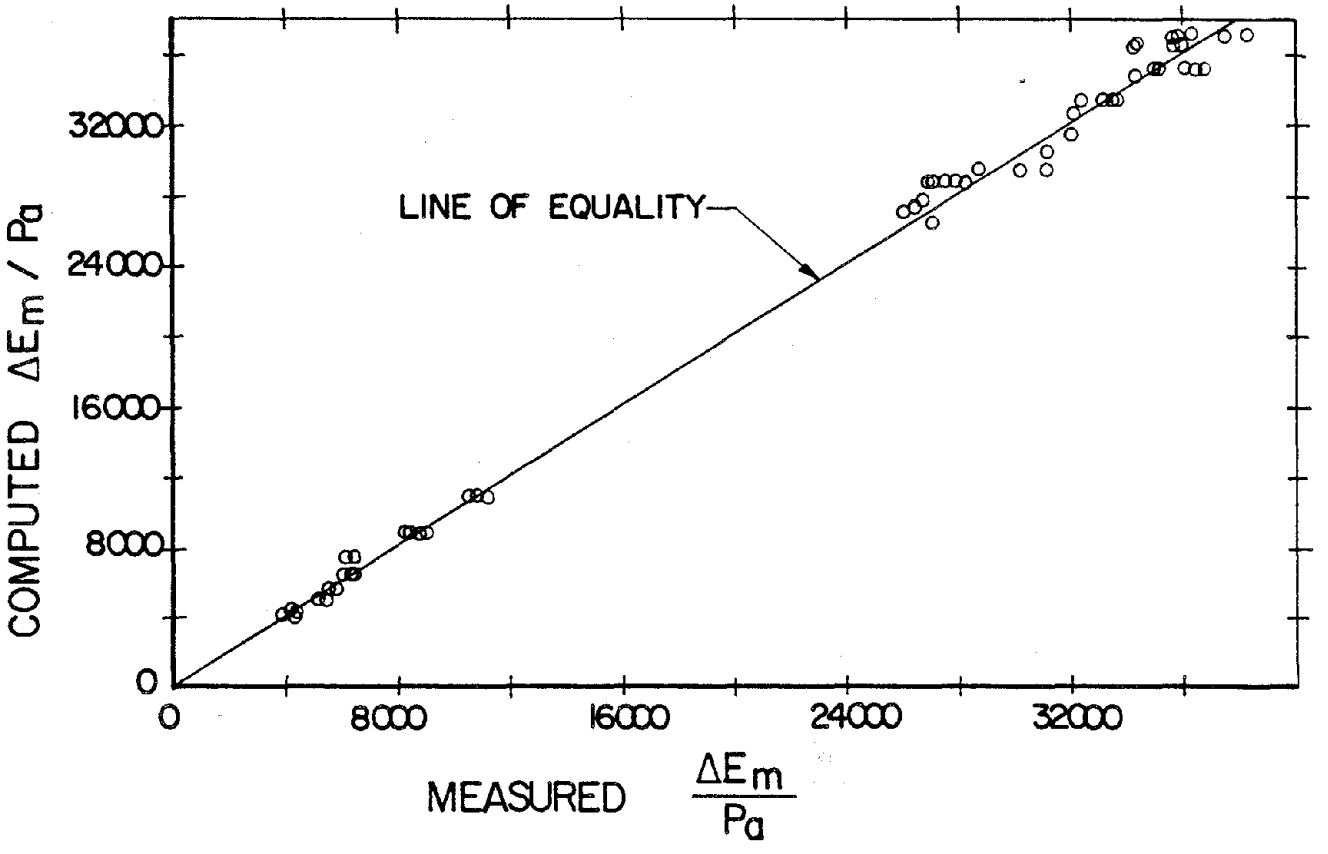

Fig.4.13 Comparison of Measured and Computed values of increase in Dynamic Maximum Young's Modulus

sands computed based on empirical relations give erroneous results. However it is interesting to observe the qualitative trends of ν with variation of different parameters. It is observed from Eqn. 4.15 that ν values decrease as effective confining pressure ($\overline{\sigma}_0$), cement content (CC) and density, all, increase.

Dynamic Shear Damping: In most of the cases, the measured damping ratios are too erratic to develop any reliable empirical relationships based on such data. This is primarily because of the uncertainties in the basis and method of their determination from experimental observations. Many investigators in the past recognized this difficulty and did not try to develop any relations for dynamic damping ratios. Even the few relations for damping values published in the literature are questioned several times in view of completely different results from field tests. In spite of these limitations, an attempt is made herein to develop relationships for damping ratios because they may provide guidance in selecting reasonable damping values if not the exact values, for practice.

In order to get a clear idea about the contribution of cementation, dynamic shear damping of cemented sands (D_s^*) is expressed as below:

$$D_s^* = D_s + \Delta D_s \tag{4.16}$$

in which D_s = dynamic shear damping of uncemented sand and ΔD_s = change in dynamic shear damping due to cementation. The damping values of cemented and uncemented sands depend very much on strain level. However it is decided to develop the relationships for all the terms in eqn. 4.16 at dynamic shear strain (γ) approximately equals to $10^{-3}\%$. Based on these relationships the D_s^* values at any other lower strains, if desired, may be appropriately selected.

A strain dependent relation for dynamic shear damping (D_s) of uncemented sands given in chapter III is as follows:

$$D_s = 9.22(\frac{\overline{\sigma}_0}{P_a})^{-0.38}(\gamma)^{0.33} \tag{4.17}$$

For $\gamma = 10^{-3}\%$, the above eqn. converts to

$$D_s = 0.94(\frac{\overline{\sigma}_0}{P_a})^{-0.38} \tag{4.18}$$

in which $\overline{\sigma}_0$ and P_a are in same units and D_s is in percent.

The reasons for increase of dynamic shear damping at lower ranges of cementation has been clearly explained previously. Unlike the observations of Chiang and Chae (1972), a decrease in shear damping has been observed at higher ranges of cementation for the reasons also explained in the previous section. The increase and decrease of dynamic shear damping (ΔD_s) at lower and higher ranges of cementation respectively are dependent on effective confining pressure ($\overline{\sigma}_0$). Based on regression analysis, the relationship for increase of dynamic shear damping at lower ranges of cementation is expressed as below:

$$\Delta D_s = 0.49(CC)^{1.07}(\frac{\overline{\sigma}_0}{P_a})^{-0.36} \tag{4.19}$$

in which $\overline{\sigma}_0$ and P_a are in same unit, CC and D_s are expressed as percentage.

The relations for D_s for uncemented sand (eqn. 4.18) and ΔD_s (eqn. 4.19), can be substituted in eqn. 4.16 to calculate the dynamic shear damping of cemented sands (D_s^*). Since all the relations are nondimensional, any system of units can be adopted.

As higher ranges of cementation are not of practical importance (for economical reasons) and also due to absence of an accurate method to exactly find the threshold cement content at which damping ratios reach their maximum values (and a further increase in cement content causes a decrease in damping values), no attempt is made to take it into account in the above relation. Therefore, it should be borne in mind that the above relation for damping is suitable only for cementation values below the threshold cement content.

A good agreement among experimentally measured values at I.I.T., calculated values from the proposed relation and also the experimental results of Chiang and Chae (1972) is obtained and shown in Fig. 4.14.

Dynamic Longitudinal Damping: As explained earlier, the effects of cementation are more pronounced on dynamic longitudinal damping (D_l^*) of cemented sands. Also, these values are found more erratic than D_s^*. To develop a relationship, D_l^* is expressed as below:

$$D_l^* = D_l + \Delta D_l \tag{4.20}$$

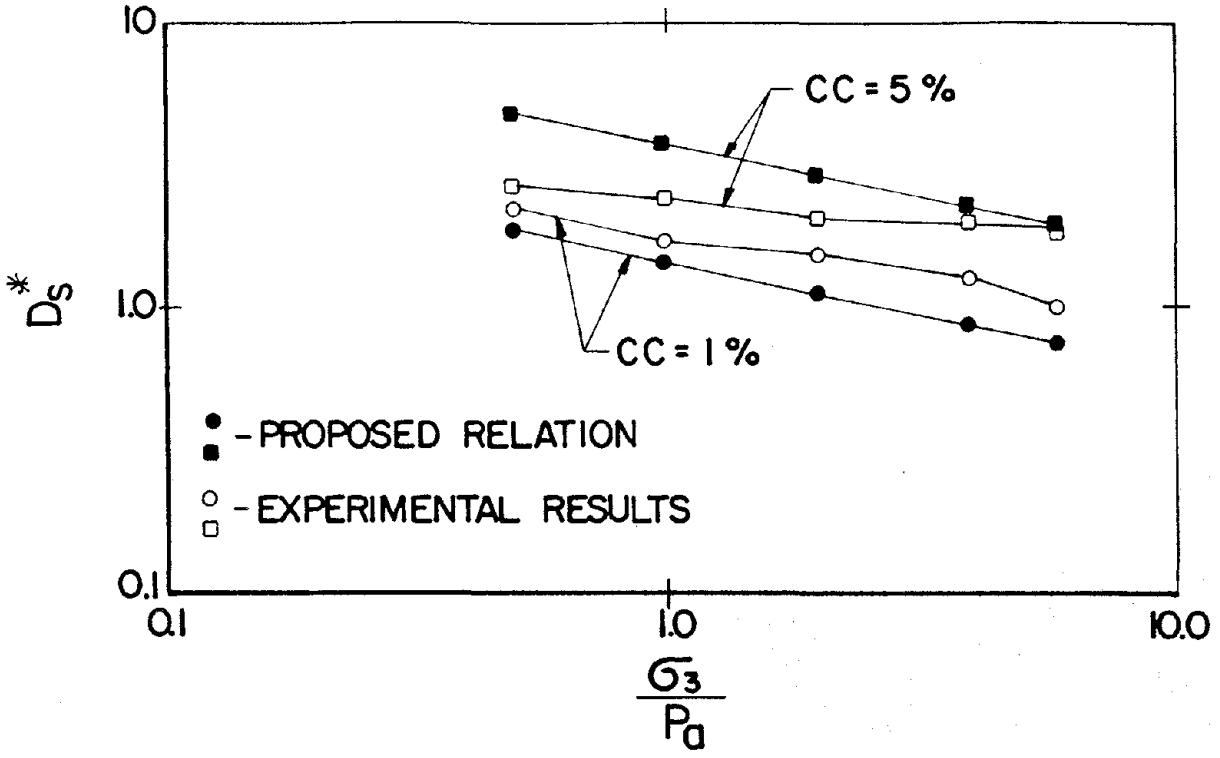

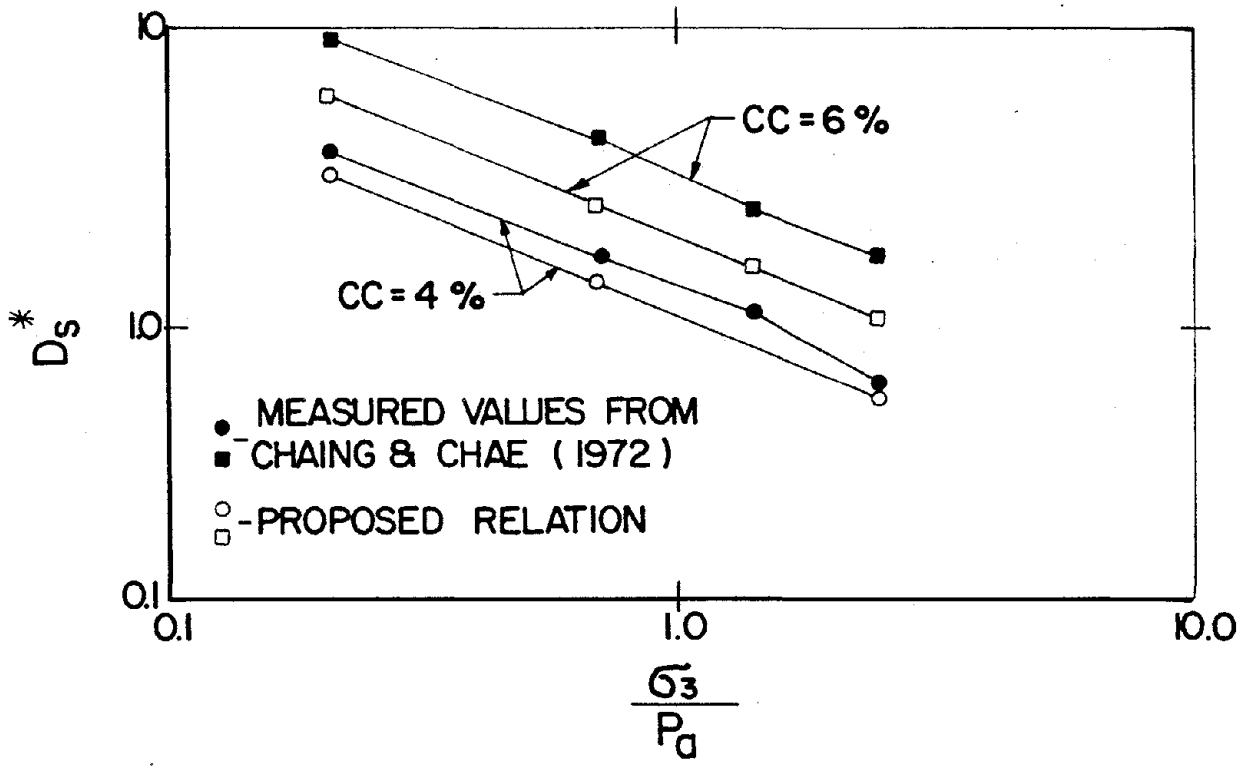

Fig.4.14 Comparison of Proposed Relation with Experimental Results for Dynamic Shear Damping

in which D_l = dynamic longitudinal damping for uncemented sands and ΔD_l = increase in damping due to cementation. According to chapter III, D_l for $\epsilon = 10^{-4}\%$ can be given as follows:

$$D_l = 0.48(\frac{\overline{\sigma}_0}{P_a})^{-0.13} \tag{4.21}$$

A statistical analysis with the measured values of damping, a relation for ΔD_l is obtained and given below:

$$\Delta D_l = 1.17(CC)^{0.75}(\frac{\overline{\sigma}_0}{P_a})^{-0.1} \tag{4.22}$$

In above all relations $\overline{\sigma}_0$ and P_a are taken in same units; D_l, D_l^* and CC are expressed in percentage. The proposed relation for D_l^* is only applicable for $\epsilon = 10^{-4}\%$ and for ranges of cementation lesser than threshold.. No literature is available on dynamic longitudinal damping because of its rare demand in practice. However there may be cases where D_l^* may be required to be evaluated. In such circumstances, the developed relations may be helpful.

4.5 CORRELATIONS WITH STATIC TRIAXIAL TESTS

The resonant column testing is costly and complicated. Whereas conventional triaxial compression tests are very common and easy to conduct. Any correlations of dynamic moduli and dynamic damping ratios obtained from resonant column tests with the results of triaxial tests are very valuable for situations when crude estimation of dynamic properties of soils at low strains is required. In this section an attempt is made in this direction.

Static Triaxial Tests: A total of 114 static strain controlled, isotropically consolidated drained triaxial compression tests were conducted on uncemented and cemented sands (chapter II). All the specimens were prepared by the method of undercompaction from Monterey No. 0 sand with relative densities 43, 60 and 80 percentages mixed with portland cement type I in 2, 5 and 8 percentages and varying curing period as 15, 30. 60 and 180 days. Samples were saturated and consolidated at different effective confining pressures of 49, 245 and 490 kpa and tested at a strain rate of 0.186% per minute. The test results were plotted as deviator stress versus axial strain, volumetric strain versus axial strain, stress paths etc.

Variation of E with ϵ : To examine the variation of E with ϵ in an extended strain range, E versus ϵ results from resonant column tests and static triaxial tests are plotted in Fig. 4.15 as an illustrative example for an uncemented and cemented case. The E values from static triaxial tests are secant modulus values and they are compatible with E determined from resonant column test. It may be observed that "smooth" extension which exists for the case of uncemented sand is not that apparent for the examined cemented case. This is an indication that as strain levels become approximately equal to 0.1%, the stiffness of the cement specimen reduced, possibly due to the breaking of the cementation bonds.

Correlations for Dynamic Moduli: Chiang and Chae (1972) are the first to report such correlations. Static undrained triaxial compression tests were conducted at a confining pressure of 20 psi. The maximum dynamic shear moduli obtained at 20 psi confining pressure were plotted against deviator stress at 1% longitudinal strain of triaxial tests for all specimens with different cement content. Following linear relationship independent of CC, density and curing time has been proposed by Chang and Chae.

$$G_m^* = 13.867 + 0.419\sigma_d \tag{4.23}$$

where σ_d is the deviator stress at 1% strain level in psi and the dynamic shear modulus G_m^* is in ksi. The above relation is applicable to only one particular case of $\overline{\sigma}_0$= 20 psi. Also, the relation is applicable only when involved parameters expressed in the above mentioned restricted systems of units.

A need to investigate the existence of such correlation with extensive static triaxial and resonant column tests for effective confining pressures other than 20 psi has been felt. A relation similar to eqn. 4.23 is of great value, however it should be adoptable to any system of units and for any effective confining pressure.

As explained in the previous sections for the present investigation the effective pressures ($\overline{\sigma}_0$) applied in resonant column tests are 49, 93, 196, 392 and 588 kpa, whereas static triaxial tests are conducted with $\overline{\sigma}_0$ = 49, 245 and 490 kpa. If the effective confining pressures for both types of tests were

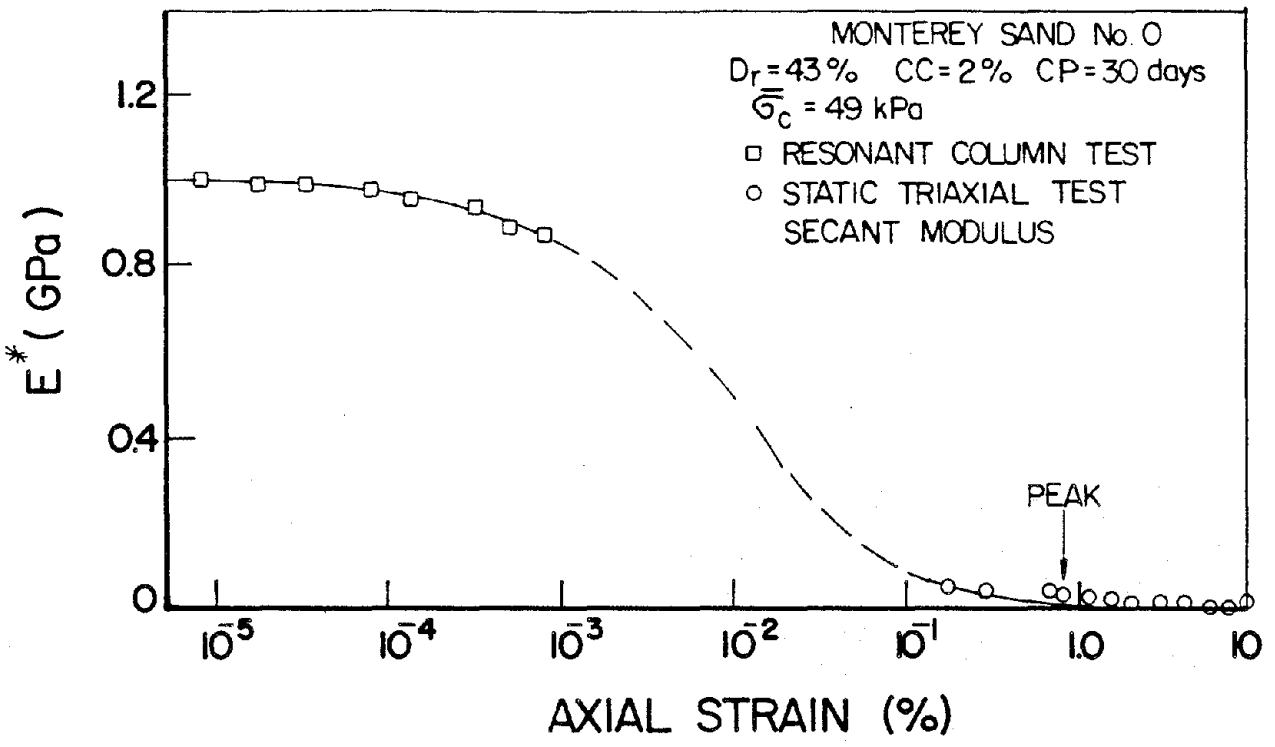

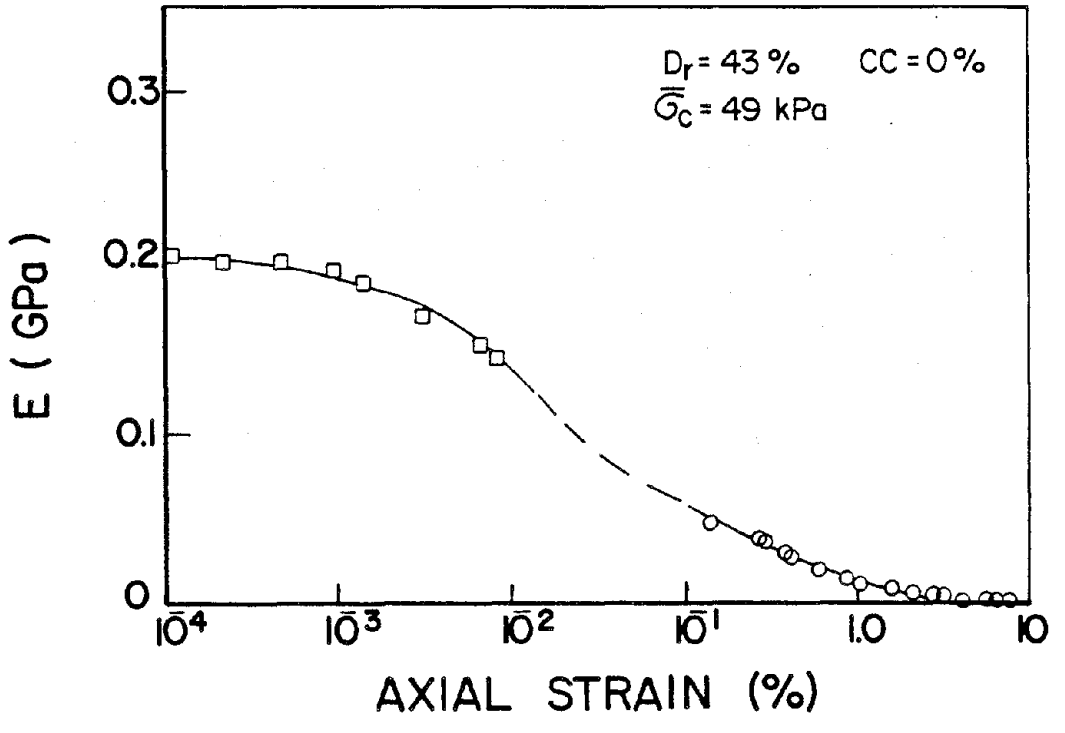

Fig.4.15 Variation of Young's Modulus with Strain as determined by the Resonant Column and by the Static Triaxial Test

same, this study would have resulted in a thorough evaluation of such correlations. However from this investigation, it is possible to correlate the maximum dynamic moduli and damping ratios from resonant column tests with static triaxial drained tests results only for $\overline{\sigma}_0 = 49$ kpa.

A correlation between maximum dynamic shear modulus (G_m^*) and deviator stress (σ_d) at 1% axial strain of static triaxial drained tests has been obtained from Fig. 4.16 as below:

$$\frac{G_m^*}{P_a} = 1109.22(\frac{\sigma_d}{P_a}) + 72.47 \tag{4.24}$$

The proposed correlation is dimensionless. The correlation is independent of density, cement content and curing period. However it is applicable for a specific case with $(\overline{\sigma}_0/P_a) = 0.49$.

A similar correlation for maximum dynamic Young's modulus (E_m^*) is obtained from Fig.4.17 and given as follows:

$$\frac{E_m^*}{P_a} = 2995.59(\frac{\sigma_d}{P_a}) + 4915.17 \tag{4.25}$$

Based on regression analysis, the coefficient of multi-square (r^2) for Eqns. 4.24 and 4.25 are found equal to 0.834 and 0.835 respectively. This fact should be remembered whenever such correlations are employed for the calculation of dynamic moduli. In view of this, the authors strongly feel that such correlations serve as a supplement to, not a replacement for, the "Resonant Column Testing."

Correlations for Damping Ratios: The values of dynamic shear damping (D_s) and dynamic longitudinal damping (D_l) are found to have no correlation with static triaxial test results. Similar observations were also made by Chaing and Chae (1972). Usually, damping values are computed by assuming Kelvin-Voight model (single degree of freedom system with linear viscous damping) and free vibrations. The absence of suitable computational technique in determining damping ratios from resonant column test measurments poses a great difficulty in developing any relationship for damping values (chapter III; Edil and Luh, 1978 etc.).

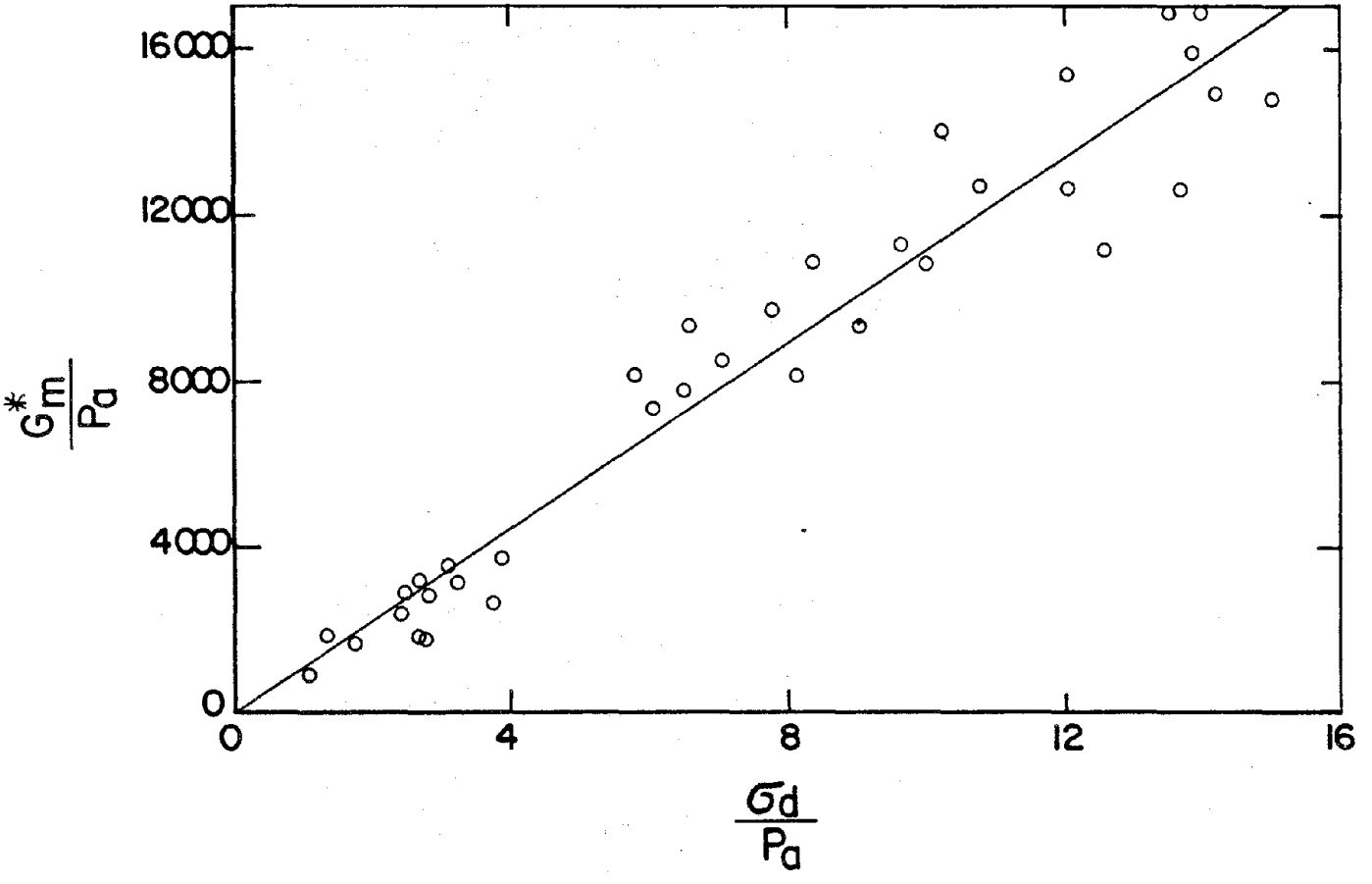

Fig.4.16 Correlation between Maximum Shear Modulus and Deviator Stress (at 1% axial strain) of Static Triaxial Tests

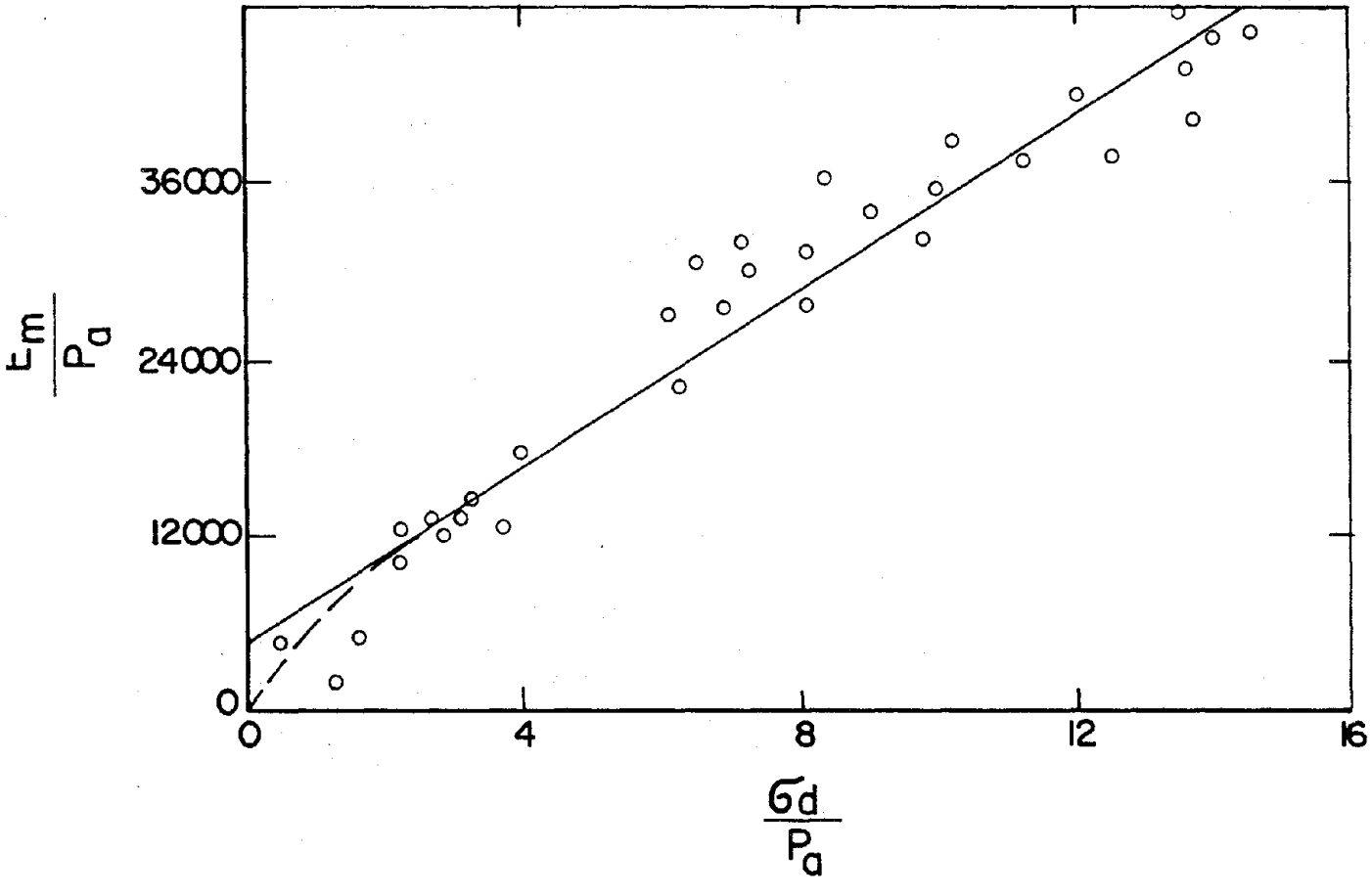

Fig.4.17 Correlation between Maximum Dynamic Young's Modulus and Deviator Stress (at 1% axial strain) of Static Triaxial Tests

4.6 SUMMARY

This study shows that a small amount of cementation increases dynamic moduli and damping ratios of sands at low strain amplitudes. However at higher cementation, though the moduli are considerably increased, the damping ratios are observed decreasing as explained by a new postulate. The major parameters governing the improved dynamic behavior of cemented sands are recognized as cement content, effective confining pressure and density. The damping ratios are however found less influenced by density.

Newly developed non-dimensional empirical relations for maximum dynamic shear and Young's moduli and dynamic shear and longitudinal damping ratios are based on reliable extensive resonant column test results and are convenient to use.

The idea of correlating static triaxial (drained) tests with resonant column tests may be objectionable in view of their fundamental testing differences, but helps in crude estimation of maximum dynamic moduli at low strains.

Chapter V

CORRELATION BETWEEN DYNAMIC MODULI AND RESISTANCE TO LIQUEFACTION OF CEMENTED SANDS

5.1 INTRODUCTION

Even though there are many studies examining the complex phenomenon of liquefaction-cyclic mobility of uncemented sands, there is only limited information regarding such behavior among cemented sands. As of today, available information dealing with naturally cemented sands is rather scarce and inconclusive mainly due to nonuniform cementation and disturbances induced during sampling, usually associated with such materials (Salomone et al.,1978 and Frydman et. al. 1980). As far as artificially cemented sands are concerned the existing studies are confined to their immediate interests (Rad and Clough, 1982; Dupas and Pecker, 1979 and Sitar et.al. 1980).

This chapter summarizes the extensive experimental program undertaken at Illinois Institute of Technology and presents relationship between resonant column test results and cyclic triaxial test results. The findings of this study will broaden the existing limited knowledge on liquefaction behavior of cemented sands which often confront the geotechnical engineer in either the artificial or natural form.

5.2 SCOPE OF PRESENT STUDY

The results of cyclic triaxial tests are discussed first. The results of resonant column tests are discussed in detail in previous chapters therefore only a brief summary is then given for completeness. Next the correlation between resonant column test results and cyclic triaxial test results is investigated. Since the samples for both types of tests were prepared identically by the method of undercompaction, any correlations developed would be free from sample preparation effects. The development of correlations become possible because of the maintainance of a one-to-one correspondence of the parameters such as cement content, curing period, density etc. for both types of tests during experimental investigation. If dynamic moduli (or wave velocities) are known from labo-

ratory or field tests, the correlations could be helpful in determining the cyclic shear strength of soil. Then any existing method such as shear wave velocity test (a brief discussion on shear wave velocity is given in next section) can be employed to identify the susceptibility of liquefaction. The correlations will also help in evaluating the feasibility of strengthening poor sandy deposits by artificial cementation.

5.3 SHEAR WAVE VELOCITY

There are several ways of determining shear wave velocity (v_s). The refraction test, downhole seismic test, crosshole seismic test etc. can be conducted to determine v_s in field. The most popular laboratory test to find v_s is resonant column test however, cyclic triaxial test, cyclic simple shear test, cyclic torsional shear test etc. can also be used. Several latest field methods are also reported in the literature and are currently under development. Under identical testing conditions, the field and laboratory tests results are found in excellent agreement. Shear wave velocity is related to shear modulus (G_{max}) by the following relation;

$$v_s = \sqrt{\frac{G_{max}}{\rho}} \tag{5.1}$$

where ρ= mass density of soil.

The shear modulus (or shear wave velocity) is the property of the material and is independent of water content and degree of saturation. The v_s is extensively used for solving dynamic soil structure interaction problems. Recently the authors found yet another utility of v_s in determining the elastic properties for granular materials while developing a constitutive model (Saxena, Reddy and Sengupta,1987). The effectiveness of stabilizing sand with cementing materials can also be evaluated from the shear wave velocity- as shown in later sections. Most importantly, in recent studies by Seed et. al(1983), Stokoe (1983) etc., v_s (or G_{max}) was used to evaluate liquefaction potential of soils.

The shear wave velocity (or G_{max}) can be used in following different ways to predict liquefaction;

(1)One way is to use the relationships between G_{max} and N as given below and then follow the simplified procedure of Seed and Idriss(1971):

Based on Seed et. al (1983):

$$G_{max} = 65N \tag{5.2}$$

Based on Ohaski and Iwasaki (1973):

$$G_{max} = 120N^{0.8} \tag{5.3}$$

G_{max} is expressed in tons per square foot in above equations. Seed also suggests an arbitrary fifty percent decrease in G_{max} in above relations to account for expected strain levels during earthquakes.

(2)Second way is to use the observations of Stokoe and Nazarian (1983) at sites of recent earthquakes in California. It was found that sands liquefy when $v_s > 550$ ft/sec and do not liquefy when $v_s < 450$ ft/sec.

(3)Third way is to use G_{max} (or v_s) to calculate threshold strain in the strain approach method proposed by Dobry et. al (1982) to predict liquefaction.

5.4 SUMMARY OF EXPERIMENTAL INVESTIGATION

The experimental results of cyclic triaxial tests and resonant column tests are briefly summarized.

(i) Cyclic Triaxial Testing

Montery No. O sand and Portland Cement Type I were used to prepare specimens in 8 layers, each layer being less than 2.54 cm, by the method of undercompaction- the method recommended by Nuclear Regulatory Commision (Ladd, 1978). This particular type of sand was selected because of extensive data available on this sand by various investigators in its uncemented form; thus, the data on cemented sand could be compared with uncemented conditions. The Portland Cement was chosen as the cementing agent because of its wide use in stabilizing poor sandy soils. The range of variables considered is given in

Table 5.1. After initial few tests, it was decided not to further test samples with cement content of 5% and 8 % as they are not susceptible to liquefaction.

Stress controlled cyclic triaxial tests were performed because such tests are easy to perform and a comparative study could be undertaken with the large body of data reported by many investigators using these tests on uncemented Montery No. O sand; thereby understand the effect of cementation. The testing procedure involves saturation, consolidation and finally applying a sinusoidal load (with preassigned stress ratio SR) initiated with compressive loading. All the tests were conducted with a frequency of 1 Hz. It has been experimentally observed that the frequency does not effect the cyclic strength (Townsend, 1977). These specifications are in accordance with those required by the Nuclear Regulatory Commission, Silver(1977). Initial liquefaction ($u_e = \overline{\sigma}_0$) is defined as the failure in all tests. Although failure could also be defined in terms of the peak to peak strain (2%, 5%, etc.) that a specimen undergoes during cyclic loading, the initial liquefaction criterion was adopted because the observed patterns concerning important parameters such as excess pore water pressure development for cemented specimens, could be compared easily with similarly obtained, well established patterns of uncemented specimens (Seed et.al,1977). For cemented sands, no significant difference in the cyclic triaxial test results was demonstrated by Rad and Clough(1982) by adopting different peak to peak strain failure criteria. The time history of load, deformation and excess pore water pressure were recorded and analysed later to determine the following values (Fig. 5.1);

1. Cyclic Stress (Single Amplitude)

$$\Delta\sigma_{sa} = \frac{\Delta P_c + \Delta P_e}{2A_c} \tag{5.4}$$

2. Dynamic Strain (Double Amplitude)

$$\epsilon_a = \frac{\delta_c + \delta_e}{l_c} \tag{5.5}$$

3. Pore Water Pressure Ratio

$$U = \frac{\Delta u_{max}}{\overline{\sigma}_0} \tag{5.6}$$

4. Stress Ratio

$$SR = \frac{\Delta\sigma_{sa}}{2\overline{\sigma}_0} \tag{5.7}$$

5. Cyclic Ratio

$$CR = \frac{N}{N_l} \tag{5.8}$$

In above definitions the area of sample-A_c; length of sample- l_c, and effective confining pressure $\overline{\sigma}_0$ correspond to after consolidation condition; N is number of cycles, N_l is the number of cycles to failure and $(\Delta P_c + \Delta P_e)$ is the double amplitude load. The results are then plotted in the conventional form. Typical results for uncemented and cemented sands are shown in Fig. 5.2 and Fig. 5.3.

(ii) Resonant Column Testing

The Drenevich Long-tor resonant column device was stiffened in order to test cemented sand specimens. The variables of the investigation include strain amplitude, effective confining pressure, void ratio (or relative density), cement content and curing period. The numerical values for the strain amplitudes were those produced by exciting forces or torques, approximately corresponding to 0.83, 1.67, 3.33, 8.3, 16.7, 33.33, 66.67, and 100 percent of the maximum force or torque produced by the apparatus. The range of values of other parameters considered is given in Table 4.1.

The test materials and specimen preparation were the same as in cyclic triaxial testing. A preliminary testing program indicated no significant effect of saturation therefore only dry specimens were tested in subsequent tests. A study of the effect of preloading and prestraining resulted the following efficient way of testing sequence.

Every specimen was first tested in the longitudinal and then in the torsional vibratory mode. For the longitudinal mode, the testing started by varying the strain amplitude from its minimum to its maximum value at the lowest applied confining pressure and the procedure repeated at the next higher confining pressure until the maximum confining pressure was reached. After testing of a sample in the longitudinal vibratory mode, and with the sample

Table 5.1 Variables and their Range of Values for Cyclic Triaxial Testing

VARIABLE	RANGE OF VALUES
Relative Density	25, 43, 60 and 80 %
Cement Content	1, 2, 5 and 8 %
Curing Period	15, 30 and 60 days
Effective confining Pressure	98 Kpa
Stress Ratio	3 values

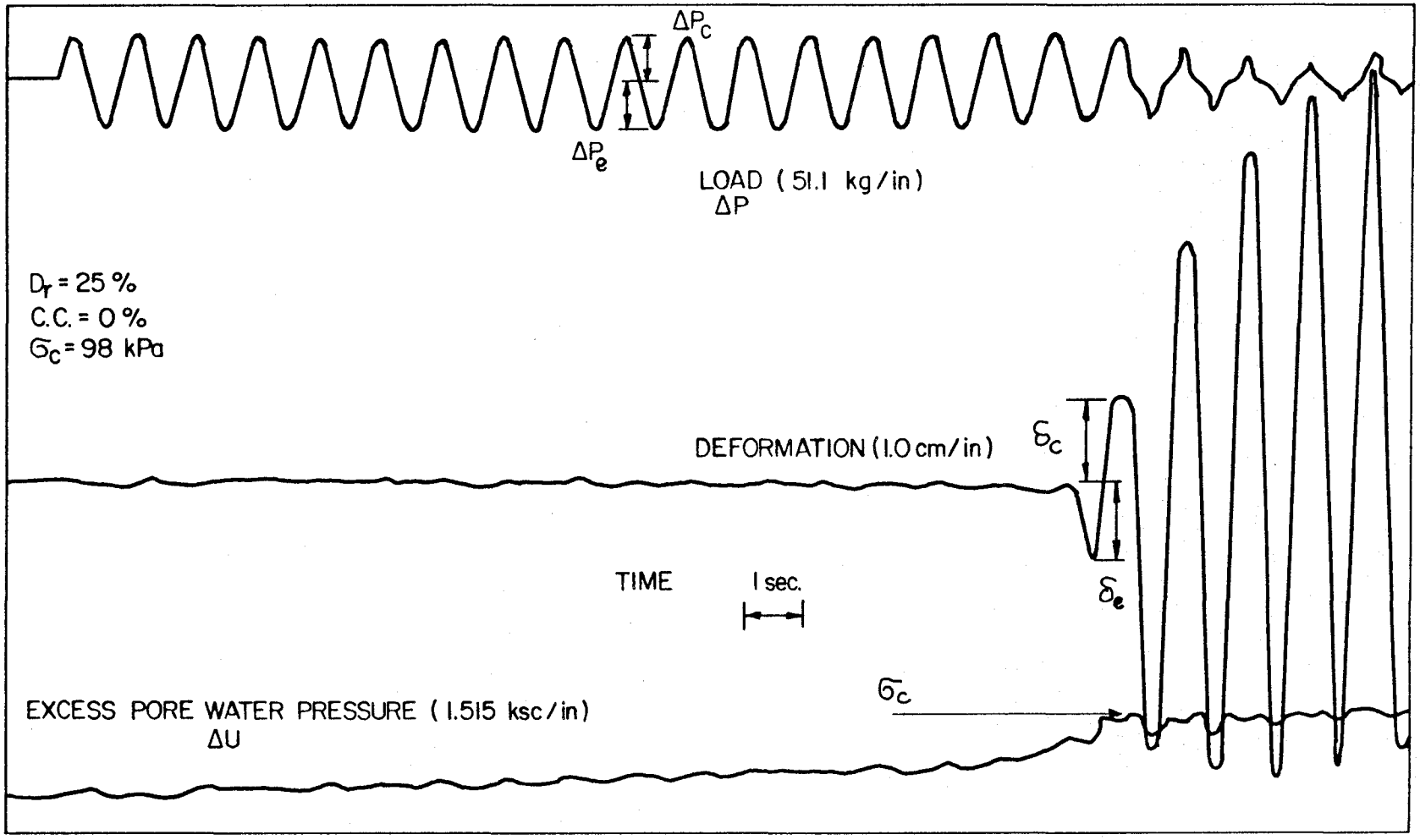

Fig.5.1 Typical Results from Cyclic Triaxial Test

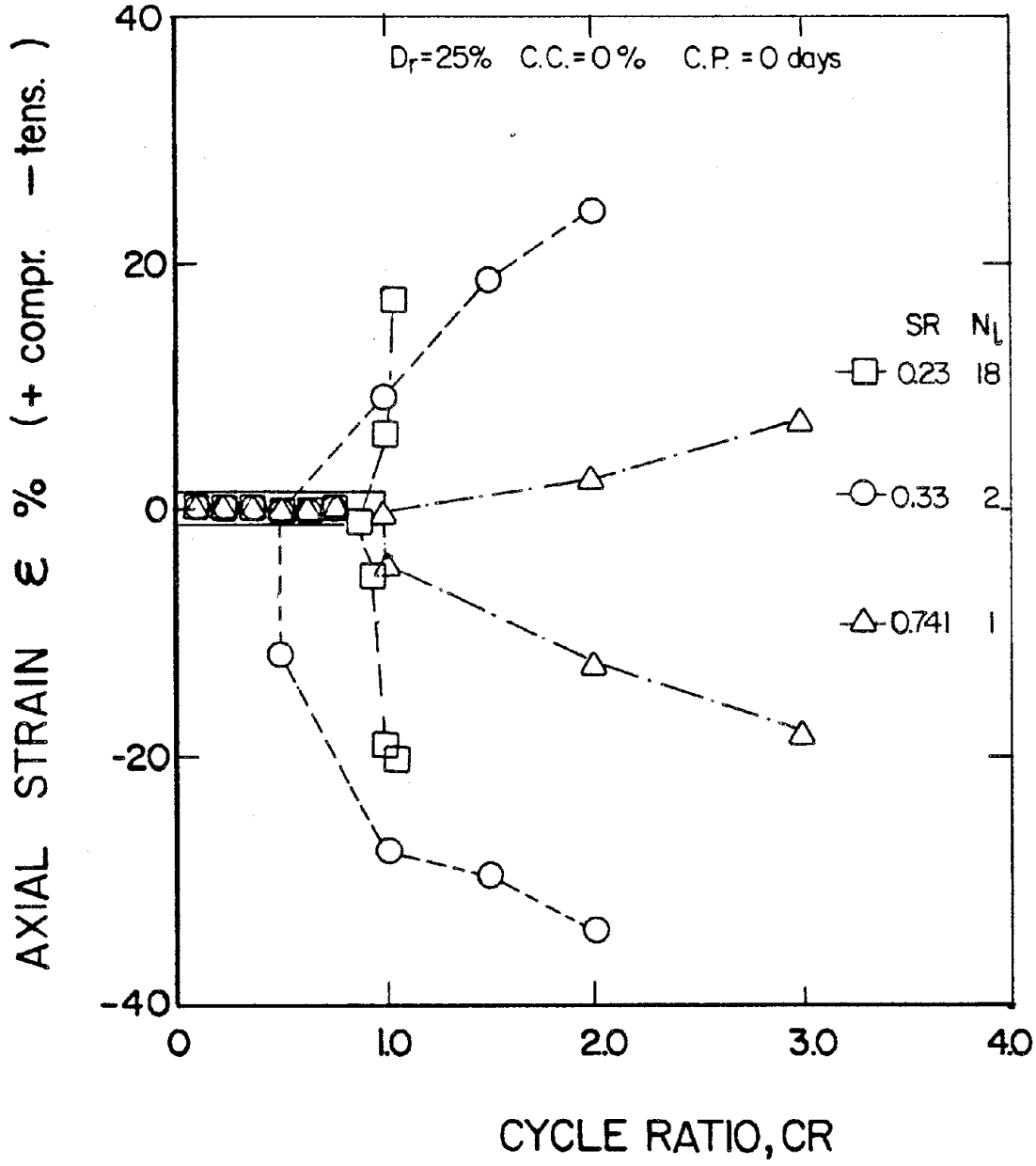

Fig.5.2(a) Axial Strain versus Cycle Ratio for Uncemented Sand

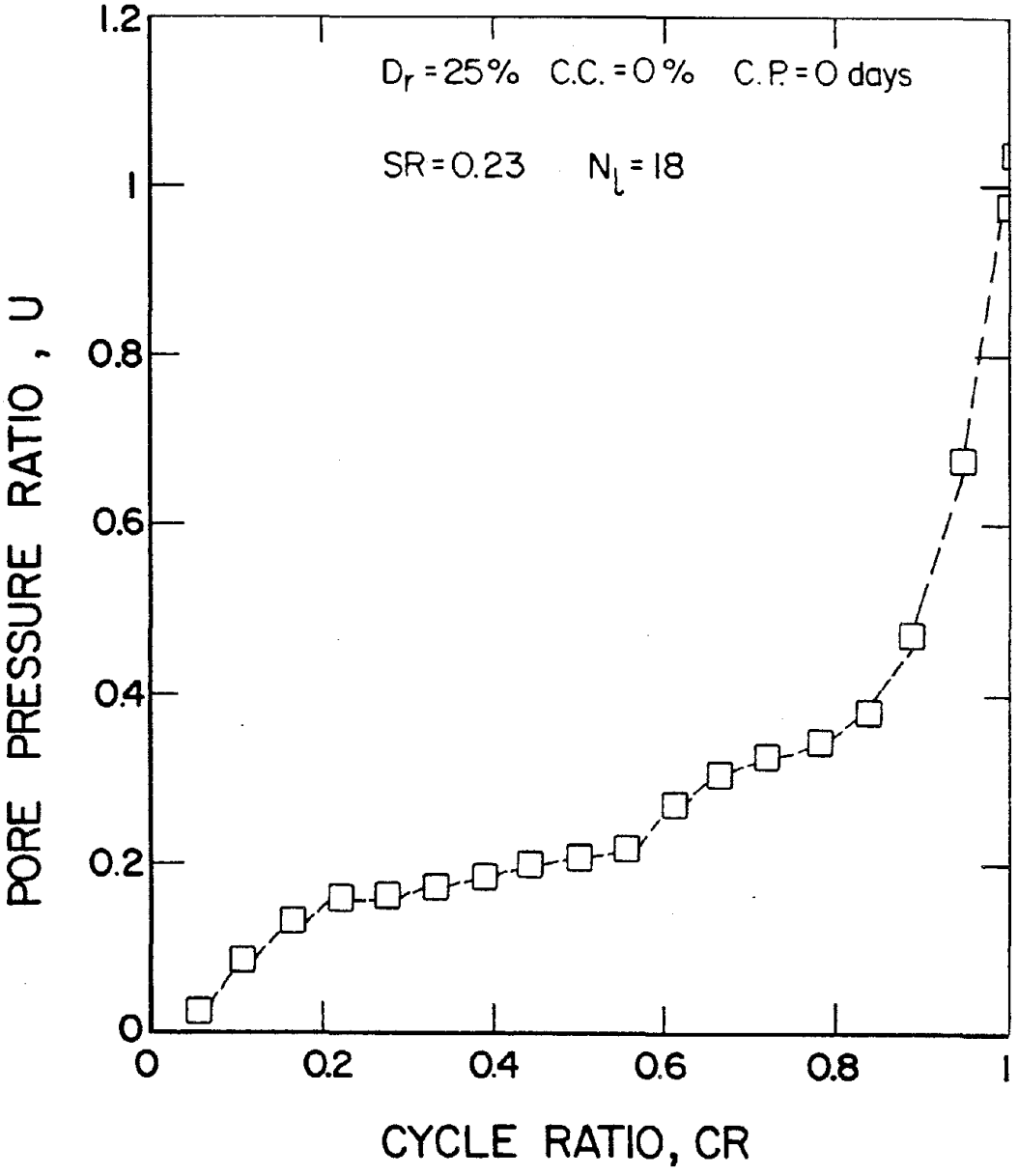

Fig.5.2(b) Pore Pressure versus Cycle Ratio for Uncemented Sand

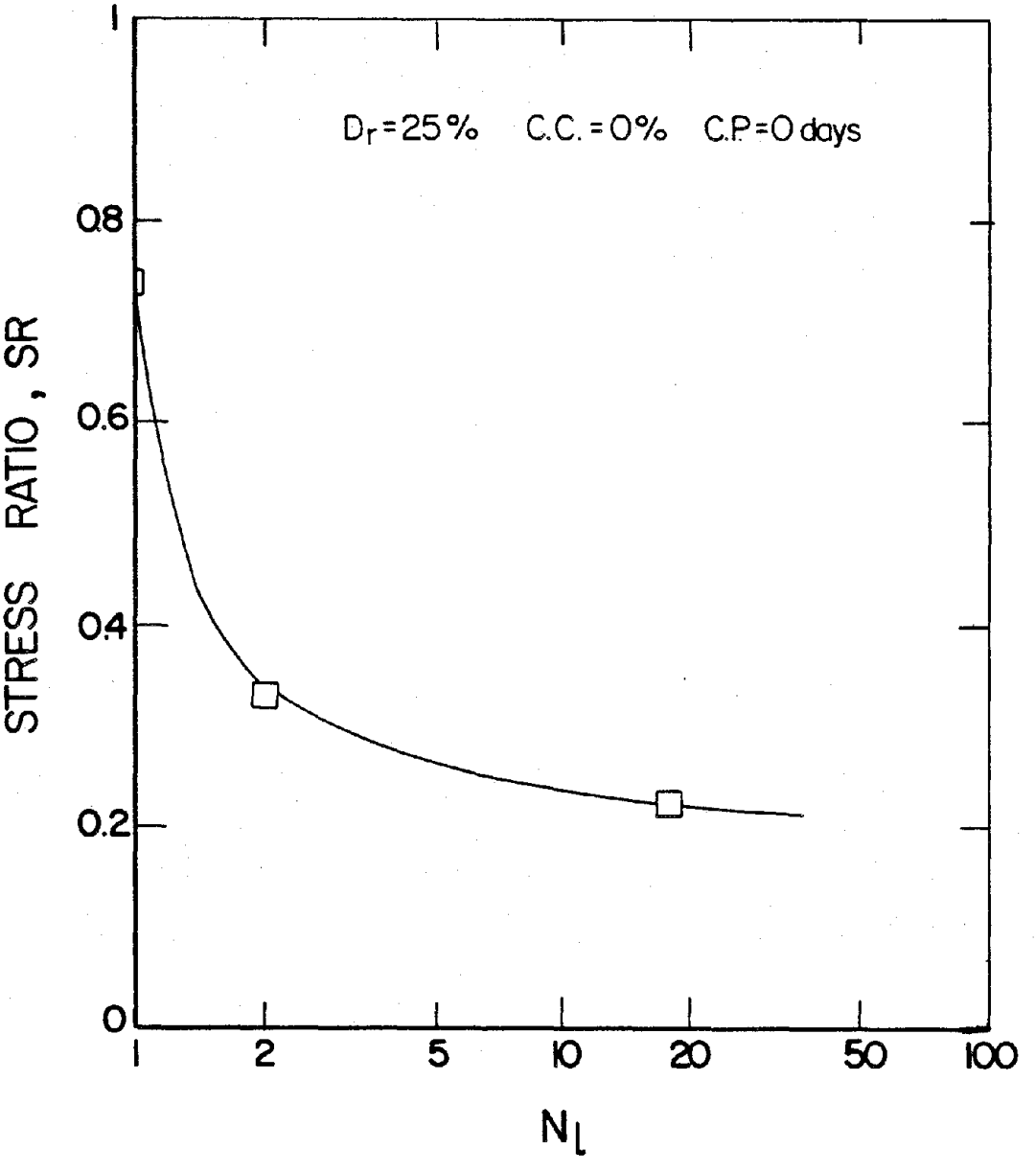

Fig.5.2(c) Stress Ratio versus Loading Cycle Number for Uncemented Sand

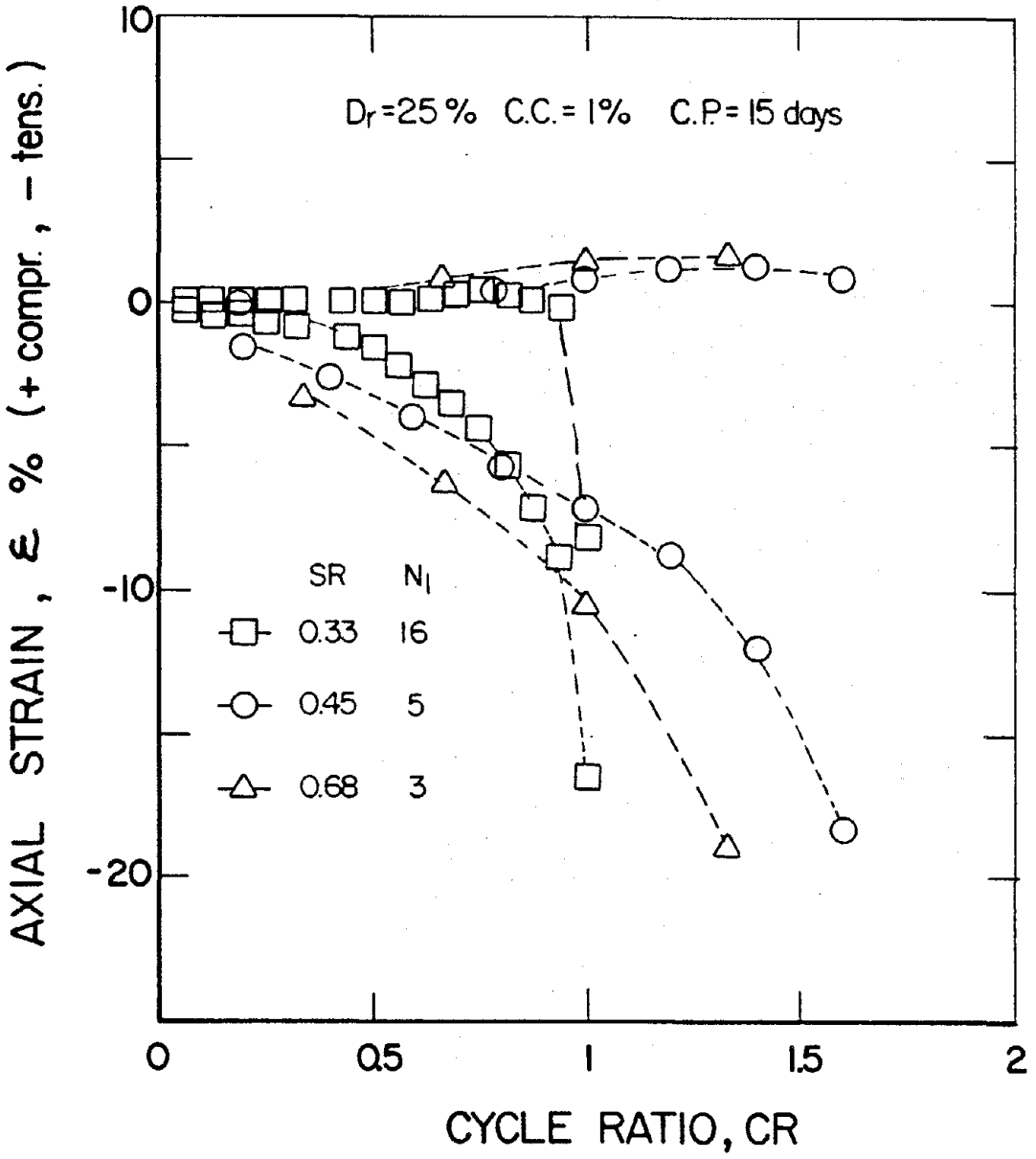

Fig.5.3(a) Axial Strain versus Cycle Ratio for Cemented Sand

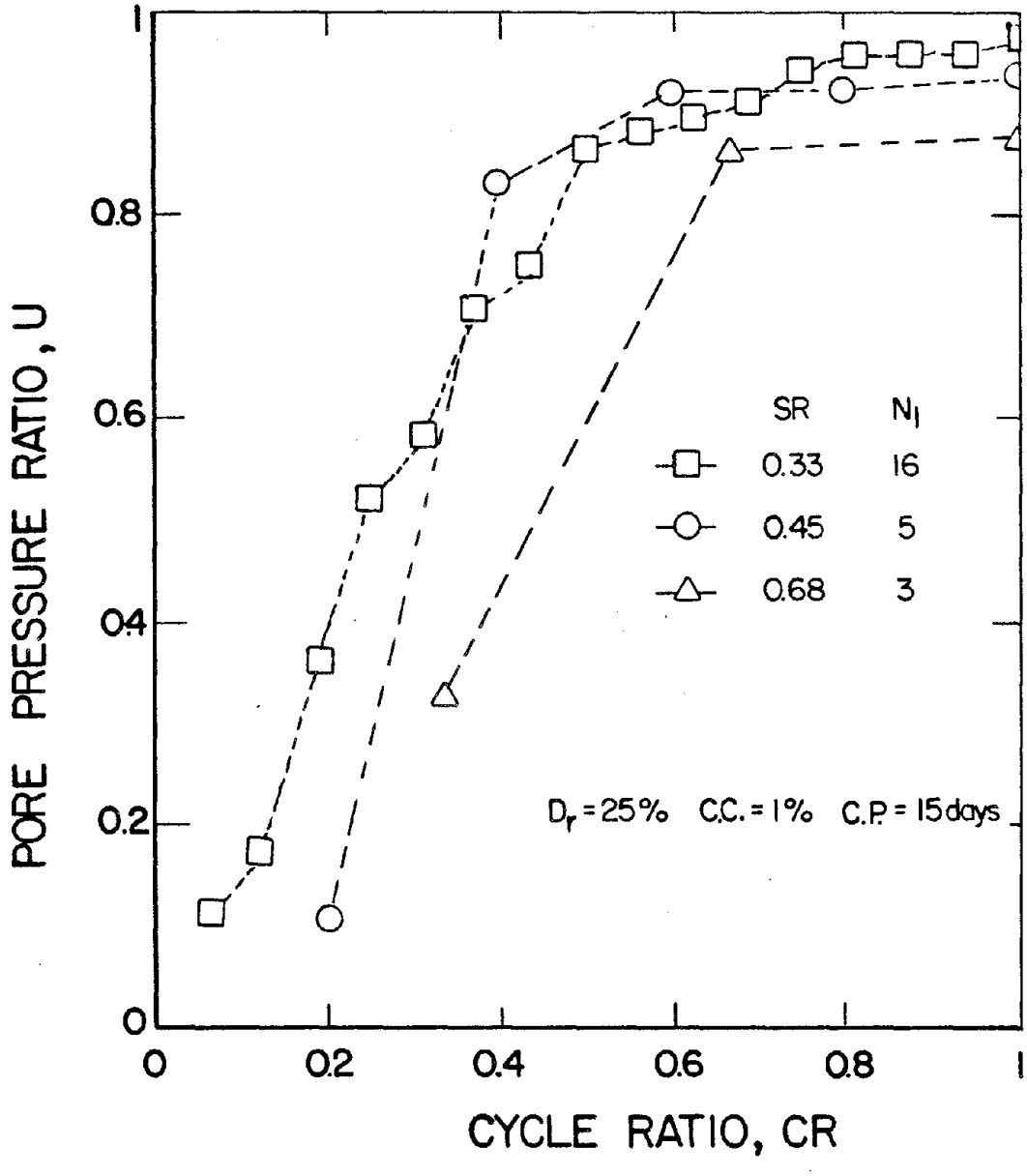

Fig.5.3(b) Pore Pressure Ratio versus Cycle Ratio for Cemented Sand

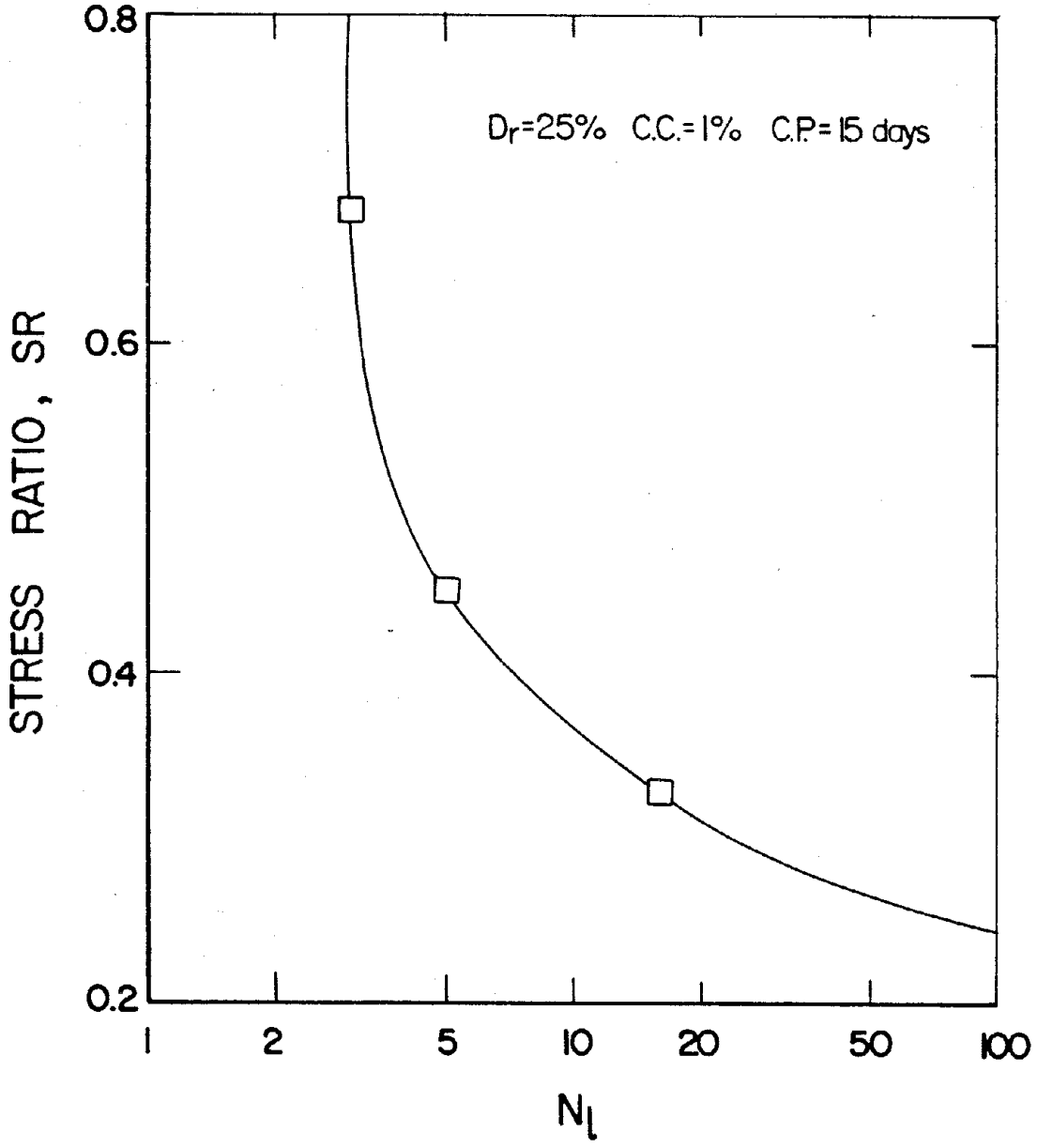

Fig.5.3(c) Stress Ratio versus Loading Cycle Number for Cemented Sand

consolidated at the highest confining pressure, testing was continued in the torsional mode by reducing the confining pressure using the same steps as in the ascending mode. With this sequence, the effects of previous operations on the parameters determined by subsequent operations were kept minimum.

Dynamic Young modulus (E^*), Dynamic Shear Modulus (G^*), Dynamic Longitudinal Damping (D_l^*), and Dynamic Shear Damping (D_s^*) were computed from the test results. Typical results for uncemented and cemented sands are shown in Figures 3.4, 3.5, 3.6, 3.7 and 4.6. The effects of different parameters on dynamic moduli and damping ratios are discussed in chapters III & IV. As cement content increases moduli are increased. Damping ratios however, initially increase as cement content increases and after a particular threshold value of cement content is reached they start decreasing.

5.5 ANALYSIS OF EXPERIMENTAL RESULTS

(i) Liquefaction Resistance

The liquefaction charactreistics of cemented sands showed similar trends of uncemented sand. Such observations were also made by other investigators (Dupas and Pecker, 1979; Rad and Clough,1982 etc.). The effect of density, cement content and curing time on the liquefaction resistance of cemented sands based on experimental results at I.I.T. is briefly discussed in this section.

Effect of Density: Fig.5.4 shows the variation of cyclic strength of uncemented sands with relative density. The number of cycles required to cause initial liquefaction for given stress ratio increases as the relative density increases. The number of loading cycles to induce initial liquefaction for stress ratio 0.4 and relative densities 25%, 43%, 60% and 80%, are approximateley 1.5 cycles, 3.5 cycles, 7.5 cycles and 18 cycles, respectively. Fig. 5.5 and Fig.5.6 show the effect of increase of cement content on the cyclic strength of sands of above mentioned densities.

Effect of Cement Content: Fig.5.7 compares the strengths of cemented and uncemented sands for a relative density of 43% and curing period of 30 days. There is a consistant increase in cyclic strength with cement content. This

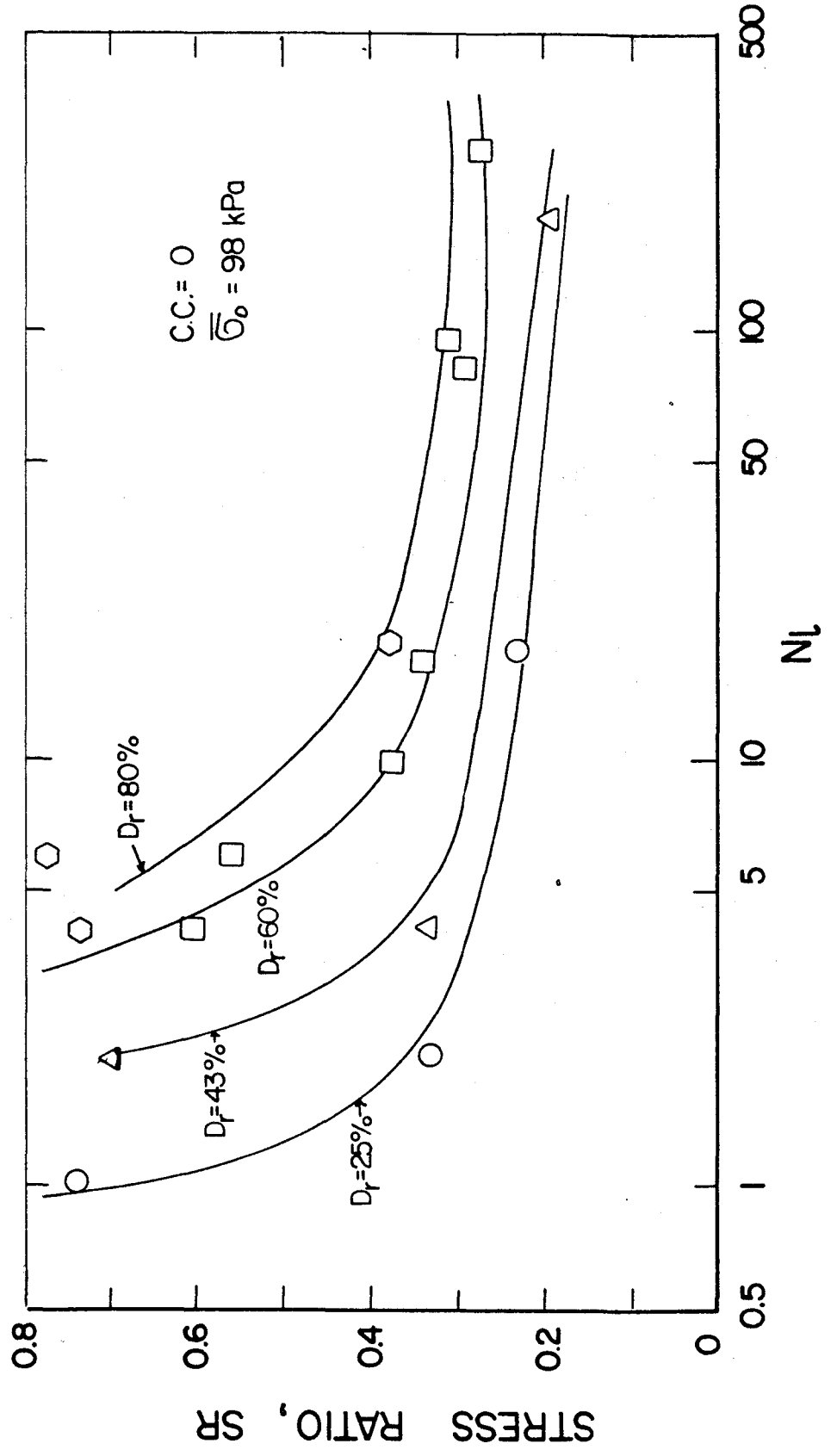

Fig.5.4 Effect of Density on Liquefaction Resistance for Uncemented Sand

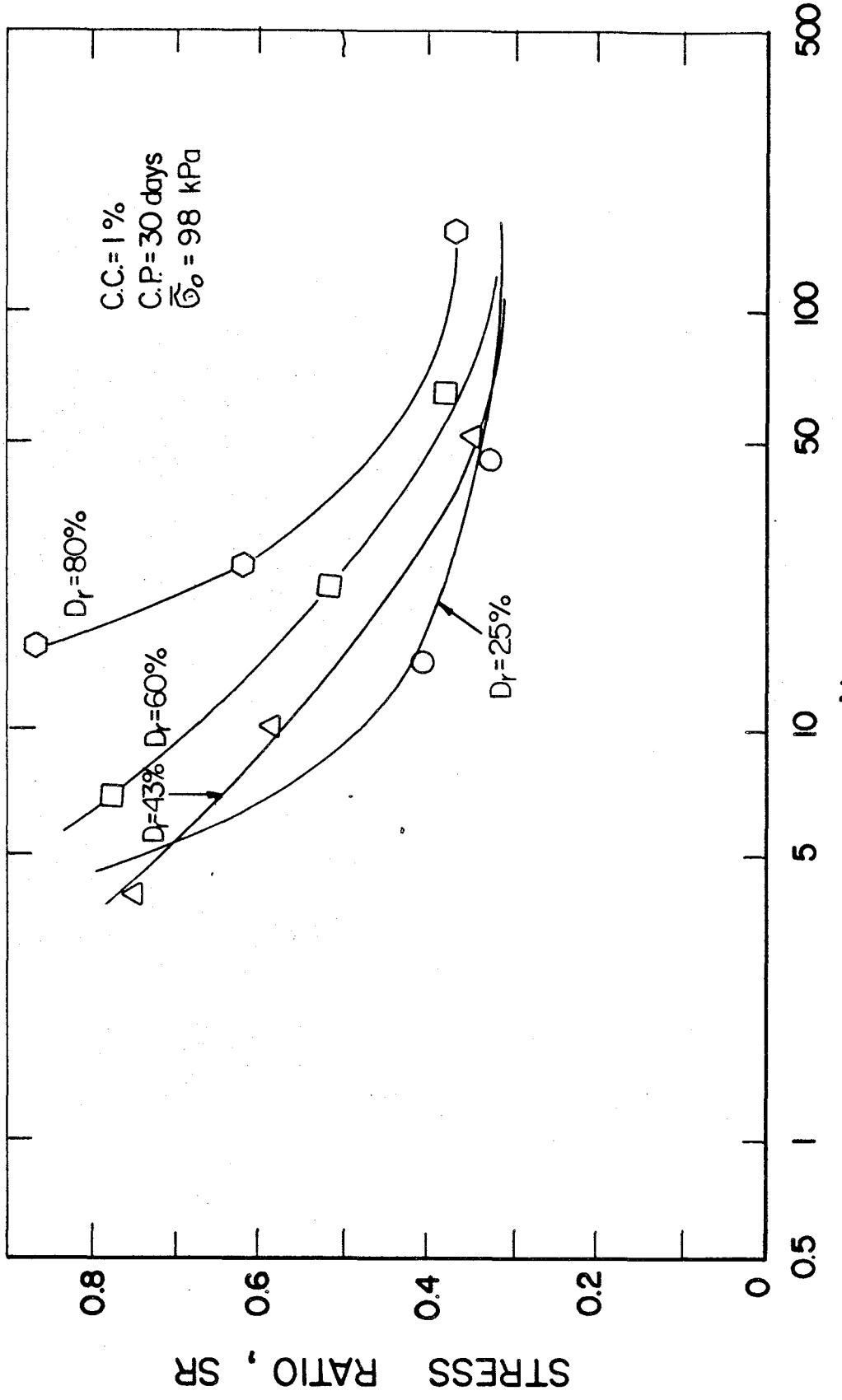

Fig.5.5 Effect of Density on Liquefaction Resistance for Cemented Sand with CC=1%

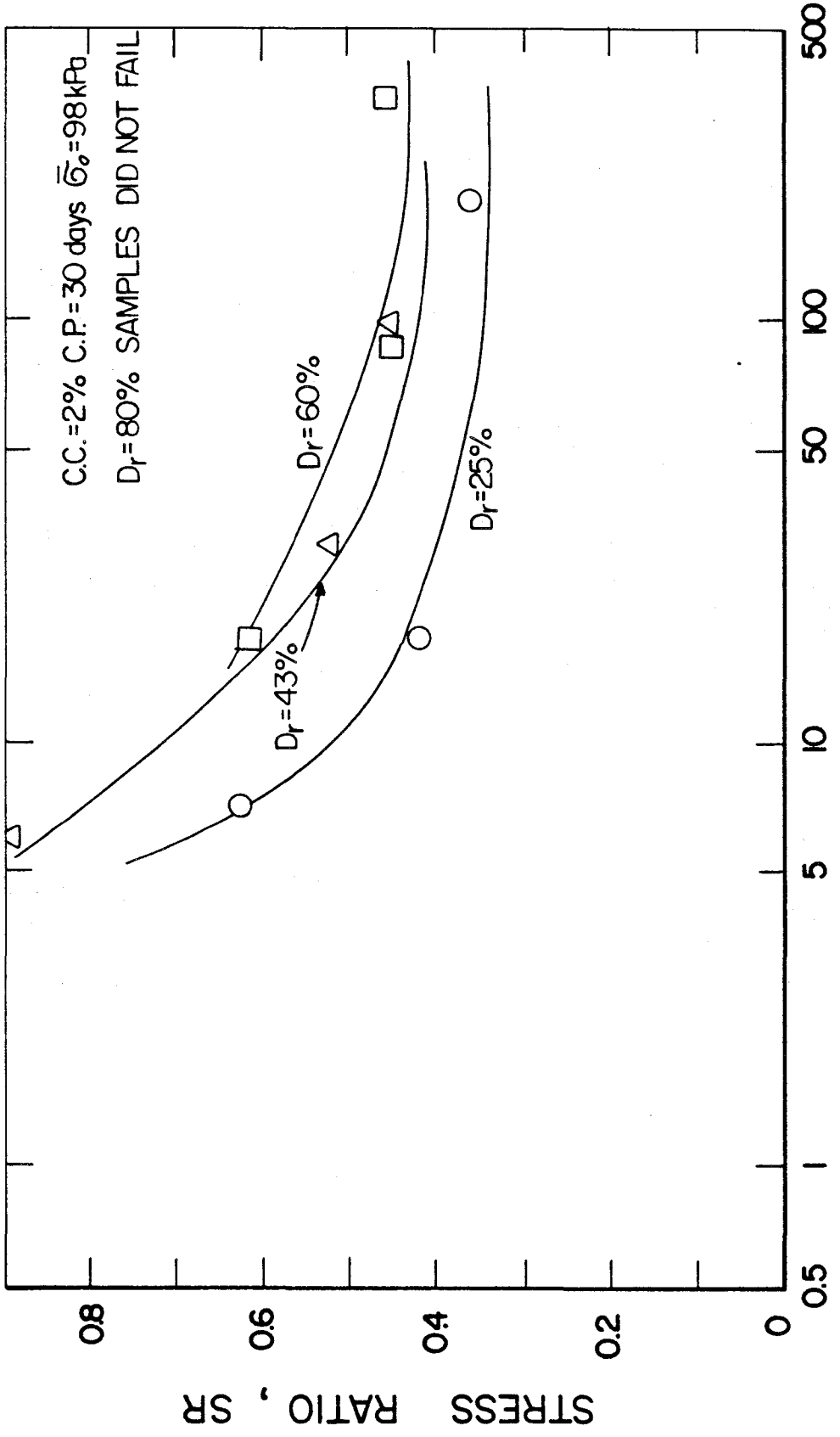

Fig.5.6 Effect of Density on Liquefaction Resistance for Cemented Sand with CC=2%

conclusion is more obvious if the stress ratio required to cause initial liquefaction in a specific number of cycles are plotted with relative density at various cement contents and a given curing period as shown in Fig.5.8 and Fig.5.9. From these figures it may be seen that a sample with D_r=25%, CC=1% and CP=60days has cyclic strength equivalent to that of an uncemented sample prepared at a relative density greater than 80%. Similar comparisons may be made for various other combinations of the various parameters.

Effect of Curing Period: Fig.5.10 shows a consistant increase of the cyclic strength with curing period and may be attributed to the nature of the cement hydration. This increase is greater for the lower range of relative densities. Furthermore the gain in strength for a curing period of 15 to 30 days is far exceeds that from 30 to 60 days. At low relative densities there being more voids, the exposed surface of the cement particles is much larger; therefore, the cement hydrates faster than at higher relative densities which have less exposed surface for a given period of time. Also at the early stages of hydration the process is faster.

Considering the overall cyclic triaxial behavior of cemented sands, the following behavioral patterns have been observed: (1) the cyclic axial strains are not symmetric. Usually the samples are strained only in tension during a complete load cycle. This happens because cement is stronger in compression than in tension; (2) in cemented sand specimens, particularly for those with 2% cement, the pore water pressures at or after initial liquefaction are not fully developed. This occurs due to the inability of the sand grains to reach a denser packing throughout the specimen, because of cementation.

(ii) Correlation between Dynamic Moduli and Cyclic Strength

Recently, studies are focussed on the easy and reliable methods of finding in-situ dynamic properties that could help as indices to judge for liquefaction potential of soils (Dobry et.al.,1981; De Alba et.al.,1984 and Tokimatsu et.al.,1986). The non-destructive shear wave velocity tests are very promising for this purpose. Since a good agreement was found between laboratory resonant column test results and in-situ shear wave velocity results, either of these

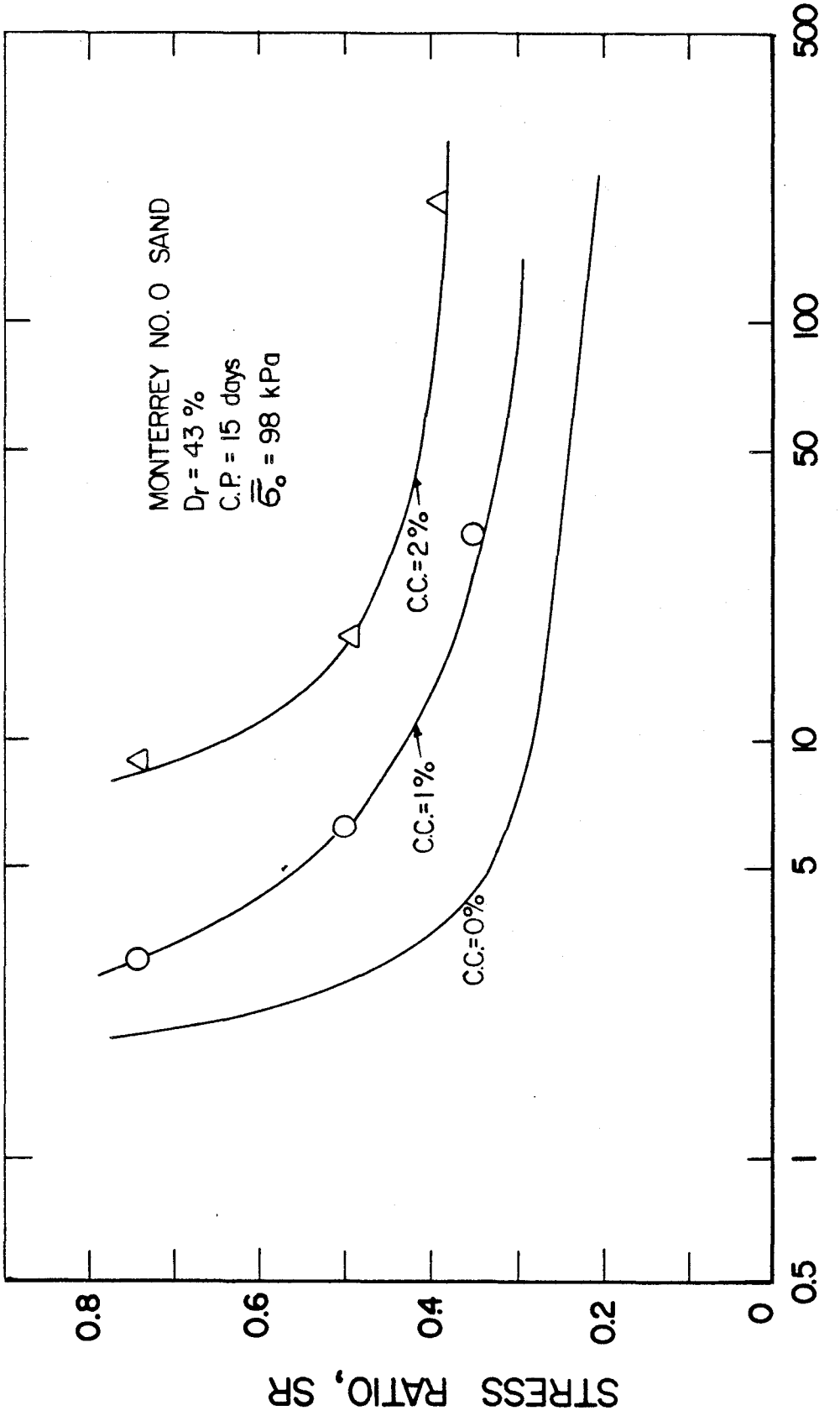

Fig.5.7 Effect of Cement Content on Liquefaction Resistance

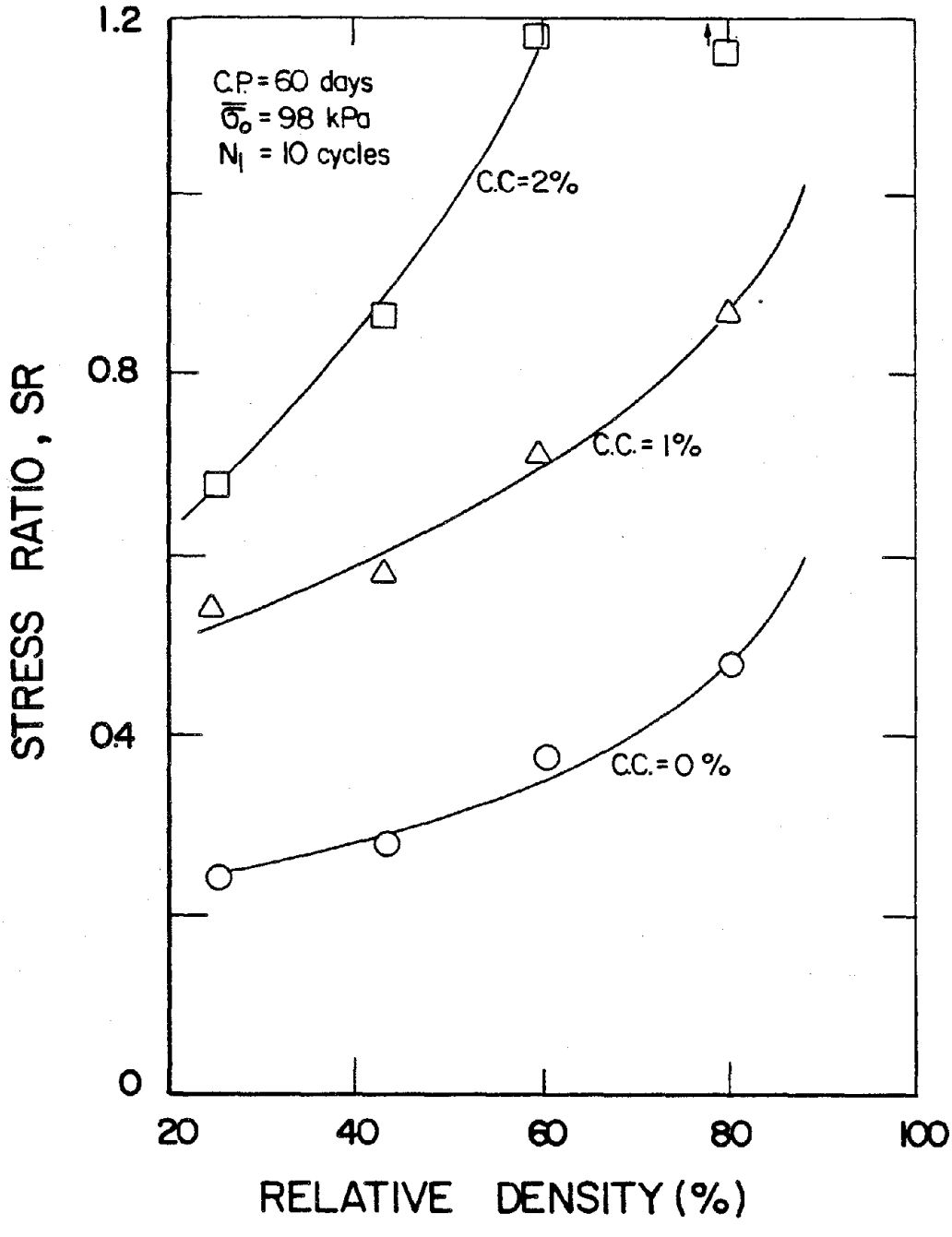

Fig.5.8 Effects of Cement Content and Density on Stress Ratio to cause Liquefaction after 10 cycles

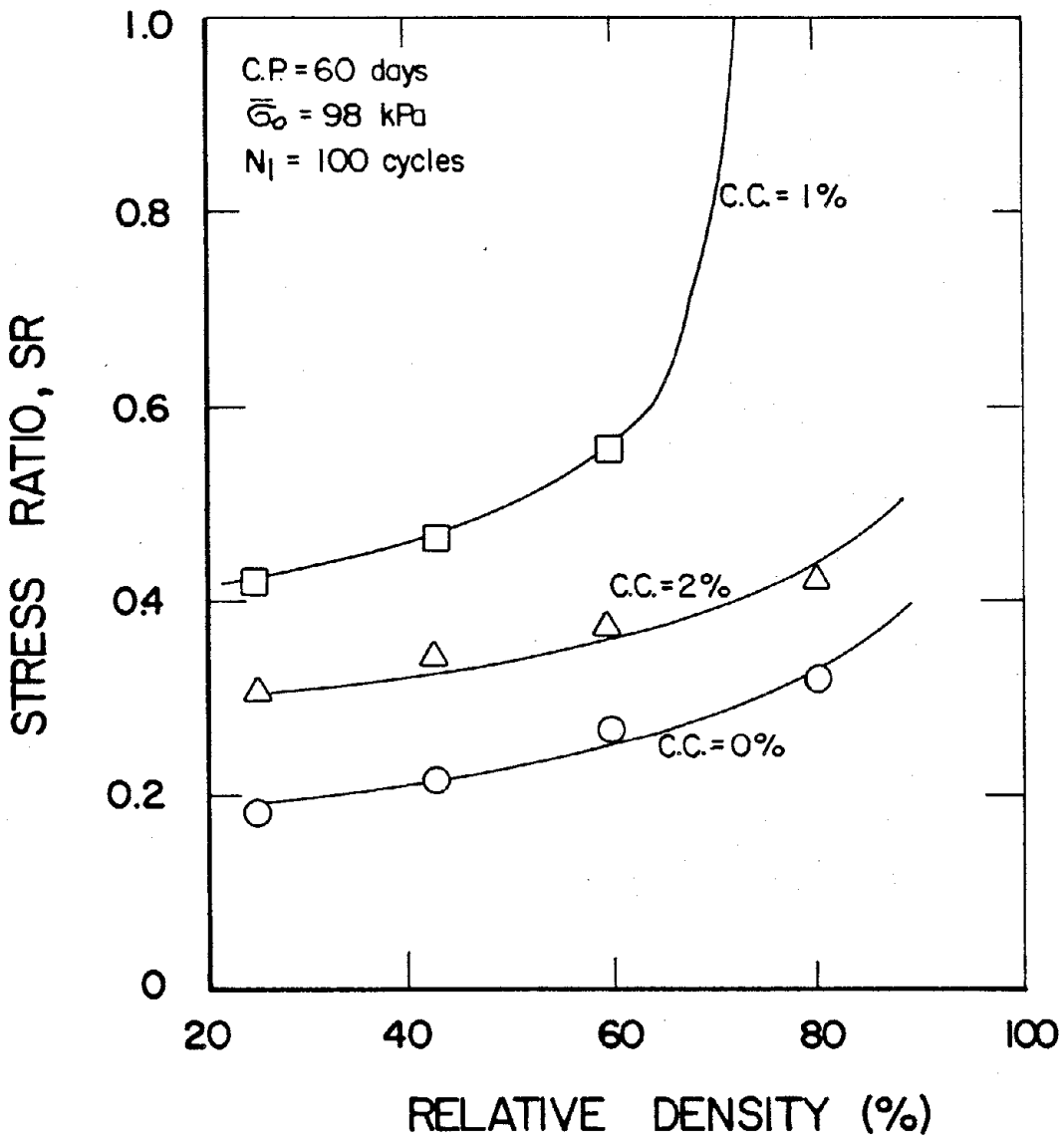

Fig.5.9 Effects of Cement Content and Density on Stress Ratio to cause Liquefaction after 100 cycles

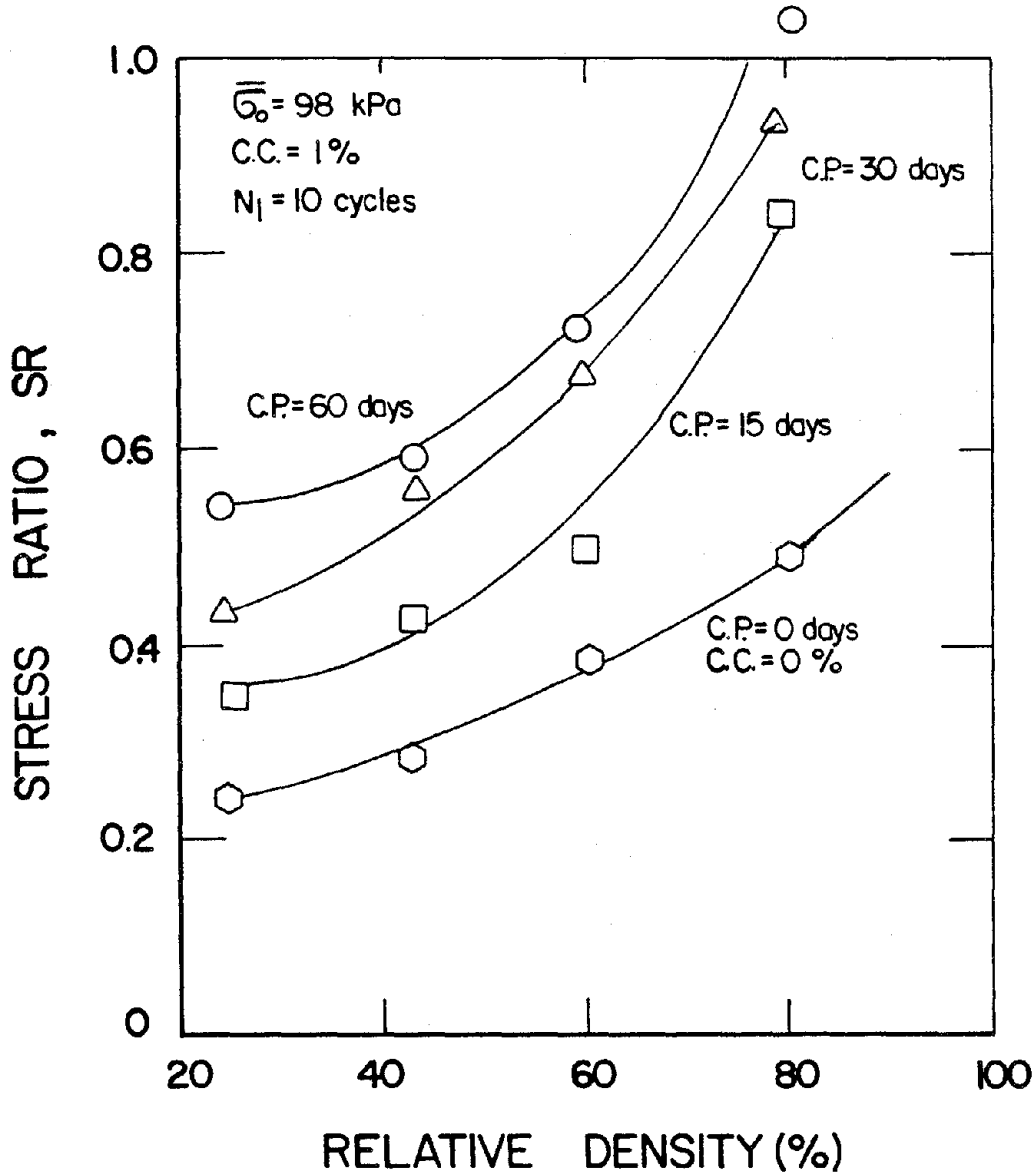

Fig.5.10 Effect of Curing Period on Liquefaction Resistance

tests can be used to determine v_s. An interesting feature observed in this study and also reported by other investigators is that the cyclic shear strength and dynamic moduli are found dependent on same factors such as density, strain, soil structure, stress history etc. Therefore the use of dynamic moduli as indices to predict liquefaction is very meaningful.

The use of dynamic moduli to predict liquefaction is particularly helpful for naturally weakly cemented sand because (i) undisturbed sampling is extremely difficult, (ii) existance of nonuniform cementation, (iii) SPT and CPT do not provide reliable results (Bachus et. al.,1981). Therefore, a relationship between cyclic strength and dynamic moduli (developed from artificially cemented sands) will be extremely useful in evaluating the effectiveness of cementation even for naturally cemented sands.

The existance of good correlation between cyclic strength and shear wave velocity has been shown in the literature for uncemented sands. Similar correlations for cemented sands, if developed could be useful for practicing engineer. The experimental results of this study with cyclic triaxial and resonant column devices provide such opportunity.

The variation of stress ratio (SR) with number of cycles to cause initial liquefaction (N_l) can be approximately expressed as below:

$$SR = a(N_l)^{-b} \tag{5.9}$$

where 'a' and 'b' are constants and are dependent on density and level of cementation. Based on statistical analyses of the experimental results obtained at I.I.T. and at Stanford University, the values of a and b are computed and are reported in Table 5.2. It may be mentioned that the normalized curve expressed in terms of $\tau/(\overline{\sigma}_0 D_r)$ versus N_l as proposed by Ferrito et.al (1979) for uncemented sands is not possible for cemented sands. For any selected number of cycle N_l for which the stress ratio is known (either from SR versus N_l data or from equation 5.9), a correlation with moduli or wave velocities is possible. An arbitrary selection of 10 cycles was reported by DeAlba et.al(1984) and 20 cycles by Tokimatsu et.al.(1986) in the similar studies related to uncemented sands. In this study, three numbers of cycles(5, 10 and 20 cycles) are selected

Table 5.2(a) Values of a and b from Present study

Cement content %	Relative Density %	$SR = a\,(N_1)^{-b}$	
		a	b
0	25	0.60	0.36
	43	0.69	0.35
	60	0.75	0.27
	80	0.89	0.23
1	25	0.85	0.33
	43	0.88	0.27
	60	0.98	0.18
	80	1.24	0.27
2	25	0.66	0.12
	43	1.45	0.25
	60	1.23	0.16
	80	no liq.	no liq.

Table 5.2(b) Values of a and b based on Rad and Clough (1982)

Cement content %	Relative Density %	$SR = a\,(N_1)^{-b}$	
		a	b
0	27	0.17	0.14
	50	0.28	0.145
	82	0.55	0.29
1	28	0.24	0.11
	51	0.45	0.18
	82	0.80	0.21
2	28	0.49	0.17
	52	0.71	0.18
	82	1.31	0.21

to develop correlations. Three values are selected to investigate the role of a particular number of cycles on the developed correlations.

The resonant column tests provide the values of dynamic moduli and damping ratios for the strain amplitudes less than 10^{-4}. Based on experimental investigations at I.I.T., relationships for maximum moduli, G_m^* and E_m^* (i.e. moduli at strains less than 10^{-5}; these moduli are independent of strain amplitude) are developed for uncemented and cemented sands (chapter III and chapter IV). These relationships are utilised here to correlate with cyclic strengths obtained from triaxial tests under identical condition of sample preparation and same variables. These relations can be easily converted to wave velocities, using relationships such as Eqn. 5.1.

Correlations for Uncemented Sand: Fig.5.11 shows the relationship between the stress ratio required to cause liquefaction in 10 cycles obtained from cyclic triaxial tests and the maximum shear modulus calculated using equation 3.16 with $\overline{\sigma}_0$=98 kpa (confining pressure used for liquefaction tests). All the data indicate a good correlation between stress ratio and shear modulus. The correlation reported by DeAlba et.al.(1984) for Monterey No.O sand is also shown in the same figure and it differs from the I.I.T. results. It may be noted that De Alba et.al(1984) presented correlations in terms of wave velocities which were converted to moduli by assuming average unit weight 97.6 pcf. The cyclic triaxial test results utilised by DeAlba et.al.(1984) correspond to effective confining pressure of 69 kpa whereas I.I.T. results correspond to $\overline{\sigma}_0$=98 kpa. Moreover, the sample preparation and testing methods adopted by De Alba et.al.(1984) are different from those at I.I.T. These may be the reasons for the difference in results. Fig.5.12 is analogous plot for maximum dynamic modulus (using equation 3.18 with $\overline{\sigma}_0$=98 kpa) versus stress ratio at 10 cycles and indicates good correlation.

To check the effect of a particular number of cycles for liquefaction (N_l) on any correlation between cyclic strength and moduli, Figs.5.13 and 5.14 are plotted for N_l=5, 10 and 20 cycles. These plots indicate the existance of a correlation of cyclic strength with moduli for any N_l. Fig.5.15 shows the correlation

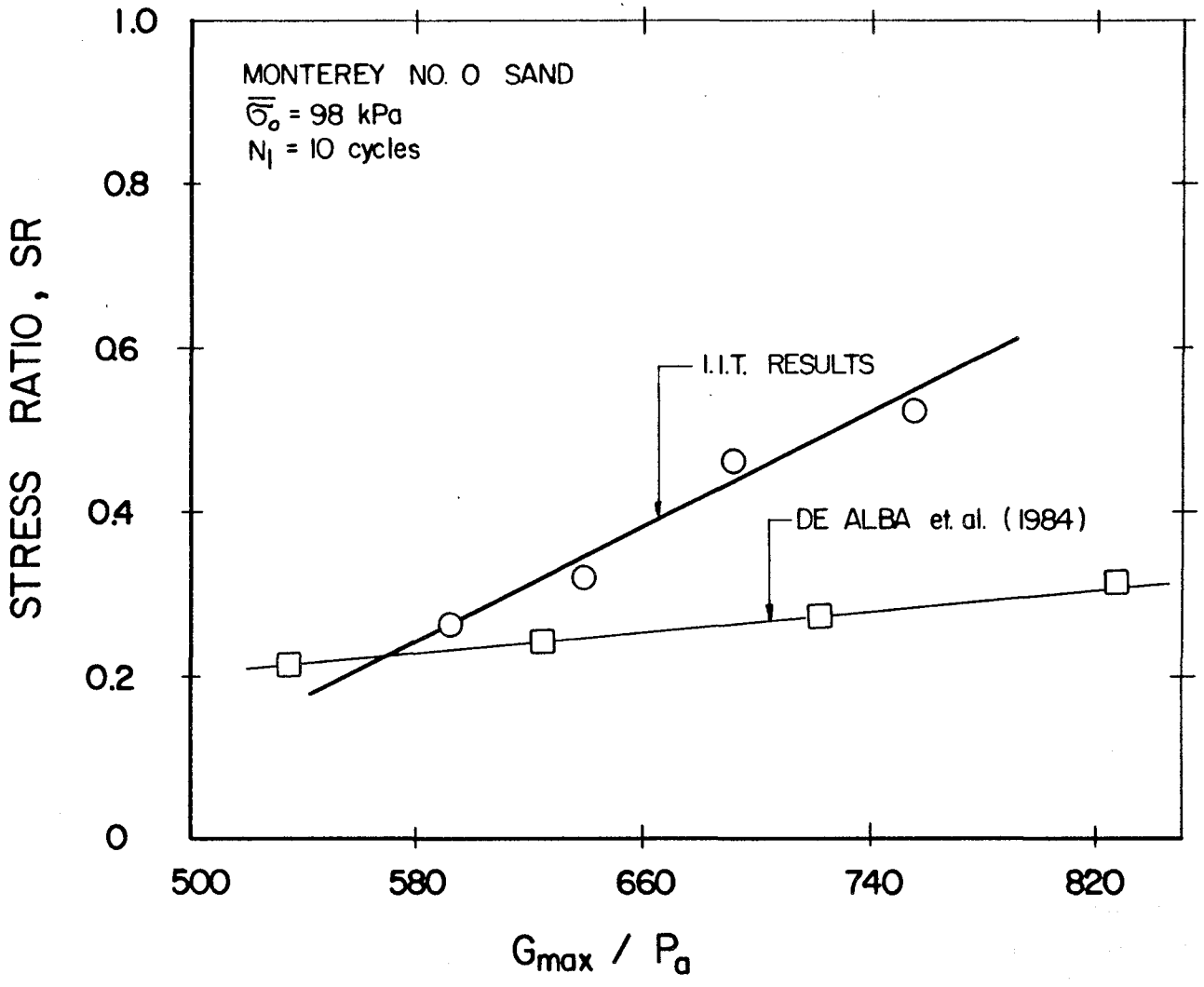

Fig.5.11 Dynamic Shear Modulus versus Liquefaction Resistance for Uncemented Sand

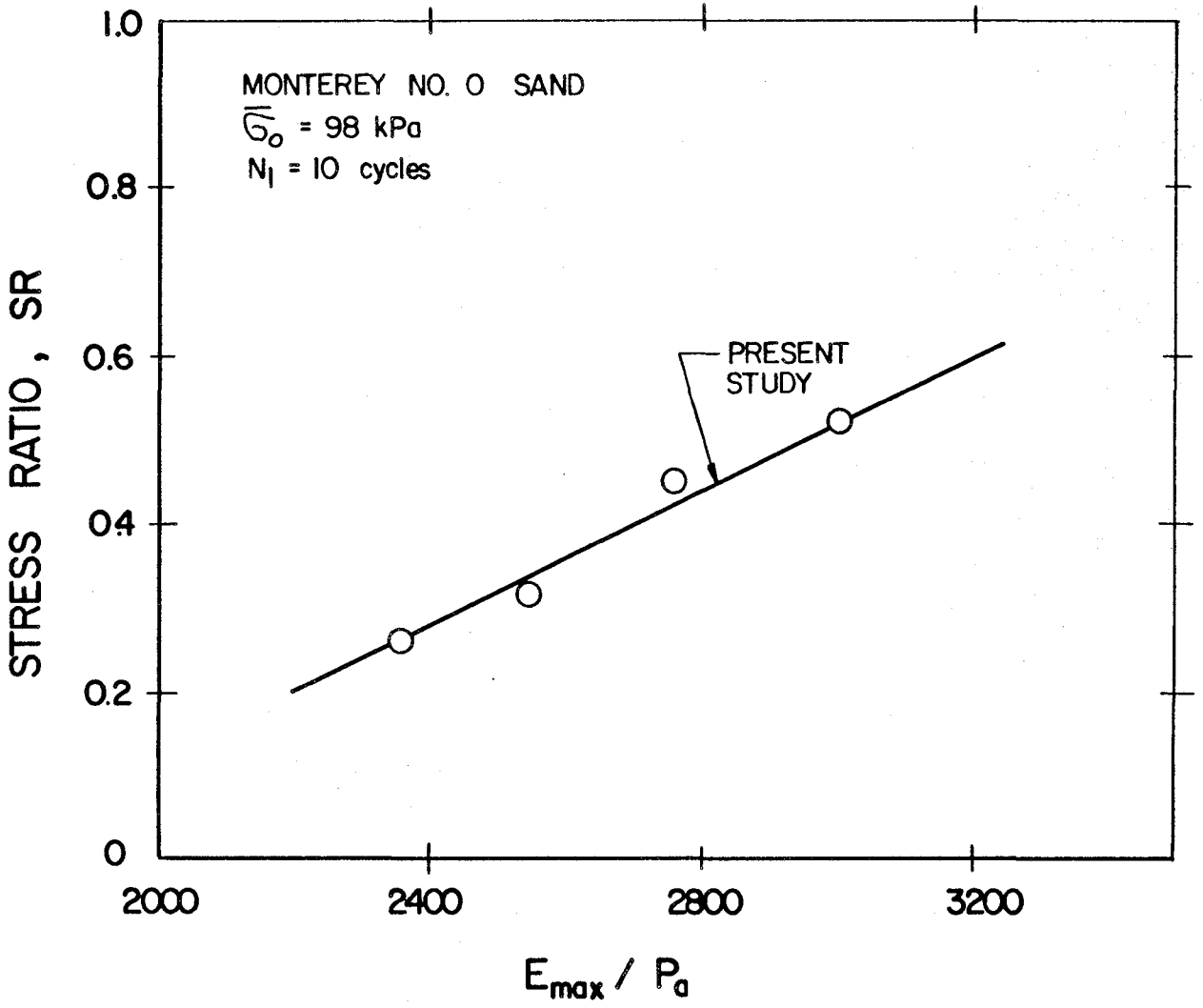

Fig.5.12 Dynamic Young's Modulus vs Liquefaction Resistance for Uncemented Sand

investigated by Tokimatsu et.al.(1986) between stress ratio and shear modulus for Niigata sand and similar correlation found from this study for Monterey No.O sand for a selected value of $\overline{\sigma}_0$ and N_l. This comparison, indicates that the correlations are material dependent and the correlations developed for a kind of soil may not be applicable for the other. This conclusion was also made by DeAlba et.al (1984) based on results for six sands of different origins and gradations.

Correlations for Cemented Sand: Fig.5.16 shows the maximum shear modulus computed from relationships reported in chapter IV and stress ratio (SR) from experimental results at I.I.T. for CC=1% and for three values of N_l. It is clear from this figure that the correlation while not as evident as for uncemented sands, does exist in some form. It is interesting to observe from the figure that a correlation can be obtained for any specific N_l and it includes the effects of density and curing time. Fig. 5.17 is similar to Fig.5.16 but for 2% cement content. Based on Fig.5.16 and Fig.5.17, the existance of correlations at all low levels of cementation (<2%) is clearly demonstrated.

Fig. 5.18 shows the maximum Young's modulus versus stress ratio for 1% cement content with N_l=5, 10 and 20 cycles. This figure clearly demonstrates that the correlation between E_m^* and SR is similar to G_m^* versus SR. This observation focuses the advantage of using dynamic Young's modulus as a direct indicator for predicting liquefaction of cemented sands; as stress ratio is not affected by $\overline{\sigma}_0$. It may be recalled (from chapter IV) that the increase in Young's modulus due to cementation (ΔE_m) is independent of $\overline{\sigma}_0$ (see Figs.4.7 and 4.8) whereas ΔG_m dependent on $\overline{\sigma}_0$ at low levels of cementation. Fig. 5.19 for CC=2% also shows the existance of good correlation between E_m^* and SR similar to G_m^* versus SR.

Discussion on Correlations: The correlations for uncemented sands are still at best in their infancy and need more data to be at a stage that they could be applied for practical use. Future field studies, perhaps may help in developing and establishing these correlations. As today, no such information for cemented sands is reported in the literature. Therefore the developed correlations between

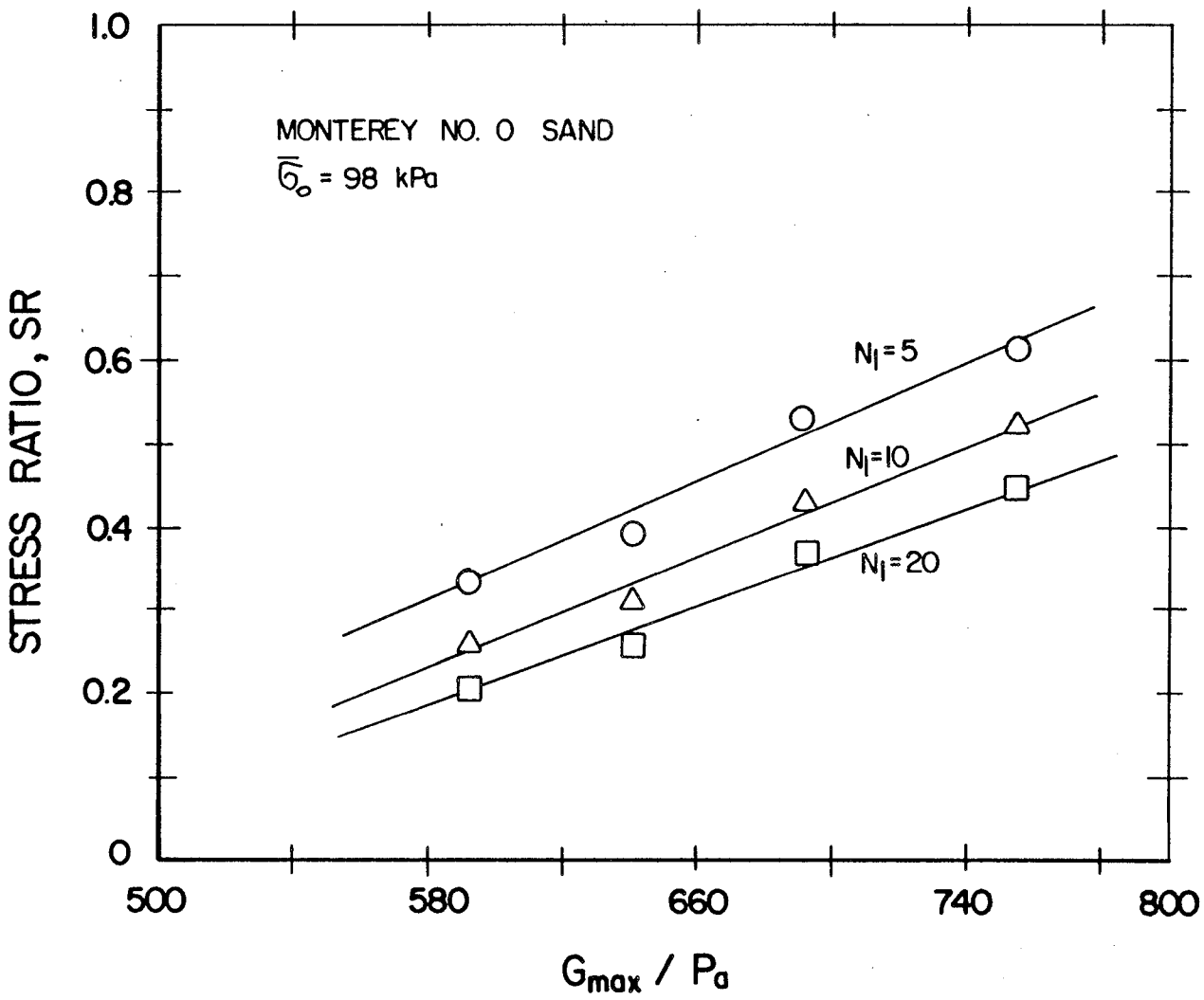

Fig.5.13 Effect of Specific Number of Cycles to cause Liquefaction on Correlation between Shear Modulus and Liquefaction Resistance for Uncemented Sand

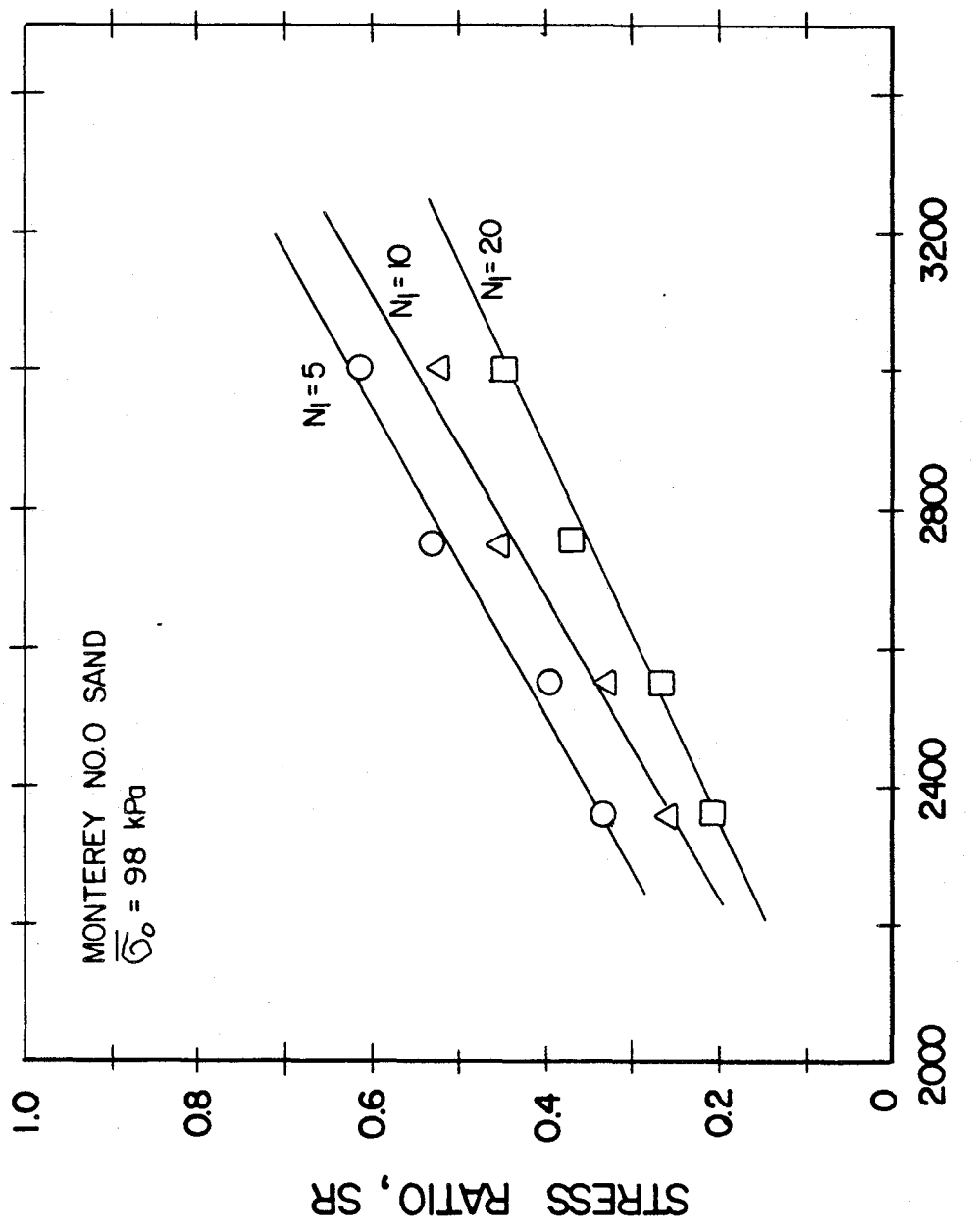

Fig.5.14 Effect of Specific Number of Cycles to cause Liquefaction on Correlation between Young's modulus and Liquefaction Resistance for Uncemented Sand

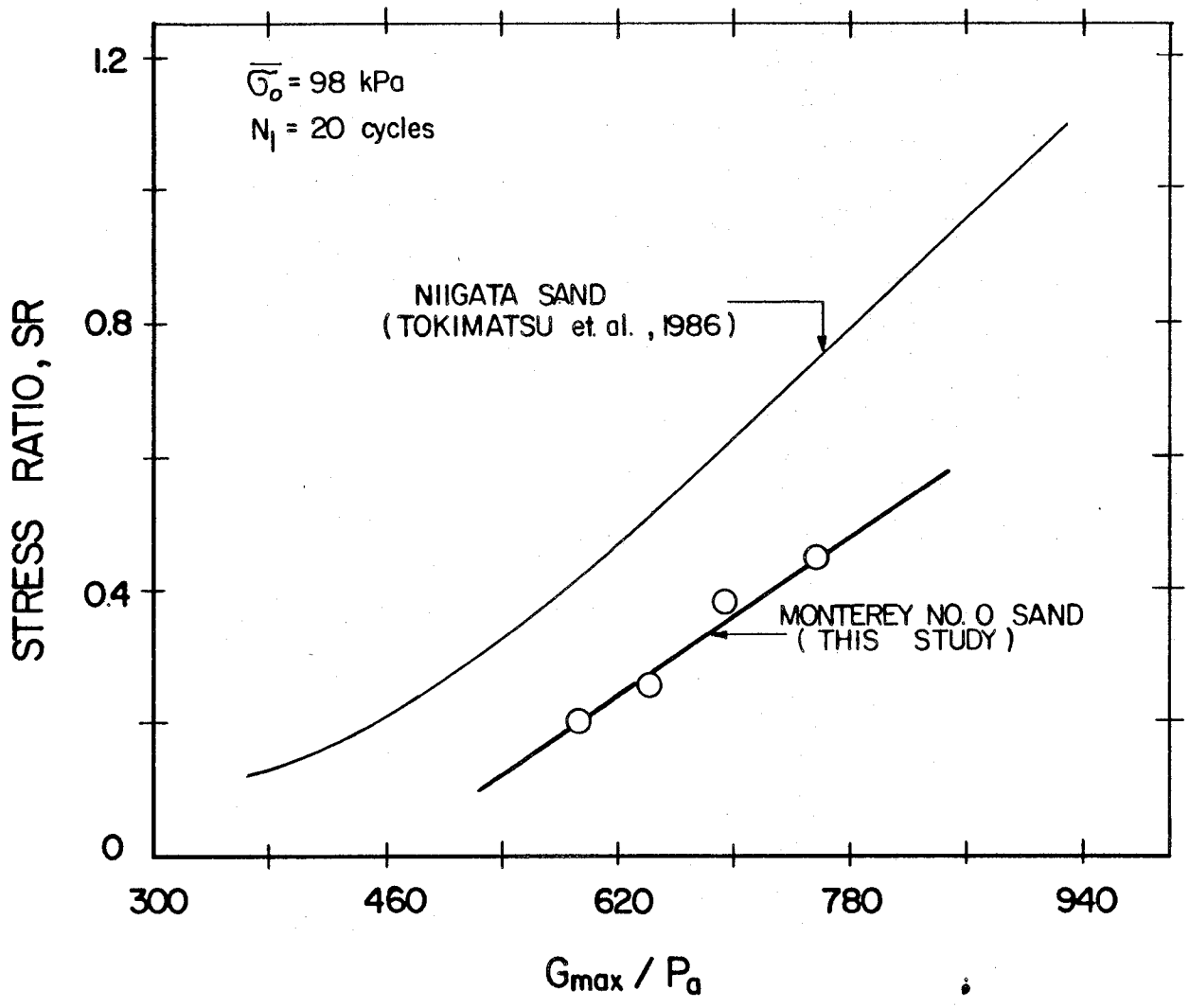

Fig.5.15 Comparison of Correlations between Dynamic Shear Modulus and Liquefaction Resistance for Uncemented Sand

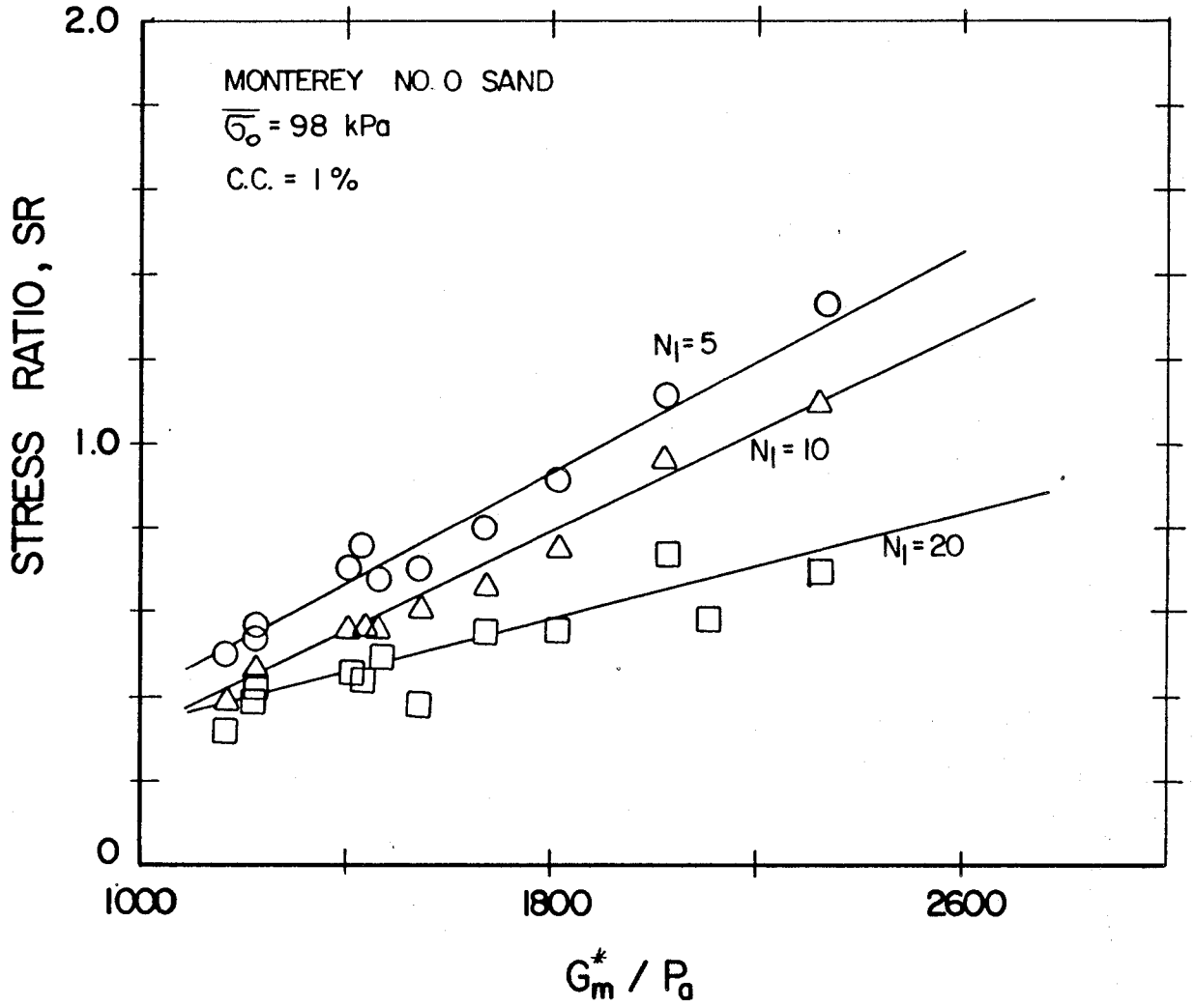

Fig.5.16 Dynamic Shear Modulus versus Liquefaction Resistance for Cemented Sand with CC=1%

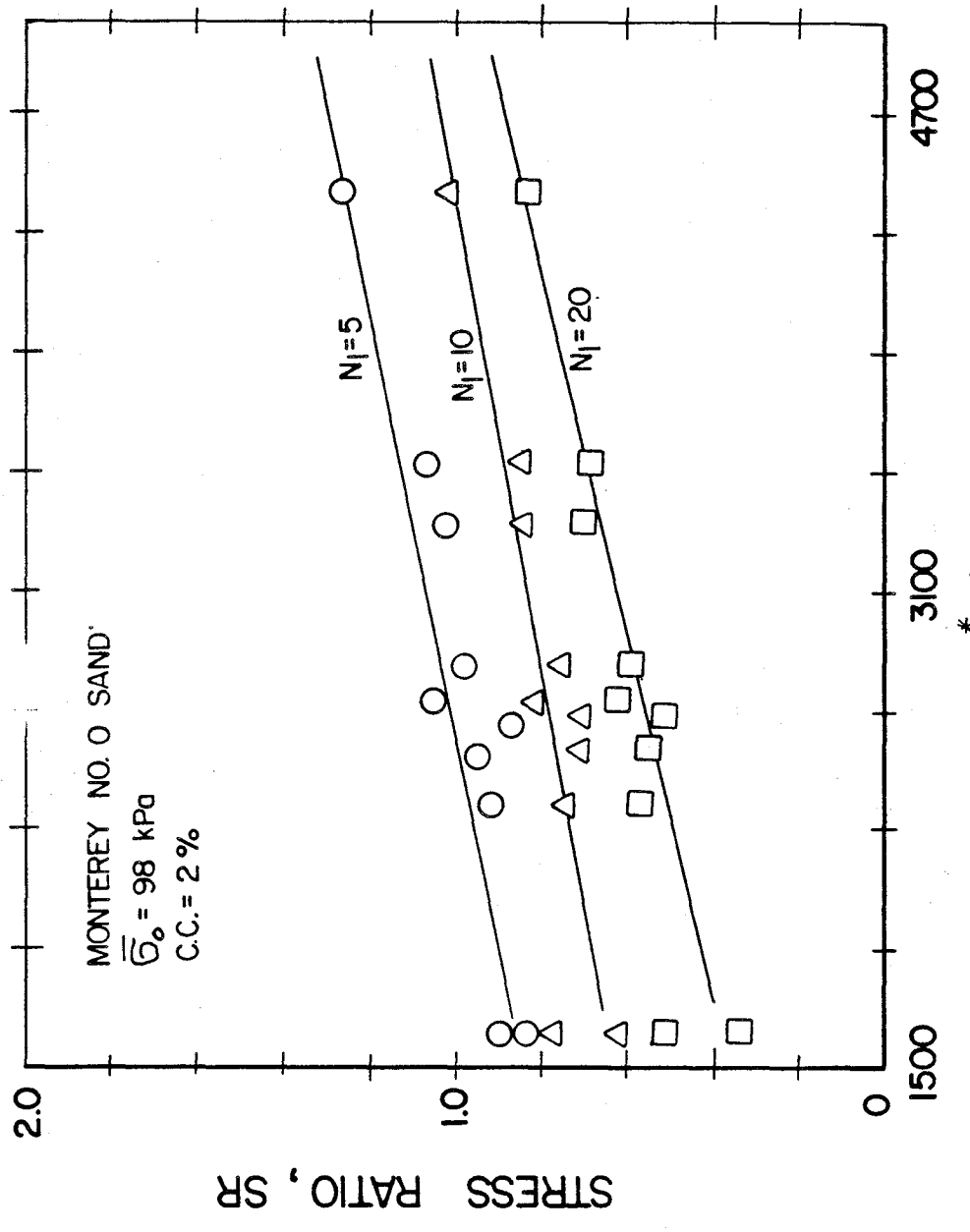

Fig.5.17 Dynamic Shear Modulus versus Liquefaction Resistance for Cemented Sand with CC=2%

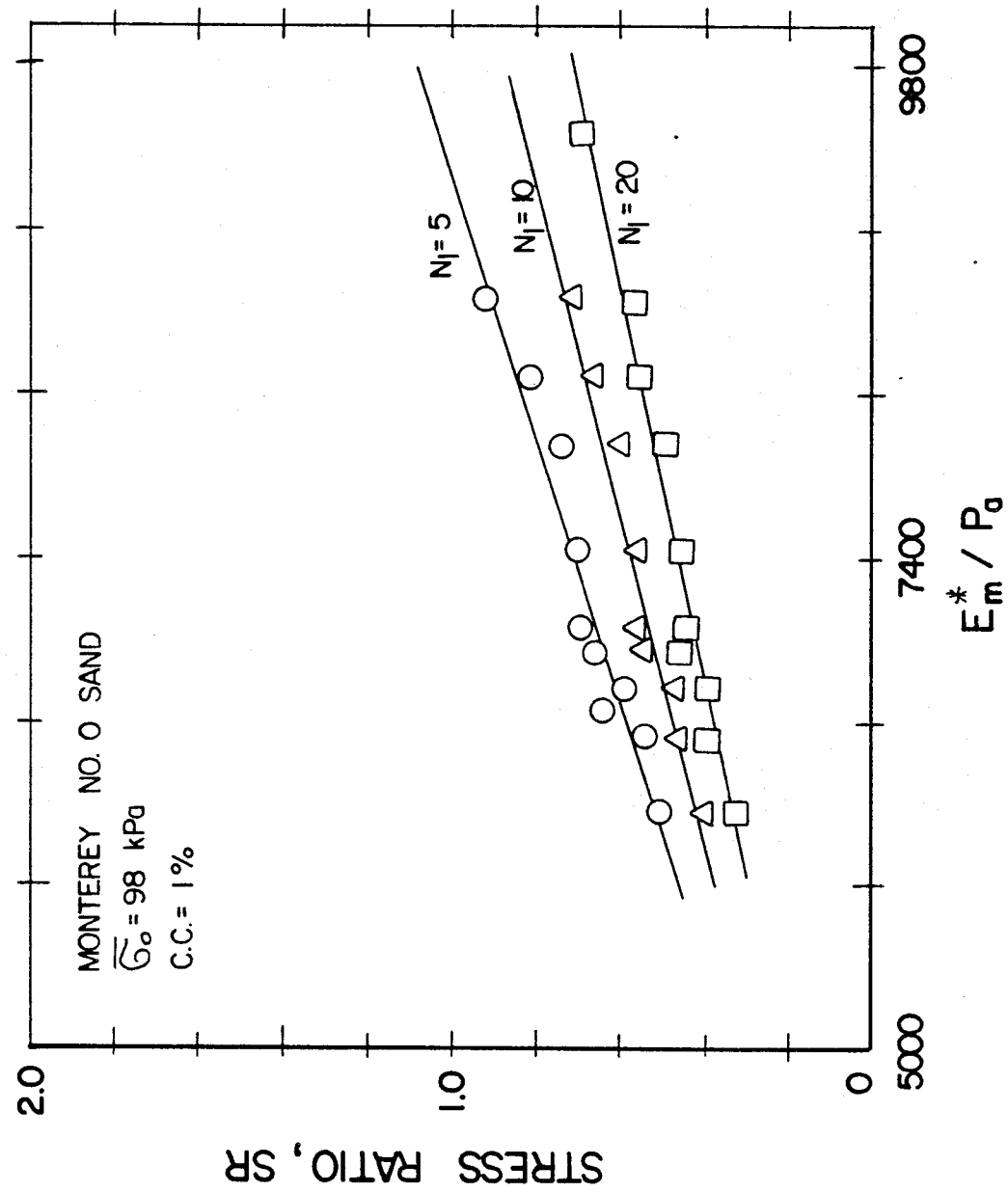

Fig.5.18 Dynamic Young's Modulus versus Liquefaction Resistance for Cemented Sand with CC=1%

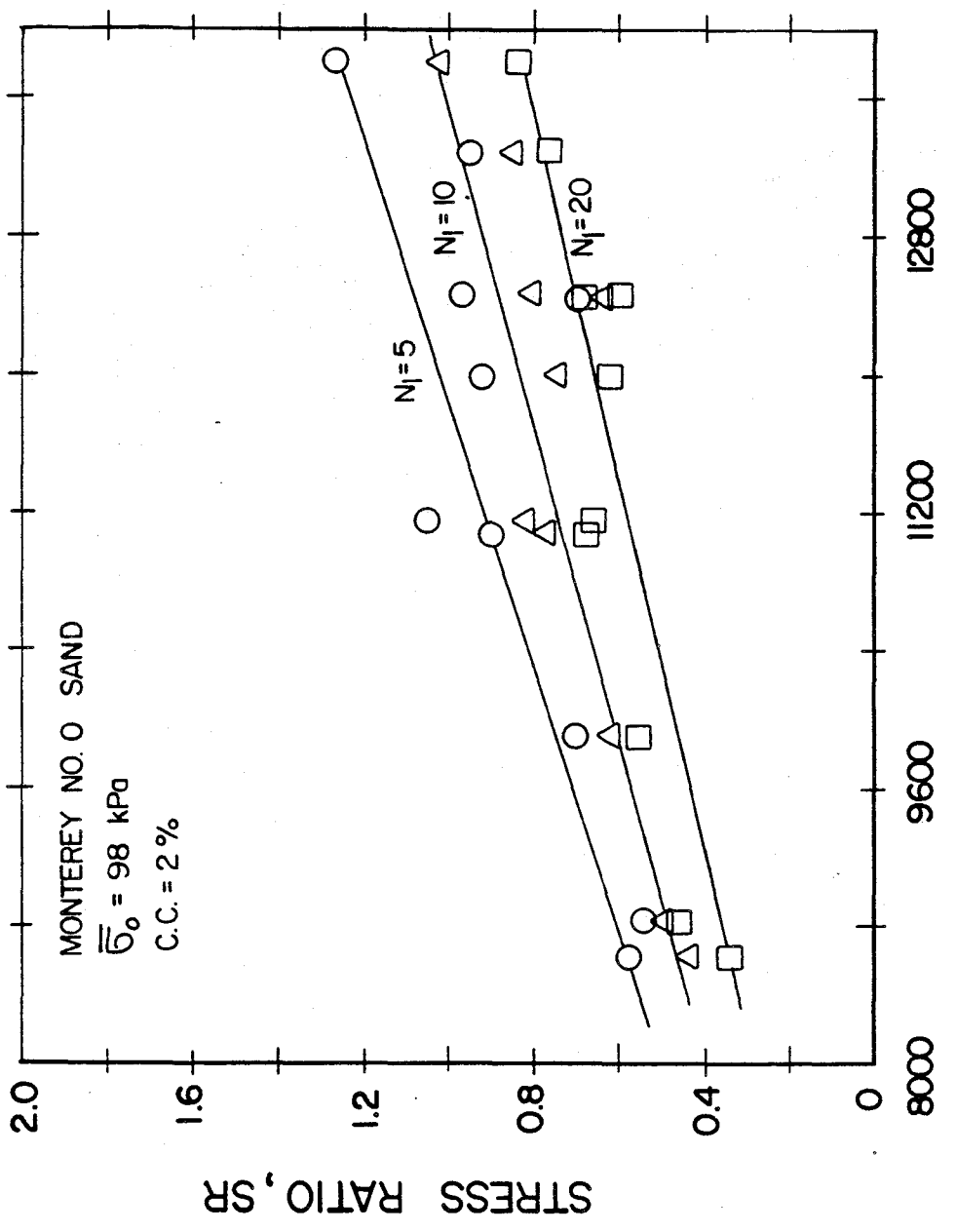

Fig.5.19 Dynamic Young's Modulus versus Liquefaction Resistance for Cemented Sand with CC=2%

dynamic moduli and cyclic strength of cemented sands can serve as preliminary base towards this direction and these relations when well established, will be of great help to practicing engineers dealing with naturally cemented or/and artificially cemented sands. The shortcomings of the developed relations are as follows: (1) Moduli and cyclic strength increase with the increase of density, confining pressure, cement content and curing period. However, the moduli values used in correlations are corresponding to confining pressure of liquefaction tests (98 Kpa). Therefore the correlations are not applicable for different $\overline{\sigma}_0$. (2) Correlations are dependent on type of sand and level of cementation however, for any particular sand and level of cementation a good correlation can be established.

Very significant difference in cyclic strength from different sample preparation methods is reported by Mulilis et.al.(1976). Therefore, several new undisturbed sampling techniques for retriving the samples for liquefaction tests are developed and reported by many investigators. Even then the duplication of stress history effects by these methods is still questionable. The existance of good correlation between moduli (wave velocities) and cyclic strength in this study indicate the following procedure to duplicate stress history effects. If any field tests providing in-situ wave velocities are conducted, then the sample prepared at field density is prestressed first until in-situ wave velocities can be measured in the sample before it is subjected to cyclic loading in conventional cyclic triaxial device. The results so obtained would provide reliable cyclic strength of that soil deposit in field.

5.6 SUMMARY

The present study is devoted to discuss the factors affecting the liquefaction resistance and also to investigate the correlation between dynamic moduli and cyclic strength of cemented sands. The results from tests with modified Drenevich resonant column device and stress controlled cyclic triaxial device on artificially cemented sands are utilised. The various parameters and method of preparation for the specimens are same for both types of tests; thereby the effects of sample preparation on correlations are avoided. A con-

sistant increase in liquefaction resistance has been observed with the increase in cement content, density and curing time. The liquefaction resistance and moduli are found dependent on same factors except $\overline{\sigma}_0$ hence, the correlations between moduli and stress ratio are developed. These correlations are similar to uncemented sands however dependent on type of sand and level of cementation and applicable to a particular $\overline{\sigma}_0$ only.

Chapter VI

CONCLUSIONS AND RECOMMENDATIONS

6.1 CONCLUSIONS

The overall investigation produced the beneficial effects of artificial cementation in quantifiable form. The following qualitative and quantitative conclusions can be made:

(1) For cemented sands, at small axial strains (0.25 – 1%) most of the shear strength is contributed from cohesion. As the strains increase, the cementation gets broken and frictional resistance increases and at or near failure, the strength entirely depends on particle to particle resistance.

(2) The tensile strength of cemented sands is related to the unconfined compressive strength and is about 13 – 15% of the unconfined compressive strength.

(3) The unconfined compressive strength of cemented sands is related to drained cohesion c' and varies with the cement content– for low cement content q_u being about twice that of c' and for high cement content q_u is about one and a half times of c'.

(4) An expression relating the initial Young's modulus of cemented sand (E_i^*) to the initial Young's modulus of uncemented sand (E_i) has been developed as follows:

$$E_i^* = RE_i$$

where R can be called modulus ratio. The value of R can be obtained from following relationship:

$$logR = log(1 + C - eC) + (0.71 - 1.3e)(C)^{(2.2-2.4e)} log\left(\frac{\overline{\sigma}_0}{P_a}\right)$$

where C is the cement content expressed in percentage , e is the void ratio and $\overline{\sigma}_0$ is the effective confining pressure. Alternate expressions for finding R by using unconfined compressive strength have also been proposed (Eqn.2.21 through Eqn.2.23).

(5) For cemented sands the typical stress-strain behavior is elastic– higher the cement content, higher is the elastic limit. However, the post peak behavior is rather complex and is a function of the brittleness.

(6) The resonant column tests provided the following relations for Monterey No.O sand:

$$G_m = \frac{428.2}{(0.3+0.7e^2)}(P_a)^{0.426}(\overline{\sigma}_0)^{0.574}$$

$$E_m = \frac{1703.57}{(0.3+0.7e^2)}(P_a)^{0.61}(\overline{\sigma}_0)^{0.39}$$

$$D_s = 9.22\left(\frac{\overline{\sigma}_0}{P_a}\right)^{-0.38}(\gamma)^{0.33}$$

$$D_l = \left(\frac{\overline{\sigma}_0}{P_a}\right)^{-0.13}(\epsilon)^{0.33}$$

where G_m, E_m,D_s, D_l, $\overline{\sigma}_0$, γ and ϵ are maximum dynamic shear modulus, maximum dynamic Young's modulus, dynamic shear damping, dynamic longitudinal damping, effective confining pressure, dynamic shear strain and dynamic longitudinal strain respectively. The dynamic strains and damping ratios are expressed in percent. The previously reported relations overpredict moduli and underpredict damping for Monterey No.O sand.

(7) A small amount of cementation increases dynamic moduli and damping ratios of sands at low strain amplitudes. However at higher cementation, though the moduli are considerably increased, the damping ratios are observed decreasing. The major parameters governing the dynamic behavior of cemented sands are cement content, effective confining pressure and density; the damping ratios, however are less influenced by density.

(8) The following relationships for cemented sands at low strain amplitude were found applicable:

For low cementation (CC<2%)

$$\frac{\Delta G_m}{P_a} = \frac{172}{(e-0.5168)}(CC)^{0.88}\left(\frac{\overline{\sigma}_0}{P_a}\right)^{(0.515e-0.13CC+0.285)}$$

$$\frac{\Delta E_m}{P_a} = \frac{2193.4}{(e-0.2262)}(CC)^{(2.03-1.739e)}$$

For high cementation (2% > CC < 8%)

$$\frac{\Delta G_m}{P_a} = \frac{773}{e}(CC)^{1.2}\left(\frac{\overline{\sigma}_0}{P_a}\right)^{(0.698e-0.04CC-0.2)}$$

$$\frac{\Delta E_m}{P_a} = \frac{2930.5}{(e-0.4921)}(CC)^{(2.692e-1.44)}$$

where ΔG_m and ΔE_m are the increase in maximum dynamic shear and Young's moduli respectively due to cementation. Similarly the increase in dynamic shear and longitudinal damping ratios (ΔD_s and ΔD_l) at low cementation (CC<2%) are developed for specific strain levels.

$$\Delta D_s = 0.49(CC)^{1.07}\left(\frac{\overline{\sigma}_0}{P_a}\right)^{-0.36} \qquad ...for\ \gamma = 10^{-3}\%$$

$$\Delta D_l = 1.17(CC)^{0.75}\left(\frac{\overline{\sigma}_0}{P_a}\right)^{-0.1} \qquad ...for\ \epsilon = 10^{-4}\%$$

(9) For cemented sands the dynamic moduli (and thus the wave velocities) are related to the cyclic shear strength (liquefaction resistance) but are applicable for a particular confining pressure only.

6.2 RECOMMENDATIONS

Further research is needed in the following directions:

(1) The methodology of incorporating the degree of brittleness into constitutive behavior needs further examination. It may also be interesting to examine if any of the available models can predict the behavior of cemented sands.

(2) More data base is required for cemented sands by using advanced soil testing devices such as true triaxial, cyclic simple shear etc. so that the behavior under nonstandard combination of principal stresses, detailed dynamic response etc. could be studied.

(3) Wherever possible the data of naturally cemented sands should be utilised to document the applicability of the study results from artificially cemented sands to the naturally cemented sands.

(4) An apparatus that would be capable of testing the same specimen under resonant column and cyclic triaxial testing conditions needs to be developed.

BIBLIOGRAPHY

Acar, Y.B., and El-Tahir, E.A.,"Low Strain Dynamic Properties of Artificially Sand," the Journal of Geotechnical Engineering, ASCE, Vol. 112, No. 11, November, 1986, pp. 1001-1015.

Afifi, S.S., and Woods, R.D.,"Long-term Pressure Effects on Shear Modulus of Soils," Journal of the Soil Mechanics and Foundations Division, ASCE, Vol. 97, No. SM10, 1971, pp. 1445-1460.

American Society of Civil Engineers, Proceedings of Geotechnical Engineering Division,"Grouting in Geotechnical Engineering," Speciality Conference, New Orleans, Feb. 10-12, 1982.

Anderson, D.G., and Woods, R.D.,"Time-Dependent Increase in Shear Modulus of Clay," Journal of the Geotechnical Engineering, ASCE, Vol. 102, No. GT5, 1976, pp. 525-537.

Anderson, D.G., and Richart, F.E.,"Effects of Straining on Shear Modulus of Clay," Journal of the Geotechnical Engineering, ASCE, Vol. 102, No. GT9, 1976, pp. 975-987.

Anderson, D.G., Espana, C., and McLamore, V.R.,"Estimating in Situ Shear Moduli at Competent Sites," proceedings of the Geotechnical Division Speciality Conference on Earthquake Engineering and Soil Dynamics, ASCE, Pasadena, Ca., Vol. 1, 1978, pp. 181-197.

Athanasopoulos, G.A., and Richart, Jr., F.E.,"Effect of Creep on Shear Modulus of Clays," Journal of the Geotechnical Engineering, Vol. 109, No. 10, 1983, pp. 1217-1232.

Au, W.C., and Chae, Y.S.,"Dynamic Shear Modulus of Treated Expansive Soils," Journal of the Geotechnical Engineering Division, ASCE, Vol. 106, No. GT3, pp. 255-273.

Avramidis, A., and Saxena, S.K., "Behavior of Cemented-Stabilized Sands Under Static and Dynamic Loads," Report No. IIT-CE85-01, Department of Civil Engineering, I.I.T., September, 1985.

Avramidis, A., and Saxena, S.K., " The Modified Stiffned Drenevich Resonant Column Apparatus," Submitted for publication in the Geotechnical Testing Journal, ASTM.

Bachus, R.C., Clough, W.G. Sitar, N., Shafii-Rad, N., Crosby, J., and Koboli, P.,"Behavior of Weakly Cemented Soil Slopes Under Static and Seismic Loading Conditions," Vol. 2, Report No. 52, The John A. Blume Earthquake Engineering Center, Stanford University, July, 1981.

Brace, W.F., "Brittle Fracture of Rocks," Proc. Int. Conf. on State of Stress in the Earth's crust, Santa Monica, Cal., May, 1963, pp. 110-174.

Chae, Y.S., and Chiang, J.C.,"Dynamic Properties of Lime and LFA Treated Soils," Proceedings of the ASCE, Geotechnical Engineering Division Speciality Conference on Earthquake Engineering and Soil Dynamics," Pasadena, CA., June, 1978, pp. 308-325.

Chiang, Y.C., and Chae, Y.S.,"Dynamic Properties of Cement Treated Soils," Highway Research Record, National Research Council, No. 379, 1972, pp. 39-51.

Chung, R.M., Yokel, F.Y., and Drenevich, V.P.,"Evaluation of Dynamic Properties of Sands by Resonant Column Testing," Geotechnical Testing Journal, GTJODJ, Vol. 7, No. 2, 1984, pp. 60-69.

Clough, G.W., Sitar, N., Bachus, R., and Rad, N.S., "Cemented Sands under Static Loading," Journal of the Geotechnical Engineering, ASCE, Vol. 107, No. GT6, June, 1981, pp. 799-817.

De Alba, P., Baldwin, K., Janoo, V., Roe, G., and Celikkol, B., " Elastic-wave Velocities and Liquefaction Potential," Geotechnical Testing Journal, GTJODJ, Vol.7, No.2, June, 1984, pp.77-87.

Dobry, R., Stokoe, K.H.II., Ladd, R.S., and Youd, T.L., " Liquefaction Susceptibility from S- Wave Velocity," Preprint 81-544, ASCE National Convention, St.Louis, October,1981.

Dobry, R., Ladd, R.S., Yokel, F.Y., Chung, R.M., and Powell, D.J., " Prediction of Pore Pressure Buildup and Liquefaction of Sands During Earthquakes

by the Cyclic Strain Method," Series 138, National Bureau of Standards, Washington, July, 1982.

Drenevich, V.P., "Recent Developments in Resonant Column Testing," Soil Mechanics Series No. 33, Dept. of Civil Engineering, University of Kentucky, Lexington, 1985.

Drnevich, V.P.,"Resonant-Column Testing Problems and Solutions," Dynamic Geotechnical Testing, ASTM, STP 654, 1978, pp. 384-398.

Duffy, J., and Mindlin, R.D.,"Stress-Strain Relations of Granular Medium," ASME, Journal of Applied Mechanics Division, Vol. 24, 1957, pp. 585-593.

Dupas, J.M., and Pecker, A.,"Static and Dynamic Properties of Sand-Cement," Journal of the Geotechnical Engineering Division, ASCE, Vol. 105, No. GT3, March, 1979, pp. 419-435.

Edil, T.B., and Luh, G.F.,"Dynamic Modulus and Damping Relationships for Sands," Proceedings of the Geotechnical Division Speciality Conference on Earthquake Engineering and Soil Dynamics, ASCE, Pasadena, CA., Vol. 1, 1978, pp. 394-409.

Ferrito, J.M., Forrest, J.B., and Wu, G., " A Compilation of Cyclic Triaxial Liquefaction Data," Geotechnical Testing Journal, Vol.2, No.2, June, 1979, pp.106-113.

Frydman, S., Hendron, D., Horn, H., Steinback, J., Backer, R., and Shoal, B., "Liquefaction Study of Weakly Cemented Sand," Journal of the Geotechnical Engineering Division, Proceedings ASCE, Vol. 106, No. GT3, March, 1980,pp. 275-297.

Griffith, A.A.,"The Phenomena of Rupture and Flows in Solids," Trans. Royal Society, Vol. 34, 1920, pp. 137-154.

Hardin, B.O., and Richart, Jr., F.E.,"Elastic Wave Velocities in Granular Soils," Journal of the Soil Mechanics and Foundation Division, ASCE, Vol. 89, No., SM1, 1963, pp. 33-65.

Hardin, B.O.,"The Nature of Stress-Strain Behavior of Soils," Proceedings of the Geotechnical Division Speciality Conference on Earthquake Engineering and Soil Dynamics, ASCE, Pasadena, CA., Vol. 1, 1978, pp.3-90.

Hardin, B.O., and Black, W.L.,"Vibrations Modulus of Normally Consolidated Clay, "Journal of the Soil Mechanics and Foundations Division, Vol. 94, No. SM2, 1968, pp. 353-369.

Hardin, B.O., and Drnevich, V.P.,"Shear Modulus and Damping in Soils; Measurement and Parameter Effect, "Journal of the Soil Mechanics and Foundations Division, ASCE, Vol. 98, No. SM6, 1972, pp. 603-624.

Hardin, B.O., and Drnevich, V.P.,"Shear Modulus and Damping in Soils; Design Equations and Curves," Journal of the Soil Mechanics and Foundation Division, ASCE, Vol. 98, SM7, 1972, pp. 667-692.

Isenhower, W.M.,"Torisonal Simple Shear/Resonant Column Properties of San Francisco Bay Mud," Geotechnical Engineering Thesis GT80-1, Civil Engineering Department, University of Texas at Austin, Austin, TX, 1979, 307 pages.

Iwasaki, T., and Tatsuoka, F.,"Effects of Grain Size and Grading on Dynamic Shear Moduli of Sands," Soils and Foundations, Vol. 17, No. 3, 1977, pp. 19-35.

Iwasaki, T., Tatsuoka, F., and Takagi, Y.,"Shear Moduli of Sands under Cyclic Torsional Shear Loading," Soils and Foundations, Japenese Society of Soil Mechanics and Foundation Engineering, Vol. 18, No. 1, 1978, pp. 39-56.

Janbu, N.,"Soil Compressibility as Determined by Oedometer and Triaxial Tests," European Conference on Soil Mechanics and Foundation Engineering, Wissbaden, Germany, Vol. 1, 1963, pp. 19-25.

Ladd, R.S.,"Preparing Test Specimens Using Undercompaction," Geotechnical Testing Journal, GTJODT, Vol. 1, No. 1, March, 1978, pp. 16-23.

Marcuson III, W.F., and Wahls, H.E.,"Time Effects on Dynamic Shear Mod-

uli or Clays," Journal of the Soil Mechanics and Foundations Division, ASCE, Vol. 98, No. SM12, 1972, pp. 1359-1373.

Marcuson III, W.F., and Curro, Jr., J.R.,"Field and Laboratory Determination of Soil Moduli," Journal of the Geotechnical Engineering Division, ASCE, Vol. 107, No. GT10, 1981, pp. 1269-1291.

McClintock, F.A., and Walsh, J.B.,"Friction on Griffith Cracks in Rocks Under Pressure," Proc. 4th U.S. Nat. Cong. Appl. Mech., Vol. 2, 1962, pp. 1015-1022.

MIT,"Conference on Soil Stabilization," Massachusetts Institute of Technology, Proceedings, Cambridge, Mass., 1952.

Mulilis, J.P., Horz, R.C., and Townsend, F.C.,"The Effects of Cyclic Triaxial Testing Techniques on the Liquefaction Behavior of Monterey No. 0 Sand," Miscellaneous paper S-76-6, Soils and Pavements Laboratory, U.S. Army Engineer Waterways Experiment Station, April, 1976.

Ohsaki, Y., and Iwasaki, R.,"On Dynamic Shear Moduli and Poisson's Ratios of Soil Deposits," Soils and Foundations, Japenese Society of Soil Mechanics and Foundation Engineering, Vol. 13, No. 4, 1973, pp. 61-73.

Rad, N.S., and Clough, W.G., "The Influence of Cementation on the Static and Dynamic Behavior of Sands," Report No.59, The Jhon A.Blume Earthquake Engineering Center, Stanford university, December, 1982.

Richart, Jr., F.E.,"Some Effects of Dynamic Soil Properties on Soil-Structure Interaction," Journal of the Geotechnical Engineering Division, ASCE, Vol. 101, No. GT12, 1975, pp. 1197-1240.

Salomone, L.A., Singh, H., and Fisher, J.A., " Cyclic Shear Strength of Variably Cemented Sands," Proceedings of the ASCE, Geotechnical Engineering Division, Speciality Conference on Earthquake Engineering and Soil Dynamics, Pasadena, Cal., Vol. 2, June, 1978, pp. 819-835.

Saxena, S.K., and Lastrico, R.M.,"Static Properties of Lightly Cemented Sand," Journal of the Geotechnical Engineering Division, Proceedings ASCE, Vol 14, No. GT12, December, 1978, pp. 1449-1463.

Saxena, S.K., and Reddy, R.K.,"A Constitutive Model for Cemented Sand," Report Under Preparation, Department of Civil Engineering, Illinois Institute of Technology, 1987.

Saxena, S.K., Reddy, R.K., and Sengupta,A., Predictions submitted to the International Workshop on Constitutive Equations for Granular Non-Cohesive Soils, Cleveland, OH, July, 1987.

Seed, H.B., and Idriss, T.M.,"Soil Moduli and Damping Factors for Dynamic Response Analyses," Earthquake Engineering research Center, Report No. EERC 70-10, University of California, Berkeley, 1970.

Seed, H.B., and Idriss, I.M., " Simplified Procedure for Evaluating Soil Liquefaction Potential," Journal of the Soil Mechanics and Foundations Division, ASCE, Vol.97, No.SM9, Sept.1971, pp. 1249-1273.

Seed, H.B., Martin, P.P., and Lysmer, J., " Pore-Water Pressure Changes During Soil Liquefaction," Journal of the Geotechnical Engineering Division, ASCE, Vol.102, No.GT4, April, 1976, pp.323-346.

Seed, H.B., Idriss, I.M., and Arango, I., " Evaluation of Liquefaction Potential Using Field Performance Data," Journal of the Geotechnical Engineering Division, ASCE, Vol.109, No.GT3, March, 1983, PP. 458-482.

Sherif, M.A., and Ishibashi, I,"Dynamic Shear Moduli For Dry Sands," Journal of the Geotechnical Engineering Division, ASCE, Vol. 102, No. GT11, 1976, pp. 1171-1184.

Sherif, M.A., Ishibashi, I., and Gaddah, A.H.,"Damping Ratio For Dry Sands," Journal of the Geotechnical Engineering Division, ASCE, Vol. 103, No. GT7, 1977, pp. 743-756.

Silver, M.L., and Park, T.K.,"Testing Procedure Effects on Dynamic Soil Behavior," Journal of the Geotechnical Engineering Division, Vol. 101, No. GT10, 1975, pp. 1061-1083.

Silver, M.L., " Laboratory Triaxial Testing Procedures to Determine the Cyclic Strength of Soils," Report No. NUREG-31, United States Nuclear Regulatory Commission, Washington, D.C., June, 1977.

Sitar, N., Clough, W.G., and Bachus, R.C.,"Behavior of Weakly Cemented Soil Slopes Under Static and Seismic Loading Conditions," Report No. 44, The John A. Blume Earthquake Engineering Center, Stanford University, June, 1980.

Skoglund, G.R., Marcuson III, W.F., and Cunny, R.W., "Evaluation of Resonant Column Test Devices," Journal of the Geotechnical Engineering Division, ASCE, Vol. 102, No. GT11, 1976, pp. 1147-1158.

Stokoe, K.H.II., and Nazarian, S., " Use of Rayleigh Waves in Liquefaction Studies," Measurment and Use of Shear Wave Velocity for Evaluating Dynamic Soil Properties, Edited by R.D. Woods, ASCE convention, Denver, CO, May, 1985, pp.1-17.

Tatsuoka, F., Iwasaki, T., and Takagi, Y.,"Hysteretic Damping of Sands under Cyclic Loading and its Relation to Shear Modulus," Soils and Foundations, Japanese Society of Soil Mechanics and Foundation Engineering, Vol. 18, No. 2, 1978, pp. 25-40.

Tokimatsu, K., Yamazaki, T., and Yoshimi, Y., " Soil Liquefaction Evaluations By Elastic Shear Moduli," Soils and Foundations, Vol.26, No.1, March, 1986, pp.25-35.

Townsend, F.C., " Review of Factors Affecting Cyclic Triaxial Tests," ASTM, STP 654, Symposium on Dynamic Geotechnical Testing, Denver, CO., June, 1977, pp. 356-383.

USNAEC,"Soil Stabilization - State of the Art Survey," Vol. 2, NAEC, Eng-7469 Code Ident. No. 80020, U.S. Naval Air Engineering Center, Philadelphia, PA, 1969.

Wilson, R.C., Warrick, R.E., and Bennett, M.J.,"Seismic Velocities of San Francisco Bayshore Sediments," Proceedings of the Geotechnical Engineering Division Speciality Conference on Earthquake Engineering and Soil Dynamics, ASCE, Pasadena, CA., Vol. 2, 1978, pp. 1007-1023.

Wissa, A.E.Z., and Ladd, C.C.,"Effective Stress-Strength Behavior of Compacted Stabilized Soils," Research Report R64-32, Soils Publication No. 164, Dept. of Civil Engineering, M.I.T., July, 1964.

Wissa, A.E.Z., and Ladd, C.C.,"Shear Strength Generation in Stabilized Soils," Research Report R65-17, Soils Publication No. 173, Department of Civil Engineering, M.I.T., June, 1965.

Wong, K.S. and Duncan, J.M.,"Hyperbolic Stress-Strain Parameters for Nonlinear Finite Element Analyses of Stresses and Movements in Soil Masses," Geotechnical Engineering Report, Department of Civil Engineering, University of California, Berkeley, July, 1974.

Woods, R.D.,"Measurement of Dynamic Soil Properties," Proceedings, ASCE, Geotechnical Engineering Division Speciality Conference on Earthquake Engineering and Soil Dynamics, Pasadena, CA., June, 1978, Vol. 1, pp. 91-178.

Wu, S., Gray, D.H., and Richart, F.E.,"Capillary Effects on Dynamic Modulus of Sands and Silts," Journal of the Geotechnical Engineering, ASCE, Vol. 110, No. 9, 1984, pp. 1188-1203.

Yu, P., and Richart, Jr., F.E.,"Stress Ratio Effects on Shear Modulus of Dry Sands," Journal of the Geotechnical Engineering, Vol. 110, No. 3, 1984, pp. 331-345.